



UNIVERSITY OF THE  
WITWATERSRAND,  
JOHANNESBURG

**The effect of cholesterol depletion on TGF- $\beta$ -induced epithelial-mesenchymal transition  
in pancreatic cancer cells.**

by

**Andrea Breytenbach**

**(1885532)**

**Dissertation**

Submitted in fulfilment of the requirements for the degree

**Master of Science**

in

**Molecular and Cell Biology**

in the Faculty of Science, University of the Witwatersrand, Johannesburg, South Africa

Supervisor: Prof. Mandeep Kaur

June 2024

## DECLARATION

I, Andrea Breytenbach (1885532), am a student registered for the degree of Master of Science (Molecular and Cell Biology) in the academic years 2022-2023.

I hereby declare the following:

- I am aware that plagiarism (the use of someone else's work without their permission and/or without acknowledging the original source) is wrong.
- I confirm that the work submitted for assessment for the above degree is my own unaided work except where explicitly indicated otherwise and acknowledged. In this context, I understand that the use of editing services is considered aided work and must be declared.
- I have not submitted this work before for any other degree or examination at this or any other University.
- The information used in the Thesis has not been obtained by me while employed by, or working under the aegis of, any person or organisation other than the University.
- I have followed the required conventions in referencing the thoughts and ideas of others.
- I understand that the University of the Witwatersrand may take disciplinary action against me if there is a belief that this is not my own unaided work or that I have failed to acknowledge the source of the ideas or words in my writing.

*Andrea Breytenbach*

Signature on the 3<sup>rd</sup> day of June 2024

## Table of Contents

Acknowledgments.....	7
List of Figures.....	8
List of Tables.....	9
List of symbols.....	9
List of abbreviations .....	11
Abstract.....	15
1 Introduction .....	16
1.1 Pancreatic cancer (PC) epidemiology .....	16
1.2 Molecular pathogenesis of PC .....	16
1.3 Current treatments options for PDAC.....	19
1.3.1 The molecular mechanisms of 5-FU and GEM.....	21
1.4 The chemoresistant characteristics of PDAC.....	23
1.5 Cellular cholesterol homeostasis.....	25
1.5.1 Metabolic reprogramming in PDAC.....	28
1.5.2 Targeting cholesterol for the treatment of PDAC .....	30
1.5.2.1 Statins.....	30
1.5.2.2 Cyclodextrins (CDs).....	31
1.6 EMT .....	33
1.6.1 Molecular mechanism of EMT .....	34
1.6.1.1 TGF- $\beta$ 1 .....	35
1.6.1.2 EMT-TFs .....	38
1.6.1.2.1 Zinc Finger protein SNAIL .....	38
1.6.1.2.2 TWIST bHLH family.....	39
1.6.1.2.3 ZEB family .....	39
1.6.1.2.4 PRRX1.....	40
1.6.2 EMT serves as a significant regulatory factor in drug resistance .....	40

1.6.3	The significance of cholesterol in EMT induction and regulation .....	41
1.7	Rationale for the current study .....	42
2	Aim and objectives .....	43
2.1	Aim.....	43
2.2	Objectives.....	43
3	Methodology.....	44
3.1	Cell culture of PANC-1 cells.....	45
3.2	Cell counting .....	45
3.3	Microscopy sample preparation .....	46
3.3.1	Immunocytochemistry .....	47
3.4	Growth curve using cell counts as a measure of proliferation .....	49
3.5	Cell viability assay .....	49
3.5.1	Cholesterol staining .....	50
3.5.1.1	Vybrant Alexa Fluor® Lipid Raft staining.....	50
3.5.1.2	BODIPY Staining.....	51
3.5.1.3	Filipin staining.....	52
3.6	MDR assay .....	52
3.7	Transwell® invasion assay.....	53
3.8	RNA extraction and purification .....	53
3.8.1	cDNA synthesis.....	55
3.9	Primer optimisation.....	56
3.9.1	PCR.....	56
3.10	RT-qPCR .....	58
3.11	Statistical analysis .....	60
4	Results .....	60
4.1	Analysing Changes in PANC-1 Cell Morphology Following TGF-β1 Treatment....	60
4.2	Confirming EMT induction using Vimentin and E-cadherin staining .....	61

4.3	Investigating the effect of TGF- $\beta$ 1-induced EMT on cell proliferation.....	63
4.4	Analysing the effect of TGF- $\beta$ 1-induced EMT on cell viability following treatment with cholesterol lowering drugs and chemotherapeutic agents.....	65
4.5	Delineating the link between TGF- $\beta$ 1-induced EMT and cholesterol in PANC-1 cells	67
4.6	Analysing the Effect of Targeting Cellular Cholesterol alone or in combination with chemotherapeutic agents on EMT.....	71
4.7	Analysing the drug resistant potential of PANC-1 cells post-EMT induction following treatment with cholesterol targeting agents and chemotherapeutic agents .....	74
4.8	Assessing the invasive potential of PANC-1 cells post-EMT induction following treatment with cholesterol targeting agents and chemotherapeutic agents .....	75
4.9	Molecular mechanism of EMT, cancer drug resistance, and cholesterol metabolism post-EMT induction following treatment with cholesterol targeting agents and chemotherapeutic agents. ....	76
5	Discussion.....	79
5.1	Alterations to Cellular Morphology and Resulting Implications following treatment with TGF- $\beta$ 1 .....	80
5.2	EMT induction alters cholesterol content, potentiates drug resistance, and promotes invasion. ....	84
5.2.1	The role of EMT in cholesterol homeostasis .....	84
5.2.2	The role of EMT in drug resistance .....	87
5.3	Targeting cholesterol content post-EMT induction promotes altered cholesterol homeostasis, increased drug resistance, invasion, and subsequently EMT.....	89
5.4	Combining cholesterol depletion with current chemotherapies 5-FU and GEM.....	94
5.4.1	Targeting cholesterol content in combination with 5-FU does not alter the EMT state or drug resistance, but does alter cholesterol homeostasis.....	94
5.4.2	Targeting cholesterol content in combination with GEM alters cholesterol homeostasis, potentiates EMT induction, chemoresistance, and invasion. ....	97
5.5	Conclusion.....	100

5.6	Limitations and future studies .....	103
6	Troubleshooting.....	104
6.1	EMT induction .....	104
6.2	MTT assay.....	104
6.3	MDR assay .....	104
6.4	Invasion Assay.....	105
6.5	RNA extraction.....	105
6.6	RT-qPCR .....	105
7	References .....	106
8	Appendix .....	136

## **Acknowledgments**

This research would not have been possible without the support and assistance of these people and institutions.

I would like to thank my supervisor Prof. Mandeep Kaur, for all her invaluable guidance, support, and encouragement throughout the course of this research. In Prof. Kaur's lab I have learned countless skills and I am truly grateful to be a part of her lab.

I would also like to thank my colleagues in GH519 for all their help and support. You all have offered me so much support, guidance, laughs, and memories I will never forget. More than anything you are all my friends and not just colleagues. I would like to extend my gratitude to the Pancreatic cancer team, I wouldn't have been able to do this without you.

A huge thank you to my family and friends for always encouraging and supporting me through this research. Thank you to my parents especially for always checking in and offering me words of wisdom, I am so grateful for you.

I would like to specially thank Matthew Woodhead, who has been the most special, encouraging, patient, and kind boyfriend. Without you I would not have made it through this and I am eternally grateful to have you in my life.

Finally, I would like to acknowledge the University of the Witwatersrand (Kirsch Foundation) for the financial assistance throughout this project. I am grateful for their financial support, which provided a great relief throughout this time. The research funding for this project through Self-Initiated Research Grant from South African Medical Research Council [SAMRC] is acknowledged.

## List of Figures

Figure 1.1: Progression and development of PDAC.....	18
Figure 1.2: Subtyping in PDAC.....	19
Figure 1.3: The molecular mechanism of GEM and 5-FU. ....	22
Figure 1.4: Mevalonate pathway.....	25
Figure 1.5: Cholesterol metabolism in PDAC .....	27
Figure 1.6: Transcriptional regulation of EMT induced by TGF- $\beta$ .....	36
Figure 1.7: Overview of the major signalling pathways involved in the EMT program in PDAC. .....	37
Figure 3.1: Summary workflow .....	44
Figure 4.1: Changes in morphology of PANC-1 cells after various TGF- $\beta$ 1 treatment times and concentrations. ....	61
Figure 4.2: Changes in vimentin fluorescence in PANC-1 cells after TGF- $\beta$ 1 treatment.....	62
Figure 4.3: Changes in E-cadherin fluorescence in PANC-1 cells after TGF- $\beta$ 1 treatment....	63
Figure 4.4: Growth curves using cell counts as a measure of proliferation of the PANC-1 cell line before and after TGF- $\beta$ 1 treatment. ....	64
Figure 4.5: Changes in Ki-67 fluorescence in PANC-1 cells after TGF- $\beta$ 1 treatment.....	65
Figure 4.6: Changes in percentage cell viability in PANC-1 cells both prior to TGF- $\beta$ 1-induced EMT and after, with combination treatments. ....	66
Figure 4.7: Changes in Vybrant Alexa Fluor® Lipid Raft staining fluorescence in PANC-1 cells as a result of TGF- $\beta$ 1-induced EMT and cholesterol-depleting agents.....	68
Figure 4.8: Changes in BODIPY staining fluorescence in PANC-1 cells as a result of TGF- $\beta$ 1- induced EMT and cholesterol-depleting agents.....	69
Figure 4.9: Changes in Filipin III staining fluorescence in PANC-1 cells as a result of TGF- $\beta$ 1- induced EMT and cholesterol-depleting agents.....	70
Figure 4.10: Changes in vimentin fluorescence in PANC-1 cells as a result of TGF- $\beta$ 1-induced EMT and combination treatments.....	72
Figure 4.11: Changes in E-cadherin fluorescence in PANC-1 cells as a result of TGF- $\beta$ 1- induced EMT and combination treatments. ....	73
Figure 4.12: Changes in MDR in PANC-1 cells after TGF- $\beta$ 1-induced EMT and combination treatments.....	74
Figure 4.13: Changes in invasive potential of PANC-1 cells after TGF- $\beta$ 1-induced EMT and combination treatments.....	76

Figure 4.14: Changes in drug-resistance, cholesterol homeostasis, and EMT genes after TGF- $\beta$ 1-induced EMT and combination treatments.....	78
Figure 5.1: A summary of the main findings of the research .....	102

## List of Tables

Table 3.1: Drug treatments and their concentrations used throughout experimentation. ....	47
Table 3.2: The primary and secondary antibodies used for target protein during immunocytochemistry.....	48
Table 3.3: Components of cDNA synthesis reaction.....	55
Table 3.4: Components of PCR reaction .....	56
Table 3.5: Cycling conditions for PCR.....	57
Table 3.6: Optimised annealing temperatures of genes of interest alongside their forward and reverse sequences.....	57
Table 3.7: Components of Luna® Universal qPCR reaction .....	59
Table 3.8: Two-step cycling conditions for RT-qPCR using the QuantStudio™ 5 Real-Time PCR System .....	59
Table 4.1: The standard deviation and significance of the log <sub>2</sub> (fold change) RT-qPCR gene expression data where *p < .05, **p < .01, ***p < .001, ****p < .0001, and ns = non-significant indicates a significant or non-significant difference to the untreated control.....	79

## List of symbols

$\alpha$	alpha
$\beta$	beta
©	copyright
°C	celsius
$\kappa$	kappa
$\mu$	micro
$\mu\text{L}$	microlitres
$\mu\text{M}$	micromolar
mM	milimolar

ng nanogram  
® registered  
™ trademark

## List of abbreviations

5-Fluorouracil	5-FU
ATP-binding cassette	ABC
Acyl-CoA: Cholesterol Acyltransferase	ACAT
Acetoacetyl-Coenzyme A	acetoacetyl-CoA
Aberrantly Differentiated Endocrine Exocrine	ADEX
acinar-to-ductal metaplasia	ADM
Anaplastic Lymphoma Kinase	ALK
Apolipoprotein A-I	apoA-I
Ataxia-Telangiectasia Mutated	ATM
Axis Inhibition Protein	AXIN
Basic Helix-Loop-Helix	bHLH
Breast Cancer 1/2	BRCA1/2
Caveolin-1	Cav-1
Cyclodextrin	CD
Cytidine Deaminase	CDA
Cyclin dependent kinase	CDK
Cyclin-Dependent Kinase Inhibitor	CDKN
Cholesteryl Ester	CE
Cholesteryl Ester Transfer Protein	CETP
Concentrative Nucleoside Transporters	CNT
Cancer Stem Cell	CSC
C-terminal-binding protein	CtBP
Deoxycytidine Kinase	DCK
2 2-Difluorodeoxycytidine	dFdC
dFdC Diphosphate	dFdCDP
dFdC Monophosphate	dFdCMP
dFdC Triphosphate	dFdCTP
2 2-Difluorodeoxyuridine Monophosphate	dFdUMP
Deoxyribonucleic Acid	DNA
Dihydropyrimidine dehydrogenase	DPD
Death Receptor	DR
Deoxythymidine Monophosphate	dTMP
Deoxythymidine Triphosphate	dTTP
Deoxyuridine Monophosphate	dUMP
Deoxyuridine Triphosphate	dUTP
Eastern Cooperative Oncology Group Performance Status	ECOG PS
Epidermal Growth Factor	EGF
Epidermal Growth Factor Receptor	EGFR
Epithelial To Mesenchymal Transition	EMT
Endoplasmic Reticulum	ER
Extracellular Signal-Regulated Kinase	ERK
16-Fluorodeoxyuridine Diphosphate	FdUDP

Fluorodeoxyuridine Monophosphate	FdUMP
Fluorodeoxyuridine Triphosphate	FdUTP
Fibroblast Growth Factor	FGF
Fluorouridine Diphosphate	FUDP
Fluorodeoxyuridine	FUDR
Fluorouridine Monophosphate	FUMP
Fluorouridine	FUR
Fluorouridine Triphosphate	FUTP
Gemcitabine	GEM
Glycogen Synthase Kinase 3 Protein	GSK3
HDL receptor	HDLR
High-density Lipoprotein	HDL
Human Equilibrative Nucleoside Transporters	hENT
hepatocyte growth factor	HGF
Hedgehog	Hh
Hypoxia-Inducible Factor 1 A	HIF1 $\alpha$
3-hydroxy-3-methyl-glutaryl CoA	HMG-CoA
HMG-CoA reductase	HMGCR
organic anionic transporter 2	hOAT2
2-Hydroxypropyl- $\beta$ -Cyclodextrin	HP $\beta$ CD
Hormone-Sensitive Lipase	HSL
I $\kappa$ B kinase	IKK
Interleukin-1/6	IL-1/6
Intraductal Papillary Mucinous Neoplasm	IPMN
Janus Kinase	JAK
Jun N-terminal kinase	JNK
Kirsten Rat Sarcoma Viral Oncogene Homolog	KRAS
lecithin-cholesterol acyltransferase	LCAT
Low-density lipoprotein	LDL
low-density lipoprotein receptor	LDLR
lymphoid enhancer-binding factor	LEF
Lin11, Isl-1 and Mec-3 kinase	LIMK
Liver X Receptor	LXR
Mitogen-Activated Protein Kinase	MAPK
Mucinous Cystic Neoplasm	MCN
Multi-drug resistance	MDR
Mitogen-Activated Protein Kinase	MEK
Mesenchymal to Epithelial Transition	MET
Matrix Metalloproteinase	MMP
Mechanistic Target of Rapamycin	mTOR
Mechanistic Target of Rapamycin Complex 1	mTORC1
4,5-Dimethylthiazol-2-yl)-2,5-Diphenyltetrazolium Bromide	MTT
Methyl- $\beta$ -Cyclodextrin	M $\beta$ CD

Nuclear Factor Kappa-Light-Chain-Enhancer of Activated B Cells	NF-κB
Nogo-B Receptor	NgBR
NAD dependent steroid dehydrogenase-like	Nsdhl
Neurotrophic Tyrosine Receptor Kinase	NTRK
Orotate Phosphoribosyltransferase	OPRT
Partner And Localizer Of BRCA	PALB
Pancreatic Intraepithelial Neoplasia	PanIN
Poly-Adp Ribose Polymerase	PARP
Pancreatic Cancer	PC
Polymerase Chain Reaction	PCR
Proprotein Convertase Subtilisin/Kexin	PCSK9
Anti-Programmed Cell Death	PD
Pancreatic Ductal Adenocarcinoma	PDAC
Platelet-Derived Growth Factor	PDGF
Phosphatidyl Inositol 3-Kinase	PI3K
Phosphoribosyl Pyrophosphate	PRPP
Paired Related Homeobox 1	PRRX1
Patched1	PTCH1
Phosphatase and Tensin Homolog	PTEN
Ras like A/B	Ral A/B
Ras homolog family member A	RhoA
Ribonucleic Acid	RNA
Rho-Associated Coiled-Coil-Containing Protein Kinase	ROCK
Ribonucleotide Reductase Regulatory Subunit M1/2	RRM1/2
Real Time-Quantitative PCR	RT-qPCR
retinoid X receptors	RXR
SREBP-Cleavage Activating Protein	SCAP
Mothers Against Decapentaplegic Homolog 4	SMAD
Smoothened	SMO
Sry-Box Transcription Factor 2	SOX2
Scavenger Receptor B1	SR-B1
Sterol Regulatory Element	SRE
Sterol Regulatory Element-Binding Protein	SREBP
Signal Transducers and Activators of Transcription	STAT
TGF-β Activated Kinase 1	TAK1
T-Cell Factor	TCF
Transforming Growth Factor- B	TGF-β
Tumour Microenvironment	TME
Tumour Necrosis Factor α	TNFα
Tumour Protein 53	TP53
Tumour Necrosis Factor Receptor Associated Factor 6	TRAF6
Tumour Necrosis Factor-Related Apoptosis-Inducing Ligand	TRAIL
Tropomyosin Receptor Kinase	TRK

Thymidylate Synthase	TS
Uridine Kinase	UK
Uridine Phosphorylase	UP
Wingless-Related Integration Site	Wnt
Zinc-Finger E-box Binding Homeobox	ZEB

## Abstract

Pancreatic ductal adenocarcinoma (PDAC) is a highly metastatic cancer that relies on the epithelial to mesenchymal transition (EMT) program for its spread. EMT is a cell plasticity program that involves the reorganization of cell structure as cells transition from an epithelial to a mesenchymal phenotype. The dysregulated cholesterol metabolism resulting from metabolic reprogramming in PDAC is thought to play a role in EMT by affecting EMT-related signalling pathways. However, no publication has yet investigated the impact of EMT on cholesterol content in PDAC. To shed light on these dynamics, EMT was induced in PANC-1 cells using TGF- $\beta$ 1, thereafter the effect of cholesterol-depleting agents (KS-01 and methyl- $\beta$ -cyclodextrin) alone or in combination with chemotherapeutic agents (Gemcitabine (GEM) and 5-Fluorouracil (5-FU)) on cholesterol content, EMT state, drug resistance, and invasion were investigated. Our results showed that mesenchymal cells rely on reduced membrane cholesterol levels, synthesis, and uptake, while storing more cholesterol and promoting efflux. EMT also promoted drug resistance via upregulation of *ABCB1* expression and reduced *hENTI* expression. Targeting cholesterol using cyclodextrins promoted a cholesterol compensatory mechanism, leading to a hybrid EMT state, drug resistance, and metastatic potential. Treating mesenchymal PANC-1 cells with GEM or 5-FU monotherapies were seen to promote EMT-transcription factors, as well as promote cholesterol efflux, synthesis, and import, an unexpected result as these chemotherapeutic agents are not known to affect cholesterol. When GEM was combined with KS-01, drug resistance, invasion, EMT-transcription factors, vimentin, and E-cadherin was promoted indicating the promotion of a hybrid EMT state. Interestingly however, combining KS-01 with 5-FU resulted in an interplay that was seen to mitigate the EMT-promoting effects typically associated with cholesterol depletion alone. The exact mechanism linking the cholesterol compensatory mechanism to EMT remains complex and unknown. Based on work presented in this dissertation, it is proposed that targeting cellular cholesterol should be continued to be investigated, particularly in understanding the repercussions of the use of cholesterol depleting agents for the treatment of other disorders in patients with PDAC.

## **1 Introduction**

### **1.1 Pancreatic cancer (PC) epidemiology**

Cancer remains a widespread global health issue, despite the existence of various modern approaches for its treatment. In the year 2020 alone, there were more than 19 million new cases and 10 million fatalities reported worldwide (Globocan, 2020d). Projections indicate that the global cancer burden is expected to increase by 47% in 2040 compared to 2020, with an anticipated 28.4 million cases (Sung *et al.*, 2021). PC ranks as the 13<sup>th</sup> most common in the world and South Africa and the 7<sup>th</sup> and 8<sup>th</sup> leading cause of cancer-related deaths in the world and South Africa, respectively (Globocan, 2020b, 2020c). Despite its lower overall prevalence, it is known to be one of the most lethal types of cancer with an exceedingly high incidence to mortality ratio of 495 773 incidences to 466 003 deaths (Globocan, 2020a). PC has no method for early detection and early symptoms of the disease are extremely non-specific, resulting a late-stage diagnosis of the disease in over 85% of patients (Smeenk *et al.*, 2005) making surgical resection impossible. PC has other difficulties, such as becoming metastatic early in tumorigenesis, even before the development of the entire tumour (Rhim *et al.*, 2012). Consequently, this highlights the critical need of discovering novel chemotherapeutic treatments in the aid of improving existing treatments and improving survival outcomes.

### **1.2 Molecular pathogenesis of PC**

Cancer can be characterised as the transformation from normal to abnormal cells, regulated by a set of fundamental processes. These include the activation of oncogenes, altered cell metabolism, inactivation of tumour suppressor genes, evasion from the immune system, resistance to apoptosis, and metastasis (Fouad and Aanei, 2017). PC can be broadly categorised into two main groups: exocrine PC and endocrine PC. Endocrine tumours arise from pancreatic endocrine cells and typically exhibit slower growth compared to exocrine tumours, which arise from exocrine cells (Jain *et al.*, 2019). Accounting for most PC cases is exocrine PC with 90-98% of cases (Xiao *et al.*, 2019) and within this group, pancreatic ductal adenocarcinoma (PDAC) stands out as the most prevalent subtype, accounting for 95% of cases (Xiao *et al.*, 2019). PDAC is a disease of multiple genetic alterations that drive the non-invasive precursor lesions, such as pancreatic intraepithelial neoplasias (PanINs), mucinous cystic neoplasms (MCNs), and intraductal papillary mucinous neoplasms (IPMNs) towards PDAC (Maitra *et al.*, 2005; Rustgi, 2006; Maitra and Hruban, 2008; Yonezawa *et al.*, 2008). PanINs are the most critical and well understood precursor lesions and are classified into three grades: PanIN-1A/B, PanIN-2, and PanIN-3 (Hruban *et al.*, 2001). The progression of each grade is predominantly

driven by specific key genetic mutations involving Kirsten rat sarcoma viral oncogene homolog (KRAS), cyclin-dependent kinase inhibitor 2A (CDKN2A), tumour protein 53 (TP53), and Mothers against decapentaplegic homolog 4 (SMAD4) as seen in Figure 1.1 (Maitra and Hruban, 2008; Biankin *et al.*, 2012; Waddell *et al.*, 2015). The most common mutation occurs in codons 12 and 13 of exon 2 of KRAS, affecting approximately 95% of PDACs (Almoguera *et al.*, 1988; Yonezawa *et al.*, 2008; Waddell *et al.*, 2015; Mizrahi *et al.*, 2020). It is responsible for the initiation of progression towards PDAC, and its constitutive activation results in the promotion of the Ras/Raf/mitogen-activated protein kinase (MEK)/extracellular signal-regulated kinase (ERK) pathway, the phosphatidylinositol 3-kinase (PI3K)/Akt/mechanistic target of rapamycin (mTOR) pathway, the Ras like A/B (RalA/B) pathway and the nuclear factor kappa-light-chain-enhancer of activated B cells (NF- $\kappa$ B) pathway, promoting proliferation, enhanced survival, and motility capabilities (Mann *et al.*, 2016; Mizrahi *et al.*, 2020). The mutation of KRAS is subsequently followed by the loss of tumour suppressor gene, CDKN2A, in PanIN2, which occurs in approximately 35% of all PDAC tumours (Jones *et al.*, 2008; Waddell *et al.*, 2015). This loss inhibits the function of p16 facilitating malignant progression and differentiation by preventing the regulation of G1/S phase transition and promoting uncontrolled cell division (Jones *et al.*, 2008). This is lastly followed by the loss of tumour suppressors TP53 and SMAD4 in PanIN3 and invasive tumours, which occurs in approximately 31% and 74% of all tumours, respectively (Waddell *et al.*, 2015). Mutated TP53 gains the ability to remodel the tumour microenvironment (TME), as well as enhance cell metabolism and loses the ability to regulate cell division, apoptosis, and deoxyribonucleic acid (DNA) repair (Jones *et al.*, 2008; Mantovani *et al.*, 2019). Mutated SMAD4, which is primarily found in high-grade precursor lesions, as well as in PDAC, alters the transforming growth factor- $\beta$  (TGF- $\beta$ ) signalling pathway, blocking downstream pathways from regulating proliferation, differentiation, cell division, apoptosis, and DNA repair (Massagué *et al.*, 2000). Additional secondary mutations responsible for PDAC progression include breast cancer 1/2 (BRCA1/2), ataxia-telangiectasia mutated (ATM), partner and localizer of BRCA2 (PALB2), and BRAF (Hu *et al.*, 2021).

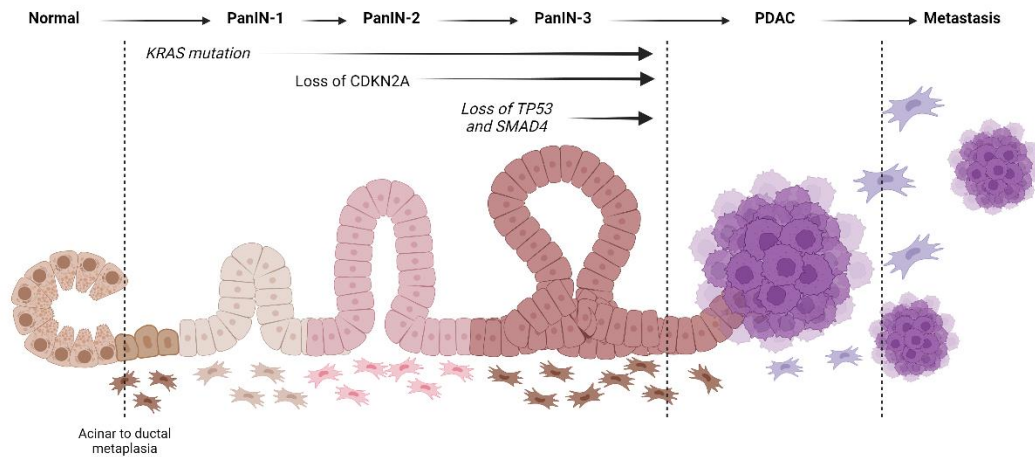


**Figure 1.1: Progression and development of PDAC.**

*Initially, acinar cells within a healthy pancreatic duct undergo transformation into ductal epithelial cells, marking the beginning of the progression through PanIN stages 1–3. Subsequently, these cells can advance into PDAC following pivotal oncogenic genetic mutations, including KRAS activation and the loss of CDKN2A/TP53/SMAD4 (Maitra and Hruban, 2008; Biankin et al., 2012; Waddell et al., 2015). (Created in BioRender.com)*

From a broader perspective, there have been eleven genetically altered key regulatory pathways implicated in PDAC (Van Heek *et al.*, 2002; Jones *et al.*, 2008; Matsuda *et al.*, 2015). There is hence an intricate interplay of genetic alterations that contribute to the complex molecular pathogenesis of PDAC. Unlike many other types of cancer, the classification of PDAC into standardised and distinct molecular subtypes is a relatively nascent field. Instead, several studies (Moffitt *et al.*, 2015; Bailey *et al.*, 2016; Puleo *et al.*, 2018; Collisson *et al.*, 2019) have introduced various terminologies and subtypes some of which show similarities or shared characteristics as seen in Figure 1.2. The absence of distinct subtyping in PDAC contributes to its treatment complexity, posing challenges in devising targeted therapeutic approaches.

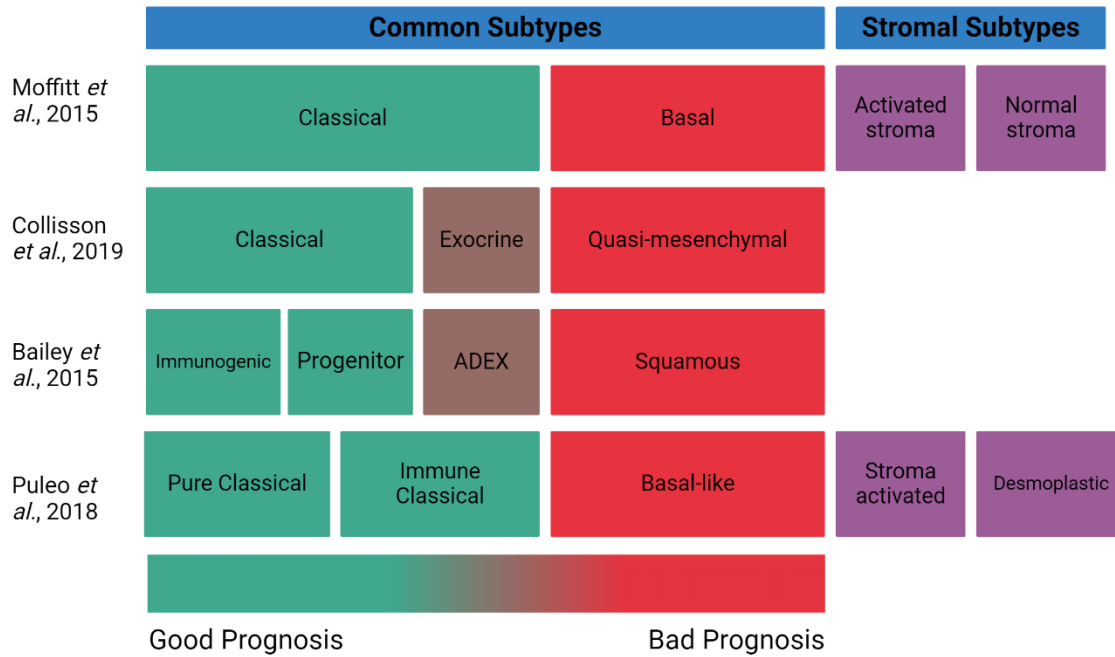


**Figure 1.2: Subtyping in PDAC.**

*The subtyping of PDAC has undergone significant evolution over the years, beginning with Collisson et al. in 2011, who delineated three transcriptional subtypes: Classical, Exocrine-like, and Quasi-mesenchymal (Collisson et al., 2019). These subtypes exhibited distinct molecular profiles and clinical behaviors. Moffitt et al. expanded this classification in 2015, defining four subtypes: Basal-like, Classical, Activated, and Normal, further elucidating the tumor and stromal subtypes (Moffitt et al., 2015). Bailey et al. added to this in 2016, introducing four gene expression subtypes: Squamous, Pancreatic Progenitor, Aberrantly Differentiated Endocrine Exocrine (ADEX), and Immunogenic, overlapping with previous classifications. The Immunogenic subtype, characterized by immune cell infiltration, and the Pancreatic Progenitor subtype, marked by specific transcriptional networks, demonstrated notable distinctions (Bailey et al., 2016). Additionally, Basal-like, Squamous, and Quasi-mesenchymal-PDAC subtypes shared similarities associated with poor prognosis and mutations in genes involved in DNA acetylation and methylation. Conversely, Progenitor and Classical subtypes exhibited better survival and susceptibility to specific treatments (Moffitt et al., 2015; Bailey et al., 2016; Collisson et al., 2019). Puleo et al. in 2018 introduced Pure Classical and Immune Classical subtypes, derived from the Classical subtype, along with Stroma Activated and Desmoplastic subtypes related to the stromal component (Puleo et al., 2018). However, the classification of these subtypes remains subject to debate, highlighting the need for further research to establish a refined classification system to guide treatment decisions effectively in PDAC. (Created in BioRender.com)*

### 1.3 Current treatments options for PDAC

The currently available treatments for PDAC are surgery, radiation therapy, chemotherapy, targeted therapy, and immunotherapy, with surgery combined with perioperative chemotherapy being the most successful in extending the long-term survival of PDAC patients.

However, this success only increases the 5-year survival from 10% to 25% and surgery can only be performed in 10-15% of all patients due to metastasis (Bilimoria *et al.*, 2007; Principe *et al.*, 2021). This dismal survival rate is a direct result of a lack of early symptoms and no effective screening strategies. When the tumour is resectable, there is an immediate resection followed by 6 months of adjuvant chemotherapy such as FOLFIRINOX (5-Fluorouracil (5-FU), leucovorin, oxaliplatin, and irinotecan), Gemcitabine (GEM) and capecitabine, or GEM and nab-paclitaxel. However, in borderline resectable PDAC, there is no set standard-of-care treatment (Jiang and Sohal, 2023). The most employed treatment for non-resectable PDAC typically involves the administration of chemotherapy regimens, such as the combination of GEM with Nab-Paclitaxel or FOLFIRINOX alone (Sohal *et al.*, 2016).

The selection of the initial treatment approach is guided by the Eastern Cooperative Oncology Group Performance Status (ECOG PS) criteria, as established by Oken *et al.* in 1982 (Oken *et al.*, 1982). The scale ranges from 0-5, with lower scores indicating a better functional status and higher scores indicating a poorer functional status of the patient, with GEM and FOLFIRINOX as the most common first line therapy (Sohal *et al.*, 2016). More recently, nanoliposomal irinotecan or a combination of oxaliplatin with 5-FU have gained approval for use as second-line treatments following initial GEM therapy (Sohal *et al.*, 2016). Moreover, a 5-FU based therapy is more commonly used in patients who previously received GEM-based regimens. (Wainberg *et al.*, 2020). Additionally, GEM remains a second-line therapy option for patients with an ECOG PS of 2 (Sohal *et al.*, 2016). In cases where high microsatellite instability and mismatch repair deficiency are present, targeted treatments like pembrolizumab, an anti-programmed cell death-1 (PD-1) antibody is administered (Marabelle *et al.*, 2020; Hosein *et al.*, 2022; Fang *et al.*, 2023). Furthermore, patients with PALB2-mutated or BRCA1/2-mutated PDAC can explore a combination of poly-ADP ribose polymerase (PARP) inhibitors with cisplatin and GEM (O'Reilly *et al.*, 2020; Hosein *et al.*, 2022). For patients with specific gene fusions, including anaplastic lymphoma kinase (ALK), (ROS1, and neurotrophic tyrosine receptor kinase (NTRK) 1–3, targeted treatments like the ROS1 inhibitor entrectinib and the selective tropomyosin receptor kinase (TRK) inhibitor larotrectinib are available (Drilon *et al.*, 2017; Hosein *et al.*, 2022; Fang *et al.*, 2023).

It is important to note that despite the array of available chemotherapeutic options for PDAC, many of them exhibit limited efficacy, offering only marginal extensions in patient survival. Notably, among these treatments, first line GEM treatment followed by a 5-FU based second-

line treatment stands out as one of the most widely utilised approaches for managing PDAC due to their clinical experience and effectiveness.

### **1.3.1 The molecular mechanisms of 5-FU and GEM**

GEM and 5-FU both use human concentrative nucleoside transporters (hCNT) proteins and human equilibrative nucleoside transporters (hENT) proteins to enter the cell. GEM primarily utilises hCNT1, hCNT3, and notably hENT1 (Principe *et al.*, 2021). On the other hand, 5-FU utilises hENT1 and hENT2, with some reports suggesting that organic anionic transporter 2 (hOAT2) is also involved (Kobayashi *et al.*, 2005; Mafi *et al.*, 2023).

5-FU is a uracil analogue with a fluorine atom at the C-5 position, replacing a hydrogen atom. The mechanism of action of 5-FU involves its transformation into active metabolites within the cell, leading to disruption of nucleic acid synthesis and DNA damage (Longley *et al.*, 2003). As depicted in Figure 1.3, 5-FU enters the cell in a similar manner to uracil. Once inside, it undergoes conversion into active metabolites, namely fluorouridine triphosphate (FUTP), fluorodeoxyuridine triphosphate (FdUTP), and fluorodeoxyuridine monophosphate (FdUMP). These metabolites interfere with ribonucleic acid (RNA) synthesis and inhibit thymidylate synthase, leading to DNA damage (Longley *et al.*, 2003) (Figure 1.3).

GEM, also known as 2,2-difluorodeoxycytidine (dFdC), shares a structural similarity with deoxycytidine but differs by having two fluoride molecules at the 2' position. As seen in Figure 1.3 once inside the cell, GEM undergoes phosphorylation through the action of deoxycytidine kinase (DCK), leading to the formation of dFdC monophosphate (dFdCMP) (Principe *et al.*, 2021). Subsequently, phosphorylation or deamination converts dFdCMP into dFdC diphosphate (dFdCDP) or 2,2-difluorodeoxyuridine monophosphate (dFdUMP), respectively (Principe *et al.*, 2021). dFdCDP impairs the function of ribonucleotide reductase regulatory subunit (RRM1/2), disrupting DNA synthesis and hindering cell proliferation. Alternatively, dFdCDP can undergo further phosphorylation to become dFdC triphosphate (dFdCTP) preventing DNA repair and synthesis, and inhibiting DNA polymerases by integrating itself into the genome (Principe *et al.*, 2021). Additionally, dFdUMP functions to inhibit thymidylate synthase (TS), leading to increased DNA damage and disruption of DNA synthesis as described previously. In summary, the distinct mechanisms of action for 5-FU and GEM underscore their efficacy as chemotherapeutic agents, disrupting crucial pathways in nucleic acid synthesis and

DNA damage, ultimately inhibiting the proliferation of cancer cells. However, it is important to note that despite their efficacy, PDAC often exhibits resistance to these chemotherapies.

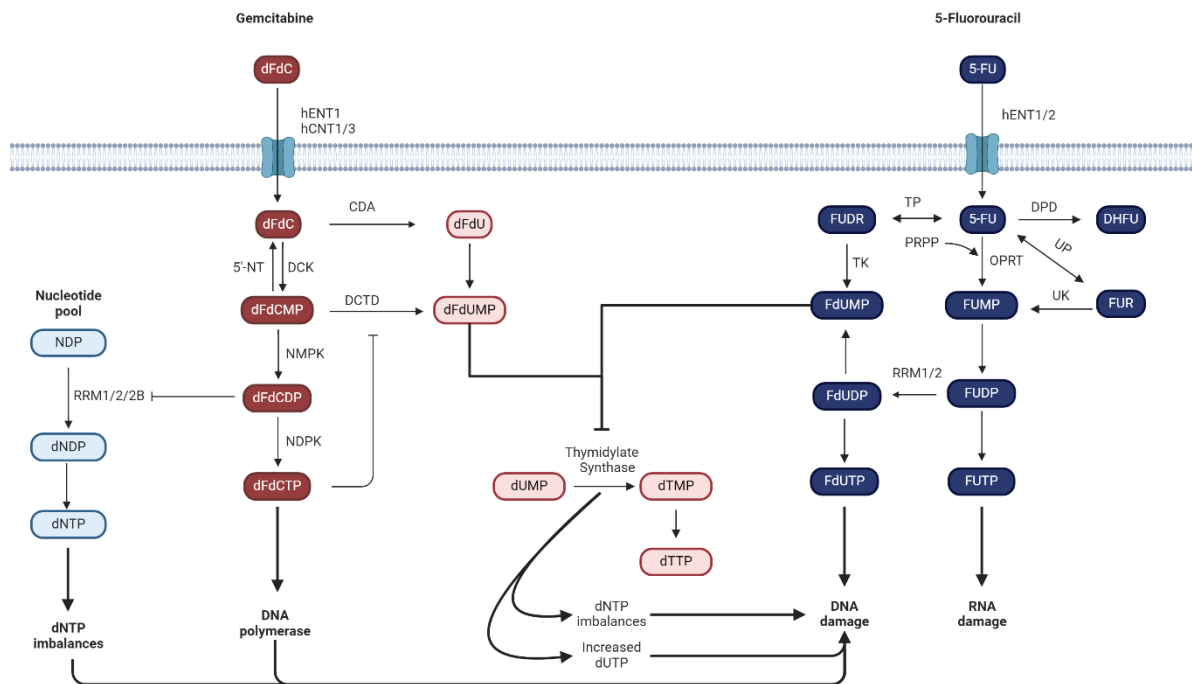


**Figure 1.3: The molecular mechanism and action of GEM and 5-FU.**

The activation pathway involves conversion of 5-FU to fluorouridine monophosphate (FUMP) via orotate phosphoribosyltransferase (OPRT) in the presence of the cofactor phosphoribosyl pyrophosphate (PRPP) or indirectly through fluorouridine (FUR) involving uridine kinase (UK) and uridine phosphorylase (UP). Further phosphorylation leads to the formation of fluorouridine diphosphate (FUDP), which can be converted to FdUDP by RRM1/2 or phosphorylated to FUTP (Longley et al., 2003). FUTP is incorporated into RNA, disrupting normal RNA processing and function. 16-Fluorodeoxyuridine Diphosphate (FdUDP) can be phosphorylated to FdUTP or dephosphorylated to FdUMP where FdUTP results in DNA damage. Another pathway involves the conversion of 5-FU to fluorodeoxyuridine (FUDR) through thymidine phosphorylase (TP), followed by phosphorylation by thymidine kinase (TK) to form FdUMP. FdUMP inhibits TS, leading to decreased deoxythymidine monophosphate (dTMP) synthesis from deoxyuridine monophosphate (dUMP) and subsequent decrease in deoxythymidine triphosphate (dTTP) (Longley et al., 2003). This results in an imbalance in the deoxynucleotide pool and decreased levels of deoxyuridine triphosphate (dUTP), hindering DNA synthesis and repair. 5-FU can also be converted to its inactive form 5,6-dihydro-5-fluorouracil (DHFU) by the enzyme dihydropyrimidine dehydrogenase (DPD) (Longley et al., 2003). GEM undergoes phosphorylation by DCK to form dFdCMP, which is further phosphorylated to dFdCDP or deaminated to dFdUMP. dFdCDP impairs RRM1/2 disrupting the formation Deoxynucleoside diphosphates (dNDPs) from nucleoside diphosphates (NDPs), subsequently decreasing levels of Deoxynucleoside triphosphates (dNTPs) thereby preventing DNA synthesis and inhibiting cell proliferation (Principe et al., 2021). dFdCDP can also be phosphorylated to form dFdCT, preventing DNA repair and synthesis and inhibiting DNA polymerases by integrating itself into the genome. Additionally, dFdUMP inhibits TS, leading

*to increased DNA damage and disruption of DNA synthesis, ultimately contributing to cell death in PDAC (Principe et al., 2021). (Created in BioRender.com)*

#### **1.4 The chemoresistant characteristics of PDAC**

PDAC exhibits inherent resistance (referred to as *de novo* resistance) to chemotherapeutic agents such as GEM or 5-FU, or they acquire resistance to these chemotherapy agents, contributing significantly to the treatment failure and poor prognosis seen in PDAC. Drug resistance in PDAC is a multifaceted phenomenon influenced by various cellular mechanisms, the first being transport mechanisms. Looking at cell entry proteins, GEM resistance has been associated with the loss of hENT1 and hCNT1, resulting in a partial uptake of GEM. Conversely, higher levels of hENT1 have been found to correlate with a better prognosis and improved overall survival for both GEM and 5-FU treated patients (Elander *et al.*, 2018; Principe *et al.*, 2021). Contradictory to these findings, several PC cell lines were found to be less sensitive to GEM and 5-FU when hENT1 mRNA levels were high (Tsujiie *et al.*, 2007). Drug resistance in PDAC is also facilitated by members of the ATP binding cassette (ABC) transporter family, which function as drug efflux pumps to confer multidrug resistant (MDR) phenotype through regulation of the transport of chemotherapeutics across the cell membrane. A number of ABC subfamily transporters (ABCB1/MDR1, ABCC1, and ABCG2) are upregulated in PDAC, promoting drug efflux for both GEM and 5-FU (Chen *et al.*, 2012). Similarly, ABCC3, ABCC4, and ABCC5 are also responsible for 5-FU efflux (Hagmann *et al.*, 2009; Li *et al.*, 2011).

Another mechanism of drug resistance in PDAC involves the alteration of the drug metabolism pathway. GEM resistance is characterised by low levels of DCK, the rate limiting step of GEM activation (Saiki *et al.*, 2012), as well as high levels of cytidine deaminase (CDA), the enzyme responsible for metabolising the active form of GEM (dFdC) to its inactive form (dFdU), after cellular uptake (Figure 1.3). This suggests that excessive conversion of the drug to its inactive form may limit the availability of the drug for activation (Bjånes *et al.*, 2020). High levels of RRM1/2 and TS are also implicated in GEM resistance, where high RRM1 and RRM2 levels are predicted to promote DNA repair and hence promote resistance (C. Wang *et al.*, 2015). Notably, inhibition of TS has been shown to activate hENT1, and its overexpression may contribute to the reduction of hENT1 expression (Komori *et al.*, 2011). Similar to GEM resistance, resistance to 5-FU is characterised by an upregulation of TS (Zhang *et al.*, 2011). Studies have shown that low intra-tumoural levels of TS, followed by adjuvant chemotherapy with 5-FU, result in higher median survival compared to high TS expression (Van Der Zee *et*

*al.*, 2012). Additionally, high levels of DPD, the initial and rate-limiting enzyme in the catabolism of 5-FU, contributes to increased resistance to 5-FU (Kurata *et al.*, 2011). However, when DPD levels are too low, it can lead to fatal toxicity from 5-FU (Fidai *et al.*, 2018).

GEM and 5-FU resistance also encompasses a range of cell survival pathways, including epidermal growth factor receptor (EGFR)/mitogen-activated protein kinase (MAPK)/ERK, NF- $\kappa$ B, Wnt/ $\beta$ -catenin, PI3K/Akt/mTOR and Raf/MEK/ERK pathways. Notably, the last two pathways are primarily activated by mutant KRAS signalling (Zheng *et al.*, 2013; Mollinedo and Gajate, 2019; Mehra *et al.*, 2021; Principe *et al.*, 2021). These pathways play a crucial role in promoting proliferation and survival while inhibiting drug-induced apoptosis. Specifically, NF- $\kappa$ B and Wnt/ $\beta$ -catenin activation inhibits apoptosis (Griesmann *et al.*, 2013; Makena *et al.*, 2019; Principe *et al.*, 2021). GEM resistance is also attributed to the Hedgehog (Hh), hypoxia-inducible factor 1  $\alpha$  (HIF1 $\alpha$ ), GLI, and SRY-Box TF 2 (SOX2) pathways, while 5-FU resistance involves signal transducer and activator of transcription 3 (STAT3) and Nogo-B receptor (NgBR) pathways. Interestingly HIF1 $\alpha$  not only promotes chemoresistance through survival, proliferation, and apoptosis inhibition but also facilitates drug efflux via ABCG2 (He *et al.*, 2016). In GEM resistant PDAC, there is also an upregulation of the glycolysis, pentose phosphate, fatty acid synthesis, and purine/pyrimidine synthesis pathways (Principe *et al.*, 2021). Furthermore, both GEM and 5-FU resistance are associated with pathways related to the extracellular matrix, cell–cell adhesion, and cell junction assembly (B. Zhao *et al.*, 2022).

Two additional significant factors that contribute to drug resistance are the TME and cancer stem cells (CSCs). The TME, which consists of a dense extracellular matrix-rich stroma, acts as a physical barrier, preventing efficient drug delivery. Furthermore, the TME provides a favourable niche environment for the survival and growth of CSCs (X. Zhao *et al.*, 2022). CSCs are a subpopulation of cells within a tumour capable of self-renewal, differentiation and tumourigenicity, and they exhibit distinctive drug-resistant characteristics. These cells are quiescent, undergo metabolic reprogramming, and possess highly active DNA repair mechanisms that confer chemoresistance (Mathews *et al.*, 2011). Interestingly, CSCs exhibit increased activity of ABC transporters, which contribute to their ability to evade the effects of 5-FU and GEM (Cho *et al.*, 2017; Gzil *et al.*, 2019; Kuo *et al.*, 2023). In particular, in the context of GEM treatment, only CSCs expressing high levels of CD44 will become even more stem-like after continuous exposure to GEM (Zhang *et al.*, 2016; Zhao *et al.*, 2019). These findings underscore the intricate interplay among genetic mutations, signalling pathways, the TME, and CSCs in the development of resistance to GEM and 5-FU in PDAC. However, the

explanation does not conclude here, as two significant mechanisms, cholesterol homeostasis and epithelial to mesenchymal transition (EMT) remain unmentioned. These mechanisms will be comprehensively explored in subsequent sections.

### 1.5 Cellular cholesterol homeostasis

Cholesterol is a structural component of cell membranes and a precursor for synthesising steroid hormones, vitamin D, and bile acids. Cholesterol does not only provide stability and fluidity to the cell membrane but also regulates cell function, playing a crucial role in maintaining cellular homeostasis (Silva Afonso *et al.*, 2018). It is a key component of plasma membranes and dynamic lipid rafts, which facilitate the interaction between signalling molecules and membrane proteins, essential for intracellular signal transduction (Ikonen, 2008). Cholesterol is synthesised via the mevalonate pathway (Cerqueira *et al.*, 2016) and is summarised in Figure 1.4.

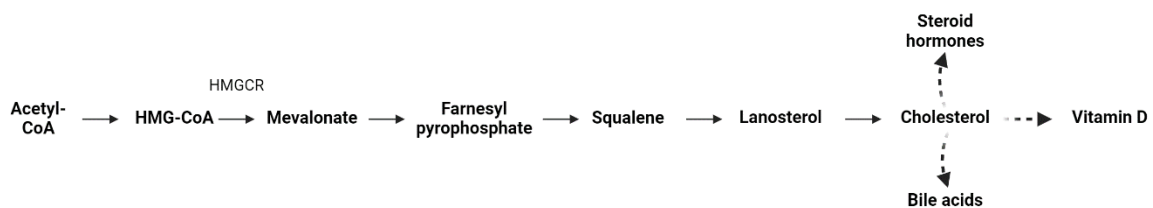


**Figure 1.4: Mevalonate pathway.**

*The mevalonate pathway is a key metabolic pathway responsible for the biosynthesis of essential biomolecules, including cholesterol, steroid hormones, and isoprenoids. This pathway begins with the conversion of acetyl-CoA to 3-hydroxy-3-methylglutaryl-CoA (HMG-CoA) through the action of HMG-CoA synthase (Cerqueira *et al.*, 2016). Subsequently, HMG-CoA is reduced to mevalonate by HMG-CoA reductase (HMGCR), a rate-limiting enzyme in the pathway (Cerqueira *et al.*, 2016). Mevalonate is next converted to the activated isoprenoids isopentenyl pyrophosphate and dimethylallyl pyrophosphate (not shown), from which farnesyl pyrophosphate originates. This is then subsequently converted to squalene, lanosterol, and lastly cholesterol is formed (Cerqueira *et al.*, 2016). (Created in BioRender.com)*

The regulation of intracellular cholesterol levels is tightly controlled through liver X receptor (LXR), which controls cholesterol uptake and sterol regulatory element-binding protein (SREBP) which controls uptake and synthesis, with SREBP2 being particularly notable as a key regulator of cholesterol biosynthesis (Gu *et al.*, 2019). Decreased levels of endoplasmic reticulum (ER) cholesterol leads to the transportation of previously ER-bound SREBPs to the Golgi via SREBP-cleavage activating protein (SCAP) (Wakana *et al.*, 2021). This leads to the proteolytic liberation of the NH<sub>2</sub>-terminal fragments of SREBP2 that are then able to translocate from the Golgi to the nucleus, where it binds to the sterol regulatory element (SRE)

promoter to initiate transcription of cholesterol synthesis and uptake genes (Brown and Goldstein, 1986; Ikonen, 2008; Luo *et al.*, 2020). SREBP2 is also able to bind to an E-box element in the proximal promoter of ABCA1 resulting in reduced cholesterol efflux (Wong *et al.*, 2006). Simultaneously, low density lipoproteins (LDLs) are delivered cholesterol into cells through receptor-mediated endocytosis facilitated by LDL receptors (LDLRs). The cell membrane and membrane-bound organelles then utilise the released free cholesterol from LDL hydrolysis (Brown and Goldstein, 1986; Ikonen, 2008) after which LDLR relocates back to the membrane for more cholesterol intake or it is degraded by proprotein convertase subtilisin/kexin (PCSK9), a serine protease that binds to LDLR when cholesterol uptake is no longer required (Kosenko *et al.*, 2013). Acyl-CoA: cholesterol acyltransferase (ACAT) then re-esterifies any excess free cholesterol to prevent free cholesterol-induced cytotoxicity (Tabas, 2002). Subsequently, it is stored in lipid droplets with the assistance of cholesteryl ester transfer protein (CETP), leading to cholesteryl ester (CE) accumulation within the lipid droplets (Figure 1.5).

Conversely, LXR is activated when intracellular cholesterol or cholesterol derived-oxysterols levels are elevated resulting in the downregulation of cholesterol synthesis and promotion of cholesterol export (Wang *et al.*, 2008). LXRs form heterodimers with retinoid X receptors (RXRs) and are bound to LXR response elements (Wang and Tontonoz, 2018). Co-repressors are bound to the LXR-RXR complex when cholesterol or oxysterol levels are low, however excess levels result in a conformational change of the complex, releasing co-repressors and recruiting co-activators, resulting in a transcriptional increase of target genes such as ABC transporters and apolipoproteins for cholesterol efflux (Sallam *et al.*, 2016; Wang and Tontonoz, 2018). Cholesterol efflux is primarily mediated by ABCA1 and ABCG1, which efflux cellular cholesterol to apolipoproteins to form discoidal high-density lipoproteins (HDLs) (Ye *et al.*, 2011; Adorni *et al.*, 2021). These HDLs are generated either passively or actively by lipid-poor or lipid-free apolipoprotein A-I (apoA-I) (Chang *et al.*, 2009; Luo *et al.*, 2020). Mature spherical HDLs are then formed by the esterification process facilitated by lecithin-cholesterol acyltransferase (LCAT) (Marques *et al.*, 2018; Adorni *et al.*, 2021). Thereafter scavenger receptor B1 (SR-B1), a type of HDL receptor (HDLR), is responsible for direct uptake of cholesterol in the liver. Alternatively, CETP can facilitate the transfer of cholesterol from HDL to LDL particles (Gracia-Rubio *et al.*, 2021). These particles can then be endocytosed by LDLR on the liver, known as the indirect reverse cholesterol transport

pathway (Marques *et al.*, 2018). Thereafter, cholesterol is either excreted or transformed into bile acids.

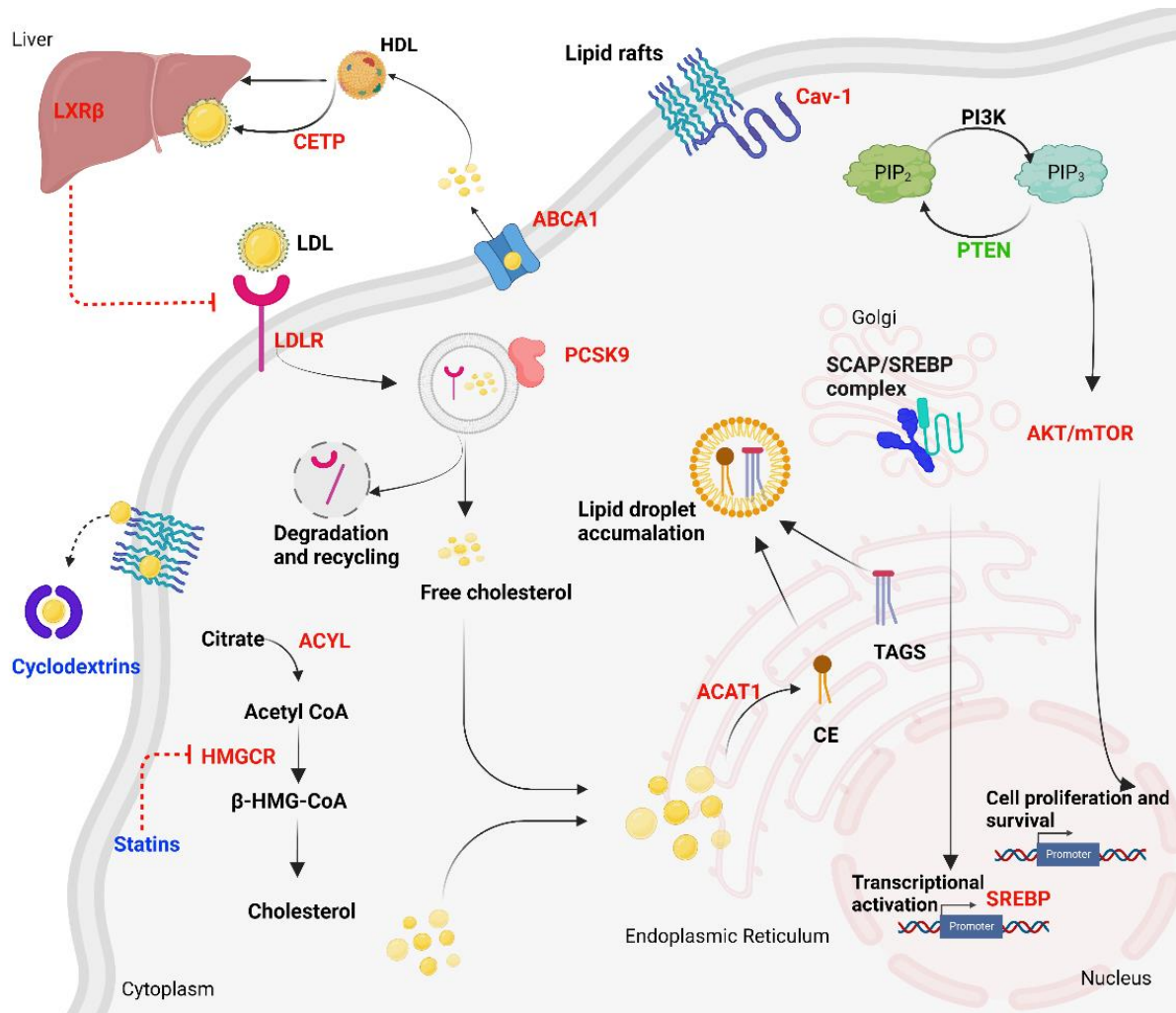


**Figure 1.5: Cholesterol metabolism in PDAC**

*Intracellular cholesterol levels are tightly controlled through a complex network of regulatory mechanisms involving several key proteins and pathways. LXR and SREBP play pivotal roles in controlling cholesterol uptake and synthesis (Gu *et al.*, 2019). LXR regulates cholesterol uptake and export, while SREBP, particularly SREBP2, is a key regulator of cholesterol biosynthesis (Gu *et al.*, 2019). Upon decreased endoplasmic ER cholesterol levels, SREBPs are transported to the Golgi via SCAP, leading to their proteolytic liberation and subsequent translocation to the nucleus, where they activate transcription of cholesterol synthesis and uptake genes (Brown and Goldstein, 1986; Ikonen, 2008; Luo *et al.*, 2020; Wakana *et al.*, 2021). Intracellularly, cholesterol biosynthesis begins with the conversion of citrate into Acetyl CoA by ATP citrate synthase (ACYL), followed by the rate-limiting step catalyzed by HMGCR to form  $\beta$ -HMG-CoA. LDLs play a crucial role in delivering cholesterol into cells through receptor-mediated endocytosis facilitated by LDLRs (Brown and Goldstein, 1986; Ikonen, 2008). Upon LDL hydrolysis by PCSK9 which degrades LDLs under high sterol conditions, free cholesterol is released and utilised by the cell membrane and organelles (Kosenko *et al.*, 2013). Excess free cholesterol produced from biosynthesis or LDL hydrolysis is re-esterified*

by ACAT) and stored in lipid droplets with the assistance of CETP (Tabas, 2002). Conversely, LXR is activated when intracellular cholesterol or oxysterol levels are elevated, leading to the downregulation of cholesterol synthesis and promotion of cholesterol export LXRs (Wang *et al.*, 2008). Cholesterol efflux is primarily mediated by efflux proteins like ABCA1, which efflux cellular cholesterol to apolipoproteins to form HDLs (Sallam *et al.*, 2016; Wang and Tontonoz, 2018). Statins inhibit HMGCR, reducing intracellular cholesterol levels, while cyclodextrins target membrane cholesterol. Extracellularly, cholesterol is transported via lipoproteins, HDLs, and LDLs. HDLs interact with SR-B1 for cholesterol clearance by the liver, while CETP shuttles cholesterol from HDLs to LDLs, which bind to LDLRs on hepatocytes for cholesterol clearance (Marques *et al.*, 2018; Adorni *et al.*, 2021). The raft-related proteins, such as caveolin-1 (Cav-1), are upregulated and stimulate cell signaling pathways and phosphatase and tensin homolog (PTEN) a protein involved in CE formation is downregulated (Simón *et al.*, 2020). Statins are a class of drugs that inhibit HMGCR, lowering cholesterol levels within the cell. Cyclodextrins are a class of drugs that form dimers with hydrophobic cores which are able to target membrane cholesterol. Red and green indicate upregulation and downregulation in PDAC, respectively. (Created in BioRender.com)

### 1.5.1 Metabolic reprogramming in PDAC

The metabolic reprogramming in PDAC results in imbalanced cholesterol levels, which promotes the progression of PDAC, as well as cell proliferation, invasion, migration, and MDR. This imbalance is caused by disruptions in synthesis, efflux, influx, and metabolism, which are all crucial processes (Figure 1.5). The KRAS mutation, as previously mentioned, particularly the KRAS<sup>G12D</sup> mutation, plays a significant role in this process by activating the PI3K/AKT/mechanistic target of rapamycin complex 1 (mTORC1) and Ras/Raf/MEK/ERK pathways. This activation specifically leads to the activation of SREBP1/2, promoting lipid and cholesterol synthesis, as well as uptake (Kuzu *et al.*, 2016; Ricoult *et al.*, 2016; Ruiz *et al.*, 2020; Li *et al.*, 2023). Additionally, KRAS is responsible for directly and indirectly promoting the storage of excess cholesterol, leading to an increased number of lipid droplets. KRAS suppresses hormone-sensitive lipase (HSL) via the MAPK/ERK pathway, redirecting its metabolism away from fatty acid oxidation and resulting in the accumulation of lipid droplets (Rozeveld *et al.*, 2020). This characteristic enables invasion and subsequent metastasis of PDAC (Rozeveld *et al.*, 2020). The accumulation of lipid droplets is also an attempt to prevent toxic levels of free cholesterol after SREBP2 activation through cholesterol esterification (Tabas, 2002). Notably, the levels of lipid droplets are 20 times higher in PC tissue and cells compared to normal cells, which acts as energy reservoirs for PC cells (Li *et al.*, 2016). KRAS mutations also affect ABC transporters ABCA1 and ABCB1 involved in cholesterol efflux and drug resistance, respectively. The activation of AKT inhibits cholesterol export via ABCA1 through mTORC1 (Dong *et al.*, 2014, 2022; Y. Zhang *et al.*, 2022). Interestingly, the tumour suppressor TP53 has been found to contribute to unregulated cholesterol synthesis in cancer

cells (Oberstein and Olive, 2013; Mukhopadhyay *et al.*, 2019). Similar to KRAS, TP53 induces the activity of SREBP 1/2 (Kuzu *et al.*, 2016), and it also enhances the expression of ACAT1. Overexpression of ACAT1 is known to reduce patient survival, promote metastasis, and contribute to lipid droplet accumulation (Li *et al.*, 2016; Oni *et al.*, 2020). Additionally, the low pH condition of the TME promotes cholesterol biosynthesis. PC cells at a pH of 6.8 and lower result in the nuclear localisation of SREBP2, leading to the transcription of cholesterol synthesis and uptake genes, as well as reducing ABCA1-mediated cholesterol efflux (Kondo *et al.*, 2017).

Not only have these signalling pathways, mutations, and TME conditions been implicated in metabolic programming, but specific lipid-related proteins are also known to be dysregulated in PDAC (Figure 1.5). Notably, proteins LDLR, caveolin-1 (Cav-1), and phosphatase and tensin homolog (PTEN) expression levels are elevated. Overexpression of LDLR is associated with an increased risk of recurrence and has also been found to contribute to GEM resistance and activation of the ERK1/2 signalling pathway, thereby promoting proliferation (Guillaumond *et al.*, 2015). Interestingly, silencing of LDLR reduces CE formation and hence lipid droplet accumulation (Guillaumond *et al.*, 2015). Similarly, overexpression of Cav-1 is associated with MDR and progression of PDAC (Chatterjee *et al.*, 2015). Cav-1 is a structural protein necessary for the formation of caveolae and membrane rafts in the cell membrane, a process dependent on cholesterol level (Simón *et al.*, 2020). Therefore, Cav-1 is involved in lipid homeostasis, signal transduction, and endocytosis (Chatterjee *et al.*, 2015). Increased expression of Cav-1, due to higher cholesterol levels, leads to decreased intrinsic apoptosis, enhanced Akt and JAK/STAT signalling, and activation of survival pathways resulting in resistance to chemotherapies such as GEM and 5-FU (Chatterjee *et al.*, 2015). Additionally, the lipid raft structural damage activates oncogenes such as c-Met, c-Src, and Src to promote tumour formation, invasion, and migration (Kuzu *et al.*, 2016). Importantly, Cav-1 overexpression may also contribute to lipid droplet accumulation due to its role in the assembly and stabilisation of lipid droplets (Kuo *et al.*, 2018). Additionally, loss of PTEN function contributes to lipid droplet accumulation through the same pathway as KRAS and TP53, leading to increased ACAT1-mediated CE formation and an overall increase in cholesterol synthesis and uptake genes. Lipid droplet accumulation can also be seen to play an integral role in PDAC whereby the accumulation of lipid droplets enables not only proliferation but also invasion and metastasis, as these lipid droplets act as an energy reservoir for this highly energy-intensive process (Li *et al.*, 2020; Rozeveld *et al.*, 2020). Lipid droplets also promote survival

in stressful conditions, such as chemotherapy treatment, where GEM-resistant PDAC cells have been found to exhibit higher levels of CEs (Guillaumond *et al.*, 2015; Cotte *et al.*, 2018; Li *et al.*, 2018). Additionally, lipid droplets protect cells from ER stress and lipotoxicity (Li *et al.*, 2020). Therefore, it is evident that altered cholesterol homeostasis plays a significant role in MDR, migration, proliferation, and cancer progression, as it is involved in several oncogenic pathways. Targeting cholesterol may thus be considered a potential therapeutic option for PDAC.

## **1.5.2 Targeting cholesterol for the treatment of PDAC**

Given cholesterol's significant involvement in cancer-related processes like differentiation, proliferation, migration, chemoresistance, and survival, alongside the observed elevated cholesterol levels in PDAC, targeting cholesterol depletion emerges as a prospective therapeutic strategy in cancer treatment. There are two broad approaches to targeting cholesterol, the first being targeting elements found in the cholesterol synthesis pathway and the second being the use of cholesterol-depleting agents to lower cholesterol levels directly.

### **1.5.2.1 Statins**

Statins are a group of drugs commonly prescribed to lower cholesterol levels, particularly in cardiovascular diseases, however recently they have been seen to be repurposed for the treatment of cancer due to their anti-cancer properties (Ward *et al.*, 2019; Jiang *et al.*, 2021). Statins act to lower cholesterol levels by competitively inhibiting HMGCR, the rate-limiting enzyme in the mevalonate pathway (Brown, 2007) hence resulting in the reduction of *de novo* cholesterol biosynthesis, as well as altering LDLR expression (Figure 1.5). The anti-cancer properties of statins are dependent on time, concentration, cell type, as well as the type of statin used. Statins have been found to target cancer by blocking cholesterol synthesis (Murai *et al.*, 2011), preventing isoprenoid formation (Gonyeau and Yuen, 2010; Corcos and le Jossic-Corcos, 2013; Gong *et al.*, 2017; Jiang *et al.*, 2021), targeting the TME (Jiang *et al.*, 2021) inducing autophagy (Panda *et al.*, 2015; Jiang *et al.*, 2021), inducing ferroptosis (Stockwell *et al.*, 2017), and lastly inducing pyroptosis (Jiang *et al.*, 2021). Specifically statins have been found to target PDAC through several mechanisms such as targeting the functional P2X7-Akt signalling in PDAC cells (Mistafa and Stenius, 2009), blocking the TGF- $\beta$ 1/growth factor independent 1 (Gfi1) axis reducing GEM resistance (Xian *et al.*, 2017), inhibition of geranylgeranylation and/or farnesylation hence impairing Ras Homolog Family Member A (RhoA) and Ras signalling pathways (Elsayed *et al.*, 2016), inhibition of protein prenylation

of the KRAS protein (Liao *et al.*, 2013), and arrest of sub-G1 and S phase cell cycle arrest (Y. H. Chen *et al.*, 2020) to name a few.

Despite the extensive use of statins, evidence for their ability to enhance the overall survival of PDAC patients and efficacy of chemotherapies in PDAC remains inconclusive, most likely due to the lack of prospective studies. Statin use is also associated with musculoskeletal side effects, increase risk of diabetes mellitus, hepatotoxicity, kidney dysfunction, and neuropathy (Ramkumar *et al.*, 2016). Therefore, further research is required prior to the approval of statins as an anti-cancer drug. An alternative strategy is to target the excess cholesterol in cancer cells as opposed to altering the synthesis process.

### 1.5.2.2 Cyclodextrins (CDs)

CDs are cyclic oligosaccharides that contain hydrophobic cavities and a relatively hydrophilic exterior (Ottinger *et al.*, 2014). They typically exist as hexamers ( $\alpha$ -CD), heptamers ( $\beta$ -CD), or octamers ( $\gamma$ -CD). These natural CDs can be further modified into randomly methylated- $\beta$ -CD, hydroxypropylated- $\beta$ -CD, sulphobutyl ether- $\beta$ CD, and hydroxypropylated- $\gamma$ -CD, which gives rise to an increase in water solubility of the CD (Davis and Brewster, 2004). Due to their structure and size, these natural CDs form inclusion complexes with different types of hydrophobic molecules (Másson *et al.*, 1999). Low molecular weight molecules or a compound with aliphatic side chains will form an inclusion complex with  $\alpha$ -CD, whereas any compound that is aromatic or heterocyclic compound will form inclusion complexes with  $\beta$ -CD. Large organic compounds however will form inclusion complexes with  $\gamma$ -CD (Li *et al.*, 2007). This is possible due to the presence of water molecules inside the apolar cavity, an energetically unfavourable state, and hence any molecule less polar than water can be encapsulated into the CD via hydrophobic interactions, hydrogen bonds, charge-transfer interactions, van der Waals forces, and electrostatic interactions (Szejtli, 1998; Cordes *et al.*, 2007). This trait has particularly attracted widespread attention to chemically modified CDs for their ability to enhance solubility, stability, and bioavailability, as well as reduce the toxicity of many drug formulations (Davis & Brewster, 2004; Loftsson *et al.*, 2005; Qiu *et al.*, 2017) .

The most used CDs in *in vitro*, *in vivo*, and pre-clinical studies are  $\beta$ -CDs, particularly methyl- $\beta$ -CD (M $\beta$ CD) with 2-Hydroxypropyl- $\beta$ -CD (HP $\beta$ CD) emerging as another commonly used CD (Gadade and Pekamwar, 2020; Karthic *et al.*, 2022; Saha *et al.*, 2023) due to their availability, simple production, and cost (Zhang *et al.*, 2015). CDs have so far been minimally used to increase drug bioavailability, increase therapeutic efficacy, and decrease toxicity in

PDAC (Dandawate *et al.*, 2012; Chapiro *et al.*, 2014; Ji *et al.*, 2016; Iacobazzi *et al.*, 2020). However, in various other types of cancer, CDs have consistently proven to be effective in achieving these outcomes. It is important to note that CDs can be toxic at high concentrations, and as a result, dose levels must be limited (Di and Kerns, 2016). Interestingly, HP $\beta$ CD has been shown to be less toxic than other  $\beta$ -CDs such as M $\beta$ CD (Gould and Scott, 2005).

$\beta$ -CDs as previously mentioned, form inclusion complexes with aromatic or heterocyclic compounds and are hence notably able to extract cholesterol and other lipid membrane components from cells (Figure 1.5) (Davis and Brewster, 2004). This forms the basis of an emerging field of use for CDs in which membrane properties such as fluidity and permeability can be altered. As aforementioned, higher amounts of membrane cholesterol are known to be responsible for a more rigid and less permeable membrane thus contributing to chemoresistance in cancer, particularly PDAC (Iacobazzi *et al.*, 2020; Preta, 2020). Reducing cholesterol levels via  $\beta$ -CDs may thus serve as a method of reducing chemoresistance, as well as preventing PDAC progression by regulating aberrant cholesterol homeostasis (López, de Vries and Marrink, 2011). Unlike other cancer types, such as breast, bladder, melanoma, rectal, prostate, and colon (Li *et al.*, 2006; Mohammad *et al.*, 2014; Resnik *et al.*, 2015; Yamaguchi *et al.*, 2015; Chowdhury *et al.*, 2017; Yang *et al.*, 2018; Gu *et al.*, 2019; Sharma *et al.*, 2019; Vona *et al.*, 2021; Zhao *et al.*, 2021; Ohno *et al.*, 2023; Saha *et al.*, 2023), there are no studies investigating the effects of CDs on PDAC progression and chemoresistance via cholesterol depletion, which only further relays the issue surrounding the lack of research in this emerging field, particularly in PDAC. The limited number of studies on the use of CDs in PDAC, compared to other types of cancer, indicates that CDs have not been able to fully demonstrate their potential as a new treatment for PDAC. Notably, there is currently only one clinical trial targeting cholesterol for the treatment of PDAC titled "A Phase 1 Feasibility Study of Cholesterol Metabolism Disruption (Evolocumab, Atorvastatin, and Ezetimibe) in Combination With FOLFIRINOX in Patients With Metastatic Pancreatic Adenocarcinoma" that is currently recruiting ([NCT04862260](https://clinicaltrials.gov/ct2/show/study/NCT04862260)). This study aims to slow or halt the progression of PDAC and reduce chemoresistance to FOLFIRINOX by depleting cholesterol using statins. Given that there is only one clinical trial focused on a target that is crucial to the development of this cancer and its significant chemoresistance, it is imperative to conduct more research and development on using cholesterol as a target, particularly in combination with current treatments.

## 1.6 EMT

PDAC is highly metastatic and utilises the EMT program for this metastasis. The process of EMT is a cell plasticity program that involves the dynamic reorganisation of cellular structure as cells transition from an epithelial to a mesenchymal phenotype. EMT is observed in various biological processes, including embryonic development, tissue regeneration, and notably the progression of cancer (Zeisberg and Neilson, 2009; Ribatti *et al.*, 2020). This mesenchymal phenotype plays a crucial role in enabling cell migration, invasion, and ultimately, metastatic dissemination (Ribatti *et al.*, 2020). EMT is regulated by specific EMT-TFs, namely, SNAIL1/2, TWIST1, Zinc-finger E-box Binding Homeobox 1/2 (ZEB1/2), and Paired Related Homeobox 1 (PRRX1), which are activated through various signalling pathways, TME conditions, and miRNAs, as discussed in more detail below.

Epithelial cells are characterised by their polygonal and cobble-stone-like morphology, apical-basal structural polarity, non-motility, expression of cytokeratin, and the ability to form cadherin-mediated adherens junctions, tight junctions, and desmosomes with surrounding cells (Thiery *et al.*, 2009; Ye and Weinberg, 2015). In contrast, mesenchymal cells are characterised by an elongated and spindle-like morphology, front-back polarity, motility, expression of vimentin, excessive expression of actin and myosin, and minimal to no junctions with surrounding cells (see Figure 1.7) (Thiery *et al.*, 2009; Ye and Weinberg, 2015). Instead, these mesenchymal cells attach to the extracellular matrix via focal adhesion (Ye and Weinberg, 2015), which confers migratory and invasive capabilities. The expression of cytokeratin is integral to the formation of intermediate filaments in epithelial cells. However, in mesenchymal cells, the function of cytokeratin is taken over by vimentin, which enhances cytoskeletal strength and contributes to the cell flexibility that is required for migration and invasion (Mendez *et al.*, 2010; Ye and Weinberg, 2015). Another hallmark of EMT is cadherin switching from E-cadherin to N-cadherin where mature, full-length E-cadherin (120 kDa) is cleaved into an extracellular N-terminal fragment (80 kDa) and an intracellular C-terminal fragment (38kDa) by secretases, metalloproteinases, and plasmin (De Wever *et al.*, 2007; David and Rajasekaran, 2012; Gagliano *et al.*, 2016; Sommariva and Gagliano, 2020). The newly soluble extracellular N-terminal fragment leads to both a reduction in adherens junctions, as well as upregulation of matrix metalloproteinase-2 (MMP-2) and MMP-9, which degrade the basement membrane. The intracellular C-terminal fragment is further cleaved, and the resulting fragments act as signalling molecules to promote junction disruption, migration and invasion through upregulation of the Wnt/ $\beta$ -catenin pathway (De Wever *et al.*, 2007; David

and Rajasekaran, 2012). Other key markers of EMT involve the loss of membrane proteins occludin and claudin, which are components of tight junctions, and the gain of fibronectin and MMPs (Thiery *et al.*, 2009; Zeisberg and Neilson, 2009; Bulle and Lim, 2020; Ribatti *et al.*, 2020).

EMT, previously believed to be a phenotypic switch, is actually a transition between intermediate states (see Figure 1.7). Cells can transition bidirectionally from an epithelial to mesenchymal state through various hybrid states, resulting in either EMT or mesenchymal to epithelial transition (MET) (Nieto, 2013; Ungefroren *et al.*, 2022). MET, in particular, is a crucial pathway responsible for metastatic colonisation, as it facilitates cell attachment and proliferation necessary for secondary tumour growth (Nieto, 2013). Although the specific number of stable and metastable transitional states remains unknown, it has been confirmed that the intermediate hybrid states of EMT, referred to as hybrid E/M states, exist (Nieto, 2013; Zadran *et al.*, 2014; Williams *et al.*, 2019; Ungefroren *et al.*, 2022). These hybrid EMT states have the highest metastatic potential due to their ability to migrate easily and attach to distant sites, forming metastatic colonies (Pastushenko *et al.*, 2018; Celià-Terrassa and Kang, 2024). Interestingly, while metastatic dissemination typically occurs in the late stages of cancers, recent evidence suggests that it can occur when pre-cancerous acinar-to-ductal metaplasia (ADM) and PanIn lesions are present, long before the formation of a clinically relevant tumour (Rhim *et al.*, 2012). This implies that PDAC cells can circulate in the body for years prior to the development of metastatic colonies. Instead, these early disseminated cells are suggested to play a role in tumour formation by promoting fibroblast infiltration and chronic tissue inflammation, creating an environment conducive to triggering EMT-TFs and promoting the progression of these pre-cancerous lesions into PDAC (Palamaris *et al.*, 2021). In addition to its role in PDAC progression, EMT has also been implicated in drug resistance and the generation of CSCs in PDAC (Satoh *et al.*, 2015).

### **1.6.1 Molecular mechanism of EMT**

In order for cells to undergo this plasticity program, signalling pathways must be activated by certain TME conditions such as inflammation, hypoxia, nutrient deficiency or oxidative stress (Zhu *et al.*, 2016; S. Wang *et al.*, 2017). As demonstrated in Figure 1.7, the most prominent signalling pathways include cytokines (TGF- $\beta$ , tumour necrosis factor  $\alpha$  (TNF $\alpha$ ), interleukin-1/6 (IL-1/6), growth factors (Epidermal growth factor (EGF)/hepatocyte growth factor (HGF)/fibroblast growth factor (FGF)/platelet-derived growth factor (PDGF)), Wnt, Hh, and

Notch (Figure 1.6) (Moustakas and Heldin, 2007; Ribatti *et al.*, 2020). Additionally, several miRNAs have also been implicated in regulating EMT. While these signalling pathways can individually induce EMT, in the context of tumours, there is a collaboration and crosstalk among these pathways leading to the amplification of EMT signalling through positive feedback loops.

#### **1.6.1.1 TGF- $\beta$ 1**

The binding of TGF- $\beta$ 1 ligand to its type II receptor (T $\beta$ R-II), a membrane-bound serine/threonine kinase receptor, initiates the formation of a hetero-tetrameric receptor complex by recruiting the type I receptor (T $\beta$ R-I) to the membrane (Figure 1.6) (Moustakas and Heldin, 2016). This complex then phosphorylates and activates T $\beta$ R-I, triggering a cascade of events (Moustakas and Heldin, 2016). Phosphorylation of SMAD2 and SMAD3 by T $\beta$ R-I results in their heterodimerisation with SMAD4, and the resulting complex translocates to the nucleus, where it cooperates with DNA binding transcription factors to activate mesenchymal genes or repress epithelial genes (Xu *et al.*, 2009; Moustakas and Heldin, 2016). T $\beta$ R-I activation also promotes non-SMAD dependent pathways that contribute to EMT. For example, it can activate p38, Jun N-terminal kinase (JNK), and I $\kappa$ B kinase (IKK)-NF- $\kappa$ B pathways through TGF- $\beta$  activated kinase 1 (TAK1) and receptor-associated tumour necrosis factor receptor associated factor 6 (TRAF6), as well the activation of the Ras/Raf/MEK/ERK signalling pathway via Shc phosphorylation (Sorrentino *et al.*, 2008; Yamashita *et al.*, 2008; Xu *et al.*, 2009; Moustakas and Heldin, 2016). Furthermore, T $\beta$ R-I activation leads to the activation of PI3K/Akt/mTOR or MAPK signalling pathways, resulting in increased SNAIL expression and cell size (Barrallo-Gimeno and Nieto, 2005; Xu *et al.*, 2009). Importantly, TGF- $\beta$ 1 was the first cytokine identified to induce EMT in PDAC cells (Grände *et al.*, 2002), and it has been shown that the TGF- $\beta$ /SMAD pathway is the most potent inducer of EMT in PDAC (Alvarez *et al.*, 2019). This is attributed to the signalling crosstalk between TGF- $\beta$ /SMAD and the Wnt and Notch pathways resulting in a robust induction of EMT (Xu *et al.*, 2009).

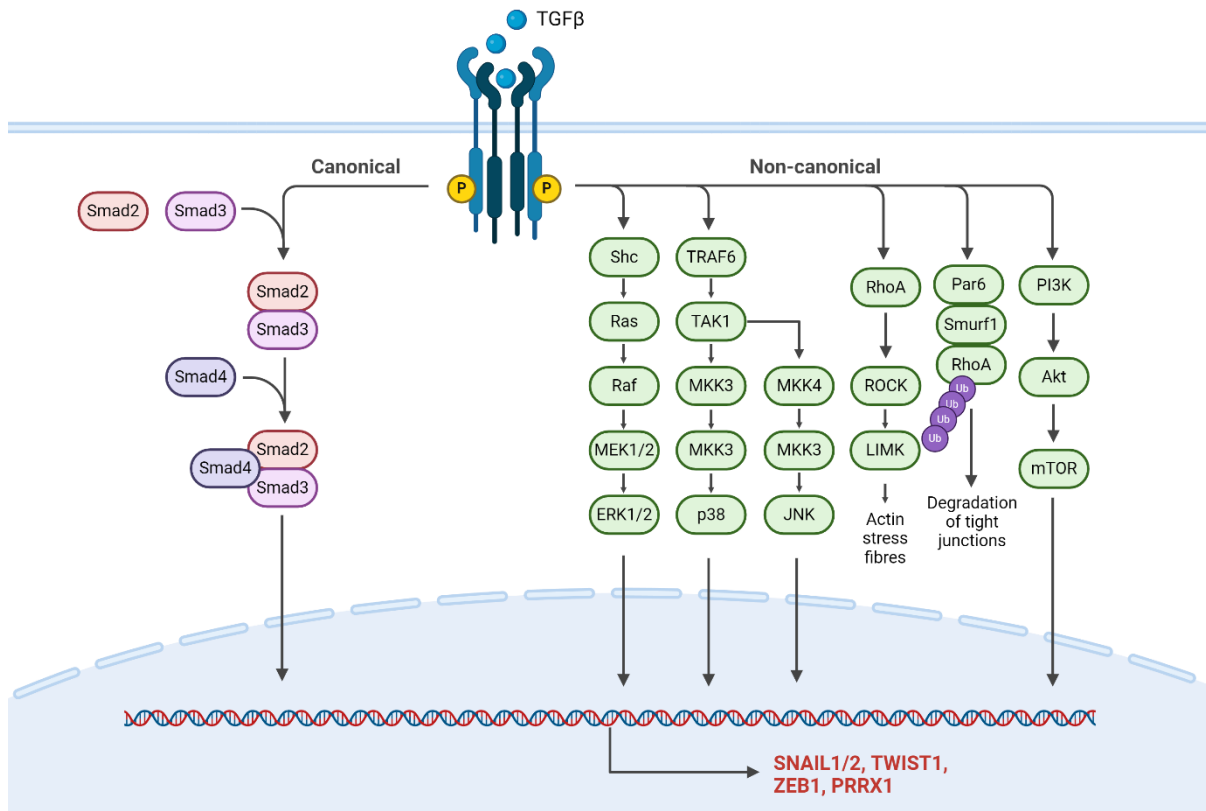


**Figure 1.6: Transcriptional regulation of EMT induced by TGF- $\beta$**

Initiation of the canonical pathway begins with the binding of TGF- $\beta$ 1 ligand to T $\beta$ R-II, a membrane-bound serine/threonine kinase receptor. This interaction recruits and activates T $\beta$ R-I, forming a hetero-tetrameric receptor complex (Moustakas and Heldin, 2016). Activation of T $\beta$ R-I phosphorylates downstream effectors, specifically SMAD2 and SMAD3, leading to their heterodimerization with SMAD4 (Moustakas and Heldin, 2016). The resulting complex translocates into the nucleus, where it collaborates with DNA binding transcription factors to regulate the expression of genes associated with EMT (Xu et al., 2009; Moustakas and Heldin, 2016). Additionally, TGF- $\beta$ 1-induced signalling pathways include non-SMAD dependent mechanisms. TGF- $\beta$ 1 stimulates the p38 mitogen-activated protein kinase kinase 3/6 (MKK3/6), JNK, mitogen-activated protein kinase kinase 4 (MKK4), and IKK-NF- $\kappa$ B pathways by activating TAK1 through receptor-associated TRAF6. It also initiates Ras/Raf/MEK/ERK signaling by recruiting and phosphorylating Shc via the T $\beta$ R-I. TGF- $\beta$  also activates RhoA leading to the activation of Rho-associated coiled-coil-containing protein kinase (ROCK) and Lin11, Isl-1 and Mec-3 kinase (LIMK), which reorganise the actin cytoskeleton into actin stress fibres. RhoA also participates in the ubiquitin-mediated degradation of tight junctions through the activation of Par6 and subsequent recruitment of Smurf1, resulting in enhanced ubiquitination of RhoA. Lastly, TGF- $\beta$  induces PI3K/Akt/mTOR signalling (Sorrentino et al., 2008; Yamashita et al., 2008; Xu et al., 2009; Moustakas and Heldin, 2016). Consequently, the EMT-related transcription factors SNAIL1/2, TWIST1, ZEB1/2, and PRRX1 (Alvarez et al., 2019). (Created in BioRender.com)

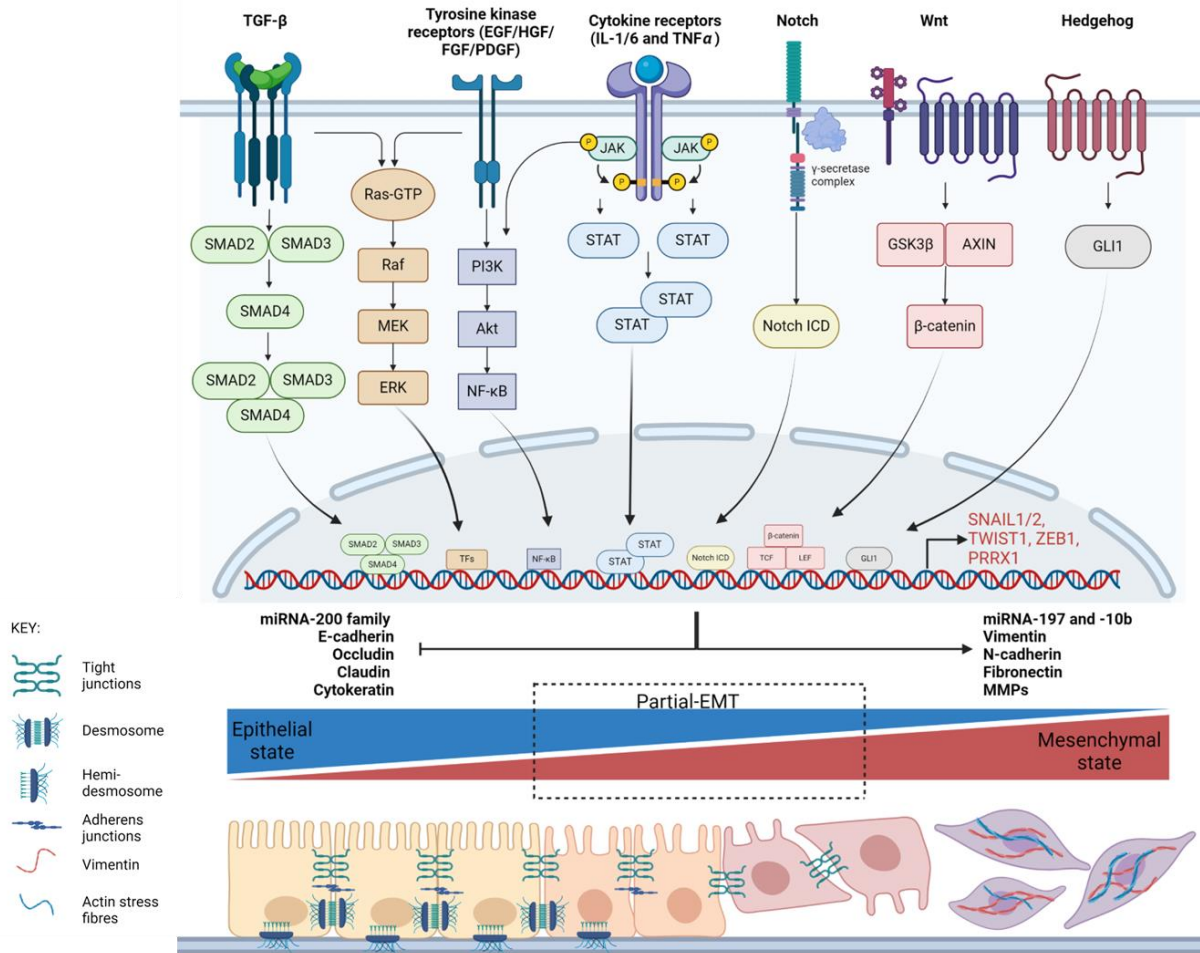


**Figure 1.7: Overview of the major signalling pathways involved in the EMT program in PDAC.**

*EMT is a fundamental process implicated in the progression PDAC, characterized by the transformation of epithelial cells into mesenchymal-like cells with enhanced migratory and invasive properties. This figure illustrates key signalling pathways driving EMT in PDAC and their molecular mechanisms. Binding of the TGF- $\beta$  proteins to the TGF- $\beta$  family of receptors leads to receptor phosphorylation and activation of SMAD complexes, which activate the EMT programme (Sorrentino et al., 2008; Yamashita et al., 2008; Xu et al., 2009; Moustakas and Heldin, 2016). SMAD proteins also interact with  $\beta$ -catenin and NOTCH- intracellular domain (ICD) (not shown here). TGF- $\beta$  signalling also promotes the Ras/Raf/MEK/ERK pathway. Tyrosine kinase signalling of EGF, HGF, FGF, and PDGF activate EMT-TFs through Ras/MAPK or PI3K/AKT pathways (Barrallo-Gimeno and Nieto, 2005). The cytokine receptors, while not as potent as TGF- $\beta$ 1, interleukin-1 (IL-1), IL-6, and tumour necrosis factor alpha (TNF $\alpha$ ) play integral roles in promoting EMT. IL-6 activates STAT3, which translocates to the nucleus and induces the expression of mesenchymal genes. IL-1 and TNF $\alpha$  activate the NF- $\kappa$ B pathway (Wu et al., 2004; Maier et al., 2010; Nagathihalli et al., 2016). Activation of Notch receptors by  $\gamma$ -secretase complex initiates proteolytic cleavages, releasing the Notch-ICD, which translocates to the nucleus to induce the expression of EMT-TFs (Timmerman et al., 2004; Kopan and Ilagan, 2009; Mazur et al., 2010; Kar et al., 2019). Canonical Wnt*

signaling stabilizes  $\beta$ -catenin, leading to the release of  $\beta$ -catenin from the glycogen synthase kinase-3 $\beta$  (GSK3 $\beta$ )– axis inhibition protein (AXIN) complex allowing its translocation to the nucleus where it forms complexes with T-cell factor/lymphoid enhancer factor (TCF/LEF) to activate EMT-TFs (Xu *et al.*, 2009; Palamaris *et al.*, 2021; Liu *et al.*, 2022). Normally dormant in the pancreas, Hh signaling becomes highly active in PDAC. Upon ligand binding, patched1 (PTCH1) releases smoothed (SMO), leading to the transcriptional activation of GLI1. These signalling pathways operate to activate the specific EMT-TFs, namely, SNAIL1/2, TWIST1, ZEB1/2, and PRRX1 (Lei *et al.*, 2013; Wang *et al.*, 2016). This results in the suppression of epithelial markers (miRNA-200 family, E-cadherin, Occludin, Claudin, and cytokeratin) and the promotion of mesenchymal markers (miRNA-197 and -10b, Vimentin, N-cadherin, Fibronectin, and MMPs). Resulting in the morphological change of epithelial cells from a polygonal morphology, apical-basal polarity, and expression of cytokeratin towards a spindle-like morphology, front-back polarity, and vimentin expression, enabling migration and invasion. Additionally, EMT, as previously believed to be a phenotypic switch, is actually a transition between intermediate states. Cells can transition bidirectionally from an epithelial to mesenchymal state through various hybrid states, resulting in either EMT or MET (Nieto, 2013; Ungefroren *et al.*, 2022). (Created in BioRender.com)

### 1.6.1.2 EMT-TFs

There's a number of EMT-TFs involved in the EMT process. The zinc finger protein SNAIL family, TWIST Basic Helix-Loop-Helix (bHLH) transcription Factor 1, ZEB family, and PRRX1 are considered master EMT-TFs (Figure 1.7). These EMT-TFs work collaboratively to modulate each other, as well as the expression of target epithelial or mesenchymal genes. Notably, SNAIL and ZEB function as strong epithelial repressors rather than mesenchymal promoters, suppressing the expression of epithelial markers such as E-cadherin, claudins, and occludins. In contrast, PRRX and TWIST have strong mesenchymal inducing properties (S. Wang *et al.*, 2017).

#### 1.6.1.2.1 Zinc Finger protein SNAIL

There are three SNAIL family proteins, namely, SNAIL 1 (Snail), SNAIL 2 (Slug), and SNAIL 3 (Smuc), with Snail and Slug being implicated in EMT (Barrallo-Gimeno and Nieto, 2005). Notably, Snail and Slug are overexpressed in over 70% and 50% of PDAC, respectively (Hotz *et al.*, 2007). Snail and Slug repress specific cell junction targets such as E-cadherin, occludins, and claudins through their N-terminal SNAG domain by directly binding transcriptional repressors to the E-box in the proximal promoter regions (Batlle *et al.*, 2000; Ikenouchi *et al.*, 2003). They can also repress targets through epigenetic remodelling complexes, including histone modifiers and DNA methyltransferases, which affect DNA and chromatin accessibility (Peinado *et al.*, 2004; Hou *et al.*, 2008). Interestingly, Snail also forms a transcriptional repressor complex with SMAD3/4 during TGF- $\beta$  induced EMT, targeting junction proteins (Vincent *et al.*, 2009). Additionally, Slug is an essential mediator of TWIST-induced EMT,

where TWIST first induces Slug to suppress epithelial phenotypes, after which TWIST and Slug act synergistically to promote EMT (Casas *et al.*, 2011). Snail also activates MMP-9 and MMP-2, resulting in basement membrane degradation (Shields *et al.*, 2011). Therefore, Snail activation is crucial for potent induction of EMT and consequently, PDAC progression and invasion.

#### **1.6.1.2.2 TWIST bHLH family**

TWIST-family bHLH proteins form dimers and recognise specific DNA sequences known as hexanucleotide E-boxes within regulatory regions, to act as transcriptional regulators (Zhu *et al.*, 2016). TWIST-1 induces the transcription of mesenchymal markers like vimentin and N-cadherin, although the exact mechanism is not fully elucidated (Lamouille *et al.*, 2014; Meng *et al.*, 2018). Moreover, TWIST-1 can directly bind to E-boxes 2 and 3 on the *CDH1* promoter to repress E-cadherin (Vesuna *et al.*, 2008). TWIST-1 is also known to cooperate with epigenetic regulators that bind to the proximal promoter of E-cadherin to repress its expression (Fu *et al.*, 2011). It is important to highlight that TWIST-1 is expressed at low levels in PDAC, with some PC cell lines only expressing it under hypoxic conditions (Hotz *et al.*, 2007). This indicates that TWIST-1 may only be a crucial TF in hypoxic conditions and may, therefore, contribute to the maintenance of EMT rather than its induction in PDAC. Unlike SNAIL, TWIST-1 may not play a significant role in PDAC progression.

#### **1.6.1.2.3 ZEB family**

ZEB transcription factors, specifically ZEB-1, have been found to exhibit high levels of expression in both tumour-associated stroma and PDAC cells (Bronsert *et al.*, 2014; Galván *et al.*, 2015). ZEB1 functions by repressing transcription through the recruitment of the C-terminal-binding protein (CtBP) corepressor to its CtBP-interacting domain (Furusawa *et al.*, 1999). This mechanism is similar to SNAIL, as both proteins bind to the two E box sequences in the promoter region of E-cadherin to suppress its expression (Wong *et al.*, 2014). Furthermore, ZEB1 can also operate in a CtBP independent manner, ZEB1 interacts with BRG1, a SWI/SNF chromatin remodelling protein to repress the E-cadherin promoter (Sánchez-Tilló *et al.*, 2010). Interestingly, SNAIL upregulates the expression of ZEB1 (Peinado *et al.*, 2007). ZEB1 plays a crucial role as an EMT-TF by driving precursor lesions, invasion, and metastasis, making it a key driver in the progression of PDAC.

#### 1.6.1.2.4 PRRX1

PRRX1 is an intriguing EMT-TF that exhibits two major isoforms, PRRX1a and PRRX1b, which undergo isoform switching in PDAC (Takano *et al.*, 2016). The PRRX1b isoform stimulates EMT by upregulating N-cadherin, Vimentin, and fibronectin (Du *et al.*, 2021), thereby promoting invasion and dedifferentiation of tumours. PRRX1 is capable of binding to the promoter regions of mesenchymal markers, such as vimentin and N-cadherin, through its homeobox DNA-binding domain, which interacts with DNA via a helix-turn-helix structure (Du *et al.*, 2021). On the other hand, the PRRX1a isoform promotes tumour differentiation and metastatic outgrowth by inducing MET (Takano *et al.*, 2016). Isoform switching thus governs plasticity, enabling metastasis in PDAC. Additionally, PRRX1 is involved in a SNAIL-independent pathway that rather drives invasiveness in conjunction with TWIST1.

#### 1.6.2 EMT serves as a significant regulatory factor in drug resistance

EMT plays a crucial role in MDR in PDAC, as supported by various studies (Buck *et al.*, 2007; Li *et al.*, 2007; Arumugam *et al.*, 2009; El Amrani *et al.*, 2019; Porter *et al.*, 2019). Involvement of EMT in MDR is multifaceted and encompasses multiple regulatory mechanisms. Firstly, the EMT inducer SNAIL promotes antiapoptotic properties by activating Akt, upregulating the expression of the pro-survival protein Bcl-XL and disrupting cell-cycle progression (Vega *et al.*, 2004; Zheng *et al.*, 2015). Furthermore, EMT-TFs inhibit oncogene-induced senescence and apoptosis, particularly through the TP53- and retinoblastoma protein-dependent pathway (Pinho *et al.*, 2011). Importantly, EMT activation diminishes E-cadherin-mediated clustering of death receptor 4 (DR4) and DR5, rendering carcinoma cells resistant to tumour necrosis factor-related apoptosis-inducing ligand (TRAIL)-induced apoptosis (Vega *et al.*, 2004). Cellular quiescence is a major contributor to MDR, in that most conventional or targeted anti-cancer agents are effective against cells passing through the S and G2/M phases of the cell cycle, with cells in an EMT state they reside in G1/G0 phase, rendering normal therapies ineffective (Ungefroren *et al.*, 2022). EMT cells enter this quiescent state due to interactions between cell cycle machinery and EMT-TF networks, leading to the upregulation of p27<sup>KIP1</sup>, p21<sup>CIP1</sup>, and p57<sup>KIP2</sup>, which inhibit proliferation and activate migration (Akhmetkaliyev *et al.*, 2023). Particularly, the potent EMT inducer, TGFβ, acts as a canonical inhibitor of the cell cycle in the G1 phase. The SMAD-mediated activation of *CDKN2B* and *CDKN1A* genes, encoding cyclin dependent kinase (CDK) inhibitors p15<sup>INK1</sup> and p21<sup>CIP1</sup>, leads to cell stagnation in the G1 phase (Ikushima and Miyazono, 2010). Additionally, EMT activation

increases the expression of ABC transporters, which enhances the efflux of therapeutic agents from cells, resulting in MDR (Saxena *et al.*, 2011). For instance, ABCB1 and ABCC1 overexpression, induced by EMT, confers resistance to nucleoside analogues like GEM (Arumugam *et al.*, 2009; Adamska and Falasca, 2018). Interestingly, EMT has also been found to reduce the expression of hENT1 and hCNT3 in PDAC cells, thereby reducing the uptake of chemotherapeutic agents, further contributing to MDR (Zheng *et al.*, 2015). Moreover, EMT facilitates the evasion of immune surveillance by upregulating PD-1 expression and inhibiting thrombospondin-1 activity, impairing the function of cytotoxic T cells (Chen *et al.*, 2014). These findings underscore the intricate involvement of EMT in mediating MDR and recurrence in PDAC.

### **1.6.3 The significance of cholesterol in EMT induction and regulation**

The process of EMT at the cellular level is a complex network that relies on the manipulation of crucial cellular signalling pathways. These pathways extensively communicate to initiate and control the EMT program. Furthermore, the dysregulated cholesterol metabolism resulting from metabolic reprogramming also plays a distinct role in EMT. As previously mentioned, this metabolic reprogramming in PDAC leads to the activation of several cell signalling pathways, namely, PI3K/Akt, Hh, and Wnt/ $\beta$ -catenin, either directly or through lipid raft disruption. All of these pathways have been implicated in the activation of EMT-TFs, as discussed above, the upregulation of these pathways may thus be implicated in the promotion of EMT-TFS and hence the promotion of EMT in PDAC. Moreover, it has been suggested that the increased cholesterol levels resulting in increased lipid raft content alters the signalling of TGF- $\beta$ , subsequently promoting EMT (Kuzu *et al.*, 2016; Abdulla *et al.*, 2021). This alteration occurs due to the dependence of the formation of the T $\beta$ RI/T $\beta$ RII/TG $\beta$ -1 complex on lipid raft integrity (S. Zhang *et al.*, 2022). Furthermore, metabolic reprogramming in PDAC also drives the accumulation of lipid droplets in PDAC. These lipid droplets are able to serve as an energy source, supporting the long-distance spread cells during invasion (Tabas, 2002; Li *et al.*, 2016; Rozeveld *et al.*, 2020). Therefore, lipid droplets do not directly stimulate EMT but rather play a role in sustaining EMT for invasion. While targeting cholesterol appears to be a potential therapeutic option in PDAC, particularly in hopes of preventing EMT, certain studies have indicated the promotion of a basal-subtype of PDAC when cholesterol is depleted. Research by Gabitova-Cornell and team demonstrates that disrupting cholesterol biosynthesis through treatment with statins such as atorvastatin and mevastatin or by NAD(P) dependent steroid

dehydrogenase-like (*Nsdhl*) knockout results in a switch from the classical to basal subtype of PDAC. This switch is facilitated by disrupted cholesterol biosynthesis prompting SREBP1 activation, inducing TGF- $\beta$ 1 expression, and ultimately promoting EMT and basal conversion. This observation was further confirmed through multiplex immunofluorescence on archival surgical PDAC tissue from 55 untreated patients with documented statin use information. The analysis indicated increased PDAC aggressiveness (Gabitova-Cornell *et al.*, 2020). Another study found that statins induced a partial EMT state that could be reversed upon discontinuation of statin use. In this, PC cells were shown to reduce the formation of secondary tumours, a resultant effect of MET, a property that could be reversed if statin resistance was developed or statin usage stopped, and hence this would drive a more metastatic and invasive form of PC (Dorsch *et al.*, 2021). The impact of cholesterol depletion on EMT using alternative methods that do not target biosynthesis currently remains unexplored. Consequently, definitive conclusions regarding the benefits or drawbacks of targeting cholesterol in the treatment of PDAC remains inconclusive.

## **1.7 Rationale for the current study**

PDAC poses significant challenges in clinical management due to its metastatic nature and resistance to conventional chemotherapies such as GEM and 5-FU. This resistance is often attributed to the activation of EMT, a process closely associated with metastasis and drug resistance. Furthermore, studies highlight that dysregulated cholesterol metabolism, a characteristic feature of PDAC, plays a significant role in EMT induction and even drug resistance. Although targeting cholesterol shows promise as a therapeutic approach to counteract EMT and drug resistance to improve treatment outcomes, recent studies have revealed that cholesterol depletion through statins may assist in secondary tumour formation, thereby complicating the treatment landscape. Additionally, the impact of cholesterol depletion on EMT using direct methods has not yet been explored in PDAC, resulting in critical gaps in our knowledge. Consequently, the depletion of excess membrane and intracellular cholesterol using M $\beta$ CD or KS-01 (our lab's novel patented cholesterol-depleting agent) will be investigated. Therefore, in this study PANC-1 cells will undergo EMT induction through treatment with TGF- $\beta$ 1 followed by treatment with the cholesterol-depleting agents, M $\beta$ CD or KS-01, standard chemotherapy regimens (GEM or 5-FU), as well as a combination between KS-01 and the standard chemotherapy regimens. Through this approach, the study aims to unravel the complex interplay among cholesterol metabolism, EMT, and drug resistance.

Ultimately, the research endeavours to shed light on the potential of cholesterol depletion as a strategy for combatting metastasis in PDAC.

## **2 Aim and objectives**

### **2.1 Aim**

To determine the effects of cholesterol-depleting agents (KS-01 and M $\beta$ CD) alone or in combination with current chemotherapy treatments (GEM and 5-FU) on mesenchymal PC cells.

### **2.2 Objectives**

1. To induce EMT in PC cells (PANC-1) by utilising TGF- $\beta$ 1 and confirming the induction through cell morphology, immunofluorescence, growth curves, and reverse transcription quantitative polymerase chain reaction (RT-qPCR)
2. To determine the impact of combination treatments on cell viability by employing a 3-(4,5-Dimethylthiazol-2-yl)-2,5-Diphenyltetrazolium Bromide (MTT) assay.
3. To investigate the influence of EMT on cholesterol content following treatments with cholesterol-depleting agents using immunofluorescence.
4. To determine the effects of single and combination treatments on EMT induction by utilising immunofluorescence.
5. To assess the MDR and invasive capabilities of cells following single and combination treatments using drug resistance and Transwell<sup>TM</sup> invasion assays, respectively.
6. To examine the effects of single and combination treatments on the expression levels of genes and proteins involved in EMT, cancer drug resistance, and cholesterol metabolism signalling pathways through RT-qPCR.

### 3 Methodology

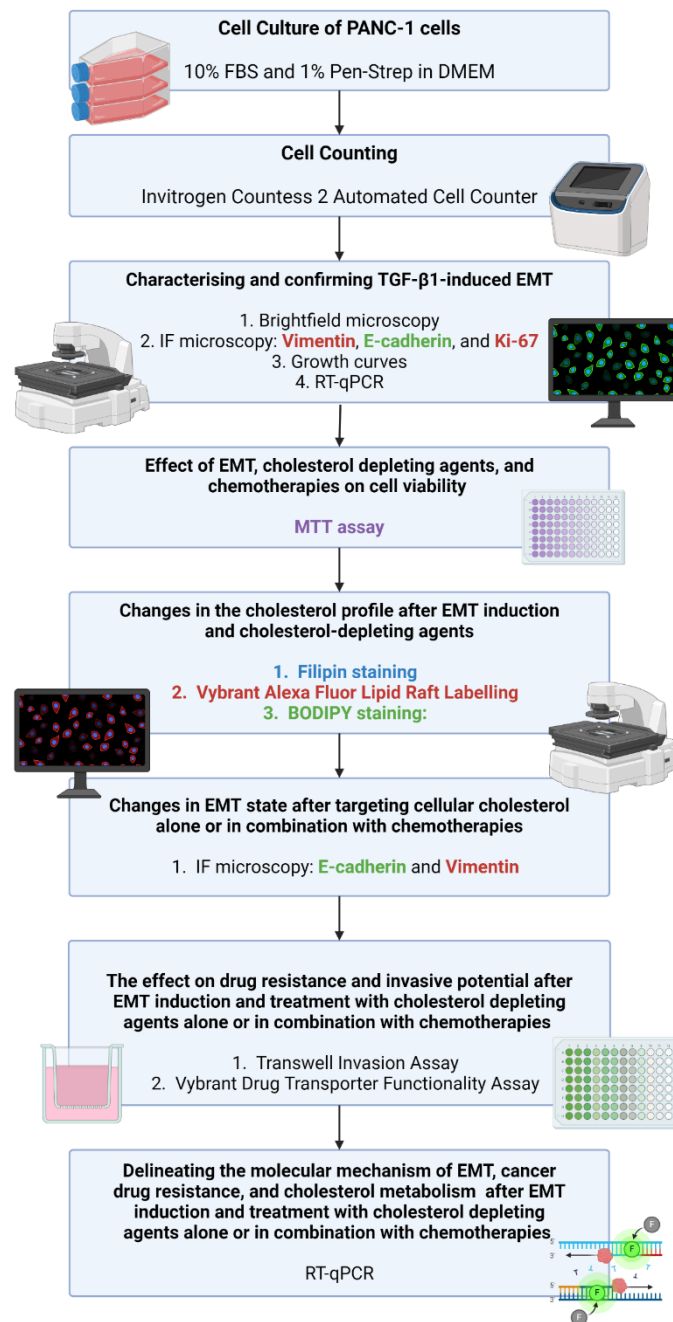


**Figure 3.1: Summary workflow**

*PANC-1 cells were cultured, counted and EMT was confirmed to be induced using brightfield microscopy, immunofluorescence microscopy, growth curves and RT-qPCR. Thereafter cell viability was analysed after EMT induction, cholesterol depleting agents, and chemotherapeutic agents. Changes in the cholesterol profile were then analysed post-EMT and with cholesterol depleting agents. Changes in the EMT state after targeting cholesterol with chemotherapies was also observed. The effect of drug resistance and invasion was then investigated after EMT, cholesterol depleting agents, and chemotherapeutic agents. Lastly, gene expression was investigated to aid in delineating the molecular mechanism of EMT, drug resistance, and cholesterol metabolism. (Created in BioRender.com)*

### 3.1 Cell culture of PANC-1 cells

In this study, the PANC-1 cell line (Cellonex, SA) was used. The PANC-1 cell line was isolated from the pancreatic duct of a 56-year-old, white, male with epithelioid carcinoma. These cells were authenticated using STR profiling with Inqaba and are confirmed to be mycoplasma free. The PANC-1 cell line is an adherent human PC epithelial cell line. It is known to exhibit both epithelial and mesenchymal phenotypes, which classifies it as a quasi-mesenchymal-cell line (Ungefroren *et al.*, 2022), hence throughout the dissertation the cells that have not been EMT-induced are referred to as partial-EMT cells and those that have been EMT-induced are referred to as post-EMT cells. PANC-1 cells were cultured in Dulbecco's Modified Eagle's Medium (DMEM) (Sigma Aldrich, UK) supplemented with 1% (v/v) Penicillin-streptomycin (Sigma Aldrich, UK) to prevent bacterial contamination and 10% (v/v) foetal bovine serum (FBS) (Celtic Molecular Diagnostics, SA) to provide all necessary hormones, adhesion and growth factors, minerals, and lipids. The cells were incubated at 37 °C with 5% CO<sub>2</sub> (Thermo Fisher Scientific, USA) to maintain a constant and normal physiological pH through the carbon dioxide–bicarbonate buffer system. These conditions closely simulate *in vivo* conditions, thereby promoting optimal growth of PANC-1 cells. Sub-cultivation of PANC-1 cells at 1:2 or 1:4 was performed once a confluency of 70% was reached.

### 3.2 Cell counting

The density of viable cells was determined prior to seeding for experiments and utilised selective staining with trypan blue. First, the media was removed from the flask, and the cells were washed twice with 1× phosphate buffered saline (PBS). Then, TrypLE™ (Thermo Fisher Scientific, USA) was added for 5-8 minutes to dissociate the cells from the flask and neutralised in a 1:1 ratio with 10% (v/v) DMEM. TrypLE™ is an animal-free trypsin product derived from recombinant bacteria and is known to be less toxic than trypsin (Nestler *et al.*, 2004; Alm *et al.*, 2014) allowing for longer incubation times to detach the cells, which is necessary for PANC-1 cells. TrypLE™ functions similarly to trypsin by cleaving peptide bonds on the C-terminal side of lysine and arginine, but with greater specificity and without affecting cell surface antigens (Tsuji *et al.*, 2017). An Invitrogen Countess 2 Automated Cell Counter (Thermo Fisher Scientific, USA) was employed to count viable cells. Specifically, 100 µl of cell suspension was diluted with 100 µl of 0.4% (v/v) trypan blue in a micro-Eppendorf tube (Sigma Aldrich, UK). Following dilution, 10 µl of the sample was placed on each side of the Countess Cell Counting Chamber Slides, which were read using the Invitrogen Countess 2 Automated Cell Counter (Thermo Fisher Scientific, USA) in which it utilises the Neubauer

method to determine cell density. The use of an automated cell counter improved time efficiency and minimised subjectivity or human error in cell counting, compared to traditional methods such as using a haemocytometer. Trypan blue stains non-viable cells due to their compromised membranes, allowing for the incorporation of trypan blue. In contrast, viable cells remained unstained, appearing clear. Subsequently, cells were seeded according to their required densities.

The total number of cells to be plated was determined using the following calculations:

*Calculation 1:*

$$\text{Volume of media required (a)} = \text{Volume to be plated} \times \text{Number of wells}$$

*Calculation 2:*

$$\text{Volume of cells required from the flask (b)} = \frac{\text{Total volume in the flask (ul)} \times \text{Number of cells to be plated} \times \text{Number of wells}}{\text{Total number of cells in the flask}}$$

*Calculation 3:*

$$\text{Volume of media to be added to the cells} = \mathbf{a - b}$$

### 3.3 Microscopy sample preparation

Prior to any fluorescent labelling, such as immunocytochemistry of E-cadherin and vimentin or cholesterol staining using Filipin, BODIPY, and Vybrant Alexa Fluor 594, it is necessary to complete sample preparation. In this study, the cells were prepared by seeding 40 000 cells/well into 24-well plates containing 12 mm round glass coverslips. The plates were then incubated overnight at 37 °C and 5% CO<sub>2</sub> to allow for cell attachment. Subsequently, concentrations of 5 ng/mL or 10 ng/mL TGF-β1 (Bio-Techne, USA) were tested for 24 and 48 hours to induce EMT. Thereafter, 10 ng/mL of TGF-β1 for 48 hours was chosen to induce EMT. Relevant drug treatments (Table 3.1) were administered during the final 4 hours of EMT induction. The drugs GEM, KS-01 and MβCD were dissolved in water and 5-FU dissolved in dimethyl sulfoxide. Concentrations of 1 μM GEM and 10 μM 5-FU were optimised previously in the PANC-1 cell line and relevant graphs can be seen in Figure A1. The 10 mM concentration of KS-01 and 1mM of MβCD concentrations were optimised by Saha et al., 2023. Following the treatment, the media in the wells was discarded and the cells were washed three times with 1×

PBS. The cells were fixed to the coverslips by exposing them to 10% Formalin (Sigma Aldrich, UK) for 10 minutes at room temperature. Formalin fixation preserves the native cellular components, such as carbohydrates, proteins, and bio-active moieties, as well as cell morphology by forming inter- and intra-molecular crosslinks (methylene bridges) within proteins, nucleic acids, and polysaccharides thus enabling further experimentation (Fox *et al.*, 1985; Paavilainen *et al.*, 2010). Following fixation, the formalin was discarded, and the coverslips were washed three times using 1× PBS and stored at 4 °C. These samples were used for future fluorescent staining which will be described in the following sections.

**Table 3.1: Drug treatments and their concentrations used throughout experimentation.**

<b>Drug Treatments</b>	<b>Concentration</b>
KS-01	10 mM
5-FU ( <i>Sigma Aldrich, UK</i> )	10 $\mu$ M
GEM ( <i>Sigma Aldrich, UK</i> )	1 $\mu$ M
KS-01 + 5-FU	10 mM + 10 $\mu$ M
KS-01 + GEM	10 mM + 1 $\mu$ M
M $\beta$ CD ( <i>Sigma Aldrich, UK</i> )	1 mM

### 3.3.1 Immunocytochemistry

Immunocytochemistry is a technique used to identify proteins and other macromolecules within cells, employing a specific combination of antibodies. In this study, the indirect method of immunocytochemistry was utilised. This method involved the use of a primary antibody that is capable of binding to a particular antigen. Subsequently, the primary antibody is incubated with a secondary antibody that is conjugated with a fluorophore that when bound to the primary antibody emits a fluorescent light allowing for the visualisation of proteins. Immunocytochemistry was utilised throughout the research project. Initially, it was used to validate EMT induction after treatment with TGF- $\beta$ 1 by detecting E-cadherin, Ki-67, and vimentin. Subsequently, it was employed to investigate the impact of chemotherapeutic agents and cholesterol-lowering drugs on the EMT state by examining the expression of E-cadherin and vimentin.

Following microscopy sample preparation, cells were permeabilised using 0.1% (v/v) Triton X-100 (Sigma Aldrich, UK), diluted in 1× PBS, for a duration of 15 minutes at room

temperature. Subsequently, the cells were blocked with 1% (w/v) bovine serum albumin (BSA) (Sisco Research Laboratories, India) prepared in 0.1% (v/v) PBST (1× PBS with 0.1% Tween 20 (Sigma Aldrich, UK)) for one hour. Blocking is performed to reduce the non-specific binding of antibodies as a result of surrounding inter-molecular forces. After this step, the primary antibody, which binds to a specific antigen, was added overnight at 4 °C (Table 3.2). The primary antibody was diluted in 0.1% (w/v) BSA prepared in 0.1% PBST (1:250 dilution). Once the incubation was complete the primary antibody was removed and recovered, and the cells were washed three times with 0.1% (v/v) PBST. The cells were treated with the corresponding secondary antibody (Table 3.2) and incubated for 45 minutes at room temperature in the dark. The secondary antibody was diluted in 0.1% (w/v) BSA prepared in 0.1% (v/v) PBST (1:1000 dilution). After the incubation, the secondary antibody was discarded, and the cells were washed three times with 0.1% (v/v) PBST. Nuclei were stained using 0.0001 mg/mL of 4',6-diamidino-2-phenylindole (DAPI) (Sigma Aldrich, UK) for 10 minutes at room temperature after which cells were washed three times with 1× PBS and coverslips were subsequently mounted on microscope slides using Fluoromount™ Aqueous Mounting Medium (Sigma Aldrich, UK). DAPI has the ability to bind to the minor grooves of double-stranded DNA, particularly areas rich in adenine-thymine (Chazotte, 2011), allowing for visualisation of the nuclei. After drying, the cells were viewed using the EVOS M7000 Imaging Station (Thermo Fisher Scientific, USA), and integrated optical density (OD) was quantified using Celleste 6 Image Analysis Software (Thermo Fisher Scientific, USA) or cells were visualised with EVOS Flouid™ Cell Imaging Station (Thermo Fisher Scientific, USA) and corrected total cell fluorescence (CTCF) was subsequently quantified using Image J where  $CTCF = \text{integrated density} - (\text{area of selected cell} \times \text{mean fluorescence of background})$  (Jakic *et al.*, 2017).

**Table 3.2: The primary and secondary antibodies used for target protein during immunocytochemistry**

<b>Target protein</b>	<b>Primary Antibody</b>	<b>Secondary antibody</b>
E-cadherin	Mouse Anti-Human E-cadherin (BD Pharmingen – 610182)	Goat Anti-Mouse Alexa Flour 488 (Thermo Fisher Scientific, A-11029)
Ki-67	Rabbit Anti-Human -Ki67 (Novus Biologicals - NB500-170)	Goat Anti-Rabbit Texas Red (Thermo Fisher Scientific, T-2767)

Vimentin	Rabbit Anti-Human Vimentin (Abcam - ab45939)	Goat Anti-Rabbit Texas Red (Thermo Fisher Scientific, T-2767)
----------	--	---

### 3.4 Growth curve using cell counts as a measure of proliferation

The growth of PANC-1 cells was analysed following treatment with or without 10 ng/mL TGF- $\beta$ 1 (Bio-Techne, USA) over a period of 96 hours. Cells were seeded in a 6-well plate at a density of 100 000 cells/well and incubated overnight at 37 °C and 5% CO<sub>2</sub> for cell attachment. Following this, cells were either treated with 10 ng/mL TGF- $\beta$ 1 (Bio-Techne, USA) or untreated for 96 hours where cells were detached and counted daily using the Invitrogen Countess 2 Automated Cell Counter (Thermo Fisher Scientific, USA) as previously described.

### 3.5 Cell viability assay

The effect of various chemotherapies and cholesterol-lowering drugs on cell viability was then measured relative to the untreated control. MTT is based on the principle that the mitochondria of viable cells possess NAD(P)H-dependent oxidoreductase enzymes. These enzymes can reduce MTT to formazan crystals, which can be solubilised, and the absorption read using a plate reader. The absorption is directly proportional to the concentration of formazan crystals and hence viable cells. While recognized for its speed and cost-effectiveness, this protocol is acknowledged for its limited sensitivity. Despite this, the MTT assay is known to be the gold standard for determining cell viability due to its simplicity, speed, and cost-effectiveness (Riss *et al.*, 2004; Aslantürk, 2018).

In a 96-well plate, 10 000 PANC-1 cells were seeded and incubated overnight at 37 °C and 5% CO<sub>2</sub> for cell attachment. EMT was then induced in the relevant wells by treating with 10 ng/mL TGF- $\beta$ 1 (Bio-Techne, USA) for 48 hours. Prior to drug treatments the media was removed, the wells were washed once with 1X PBS, and fresh 10% (v/v) DMEM was placed into the wells. In contrast, drug treatments commenced immediately after seeding and attachment in non-EMT induced cells. Partial- and post- EMT cells were subject to appropriate treatments, as described in Table 3.1 above, for 48 hours in which the positive control was 40  $\mu$ M plumbagin (Sigma Aldrich, UK). Plumbagin is a known inducer of apoptosis in PC cells by activating NF- $\kappa$ B regulated mitochondrial-mediated pathway which involves the activation of reactive oxygen species (Chen *et al.*, 2009; Xu *et al.*, 2013), reactive oxygen species also triggers ER stress-mediated apoptosis (Huang *et al.*, 2018). The blank wells contained only media. Blank wells were used to remove background interference in which the absorbance from the blank was

subtracted from all other wells, preventing the results from being skewed. After drug treatments, 0.5 mg/mL MTT (Thermo Fisher Scientific, USA) was added to each well for a three-hour incubation at 37 °C and 5% CO<sub>2</sub> which was then followed by overnight solubilisation in a solution of 10% (w/v) sodium dodecyl sulphate (SDS) (Sigma Aldrich, UK) and 10 mM hydrochloric acid (HCl) (Thermo Fisher Scientific, USA). This solution solubilised the formazan crystals that formed after treating the cells with MTT to produce a purple colour that can be measured spectrophotometrically. A VICTOR™ Nivo plate reader (Revvity Health Sciences, USA) was then used to measure absorbance at 570 nm. Viability of each treated sample was calculated as a percentage relative to the untreated control.

### **3.5.1 Cholesterol staining**

To assess the impact of EMT induction on cholesterol levels and the effect of cholesterol-depleting agents KS-01 and M $\beta$ CD on EMT, three stains were utilised. To stain and visualise lipid rafts the Vybrant Alexa Fluor® Lipid Raft staining kit (Thermo Fisher Scientific, USA) was utilised. In order to visualise lipid droplets as a manner of estimating CE content 4-difluoro-1,3,5,7,8-pentamethyl-4-bora-3a,4a-diaza-s-indacene (Cholesteryl BODIPY™ FL C12, Thermo Fisher Scientific, USA) stain was utilised. Lastly, in order to visualise the effects on free cholesterol, Filipin III (Sigma-Aldrich, UK) was utilised. The concentrations for KS-01 and M $\beta$ CD as mentioned in Table 3.1 have been extensively tested in breast and colorectal cancers in a laboratory setting and have been found to significantly deplete all cholesterol levels in these cancers after 2 to 4 hours of treatment, thus these concentrations were continued for further investigation in PC and utilised during the final 4 hours of EMT induction (Saha *et al.*, 2023, Perumel, *et al* unpublished article based on three research studies conducted in the lab). M $\beta$ CD served as a positive control, providing a basis for comparison with the effects of KS-01.

#### **3.5.1.1 Vybrant Alexa Fluor® Lipid Raft staining**

The Vybrant Alexa Fluor® Lipid Raft labelling kit (Thermo Fisher Scientific, USA) allows for the fluorescent labelling of lipid rafts in cells. The cholera toxin subunit B conjugate is able to bind to the ganglioside GM1, which is known to be enriched in lipid rafts found in the plasma membrane. The Alexa Fluor® 594 labelled cholera toxin subunit B then binds to the conjugate, cross-linking the lipid rafts into distinct patches that can be visualised.

Following microscopy sample preparation in which partial- and post-EMT cells were only treated with the cholesterol-lowering agents KS-01 and M $\beta$ CD with concentrations described in Table 3.1, cells were permeabilised using 0.1% (v/v) Triton X-100 (Sigma Aldrich, UK), diluted in 1X PBS, for 15 minutes at room temperature. Subsequently the 0.1% (v/v) Triton X-100 was removed and the cells were washed three times with 1X PBS. This was followed by the addition of 1  $\mu$ l/mL of Alexa Fluor® 594 cholera toxin subunit B conjugate diluted in 1 $\times$  PBS for 30 minutes at 37 °C. Thereafter, the solution was removed, and the cells were washed three times with 1X PBS. The anti-cholera toxin subunit B antibody was added in a 1:500 dilution for 30 minutes in the dark at 37 °C. Subsequently, the anti-cholera toxin subunit B solution was removed and the cells were washed three times with 1X PBS. Nuclei were stained using 0.0001 mg/mL DAPI (Sigma Aldrich, UK) for 10 minutes at room temperature. After staining, DAPI was recovered, and cells were washed three times with 1X PBS. The coverslips were then mounted on microscope slides using Fluoromount™ Aqueous Mounting Medium (Sigma Aldrich, UK) and was allowed to dry. Subsequently, cells were viewed using the EVOS M7000 Imaging Station (Thermo Fisher Scientific, USA), and fluorescence intensity was quantified using Celleste 6 Image Analysis Software (Thermo Fisher Scientific, USA).

### **3.5.1.2 BODIPY Staining**

Cholesteryl BODIPY™ FL C12 (Thermo Fisher Scientific, USA) is a neutral, lipophilic stain used to detect lipid droplets in cells by localising within the polar lipids of the cell.

Following microscopy sample preparation in which partial-and post-EMT cells were only treated with the cholesterol-lowering agents KS-01 and M $\beta$ CD with concentrations described in Table 3.1, cells were permeabilised using 0.1% (v/v) Triton X-100 (Sigma Aldrich, UK), diluted in 1X PBS, for 15 minutes at room temperature. Subsequently, the 0.1% (v/v) Triton X-100 was removed, and the cells were washed three times with 1X PBS. This was followed by the addition of 4  $\mu$ l/mL of BODIPY™ FL C12 diluted in 70% (v/v) ethanol for 30 minutes in the dark at 37 °C. The BODIPY™ FL C12 was then discarded and the cells were washed three times with 1X PBS. Nuclei were stained using 0.0001 mg/mL DAPI (Sigma Aldrich, UK) for 10 minutes at room temperature after which DAPI was recovered and cells were washed three times with 1X PBS. The coverslips were then mounted on microscope slides using Fluoromount™ Aqueous Mounting Medium (Sigma Aldrich, UK). After drying, cells were then viewed using the EVOS M7000 Imaging Station (Thermo Fisher Scientific, USA), and fluorescence intensity was quantified using Celleste 6 Image Analysis Software (Thermo Fisher Scientific, USA).

### 3.5.1.3 Filipin staining

Filipin III (Sigma-Aldrich, UK) is a polyene macrolide antibiotic derived from *Streptomyces filipinensis* that binds to cholesterol but not esterified sterols. This staining method is used to detect free cholesterol levels in fixed cells only (Maxfield and Wüstner, 2012).

Following microscopy sample preparation in which cells were only treated with the cholesterol-lowering agents KS-01 and M $\beta$ CD with concentrations described in Table 3.1, the cells were treated with 6  $\mu$ l/mL of Filipin III diluted in 1 $\times$  PBS in the dark for 2 hours at room temperature. In the final 10 minutes of incubation, the nuclei were stained red with NucRed<sup>TM</sup> Dead 647 (Thermo Fisher Scientific, USA). This staining solution was then removed, and the cells were washed three times with 1X PBS. The coverslips were then mounted on microscope slides using Fluoromount<sup>TM</sup> Aqueous Mounting Medium. After drying, cells were then viewed using the EVOS M7000 Imaging Station (Thermo Fisher Scientific, USA), and fluorescence intensity quantified using Celleste 6 Image Analysis Software (Thermo Fisher Scientific, USA).

### 3.6 MDR assay

The Vybrant<sup>®</sup> MDR Assay Kit (Thermo Fisher Scientific, USA) was used in order to screen the functionality of ABCB1. This assay relies on the principle that the fluorogenic dye calcein acetoxymethyl ester (calcein AM) acts as a substrate for efflux via ABCB1. When calcein AM enters the cell its ester bonds are cleaved resulting in a hydrophilic and fluorescent calcein, however when cells express high levels of ABCB1 the non-fluorescent calcein is expelled via the pump resulting in a lower fluorescence.

In a 96-well plate, 10 000 PANC-1 cells were seeded and incubated overnight at 37 °C and 5% CO<sub>2</sub> for cell attachment. EMT was then induced in the relevant wells as previously described, after which drug treatments (Table 3.1) were administered in the final 4 hours of EMT induction. In post-EMT cells, 20  $\mu$ M Verapamil, a known ABCB1 inhibitor, served as the positive control and was administered for the same amount of time. Following drug treatments, 0.25  $\mu$ M of calcein-AM was administered to each well and subsequently incubated at 37 °C and 5% CO<sub>2</sub> for 30 minutes in the dark. This was followed by two washes with 200  $\mu$ l 1 $\times$  PBS after which 45  $\mu$ l of 1 $\times$  PBS was placed into each well for imaging using the EVOS M7000 Imaging Station (Thermo Fisher Scientific, USA). The fluorescence was then quantified using the Celleste 6 Image Analysis Software (Thermo Fisher Scientific, USA). The MDR activity

was assessed based on calcein retention in cells and hence corresponding fluorescence in the cell.

### **3.7 Transwell® invasion assay**

Invasion is the key mechanism for cancer metastasis and cell invasion assays allow for the quantification of the invasive potential of cells by viewing their response to chemo-attractants such as growth factors and lipids. The Transwell® Cell invasion assay relies on the principle that metastatic cells are able to invade through extracellular matrix materials, like GelTrex™ or Matrigel™ matrix, followed by a porous membrane as a response to a chemotactic gradient. This mimics the invasion of these cells in the body as cancer cells are able to migrate and invade through the extracellular matrix to the blood and finally attach to a different site.

In a 24-well plate, 40 000 PANC-1 cells were seeded and incubated overnight at 37 °C and 5% CO<sub>2</sub> for cell attachment. EMT was then induced in the relevant wells as previously described after which drug treatments (Table 3.1) were administered in the final 4 hours of EMT induction. The cells in each well were then detached, counted using the Invitrogen Countess 2 Automated Cell Counter (Thermo Fisher Scientific, USA), and diluted to 300 000 cells/mL in serum-free media supplemented with 0.2% (w/v) BSA. BSA was used to support the continuous growth and survival of the cells. Thereafter, 80 µL of the PANC-1 cell suspension was mixed with 20 µL of GelTrex™ (Thermo Fisher Scientific, USA) and seeded in the Millicell® cell culture inserts (Sigma Aldrich, UK) containing 0.8 µm pores. The lower chamber contained 500 µL of DMEM supplemented with 10% (v/v) FBS to allow for chemotaxis. Cells were then incubated for 24 hours at 37 °C and 5% CO<sub>2</sub> after which the non-invasive cells were removed using cotton swabs. Invasive cells on the underside of the membrane were then fixed using 10% Formalin for 10 minutes at room temperature followed by dipping of the membrane in 1× PBS to gently wash. Cells were subsequently stained using 0.0001 mg/mL DAPI (Sigma Aldrich, UK) for 10 minutes at room temperature for future visualisation. The membrane was again gently washed through dipping in 1× PBS three times. The invasive PANC-1 cells were then viewed using the EVOS M7000 Imaging Station (Thermo Fisher Scientific, USA), and the total cell number per membrane was quantified using Celleste 6 Image Analysis Software (Thermo Fisher Scientific, USA).

### **3.8 RNA extraction and purification**

The E.Z.N.A.® HP Total RNA Isolation Kit (Omega Bio-Tek, USA) was utilised for RNA extraction. Initially, 300 000 cells were plated in 6-well plates and incubated overnight at 37

°C and 5% CO<sub>2</sub> for cell attachment. EMT was then induced in the relevant wells by treating with 10 ng/mL TGF-β1 (Bio-Techne, USA) for 48 hours. Relevant drug treatments, from Table 3.1 above, were administered in the final 4 hours of EMT induction. Cells were then harvested and centrifuged at 1 400 rpm for 8 minutes to pellet the cells. These pellets were resuspended in 350 μL GTC lysis buffer supplemented with β-mercaptoethanol (Sigma Aldrich, UK) and vortexed for 30 seconds. The β-mercaptoethanol eliminates RNases released during cell lysis (Van Der Poel-Van De Luytgarde *et al.*, 2013; Masoodi *et al.*, 2021). The lysate was then passed through an RNA homogenizer mini-column at maximum speed for 1 minute allowing for the complete breakdown of the cell and its constituents. The filtrate was then mixed with an equal volume of 70% (v/v) ethanol to precipitate out nucleic acids (Rio *et al.*, 2010). This mixture was vortexed for 30 seconds and passed through a HiBind® RNA Mini Column at 12 100 rpm for 1 minute after which the flow through was discarded. The column was then centrifuged once at 12 100 rpm for 30 seconds with 500 μL RNA Wash Buffer I. This was followed by two centrifugation steps with 500 μL RNA Wash Buffer II diluted in 100% (v/v) ethanol at 12 100 rpm for 30 seconds. These steps act to wash the RNA, removing any remaining salts and proteins, as well as concentrate the nucleic acids (Farrell, 2010). The flow-through was discarded after all RNA wash steps. The HiBind® RNA Mini Column was then spun at maximum speed for 7 minutes to ensure all the ethanol had evaporated from the RNA. Lastly, RNA was eluted, and the sample resuspended in 40 μL of DNase/Rnase Free water (Omega Bio-Tek, USA).

The purity and quality of the RNA were then investigated prior to cDNA synthesis, polymerase chain reaction (PCR) and real time-quantitative PCR (RT-qPCR). The Nanodrop 1000 spectrophotometer (Thermo Fisher Scientific, USA) was used to quantify the RNA concentration (ng/μl), as well as indicate the purity of the RNA using the A<sub>260</sub>/A<sub>280</sub> and A<sub>260</sub>/A<sub>230</sub> ratios. The A<sub>260</sub>/A<sub>280</sub> ratio allows for the confirmation of RNA purity and lack of protein contamination by comparing the absorbance wavelengths of 260 nm and 280 nm which are the wavelengths that display a maximum absorbance for the aromatic compounds in nucleic acids and proteins respectively. In addition, the A<sub>260</sub>/A<sub>230</sub> ratio indicates any contaminants which display a maximum absorbance at 230 nm such as carbohydrates, salts, phenol, and EDTA.

Furthermore, the integrity of the RNA was assessed by mixing 500 ng of RNA with 2 μl 2X RNA loading dye (Thermo Fisher Scientific, USA) which were then loaded carefully into the wells of a 1% (w/v) agarose gel (0.5 g agarose powder in 50 ml 1× Tris-borate EDTA (TBE)

buffer) containing ethidium bromide (Thermo Fisher Scientific, USA) alongside the RiboRuler High Range RNA Ladder (Thermo Fisher Scientific, USA). The gel was subsequently electrophoresed at 80 V for approximately 1 hour and then viewed using the ChemiDoc™ XRS+ System (BioRad, USA) to visualise the 18S and 28S rRNA subunits. RNA with an A260/280 ratio of 2.0 and A260/230 ratio of 2.0-2.2, and good integrity was accepted for cDNA synthesis.

### 3.8.1 cDNA synthesis

Following RNA extraction, cDNA synthesis was performed using the RevertAid First Strand cDNA Synthesis Kit (Thermo Fisher Scientific, USA) for each treatment type. The reaction mixture was prepared according to Table 3.3 and dispensed into 0.2 mL microcentrifuge tubes. The tubes were mixed gently and centrifuged in a microcentrifuge (Starlab, Germany; Celtic Molecular Diagnostics, SA) to eliminate air bubbles.

**Table 3.3: Components of cDNA synthesis reaction**

Component	Volume (µL)
RevertAid Reverse Transcriptase (200 U/µL)	1
RiboLock RNase Inhibitor (200 U/µL)	1
5X Reaction Buffer (250 mM Tris-HCl (pH 8.3), 250 mM KCl, 20 mM MgCl <sub>2</sub> , 50 mM DTT)	4
10mM dNTP Mix	2
Oligo(dT) <sub>18</sub> Primer (100 µM)	1
RNA (1µg)	x
Nuclease-free water	x
<b>Total Volume</b>	<b>20</b>

A no template control (NTC) was used to confirm that amplification was as a result of the presence of RNA and not contamination of the reaction mixture. The reaction tubes were then placed in a T100™ Thermal Cycler at the following conditions: 1 cycle at 42 °C for 1 hour, 1 cycle at 70 °C for 5 minutes. Subsequently, samples were either immediately placed on ice for use in PCR or RT-qPCR or stored at -20°C for long-term storage.

### 3.9 Primer optimisation

In this study, PCR was utilised to optimise the annealing temperatures of selected primers involved in EMT, cholesterol homeostasis and drug resistance. Initially, primer sequences were selected from the PrimerBank database (<http://pga.mgh.harvard.edu/primerbank/>). Thereafter the primers were validated to target the correct gene, have a GC content of 35-65%, length of 18-22 base pairs, and an amplicon length of 70-140 base pairs using the UCSC In-Silico PCR Genome Browser (<https://genome.ucsc.edu/cgi-bin/hgPcr>), the NCBI Primer-BLAST website (<https://www.ncbi.nlm.nih.gov/tools/primer-blast/>), and the Integrated DNA Technologies (IDT) OligoAnalyzer™ Tool (<https://eu.idtdna.com/pages/tools/oligoanalyzer>). The validated primer sequences were then synthesised by IDT (Whitehead Scientific, SA).

#### 3.9.1 PCR

In order to find the annealing temperature for each primer pair to be used in RT-qPCR, PCR had to first be performed. The reaction mixture was prepared according to Table 3.4 and dispensed into 0.2 mL microcentrifuge tubes. The OneTaq® 2X Master Mix with Standard Buffer (New England Biolabs, USA) allowed for the amplification of amplicons without altering the pH.

*Table 3.4: Components of PCR reaction*

Component	Volume (µL)
OneTaq® 2X Master Mix with Standard Buffer	6.25
Forward primer (10 µM)	0.4
Reverse primer (10 µM)	0.4
RNase-free water	3.45
Template cDNA	2
<b>Total volume</b>	<b>12.5</b>

An NTC was again used to confirm that amplification was as a result of the presence of cDNA and not contamination of the reaction mixture. The reaction tubes were then placed in a T100™ Thermal Cycler with the following parameters in Table 3.5.

**Table 3.5: Cycling conditions for PCR**

Step	Time	Temperature (°C)	Cycle number
Initial activation	10 minutes	95	1
Denaturation	10 seconds	95	40
Annealing	15 seconds	Temperature range for each primer pair based on $T_m$	
Extension	20 seconds	72	
Final extension	1 minute	72	1

Subsequently, samples were either immediately placed on ice for visualisation on a 1% (w/v) agarose gel or stored at -20°C for long-term storage. Each PCR product was gently mixed with 6X DNA loading dye (Thermo Fisher Scientific, USA) which were then loaded into each well of the gel alongside a 50 bp DNA ladder (New England Biolabs, USA) to determine the amplicon size and to determine if any primer-dimers were present. The gel was subsequently electrophoresed at 80 V for approximately 1 hour and then viewed using the ChemiDoc™ XRS+ System (BioRad, USA). Annealing temperatures with the brightest bands and without any non-specific primer dimers were then chosen to be used in RT-qPCR (Table 3.6).

**Table 3.6: Optimised annealing temperatures of genes of interest alongside their forward and reverse sequences**

Gene	Primer Sequence (5'- 3')	Annealing temperature (°C)
<i>SNAIL1</i>	F: TCGGAAGCCTAACTACAGCGA	61
	R: AGATGAGCATTGGCAGCGAG	
<i>TGF-β1</i>	F: TACCTGAACCCGTGTTGCTCTC	62
	R: GTTGCTGAGGTATCGCCAGGAA	
<i>SREBF2</i>	F: CTGCAACAACAGACGGTAATGA	63
	R: CCATTGGCCGTTTGTGTCAG	
<i>LDLR</i>	F: ACCAACGAATGCTTGGACAAC	61
	R: ACAGGCACTCGTAGCCGAT	
<i>ABCA1</i>	F: ACCCACCCTATGAACAACATGA	61
	R: GAGTCGGGTAACGGAAACAGG	

<i>hENT1</i>	F: CTCCAACCTCTCAGCCCACCAATGA R: GAAGTAACGTTCCCAGGTGCTGC	61
<i>ABCC5</i>	F: AGTCCTGGGTATAGAAGTGTGAG R: ATTCCAACGGTTCGAGTTCTCC	63
<i>ABCG2</i>	F: CAGGTGGAGGCAAATCTTCGT R: ACCCTGTTAATCCGTTTCGTTTT	60
<i>ABCB1</i>	F: TTGCTGCTTACATTCAGGTTTCA R: AGCCTATCTCCTGTTCGCATTA	62
<i>GAPDH</i>	F: GGAGCGAGATCCCTCCAAAAT R: GGCTGTTGTCATACTTCTCATGG	62

### 3.10 RT-qPCR

To quantify gene expression of genes involved in drug resistance, cholesterol homeostasis, and EMT, the Luna® Universal qPCR Master Mix (New England Biolabs, USA) was utilised to conduct RT-qPCR. During the annealing and extension stages of RT-qPCR Luna® is able to bind to the minor grooves of double-stranded DNA (dsDNA). By monitoring the fluorescence output after each amplification cycle the relative quantification of the amount of DNA present can be calculated.

The RT-qPCR reaction mixture was prepared according to Table 3.7 for each gene and sample type after which 10 µL of the reaction mixture was dispensed into optically clear strip PCR tubes, sealed with optically clear flat caps, and centrifuged in a microcentrifuge (Starlab, Germany; Celtic Molecular Diagnostics, SA) to eliminate air bubbles. The QuantStudio™ 5 Real-Time PCR system (Thermo Fisher Scientific, USA) was then used with the cycling conditions as described in Table 3.8. Subsequently, the C<sub>q</sub> values were found using the Design & Analysis 2 software (Thermo Fisher Scientific, USA) after setting a quantification threshold. Glyceraldehyde 3-phosphate dehydrogenase (GAPDH) was used as a reference gene for expression normalization during fold change calculations. Reference genes, also known as housekeeping genes, are fundamental constitutively expressed genes utilised in RT-qPCR to normalize gene expression levels (Ong, 2018). These genes play a critical role in mitigating the limitations associated with RT-qPCR, including primer specificity, uniform RNA quality, inhibitor presence, reverse transcription efficiency and ensuring equal cDNA levels across samples for accurate expression normalization and data interpretation (Turabelidze *et al.*, 2010). Following RT-qPCR gene expression was quantified using the Livak method of relative

quantification (Livak and Schmittgen, 2001) and data was presented as log<sub>2</sub> of this fold change.

The log<sub>2</sub> fold change was calculated using the following calculations:

*Calculation 1:*

$$\Delta Ct = Ct (\text{target gene}) - Ct (\text{endogenous control GAPDH})$$

*Calculation 2:*

$$\Delta\Delta Ct = \Delta Ct (\text{experimental sample}) - \Delta Ct (\text{normal sample})$$

*Calculation 3:*

$$\text{Normalised target gene expression in sample (fold change)} = 2^{-\Delta\Delta Ct}$$

*Calculation 4:*

$$\begin{aligned} \log_2 \text{ fold change of expression of the sample} \\ = \log_2 (\text{Normalised target gene expression of sample}) \end{aligned}$$

**Table 3.7: Components of Luna® Universal qPCR reaction**

Component	Volume (µL)
Luna® Universal qPCR Master Mix	5
Forward Primer	0.25
Reverse Primer	0.25
cDNA	0.5
Nuclease-free water	4
<b>Total Volume</b>	<b>10</b>

**Table 3.8: Two-step cycling conditions for RT-qPCR using the QuantStudio™ 5 Real-Time PCR System**

Step	Time (Seconds)	Temperature (°C)	Cycle number
Initial denaturation	60	95	1

Denaturation	15	95	
Annealing	30	Optimised primer temperature	40
Extension	30 (+ plate read)	60	

### 3.11 Statistical analysis

All statistical analysis was performed using GraphPad Prism version 8.4.3, with all experiments conducted in both technical and biological duplicate or triplicate where possible. To measure the statistical significance of the results, an analysis of variance (ANOVA) test was run to compare the means among three or more groups (Mishra et al., 2019). This was followed by a Tukey post hoc test to determine the statistical comparisons between the means of the group. To measure the statistical significance of smaller data sets with fewer than three groups or in cases where an ANOVA was not possible, a two-tailed student's t-test was utilised. This tests for changes in the variable, and determines if there are any significant differences between the means of the groups. Values were considered significant at  $p < 0.05$ . For any assays conducted in a 96-well plate, a Z-factor was calculated (Zhang *et al.*, 1999). This value indicated the robustness and reliability of the scientific data produced, with a Z-factor above  $> 0.6$  considered the acceptable range for use.

## 4 Results

### 4.1 Analysing Changes in PANC-1 Cell Morphology Following TGF- $\beta$ 1 Treatment

The PANC-1 cell line is an adherent human PC epithelial cell line. It is known to exhibit both epithelial and mesenchymal phenotypes, which classifies it as a quasi-mesenchymal-cell line (Ungefroren *et al.*, 2022). Previous studies have indicated that the PANC-1 cell line can undergo a shift towards a more mesenchymal or epithelial phenotype (Ungefroren *et al.*, 2022). Following the treatment with 5 ng/mL and 10 ng/mL TGF- $\beta$ 1 for incubation periods of 24 or 48 hours, the cells exhibited characteristics associated with the mesenchymal phenotype particularly after 48 hours of treatment (Figure 4.1d and e). After 48 hours of treatment, and specifically with a concentration of 10 ng/mL of TGF- $\beta$ 1, there was a notable loss of cell-cell contacts and a transition to an elongated, spindle-like morphology. Consequently, further investigation was conducted using a 48-hour treatment with concentrations of 5 ng/mL and 10 ng/mL.

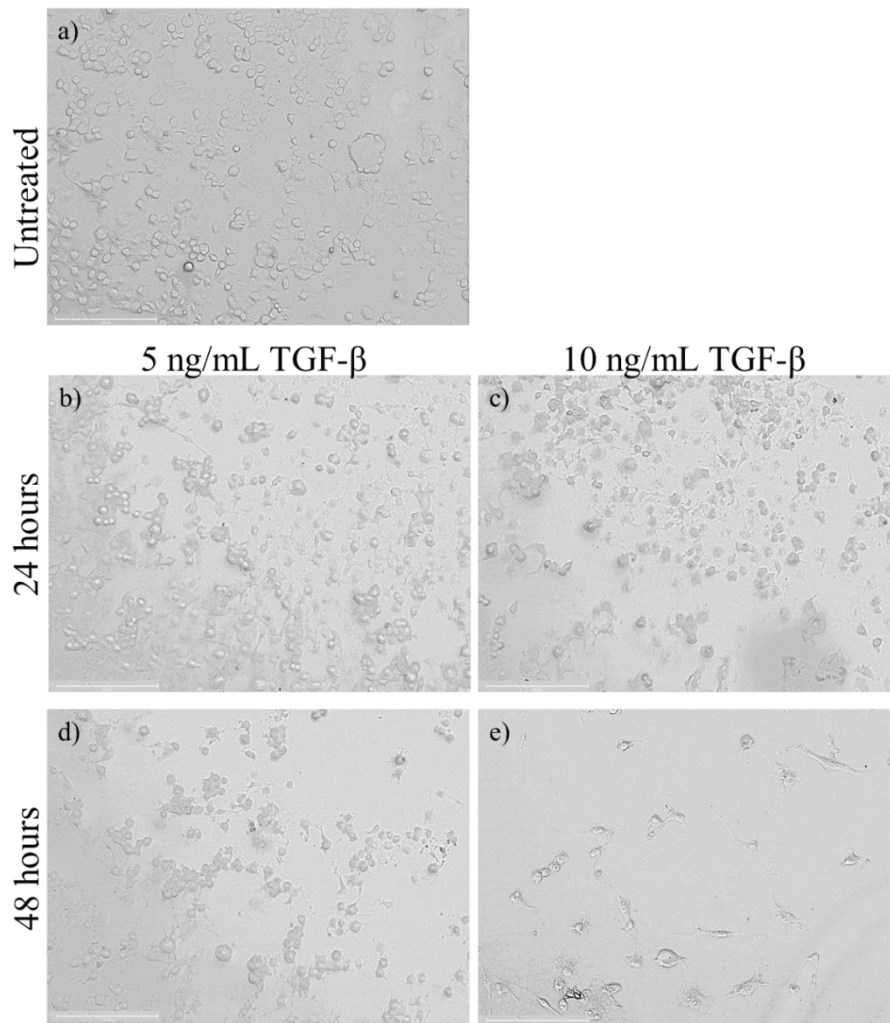


**Figure 4.1: Changes in morphology of PANC-1 cells after various TGF- $\beta$ 1 treatment times and concentrations.**

*The images depict the morphological changes observed in PANC-1 cells following treatment with various concentrations and durations of TGF- $\beta$ 1. The images correspond to the following conditions: (a) Untreated, (b) 5 ng/mL TGF- $\beta$ 1 for 24 hours, (c) 10 ng/mL TGF- $\beta$ 1 for 24 hours, (d) 5 ng/mL TGF- $\beta$ 1 for 48 hours, and (e) 10 ng/mL TGF- $\beta$ 1 for 48 hours. Cells were imaged using the EVOS M7000 Imaging Station at 20 $\times$  magnification. Scale bar represents 150  $\mu$ M. Notably, the most pronounced mesenchymal-like morphology was observed after 48 hours of treatment, particularly at a concentration of 10 ng/mL of TGF- $\beta$ 1.*

#### **4.2 Confirming EMT induction using Vimentin and E-cadherin staining**

Following morphological analysis to visualise EMT induction in PANC-1 cells, immunofluorescence microscopy was utilised to study the expression of key EMT markers following TGF- $\beta$ 1 administration. E-cadherin is a cell junction protein, indicative of an

epithelial phenotype, whereas vimentin, an intermediate filament, is the marker indicative of a mesenchymal phenotype (Thiery *et al.*, 2009; Ye and Weinberg, 2015). As seen in Figure 4.2 vimentin expression increased by 16% after 24 hours and 44% after 48 hours of treatment with 10 ng/mL TGF- $\beta$ 1, the only statically significant increase was after 48 hours. As seen in Figure 4.3, E-cadherin expression decreased by 49%. These markers indicate the promotion of an EMT state. Therefore, treatment conditions of 10 ng/mL TGF- $\beta$ 1 for 48 hours was selected to induce complete EMT in PANC-1 cells.

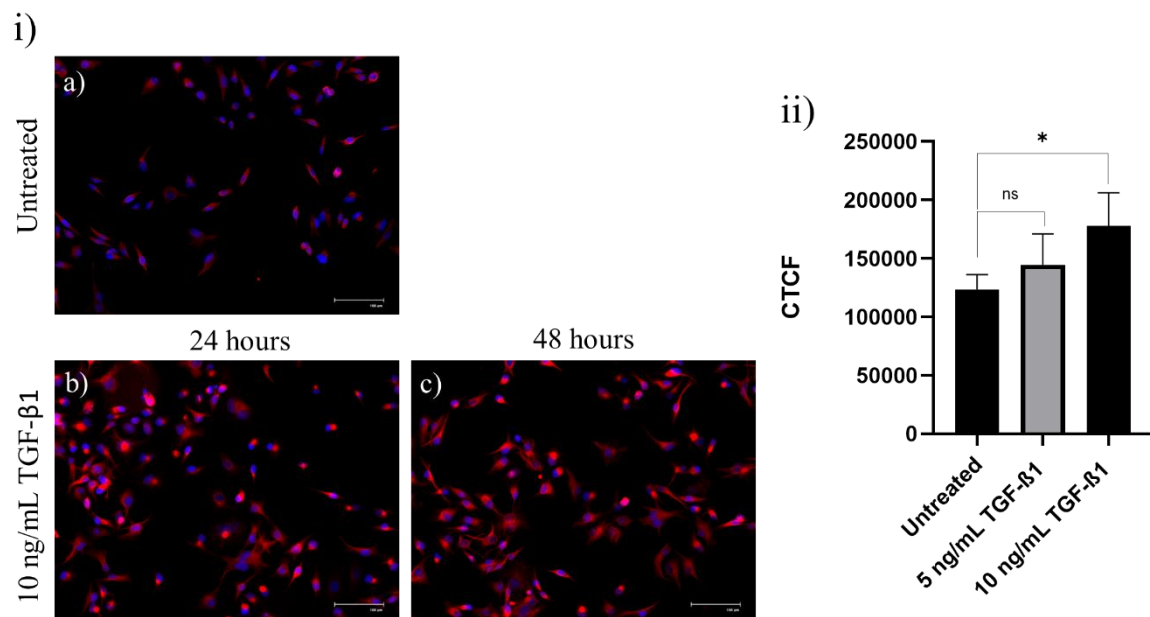


**Figure 4.2: Changes in vimentin fluorescence in PANC-1 cells after TGF- $\beta$ 1 treatment**

The representative immunofluorescent images illustrate the impact of various TGF- $\beta$ 1 treatments on vimentin expression levels. (i) The images correspond to the following conditions: (a) Untreated, (b) 5 ng/mL TGF- $\beta$ 1 for 48 hours, and (c) 10 ng/mL TGF- $\beta$ 1 for 48 hours. Cells were labelled with Rabbit Anti-Human Vimentin primary antibody and Goat Anti-Rabbit Texas Red secondary antibody. Nuclei are stained with DAPI and shown in blue, and vimentin in red. (ii) Quantification revealed a significant increase vimentin, a mesenchymal marker, only after treatment with 10 ng/mL of TGF- $\beta$ 1 for 48 hours. Images were captured using EVOS Flويد™ Cell Imaging Station at 20 $\times$  magnification and subsequently quantified using Image J. A corresponding bar graph depicting mean values of the corrected total cell fluorescence (CTCF) from three independent repeats, is included. Treatment groups were compared to the untreated control. Scale bar represents 100  $\mu$ M. Data are mean  $\pm$  SD; (n = 3) from raw data. Treatment groups were compared to the untreated control. Statistical analysis was calculated using a two-tailed students t-test, where \* $p$  < .05, \*\* $p$  < .01, \*\*\* $p$  < .001, \*\*\*\* $p$  < .0001, and ns = non-significant indicates a significant or non-significant difference to the untreated control.

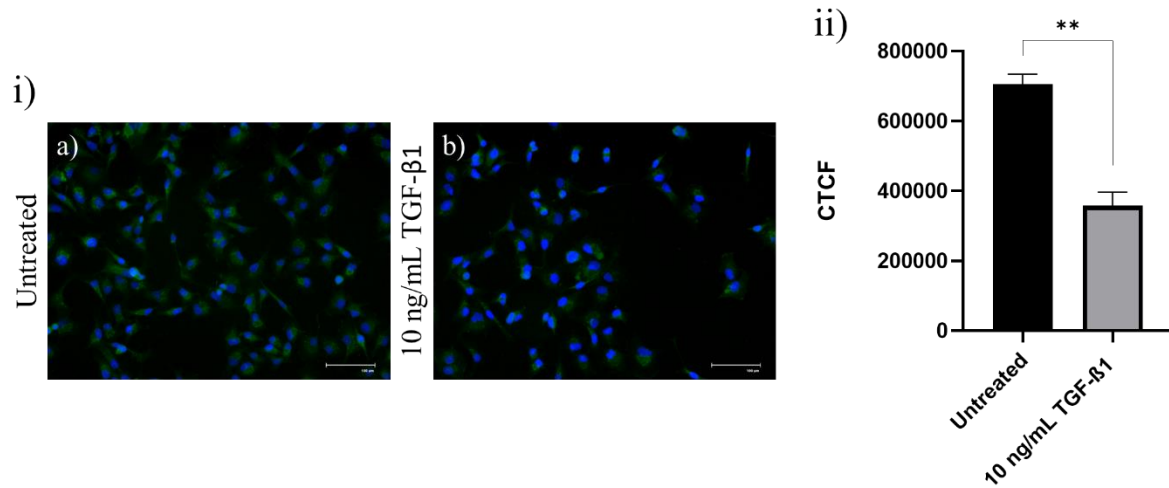


**Figure 4.3: Changes in E-cadherin fluorescence in PANC-1 cells after TGF-β1 treatment.**

The representative immunofluorescent images depict the impact of 10ng/mL TGF-β1 treatment for 48 hours on E-cadherin expression levels. (i) The images correspond to the following conditions: (a) Untreated and (b) 10 ng/mL TGF-β1 for 48 hours. PANC-1 cells were exposed to 10 ng/mL of TGF-β1 for 48 hours. Cells were labelled with Mouse Anti-Human E-cadherin primary antibody and Goat Anti-Mouse Alexa Fluor 488 secondary antibody. Nuclei are stained with DAPI and shown in blue, and E-cadherin in green. (ii) Quantification revealed a significant decrease in E-cadherin, an epithelial marker, after 10 ng/ml of TGF-β1 for 48 hours. Images were captured using EVOS FLoid™ Cell Imaging Station at 20× magnification and subsequently quantified using Image J. A corresponding bar graph depicting mean values of the corrected total cell fluorescence CTCF from three independent repeats, is included. Treatment groups were compared to the untreated control. Scale bar represents 100 μM. Data are mean ± SD; (n = 3) from raw data, where n is the total number of cells quantified per condition. Treatment groups were compared to the untreated control. Statistical analysis was calculated using a two-tailed students t-test, where \*p < .05, \*\*p < .01, \*\*\*p < .001, \*\*\*\*p < .0001, and ns = non-significant indicates a significant or non-significant difference to the untreated control.

### 4.3 Investigating the effect of TGF-β1-induced EMT on cell proliferation

Since the induction of EMT has been linked to cell quiescence (Akhmetkaliyev *et al.*, 2023), it was crucial to investigate the impact of 10 ng/mL TGF-β1 treatment for 48 hours on cell proliferation. This was done by analysing growth curves and immunofluorescence of Ki-67, a cell proliferation marker that is present in all active phases of the cell cycle, namely G1, S, G2 and M-phase where low levels of Ki-67 can indicate a stagnation in the G1/S checkpoint phase (Miller *et al.*, 2018). The growth curves, depicted in Figure 4.4, clearly demonstrate that the growth of PANC-1 cells reached a plateau after 48 hours of treatment with 10 ng/mL TGF-β1, whereas the untreated cells continued to proliferate exponentially until 96 hours. Subsequently, the expression of Ki-67 was examined, revealing a significant 53% decrease in expression after

48 hours of treatment with 10 ng/mL TGF- $\beta$ 1 (Figure 4.5ia, ib, and ii). These findings confirm a reduction in cell proliferation and a halt in the cell cycle following treatment with 10ng/mL TGF- $\beta$ 1. The morphological changes observed, such as a transition to a more spindle-like shape (Figure 4.1), along with the promotion and reduction in the expression of vimentin and E-cadherin respectively (Figure 4.2 and Figure 4.3), and lastly the reduction in proliferation and halt of the cell cycle (Figure 4.4 and Figure 4.5) as seen after treatment with 10 ng/mL TGF- $\beta$ 1 confirmed the induction of EMT and was chosen for future experiments to induce EMT.

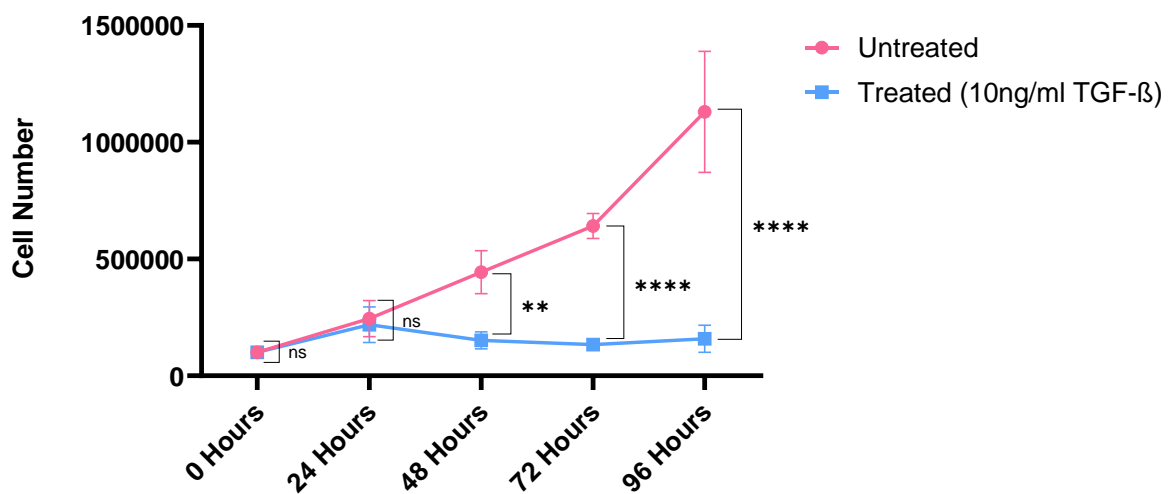


**Figure 4.4: Growth curves using cell counts as a measure of proliferation of the PANC-1 cell line before and after TGF- $\beta$ 1 treatment.**

*Cell numbers were analysed daily using the trypan blue cell counting method using the Invitrogen Automated Cell Counter in triplicates after treatment with 10 ng/ml TGF- $\beta$ 1. Cell numbers reduced and stagnated after EMT induction whereas the untreated cells continued to proliferate exponentially. Data represents the mean  $\pm$  SD; (n = 3). Treatment groups were compared to the untreated control. Statistical analysis was calculated using a two-way ANOVA followed by a Tukey post-hoc test to compare individual differences, where \*p < .05, \*\*p < .01, \*\*\*p < .001, \*\*\*\*p < .0001, and ns = non-significant indicates a significant or non-significant difference to the untreated control.*

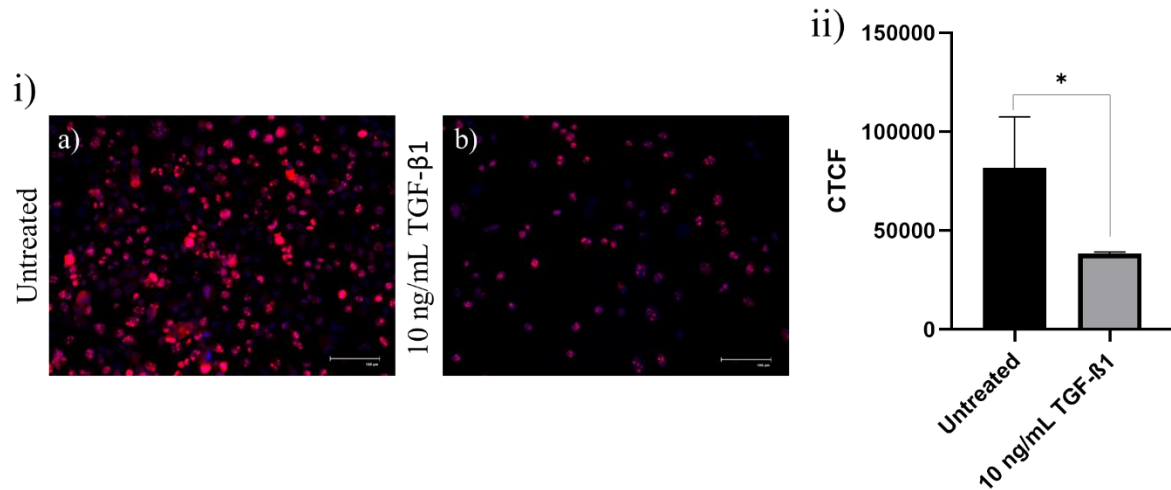


**Figure 4.5: Changes in Ki-67 fluorescence in PANC-1 cells after TGF-β1 treatment.**

The representative immunofluorescent images illustrate the effects of EMT on Ki-67 levels. (i) (i) The images correspond to the following conditions: (a) Untreated, and (b) 10 ng/mL TGF-β1 for 48 hours. PANC-1 cells were treated with 10 ng/ml of TGF-β1 for 48 hours. Cells labelled with a rabbit Anti-Human Ki-67 primary antibody followed by the secondary antibody, Goat Anti-Rabbit Texas Red. (ii) Quantification revealed that Ki-67, a proliferation marker, was reduced after 10 ng/ml of TGF-β1 for 48 hours. Nuclei are stained with DAPI and shown in blue, and Ki-67 in red. (ii) Images were captured using EVOS FLoid™ Cell Imaging Station at 20× magnification and subsequently quantified using Image J. A corresponding bar graph depicting mean values of the CTCF from three independent repeats, is included. Scale bar represents 100 μM. Data are mean ± SD; (n = 3) from raw data. Treatment groups were compared to the untreated control. Statistical analysis was calculated using a two-tailed students t-test, where \*p < .05, \*\*p < .01, \*\*\*p < .001, \*\*\*\*p < .0001, and ns = non-significant indicates a significant or non-significant difference to the untreated control.

#### 4.4 Analysing the effect of TGF-β1-induced EMT on cell viability following treatment with cholesterol lowering drugs and chemotherapeutic agents.

In order to examine the effects of TGF-β1-induced EMT on cell viability following treatment with cholesterol lowering drugs and chemotherapeutic agents, MTT assays were performed on partial- and post-EMT cells. It was found that in cells without EMT induction there was a significant 86% and 30% reduction in viability when treated with KS-01 or MβCD, respectively. Notably, there was no significant reduction in viability when treated with 5-FU or GEM alone. However, when 5-FU or GEM was combined with KS-01 there was a significant reduction in viability (45% and 57% respectively). In EMT-induced cells, the same was not seen, instead, there was a significant 76% increase in viability when treated with KS-01 or no effect when treated with MβCD alone. Again, it was seen that there was no significant reduction in viability when treated with 5-FU or GEM alone. It was however seen that there

was a significant increase in viability when 5-FU or GEM were combined with KS-01 (63% and 54% respectively). Notably, in partial-EMT, the positive control plumbagin reduced cell viability by 86% but in post-EMT cells there was only a 46% decrease. Lastly, the viability in untreated partial-EMT was 199% higher than in untreated post-EMT. EMT seems to impact the growth of PANC-1 cells as previously seen in Figure 4.4 and Figure 4.5, and when combined with treatments particularly KS-01 as seen in Figure 4.6 there is an increase in the viability but not to the extent as partial-EMT cells without treatment (Figure 4.6b).

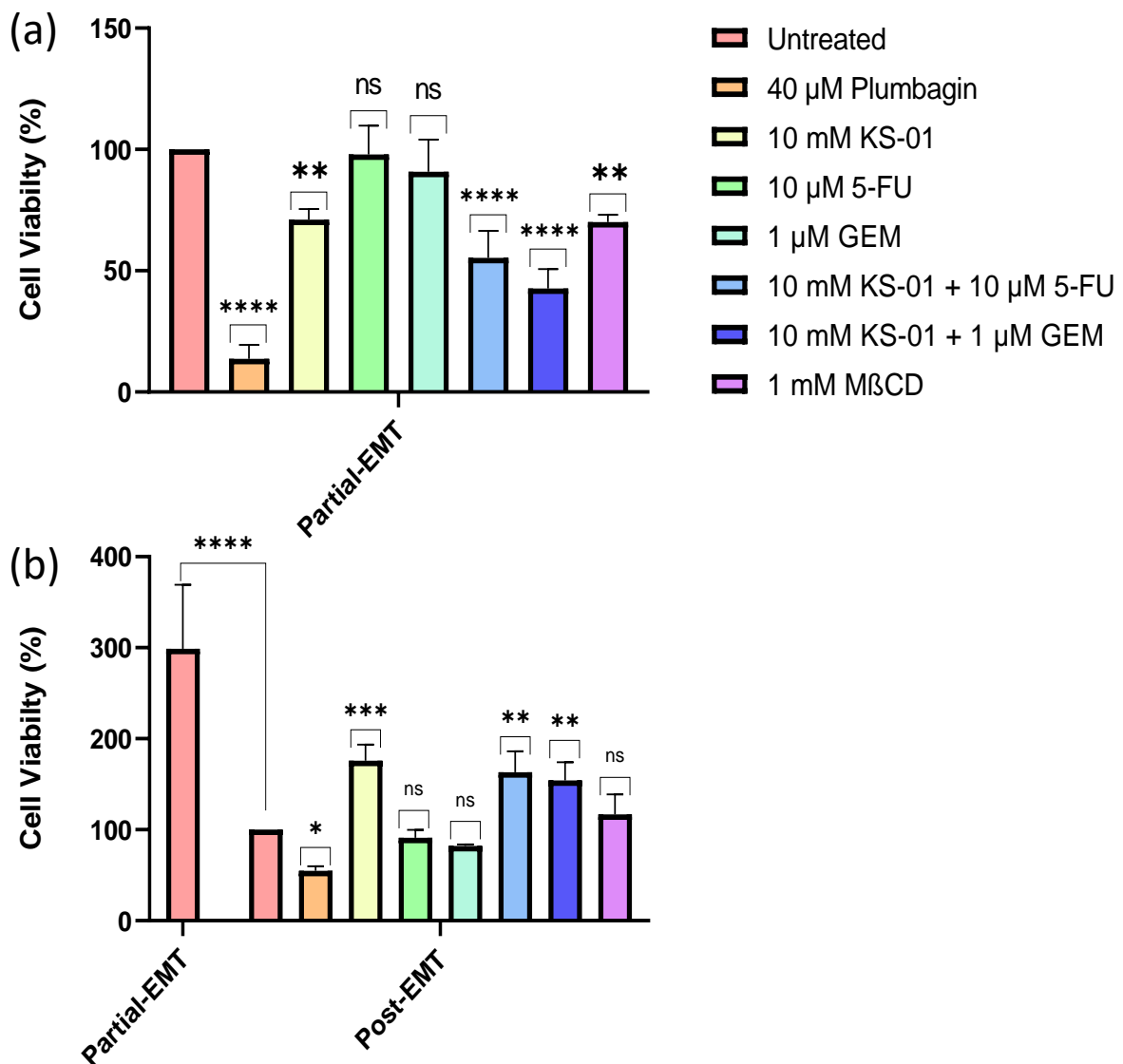


**Figure 4.6: Changes in percentage cell viability in PANC-1 cells both prior to TGF- $\beta$ 1-induced EMT and after, with combination treatments.**

*The graphs depict (a) The percentage cell viability of PANC-1 cells prior to EMT induction with various treatments, normalised to untreated (partial-EMT). (b) The percentage cell*

viability of PANC-1 cells after TGF- $\beta$ 1-induced EMT with various treatments, normalised to untreated (post-EMT). (a) Cells were then either immediately treated for 48 hours with the necessary drugs or (b) EMT was induced using 10 ng/ml of TGF- $\beta$ 1 for 48 hours after which cells were treated for 48 hours with the necessary drugs. MTT was then added for 4 hours, formazan crystals solubilised overnight, and viewed using a VICTOR™ Nivo plate reader at 570 nm. Cells were treated with 10 mM KS-01, 10  $\mu$ M 5-FU, 1  $\mu$ M GEM, 10 mM KS-01+10  $\mu$ M 5-FU, 10 mM KS-01+1  $\mu$ M GEM, and 1 mM M $\beta$ CD. A positive control (Plumbagin at 40  $\mu$ M) was used for all conditions, as it is known to have pro-apoptotic properties. Quantification indicated that in cells without EMT induction (a) there was a significant reduction in viability when treated with KS-01 or M $\beta$ CD alone, there was no significant reduction in viability when treated with 5-FU or GEM alone, however when 5-FU or GEM was combined with KS-01 there was a significant reduction in viability. In EMT-induced cells (b) the same was not seen, instead, there was a significant increase in viability when treated with KS-01 or no effect when treated with M $\beta$ CD alone. Again, it was seen that there was no significant reduction in viability when treated with 5-FU or GEM alone. Contrastingly, it was also seen that there was a significant increase in viability when 5-FU or GEM were combined with KS-01. Treatment groups were compared to the (a) untreated control and (b) untreated control for post-EMT. Cell viability was assessed using an MTT assay relative to the untreated control (100% viability). Data are mean  $\pm$  SD; (n = 3) from raw data. Statistical analysis was calculated using a one-way ANOVA followed by a Tukey post-hoc test to compare individual differences, where \* $p$  < .05, \*\* $p$  < .01, \*\*\* $p$  < .001, \*\*\*\* $p$  < .0001, and ns = non-significant indicates a significant or non-significant difference to the untreated control. The z-factor was >0.6 for each 96-well plate.

#### 4.5 Delineating the link between TGF- $\beta$ 1-induced EMT and cholesterol in PANC-1 cells

The process of EMT at the cellular level is a complex network that relies on the manipulation of crucial cellular signalling pathways. These pathways extensively communicate to initiate and control the EMT program. Furthermore, dysregulated cholesterol metabolism resulting from metabolic reprogramming has also been found to play a distinct role in EMT. As previously mentioned, this metabolic reprogramming in PDAC leads to the activation of several cell signalling pathways that are implicated in the activation of EMT-TFs.

In order to examine the effects of TGF- $\beta$ 1-induced EMT on membrane cholesterol levels, Vybrant Lipid Raft labelling was completed. Following the induction of EMT there was a notable 43% decrease in membrane lipid rafts (Figure 4.7ia, ib, and ii). In partial-EMT PANC-1 cells, treatment with cholesterol-depleting agents KS-01 and M $\beta$ CD resulted in a significant 74% increase after KS-01, but no significant change was observed when treated with M $\beta$ CD (Figure 4.7ic, ie, and ii). Interestingly, in post-EMT cells, the treatment with KS-01 and M $\beta$ CD resulted in a significant 128% and 57% increase in membrane lipid rafts, respectively (Figure 4.7id, ie, and ii).

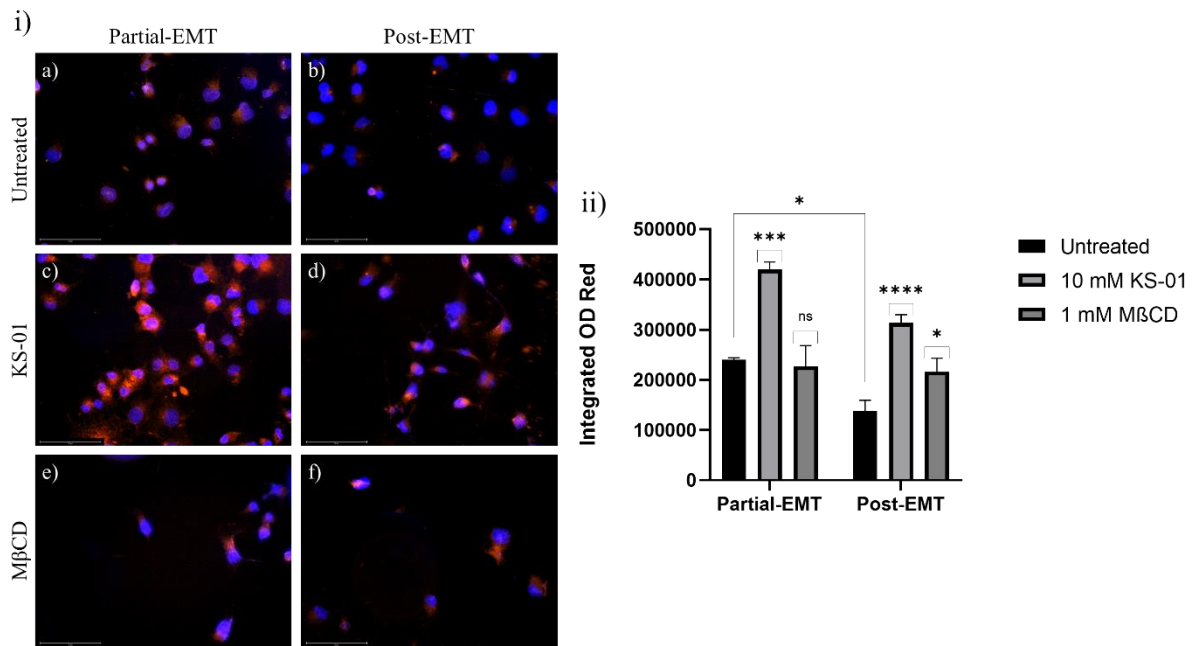


**Figure 4.7: Changes in Vybrant Alexa Fluor® Lipid Raft staining fluorescence in PANC-1 cells as a result of TGF-β1-induced EMT and cholesterol-depleting agents.**

The representative immunofluorescent images illustrate the impact of EMT and cholesterol-depleting agents on lipid rafts. (i) The images correspond to the following conditions: (a) Untreated partial-EMT, (b) Untreated post-EMT, (c) 10 mM KS-01 partial-EMT, (d) 10 mM KS-01 post-EMT, (e) 1 mM MβCD partial-EMT, (f) 1 mM MβCD post-EMT. PANC-1 cells were treated with 10 ng/ml of TGF-β1 for 48 hours after which relevant drug treatments (KS-01 and MβCD) were administered during the final 4 hours of EMT induction. Cells were stained with Vybrant Alexa Fluor® Lipid Raft stain and DAPI. (ii) Quantification revealed a significant decrease in lipid raft content after EMT induction as well as an increase in lipid raft content after treatment with KS-01 in both partial- and post-EMT. MβCD had no significant effect in partial-EMT but increased significantly post-EMT. Nuclei are stained with DAPI and shown in blue, and lipid rafts in red. Images were captured using EVOS M7000 Imaging Station at 40× magnification and subsequently quantified using Celleste 6 imaging software. A corresponding bar graph depicting mean values of the integrated optical density (OD) from three independent repeats, is included. Scale bar represents 150 μM. Data are mean ± SD; (n = 3) from raw data. Treatment groups were compared to the untreated control for either partial- or post-EMT. Statistical analysis was calculated using a one-way ANOVA followed by a Tukey post-hoc test to compare individual differences, where \*p < .05, \*\*p < .01, \*\*\*p < .001, \*\*\*\*p < .0001, and ns = non-significant indicates a significant or non-significant difference to the untreated control.

In addition to lipid raft staining, we then looked at stored cholesterol. In order to examine the influence of TGF-β1-induced EMT on CEs, the quantification of lipid droplets was conducted. Following the induction of EMT there was a notable 70% increase in lipid droplets (Figure 4.8ia, ib, and ii). In partial-EMT PANC-1 cells, treatment with cholesterol-depleting agents

KS-01 and M $\beta$ CD did not yield any significant differences in the number of lipid droplets by the integrated OD (Figure 4.8ic, ie, and ii). Conversely, in post-EMT cells, the treatment with KS-01 and M $\beta$ CD resulted in a significant 32% and 30% decrease in lipid droplets, respectively (Figure 4.8id, if, and ii).

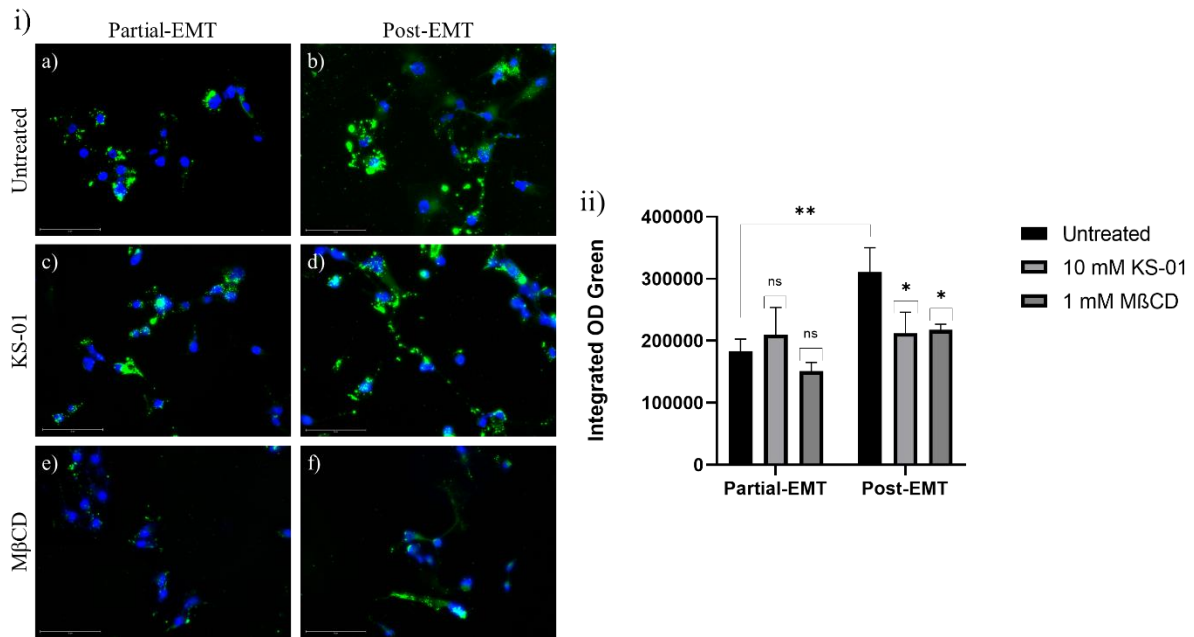


**Figure 4.8: Changes in BODIPY staining fluorescence in PANC-1 cells as a result of TGF- $\beta$ 1-induced EMT and cholesterol-depleting agents.**

The representative immunofluorescent images illustrate the impact of EMT and cholesterol-depleting agents on LDs. (i) The images correspond to the following conditions: (a) Untreated partial-EMT, (b) Untreated post-EMT, (c) 10 mM KS-01 partial-EMT, (d) 10 mM KS-01 post-EMT, (e) 1 mM M $\beta$ CD partial-EMT, (f) 1 mM M $\beta$ CD post-EMT. PANC-1 cells were treated with 10 ng/ml of TGF- $\beta$ 1 for 48 hours after which relevant drug treatments (KS-01 and M $\beta$ CD) were administered during the final 4 hours of EMT induction. Cells were stained with BODIPY<sup>TM</sup> FL C12 and DAPI. (ii) Quantification revealed a significant increase in LDs post-EMT as well as a significant decrease in LDs after KS-01 and M $\beta$ CD post-EMT. There were no significant changes in LDs when KS-01 or M $\beta$ CD was administered. Nuclei are stained with DAPI and shown in blue, and LDs in green. Images were captured using EVOS M7000 Imaging Station at 40 $\times$  magnification and subsequently quantified using Celleste 6 imaging software. A corresponding bar graph depicting mean values of the integrated optical density (OD) from three independent repeats, is included. Scale bar represents 150  $\mu$ m. Data are mean  $\pm$  SD; (n = 3) from raw data. Treatment groups were compared to the untreated control for either partial- or post-EMT. Statistical analysis was calculated using a one-way ANOVA followed by a Tukey post-hoc test to compare individual differences, where \* $p$  < .05, \*\* $p$  < .01, \*\*\* $p$  < .001, \*\*\*\* $p$  < .0001, and ns = non-significant indicates a significant or non-significant difference to the untreated control.

Finally, free cholesterol was analysed. To investigate the impact of TGF- $\beta$ 1-induced EMT on free cellular cholesterol levels, Filipin III staining was conducted. Free cholesterol plays a crucial role in lipid rafts and can be stored as CEs. Following the induction of EMT there was a notable 126% increase in free cholesterol levels (Figure 4.9ia, ib, and ii). In partial-EMT PANC-1 cells, treatment with cholesterol-depleting agents KS-01 and M $\beta$ CD led to a respective 105% and 90% increase in free cholesterol levels, as evidenced by the rise in the integrated OD (Figure 4.9ic, ie, and ii). Conversely, in post-EMT cells, treatment with KS-01 and M $\beta$ CD resulted in a slight decrease in free cholesterol 17% and 21% respectively; however, findings were not statistically significant (Figure 4.9id, if, and ii).

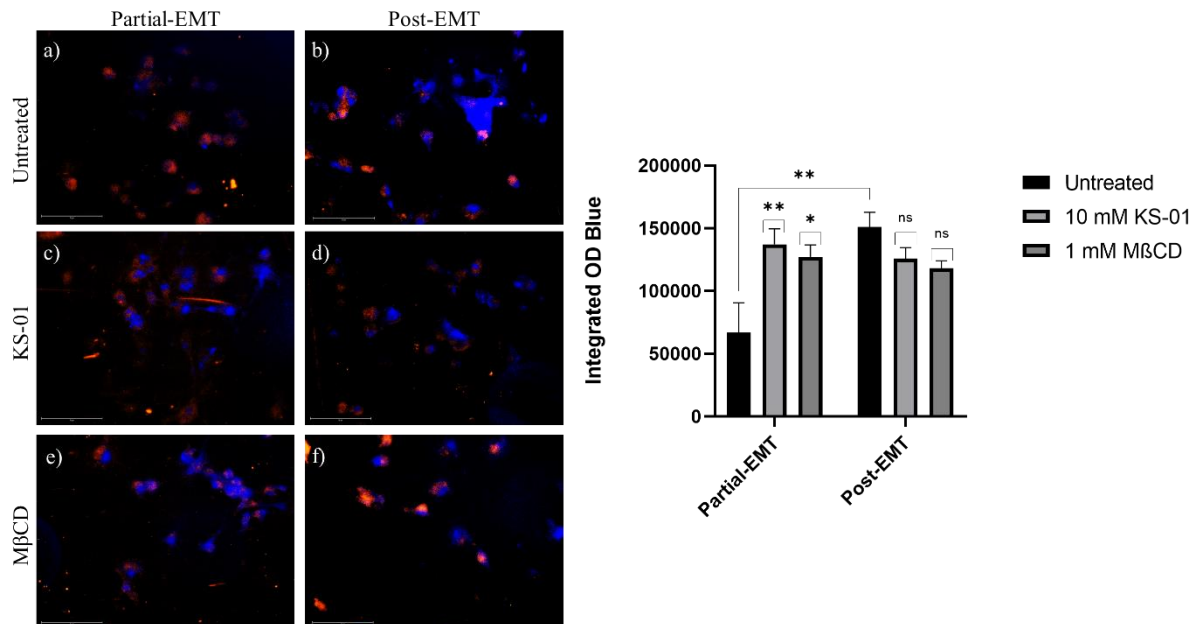


**Figure 4.9: Changes in Filipin III staining fluorescence in PANC-1 cells as a result of TGF- $\beta$ 1-induced EMT and cholesterol-depleting agents.**

*The representative immunofluorescent images illustrate the impact of EMT and cholesterol-depleting agents on free cholesterol. (i) The images correspond to the following conditions: (a) Untreated partial-EMT, (b) Untreated post-EMT, (c) 10 mM KS-01 partial-EMT, (d) 10 mM KS-01 post-EMT, (e) 1 mM M $\beta$ CD partial-EMT, (f) 1 mM M $\beta$ CD post-EMT. PANC-1 cells were treated with 10 ng/ml of TGF- $\beta$ 1 for 48 hours after which relevant drug treatments (KS-01 and M $\beta$ CD) were administered during the final 4 hours of EMT induction. Cells were stained with Filipin III and DAPI. (ii) Quantification revealed a significant increase in free cholesterol content after EMT induction. Additionally, there was a significant increase in free cholesterol after treatment with KS-01 and M $\beta$ CD in partial-EMT PANC-1 cells. In post-EMT cells, however, there was no significant change in free cholesterol. Nuclei are stained with NucRed™ Dead 647 and shown in red, and free cholesterol in blue. Images were captured using EVOS M7000 Imaging Station and subsequently quantified using Celleste 6 imaging*

software. A corresponding bar graph depicting mean values of the integrated optical density (OD) from three independent repeats, is included. Scale bar represents 150  $\mu$ M. Data are mean  $\pm$  SD; (n = 3) from raw data. Treatment groups were compared to the untreated control for either partial- or post-EMT. Statistical analysis was calculated using a one-way ANOVA followed by a Tukey post-hoc test to compare individual differences, where \* $p$  < .05, \*\* $p$  < .01, \*\*\* $p$  < .001, \*\*\*\* $p$  < .0001, and ns = non-significant indicates a significant or non-significant difference to the untreated control.

#### **4.6 Analysing the Effect of Targeting Cellular Cholesterol alone or in combination with chemotherapeutic agents on EMT**

Based on the observation that levels of free cholesterol and stored cholesterol levels are higher after EMT induction, as well as the variable responses of cell viability, membrane lipid raft cholesterol, free cholesterol, and CEs to cholesterol-depleting agents, together with scientific evidence implicating cholesterol in regulating EMT-related signalling pathways and lipid droplet accumulation in invasion, we aimed to elucidate the effect of targeting cholesterol alone and in combination with chemotherapeutic agents on the EMT state of PANC-1 cells. This was achieved by investigating the expression of EMT markers vimentin and E-cadherin. As expected, there was a significant increase in vimentin expression by 27% after EMT induction (Figure 4.10ia, ib, and ii). Unexpectedly, treatment with KS-01, KS-01 + GEM, and M $\beta$ CD further promoted vimentin expression by 115%, 88%, and 157%, respectively (Figure 4.10ic, ig, ih and ii). Interestingly, when KS-01 was combined with 5-FU, there was no significant change in vimentin expression (Figure 4.10if and ii). None of the other treatments significantly altered vimentin expression (Figure 4.10id, ie, and ii).

E-cadherin expression, as expected, significantly decreased after EMT induction by 54% (Figure 4.11ia, ib, and ii). However, the treatment groups that promoted vimentin also increased E-cadherin expression (KS-01 by 45% and KS-01 + GEM by 35%) or had no effect (M $\beta$ CD). This is an unexpected result as vimentin expression is usually accompanied by reduced E-cadherin expression (Figure 4.11ic, ig, ih, and ii). Targeting cholesterol in PDAC may thus promote a specific EMT state that fosters the expression of both mesenchymal and epithelial phenotypes.

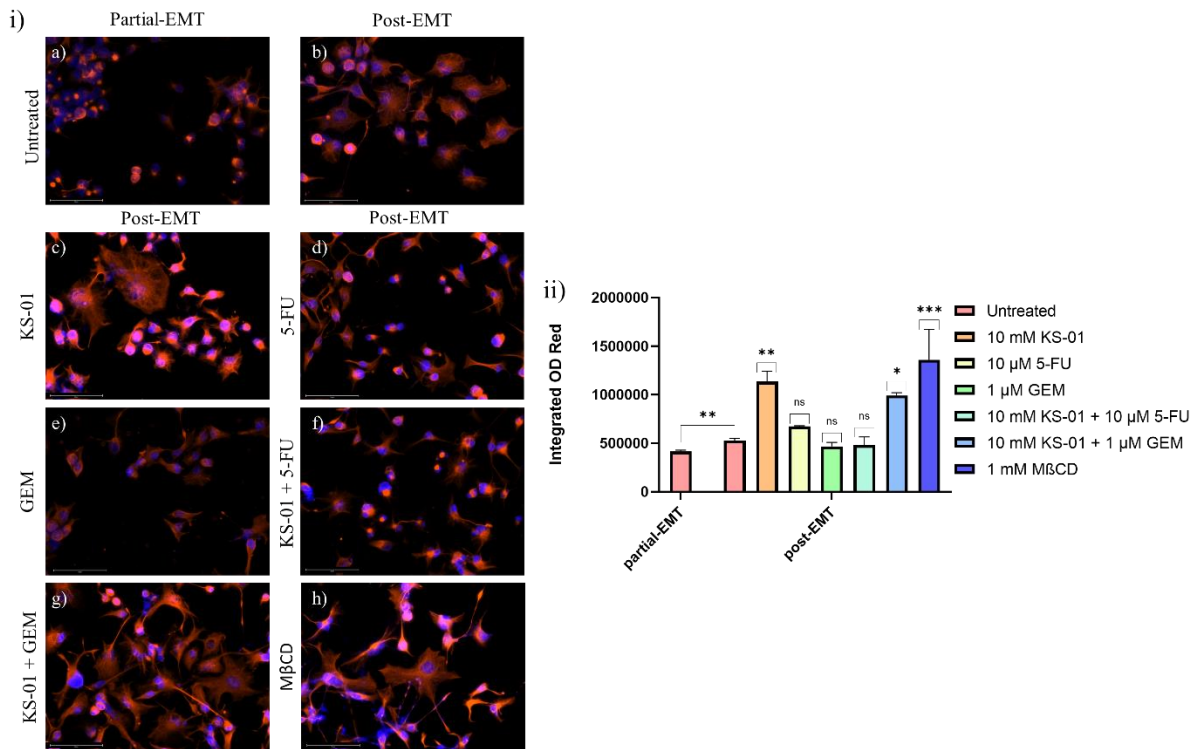


**Figure 4.10: Changes in vimentin fluorescence in PANC-1 cells as a result of TGF- $\beta$ 1-induced EMT and combination treatments.**

The representative immunofluorescent images illustrate the impact of EMT on vimentin expression levels. (i) The images correspond to the following conditions: (a) Untreated partial-EMT, (b) Untreated post-EMT, (c) 10 mM KS-01, (d) 10  $\mu$ M 5-FU, (e) 1  $\mu$ M GEM, (f) 10 mM KS-01 + 10  $\mu$ M 5-FU, (g) 10 mM KS-01 + 1  $\mu$ M GEM, and (h) 1 mM M $\beta$ CD. PANC-1 cells were treated with 10 ng/ml of TGF- $\beta$ 1 for 48 hours after which relevant drug treatments were administered during the final 4 hours of EMT induction. Cells were labelled with Rabbit Anti-Human Vimentin primary antibody and Goat Anti-Rabbit Texas Red secondary antibody. (ii) Quantification revealed a significant increase in vimentin after EMT induction and treatment with KS-01, KS-01 + GEM, and M $\beta$ CD further promoted its expression. Nuclei are stained with DAPI and shown in blue, and vimentin in red. Images were captured using EVOS M7000 Imaging Station at 40 $\times$  magnification and subsequently quantified using Celleste 6 imaging software. A corresponding bar graph depicting mean values of the integrated optical density (OD) from three independent repeats, is included. Scale bar represents 150  $\mu$ M. Data are mean  $\pm$  SD; (n = 3) from raw data. Treatment groups were compared to the untreated control for post-EMT. Statistical analysis was calculated using a two-tailed student's t-test, where \* $p$  < .05, \*\* $p$  < .01, \*\*\* $p$  < .001, \*\*\*\* $p$  < .0001, and ns = non-significant indicates a significant or non-significant difference to the untreated control.

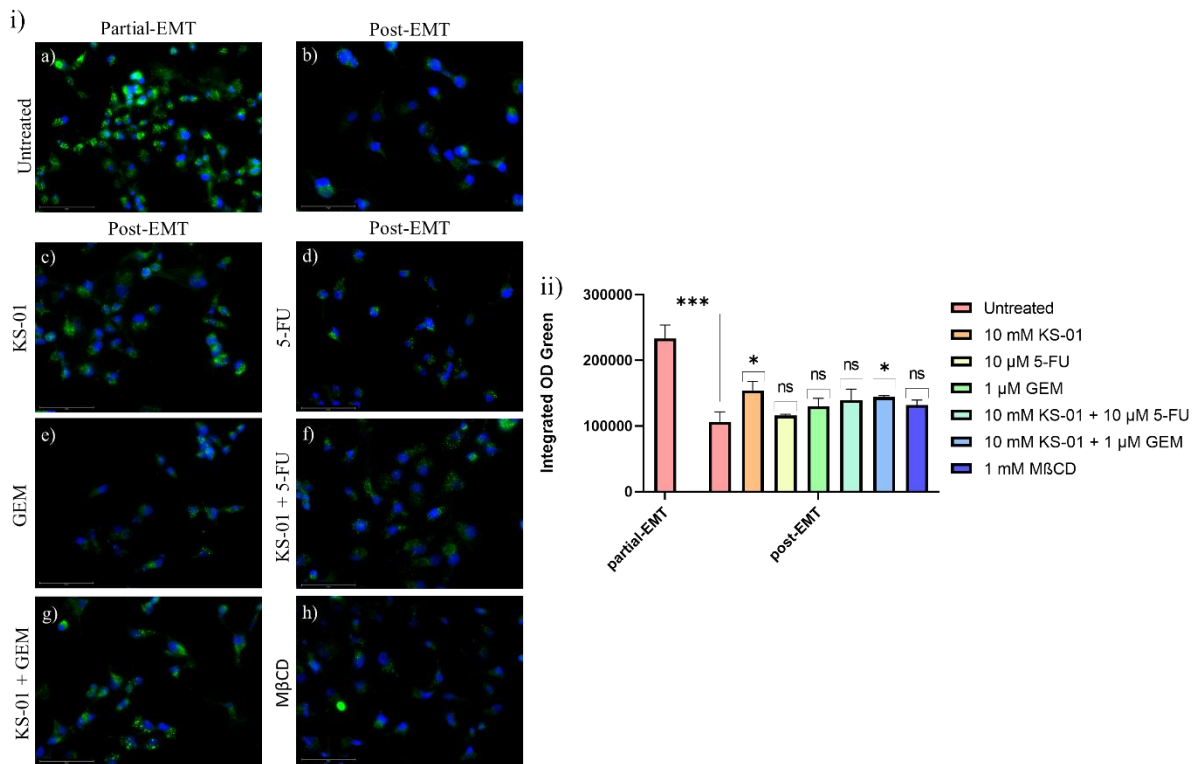


**Figure 4.11: Changes in E-cadherin fluorescence in PANC-1 cells as a result of TGF- $\beta$ 1-induced EMT and combination treatments.**

The representative immunofluorescent images illustrate the impact of EMT on vimentin expression levels. (i) The images correspond to the following conditions: (a) Untreated partial-EMT, (b) Untreated post-EMT, (c) 10 mM KS-01, (d) 10  $\mu$ M 5-FU, (e) 1  $\mu$ M GEM, (f) 10 mM KS-01 + 10  $\mu$ M 5-FU, (g) 10 mM KS-01 + 1  $\mu$ M GEM, and (h) 1 mM M $\beta$ CD. PANC-1 cells were treated with 10 ng/ml of TGF- $\beta$ 1 for 48 hours after which relevant drug treatments were administered during the final 4 hours of EMT induction. Cells labelled with Mouse Anti-Human E-cadherin primary antibody and Goat Anti-Mouse Alexa Fluor 488 secondary antibody. (ii) Quantification revealed a significant increase in decrease in E-cadherin after EMT induction. Contrastingly, the treatment with KS-01 and KS-01 + GEM significantly increased E-cadherin but not to levels found in partial-EMT. Nuclei are stained with DAPI and shown in blue, and E-cadherin in green. Images were captured using EVOS M7000 Imaging Station at 40 $\times$  magnification and subsequently quantified using Celleste 6 imaging software. A corresponding bar graph depicting mean values of the integrated optical density (OD) from three independent repeats, is included. Scale bar represents 150  $\mu$ M. Data are mean  $\pm$  SD; (n = 3) from raw data. Treatment groups were compared to the untreated control for post-EMT. Statistical analysis was calculated using a two-tailed student's t-test, where \* $p$  < .05, \*\* $p$  < .01, \*\*\* $p$  < .001, \*\*\*\* $p$  < .0001, and ns = non-significant indicates a significant or non-significant difference to the untreated control.

#### 4.7 Analysing the drug resistant potential of PANC-1 cells post-EMT induction following treatment with cholesterol targeting agents and chemotherapeutic agents

There is a well-documented link between EMT and MDR in PDAC. Previous studies have highlighted the multifaceted role of cholesterol in MDR, particularly in its impact on ABC transporters such as ABCB1 (Arumugam *et al.*, 2009; Adamska and Falasca, 2018). To evaluate the functionality of the ABCB1 transporter following cholesterol depletion and various chemotherapy treatments, the intracellular retention of calcein was measured. Induction of EMT by TGF- $\beta$ 1 significantly increased MDR potential, as evidenced by a 19% decrease in calcein retention. Interestingly, the cholesterol-depleting agent KS-01 had no impact on MDR potential, while treatment with M $\beta$ CD resulted in a 27% increase in calcein retention, and hence a reduction in MDR potential. Similarly, individual chemotherapy treatments with 5-FU and GEM reduced MDR potential by 44% and 39%, respectively, with 5-FU showing a significant reduction. However, treating post-EMT cells with a combination of KS-01 and GEM promoted MDR potential, decreasing calcein retention by 25%. Lastly, the positive control for reducing MDR, Verapamil, a known ABCB1 inhibitor, exhibited a drastic increase in calcein retention (Figure 4.12).

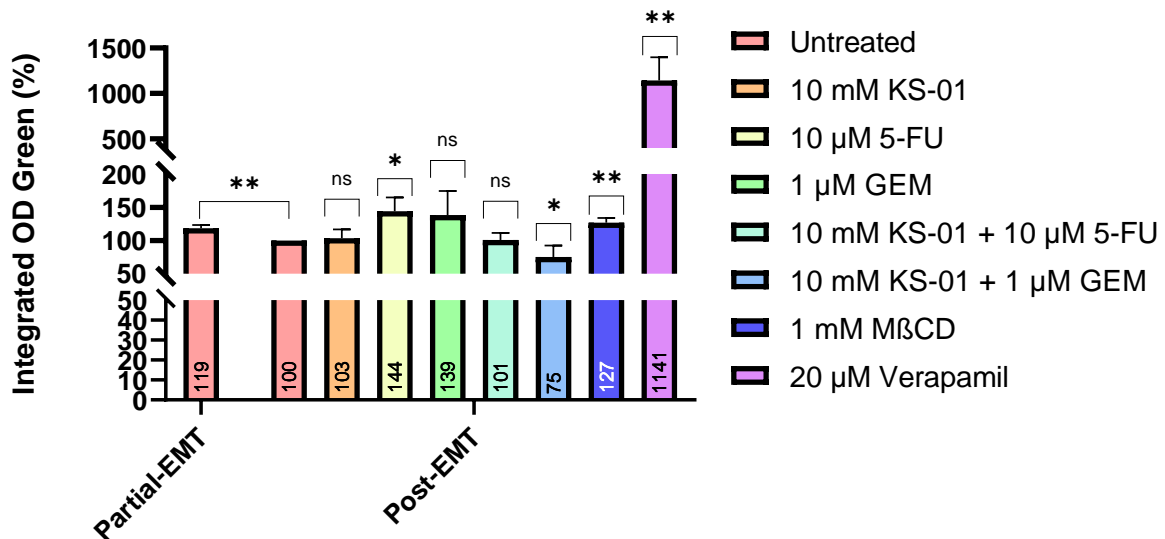


**Figure 4.12: Changes in MDR in PANC-1 cells after TGF- $\beta$ 1-induced EMT and combination treatments.**

The graph depicts the percentage integrated optical density (OD) green in PANC-1 cells under different treatment conditions normalised to the Untreated (post-EMT), representing levels of MDR. Higher levels of fluorescence correspond to reduced drug resistance. In a 96-well plate, 10 000 PANC-1 cells were seeded after which cells were incubated overnight for attachment. PANC-1 cells were treated with 10 ng/ml of TGF- $\beta$ 1 for 48 hours after which relevant drug

treatments were administered in the final 4 hours of EMT induction. Cells were treated with 10 mM KS-01, 10  $\mu$ M 5-FU, 1  $\mu$ M GEM, 10 mM KS-01 + 10  $\mu$ M 5-FU, 10 mM KS-01 + 1  $\mu$ M GEM, and 1 mM M $\beta$ CD. A positive control (20  $\mu$ M Verapamil) was used for all conditions, as it is known ABCB1 inhibitor. Quantification revealed a significant increase in MDR when EMT was induced in PANC-1 cells. Treatments with KS-01, GEM, and KS-01 + 5-FU showed no significant further effect on MDR, whereas treatment with KS-01 + GEM significantly promoted MDR. In contrast, treatments with 5-FU, and M $\beta$ CD reduced MDR. Fluorescence data was captured using EVOS M7000 Imaging Station and subsequently quantified using Celleste 6 imaging software relative to the untreated (post-EMT) control (100% integrated OD). Data are mean  $\pm$  SD; (n = 3) from raw data. Statistical analysis was calculated using a two-tailed student's t-test, where \* $p$  < .05, \*\* $p$  < .01, \*\*\* $p$  < .001, \*\*\*\* $p$  < .0001, and ns = non-significant indicates a significant or non-significant difference to the untreated control.

#### **4.8 Assessing the invasive potential of PANC-1 cells post-EMT induction following treatment with cholesterol targeting agents and chemotherapeutic agents**

The Transwell<sup>TM</sup> invasion assay is a widely employed technique aimed at understanding the invasive behaviour of cancer cells, which is a crucial step in metastasis. Following the observation that the cholesterol-depleting agents and certain combination therapies promoted the expression of vimentin and displayed varied effects on E-cadherin expression, the following step was to investigate the effects of these treatments on the invasive potential of the post-EMT groups.

EMT induction increased invasion by 51%, while the treatment groups 5-FU, GEM, and KS-01 + 5-FU had no significant effect on invasion compared to post-EMT. However, treatment with cholesterol-depleting agents alone significantly increased invasion by 72% and 88%, respectively. Notably, the combination of KS-01 and GEM also promoted invasion by 54% (Figure 4.13). These findings suggest a potential relationship between targeting cholesterol in PDAC and metastasis, particularly when combined with GEM.

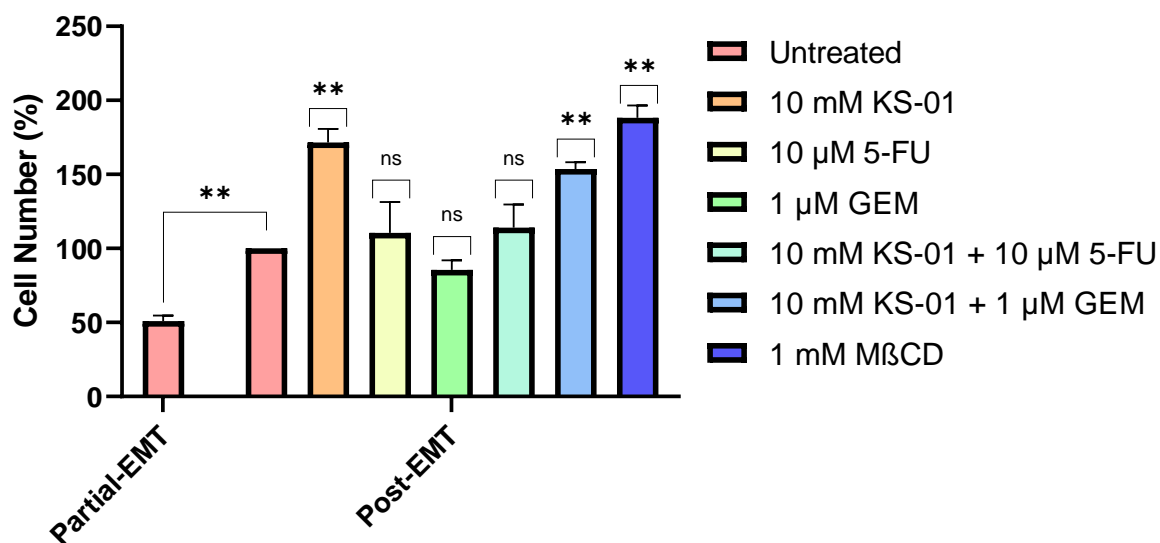


**Figure 4.13: Changes in invasive potential of PANC-1 cells after TGF- $\beta$ 1-induced EMT and combination treatments.**

The graph depicts the percentage of invaded PANC-1 cells under various treatment conditions after TGF- $\beta$ 1-induced EMT normalised to the untreated (post-EMT) control, as determined by a Transwell® invasion assay. The higher the percentage the more invasive the PANC-1 cells are. After 48 hours of TGF- $\beta$ 1-induced EMT and relevant drug treatments in the final 4 hours of EMT induction 300000 PANC-1 cell/mL of serum free media were seeded in the upper chamber of a Transwell® invasion insert coated with GelTrex™ for 24 hours. The lower chamber containing DMEM supplemented with 10% FBS acted as a chemoattractant. Invasive cells were then stained with DAPI. Cells were treated with 10 mM KS-01, 10  $\mu$ M 5-FU, 1  $\mu$ M GEM, 10 mM KS-01 + 10  $\mu$ M 5-FU, 10 mM KS-01 + 1  $\mu$ M GEM, and 1 mM M $\beta$ CD. Quantitative analysis revealed a significant increase in the invasive ability of PANC-1 cells following EMT induction. Treatment with KS-01, KS-01 + GEM, and M $\beta$ CD significantly further promoted invasion. Conversely, all other treatments had no additional effects on invasion. Fluorescent Data was captured using EVOS M7000 Imaging Station and cell number quantified using Celleste 6 imaging software relative to the untreated (post-EMT) control (100% cell number). Data are mean  $\pm$  SD; (n = 2) from raw data. Statistical analysis was calculated using a two-tailed student's t-test, where \* $p$  < .05, \*\* $p$  < .01, \*\*\* $p$  < .001, \*\*\*\* $p$  < .0001, and ns = non-significant indicates a significant or non-significant difference to the untreated control.

#### **4.9 Molecular mechanism of EMT, cancer drug resistance, and cholesterol metabolism post-EMT induction following treatment with cholesterol targeting agents and chemotherapeutic agents.**

The expression levels of relevant genes were observed using RT-qPCR. The EMT related genes analysed using RT-qPCR included: *SNAIL1* and *TGF- $\beta$ 1*, the drug resistance related genes

included: *ABCC5*, *ABCB1*, *ABCG2*, and *hENT1*, and the cholesterol homeostasis genes included: *LDLR*, *ABCA1*, and *SREBF2*.

Treatment with TGF- $\beta$ 1, as expected, induced EMT and promoted the expression of *SNAIL1*, *TGF- $\beta$ 1* and *ABCB1*. The expression of the other cancer drug efflux genes, particularly *ABCG2*, were downregulated. EMT seems to promote drug resistance by upregulating drug export through *ABCB1*. EMT induction also downregulated *LDLR* and *SREBF2*, genes involved in cholesterol uptake and synthesis, while increasing the expression of *ABCA1*, a gene involved in cholesterol efflux. Overall, all treatment groups promoted the expression of the EMT-TF *SNAIL1*. Among the treatment groups, KS-01, GEM, and KS-01 + GEM promoted the expression of TGF- $\beta$ 1 the most, with KS-01 and KS-01 + GEM having the highest promotion. The combination treatment of KS-01 + GEM promoted EMT more than GEM alone, while 5-FU alone promoted EMT more than its combination with KS-01 (Figure 4.14). All treatment groups did not have a significant further effect on *ABCG2* expression, while *ABCC5* expression was significantly promoted by KS-01, KS-01 + GEM, and M $\beta$ CD.

Interestingly, the combination treatments promoted the expression of *ABCC5* more than the 5-FU and GEM treatments alone, but less than KS-01 alone. *ABCB1* expression was significantly downregulated by treatment with KS-01, and M $\beta$ CD further promoted its expression. The expression of *hENT1*, a drug import pump, was promoted significantly in all treatment groups except for M $\beta$ CD, where there was no noticeable change. The treatment with KS-01, 5-FU, and GEM alone particularly upregulated *hENT1* expression, with the combination treatments promoting its expression less than the single treatments (KS-01, 5-FU, and GEM). All the cholesterol homeostasis genes were significantly upregulated in all of the treatment groups. However, the combination treatments had reduced expression of *ABCA1* compared to the single treatments (KS-01, 5-FU, and GEM), while there was an increase in expression of *LDLR* in the combination treatments, KS-01, and M $\beta$ CD, compared to the single treatments (5-FU and GEM). Lastly, *SREBF2* was significantly highly expressed in the KS-01 and KS-01 + GEM treatment groups, with the combination groups again having a higher expression than the single treatments (5-FU and GEM). Targeting cholesterol in PDAC promotes aberrant cholesterol homeostasis, EMT, and drug resistance particularly when combined with GEM (Figure 4.14 and Table 4.1).

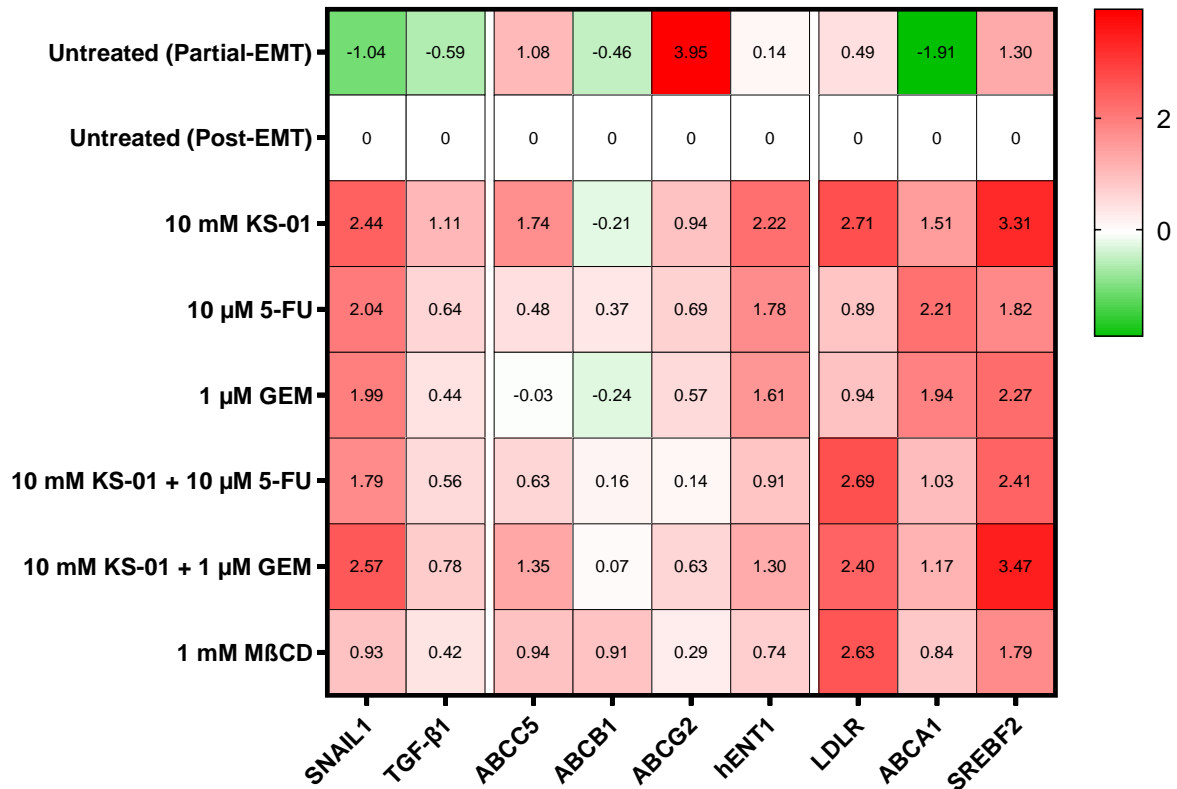


**Figure 4.14: Changes in drug-resistance, cholesterol homeostasis, and EMT genes after TGF-β1-induced EMT and combination treatments.**

The heatmap depicts the log<sub>2</sub> fold change of genes involved in EMT (*SNAIL1* and *TGF-β1*), drug resistance (*ABCC5*, *ABCB1*, *ABCG2*, and *hENT1*), and cholesterol homeostasis (*LDLR*, *ABCA1*, and *SREBF2*) in PANC-1 cells relative to the untreated (post-EMT) group. Each gene is represented on the x-axis and each treatment group on the y-axis where the red represents a positive log<sub>2</sub> fold change (increase), white represents no change and green a negative log<sub>2</sub> fold change (decrease) compared to the untreated (post-EMT). Cells were treated with 10 mM KS-01, 10 μM 5-FU, 1 μM GEM, 10 mM KS-01 + 10 μM 5-FU, 10 mM KS-01 + 1 μM GEM, and 1 mM MβCD. TGF-β1-induced EMT promotes the gene expression of drug efflux pumps *ABCB1* and *ABCC5*, and cholesterol efflux gene *ABCA1*. EMT does however, reduce the expression of cholesterol import and export genes *LDLR* and *SREBF2*, respectively. All drug treatments resulted in the further promotion of EMT, some drug efflux, and all cholesterol related genes. The heatmap was generated by GraphPad software. Relative log<sub>2</sub> fold change was assessed relative to the untreated control (0-fold change). Data are mean ± SD; (n = 2) from raw data.

**Table 4.1: The standard deviation and significance of the log<sub>2</sub>(fold change) RT-qPCR gene expression data where \**p* < .05, \*\**p* < .01, \*\*\**p* < .001, \*\*\*\**p* < .0001, and ns = non-significant indicates a significant or non-significant difference to the untreated control**

Treatment group	SNAIL1		TGF-β		ABCC5		ABCG2		ABCB1		ENT1		LDLR		ABCA1		SREBF2	
	Standard Deviation	Significance	Standard Deviation	Significance	Standard Deviation	Significance	Standard Deviation	Significance	Standard Deviation	Significance	Standard Deviation	Significance	Standard Deviation	Significance	Standard Deviation	Significance	Standard Deviation	Significance
Untreated (Partial-EMT)	0,005	*	0,098	*	0,080	**	0,135	**	0,085	*	0,009	**	0,060	*	0,095	**	0,047	**
Untreated (Post-EMT)	0,000		0,000		0,000		0,000		0,000		0,000		0,000		0,000		0,000	
10 mM KS-01	0,150	****	0,238	**	0,171	**	0,443	ns	0,225	***	0,214	***	0,206	**	0,034	*	0,022	***
10 μM 5-FU	0,174	***	0,017	ns	0,229	ns	0,295	ns	0,271	ns	0,374	*	0,151	*	0,322	*	0,089	**
1 μM GEM	0,065	***	0,072	**	0,076	ns	0,283	ns	0,003	ns	0,059	*	0,123	*	0,190	***	0,182	**
10 mM KS-01 + 10 μM 5-FU	0,175	***	0,217	ns	0,294	ns	0,186	ns	0,113	ns	0,162	*	0,059	***	0,011	***	0,239	**
10 mM KS-01 + 1 μM GEM	0,042	****	0,026	**	0,067	**	0,241	ns	0,058	ns	0,090	**	0,253	*	0,021	***	0,296	**
1 mM MβCD	0,328	*	0,335	ns	0,023	***	0,130	ns	0,026	***	0,179	ns	0,018	****	0,170	*	0,046	***

## 5 Discussion

The challenges posed by PDAC in clinical management are substantial, primarily due to its metastatic nature and resistance to conventional chemotherapies like GEM and 5-FU. Given cholesterol's significant involvement in cancer-related processes like differentiation, proliferation, migration, chemoresistance, and survival, alongside the observed elevated cholesterol levels in PDAC, targeting cholesterol depletion emerges as a prospective therapeutic strategy in cancer treatment. In addition to its role in PDAC progression, EMT has also been implicated in drug resistance and the generation of CSCs in PDAC (Sato *et al.*, 2015). The process of EMT at the cellular level is a complex network that relies on the manipulation of crucial cellular signalling pathways. These pathways extensively communicate to initiate and control the EMT program. Furthermore, the dysregulated cholesterol metabolism resulting from metabolic reprogramming may also play a distinct role in EMT. This study was carried out with the aim of determining whether targeting cellular cholesterol in these cells could offer a new approach to addressing aggressive cancer characteristics, while also restoring drug sensitivity. Using PANC-1 cells as a model, EMT was induced through TGF-β1 treatment, followed by exposure to the cholesterol-depleting agent KS-01 in combination with standard chemotherapy regimens (GEM and 5-FU). Through this approach, the current study aimed at elucidating the intricate interplay between cholesterol metabolism, EMT, and drug resistance in PDAC.

## 5.1 Alterations to Cellular Morphology and Resulting Implications following treatment with TGF- $\beta$ 1

PDAC utilises the EMT program to facilitate its highly metastatic nature. EMT is characterised as a cellular plasticity program and entails the dynamic reorganization of cellular components, enabling migration, invasion, and metastatic spread. EMT is governed by specific EMT-TFs, signalling pathways, and miRNAs. Furthermore, it is crucial to note that EMT is not a simple binary switch, but rather a transition between intermediate states, including hybrid E/M states that exhibit heightened metastatic potential.

In this study, we first established that the PANC-1 cell line underwent EMT after treatment with TGF- $\beta$ 1. Following treatment with TGF- $\beta$ 1, PANC-1 cells displayed time and concentration dependent changes in morphology, shifting from a classic polygonal or cobblestone shape to an elongated and spindle-like morphology. The most pronounced mesenchymal phenotype was observed after 48 hours with a concentration of 10 ng/mL of TGF- $\beta$ 1 (Figure 4.1e). This phenotypic transition was accompanied by a significant decrease in the expression of E-cadherin, an epithelial marker, and a significant increase in vimentin, a mesenchymal marker (Figure 4.2 and Figure 4.3), which serve as established indicators of EMT induction. Additionally, the expression of *SNAIL1* and *TGF-B1* (Figure 4.14) was significantly upregulated following TGF- $\beta$ 1 treatment. These findings are consistent with previous studies that have documented treating cells with 10 ng/mL TGF- $\beta$ 1 for 48 hours promoted spindle-like morphology, increased vimentin expression, decreased E-cadherin expression, and promoted *SNAIL1/2* expression (Ellenrieder *et al.*, 2001; Kabashima *et al.*, 2009; Wang *et al.*, 2012; Ungefroren *et al.*, 2022). Interestingly, immunofluorescent analysis of the PANC-1 cells revealed high levels of vimentin expression and low levels of E-cadherin expression even before EMT induction, as depicted in Figure 4.2 and Figure 4.3. This characteristic is attributed to the fact that PANC-1 cells are considered a complete-EMT cell line, specifically classified as a quasi-mesenchymal cell line. Prior studies have consistently reported that the PANC-1 cell line inherently exhibits high vimentin levels and low E-cadherin levels (Shichi *et al.*, 2019; Ungefroren *et al.*, 2022). Being a quasi-mesenchymal cell line, PANC-1 cells can display various EMT phenotypes and transition between these states either spontaneously or in response to external signals (Ungefroren *et al.*, 2022). Although it is considered a complete-EMT cell line, promotion towards a more mesenchymal phenotype has been documented (Ungefroren *et al.*, 2022). This unique characteristic makes PANC-1 cells valuable for studying clonal heterogeneity and EMT subtype shifting. However, these aspects were not explored in

the present study. Previous research conducted by Aiello *et al.* has shown that tumour cells in the quasi-mesenchymal/squamous/basal subtype of PDAC primarily lose their epithelial phenotype through transcriptional changes, while those in the classical/pancreatic progenitor/ADEX subtype undergo EMT mainly through E-cadherin re-localization to transition from their epithelial phenotype (Aiello *et al.*, 2018). The loss of E-cadherin demonstrated in Figure 4.3 supports these findings.

TGF- $\beta$ 1 is an established and essential signalling pathway involved in the induction of EMT. It exerts its effects through both SMAD-dependent and SMAD-independent pathways (Figure 1.6). The induction of EMT by TGF- $\beta$ 1 can occur through the activation of EMT-TFs, particularly the Snail family (Lamouille *et al.*, 2014), as well as through its influence on cytoskeleton organisation, cell growth, and survival (Figure 1.7). Specifically, the upregulation of SNAIL1, by TGF- $\beta$ 1 directly or indirectly represses the expression of E-cadherin, claudin, and occludin through binding of the transcriptional repressors to the E-box in the proximal promoter regions. This repression is mediated by the N-terminal SNAG domain of *SNAIL1* (Batlle *et al.*, 2000; Ikenouchi *et al.*, 2003). Additionally, TGF- $\beta$ 1-induced EMT-TFs can repress target genes through the action of epigenetic remodelling complexes, such as histone modifiers and DNA methyltransferases, which impact DNA and chromatin accessibility (Peinado *et al.*, 2004; Hou *et al.*, 2008). Although EMT-TFs induced by TGF- $\beta$ 1 also promote the expression of mesenchymal markers, such as vimentin, it is worth noting that vimentin itself possesses a NF- $\kappa$ B and TGF- $\beta$  response element in its promoter region (Cano *et al.*, 2000). This suggests a dual promotion of vimentin expression upon treatment with TGF- $\beta$ 1 (Wu *et al.*, 2007; Baba *et al.*, 2022). Furthermore, TGF- $\beta$ 1 treatment has been found to result in an autocrine signalling loop, further amplifying its expression. This is evident from the increase in *TGF- $\beta$ 1* expression observed (Figure 4.14). Autocrine signalling has been recognised as playing a significant role in cancer development and progression. In various cell lines, it has been observed that treatment with TGF- $\beta$ 1 positively regulates its own expression (Bascom *et al.*, 1989; Ungefroren *et al.*, 2022).

Treatment with TGF- $\beta$ 1 has a significant impact on adherens junctions and tight junctions, both of which play crucial roles in maintaining the epithelial program. Central to the functionality of adherens junctions is the presence of E-cadherin, which acts as a key mediator and effectively suppresses the activation of the Wnt/ $\beta$ -catenin pathway and the RTK/PI3K pathway in epithelial cells (Loh *et al.*, 2019). The adherens junctions themselves are composed of cadherins, which bind to  $\alpha$ -,  $\beta$ -, and  $\gamma$ -catenins, thereby establishing a connection with the actin

cytoskeleton (Loh *et al.*, 2019). During EMT, E-cadherin is cleaved resulting in the conversion to N-cadherin. This cleavage event leads to the destabilisation of adherens junctions, facilitating the release of  $\beta$ -catenin and disrupting vital cell-cell and cell-extracellular matrix interactions (Nagafuchi, 2001). This phenomenon can be directly attributed to the increased solubility of N-cadherin fragments, which subsequently reduces the presence of adherens junctions. Additionally, EMT involves the upregulation of MMPs, which contribute to the degradation of the basement membrane (De Wever *et al.*, 2007; David and Rajasekaran, 2012).

Furthermore, PANC-1 cells exhibited an increase in vimentin, a type III intermediate filament, after treatment with TGF- $\beta$ 1 (Figure 4.2). It has been established that vimentin plays a crucial role in maintaining the integrity of cells and tissues. Importantly, vimentin replaces the function of cytokeratin in mesenchymal cells. It enhances the cytoskeletal strength and contributes to the cell's flexibility required for migration and invasion (Mendez *et al.*, 2010; Ye and Weinberg, 2015). Moreover, vimentin protects cancer cells from mechanical stresses endured during migration or even manoeuvring through narrow spaces. This is accomplished by providing an intricate cage-like network capable of supporting the positioning and integrity of organelles and the nucleus, thereby preventing genomic damage (Lowery *et al.*, 2015; Patteson *et al.*, 2019). Studies have indicated that vimentin, when introduced into epithelial cells, elicits a reversible mesenchymal shape, reducing desmosomal interactions and increasing motility. Interestingly, vimentin works in conjunction with microtubules to direct their accumulation at the nucleus, facilitating directed cell migration (Usman *et al.*, 2021). Consequently, this leads to front-back polarity rather than apical-basal (Thiery *et al.*, 2009; Ye and Weinberg, 2015). Additionally, vimentin directly associates with actin stress fibres thereby regulating their modulation and cell migration (Esue *et al.*, 2006). Notably, vimentin has been shown to promote and even be crucial to the formation of actin-rich protrusions called lamellipodia, primarily located at the leading edge, thereby facilitating the development of secondary tumours (Yang *et al.*, 2019). The upregulation of vimentin in PANC-1 cells during EMT, not only facilitates the transition to a mesenchymal phenotype but also contributes to enhanced cell motility, protection against mechanical stresses, and reorganization of the cytoskeleton in preparation for metastasis.

In addition, treatment with TGF- $\beta$ 1 was found to reduce cell proliferation from as early as 48 hours up to 96 hours of treatment. Specifically, PANC-1 cells reached a plateau after 48 hours of treatment with 10 ng/mL TGF- $\beta$ 1, while the untreated cells continued to proliferate exponentially until 96 hours (Figure 4.4). This can also be seen in Figure 4.1e which visually

displayed a reduction in cell number. The expression of Ki-67, a marker of cell proliferation, present in all active phases of the cell cycle (G1, S, G2 and M-phase), was observed to decrease post-EMT induction (Figure 4.5). Additionally, the viability of post-EMT cells decreased by 199% as seen in Figure 4.6. This phenomenon has been previously documented in various studies. Ungefroren *et al.* and Wang *et al.* demonstrated that treatment with TGF- $\beta$ 1 resulted in growth inhibition of PANC-1 cells, wherein it was demonstrated that TGF- $\beta$ 1 induced growth inhibition is selectively regulated by SMAD3 (Ungefroren *et al.*, 2011; Wang *et al.*, 2012). Another study demonstrated that PANC-1 cells exhibiting EMT characteristics after culturing in a stem cell-specific media attained a quiescent state (Ambrosini *et al.*, 2020). EMT and the cell cycle are interconnected, as described as the "Go or Grow" hypothesis, which proposes a dichotomy in cancer cell behaviour, suggesting that cancer cells can either proliferate rapidly (grow) or migrate and invade surrounding tissues (go). In the context of EMT, this hypothesis suggests that cancer cells undergoing EMT may prioritize migration and invasion (go) over proliferation (grow) (Akhmetkaliyev *et al.*, 2023). The pivotal pathway that integrates signals promoting growth with those inhibiting growth to determine cell fate is the retinoblastoma-E2F pathway. This pathway is regulated by CDK complexes, including cyclin D-CDK4/6 and cyclin E-CDK2, which phosphorylate retinoblastoma to facilitate progression through the G1 phase and initiation of the S phase (Topacio *et al.*, 2019; Akhmetkaliyev *et al.*, 2023). Cyclin-dependent kinase inhibitors, such as p27<sup>KIP1</sup>, p21<sup>CIP1</sup>, and p57<sup>KIP2</sup>, are crucial regulators of CDK activity. EMT cells enter a quiescent state mediated by interactions between cell cycle machinery and EMT-TF networks, resulting in the upregulation of above-mentioned cyclin dependent kinase inhibitors. These inhibitors prevent proliferation and promote migration (Akhmetkaliyev *et al.*, 2023). Interestingly, invadopodia components are upregulated in the G1 phase, and cells in G1 exhibit higher levels of extracellular matrix degradation (Bayarmagnai *et al.*, 2019). Notably, the activation p27<sup>KIP1</sup> promotes migration and metastasis by promoting PAK1/cortactin, increasing the turnover of invadopodia (Jeannot *et al.*, 2017). Cell cycle arrest is not only a consequence of EMT but also a factor contributing towards metastasis. This explains the decrease in Ki-67 levels observed after treatment with TGF- $\beta$ 1 (Figure 4.5), as Ki-67 is a proliferation marker, that is degraded when cells are in the G0 or G1 phases and unable to pass through the G1/S checkpoint (Miller *et al.*, 2018). Additionally, TGF- $\beta$ , acts as a canonical inhibitor of the cell cycle in the G1 phase through SMAD-mediated activation of *CDKN2B* and *CDKN1A* genes, encoding cyclin-dependent kinase inhibitors p15<sup>INK1</sup> and p21<sup>CIP1</sup>, which leads to cell stagnation in the G1 phase (Ikushima and Miyazono, 2010).

## **5.2 EMT induction alters cholesterol content, potentiates drug resistance, and promotes invasion.**

### **5.2.1 The role of EMT in cholesterol homeostasis**

During EMT, metabolic alterations occur that support the transition to a mesenchymal phenotype. Cholesterol metabolism has been raised to be intricately linked to these changes, however the exact mechanism remains elusive, particularly in PDAC. There have been some speculations that the upregulation of signalling pathways due to elevated levels of cholesterol are implicated in the promotion of EMT-TFS, hence the promotion of EMT in PDAC, since these signalling pathways are common to both pathways. Although metabolic profiling has taken place, only glycolysis, diverted glutamine consumption, and anomalous pentose phosphate pathway have been extensively elucidated to play a role in mesenchymal tumours of PDAC (Blum and Kloog, 2014; Daemen *et al.*, 2015). Overall, proliferating cancer cells are characterized by increased lipids and cholesterol dependency (Morandi *et al.*, 2017). This study aimed to shed light on the dynamics of the relationship between cholesterol and EMT. In this study, EMT induction orchestrated significant changes in cholesterol homeostasis, lowering membrane cholesterol levels by 43% and increasing free and stored cholesterol by 126% and 70% respectively (Figure 4.7, Figure 4.8, and Figure 4.9).

Dysregulated cholesterol metabolism is thought to activate key pathways like PI3K/Akt, Hh, and Wnt/ $\beta$ -catenin, either directly or through lipid raft disruption, all implicated in EMT-TF activation (Figure 1.7). It has been speculated that elevated cholesterol levels, increasing lipid raft content, may further alter TGF- $\beta$  signalling, promoting EMT (Kuzu, Noory, & Robertson, 2016; Abdulla, Vincent, & Kaur, 2021). The increased presence of cholesterol in lipid rafts within plasma membranes is significant, particularly in cancer cells such as those found in breast, prostate, and melanoma (Zhuang *et al.*, 2005; Mikesch *et al.*, 2010; Donatello *et al.*, 2012; Zhao *et al.*, 2016). Lipid rafts possess a crucial characteristic of compartmentalizing various signalling pathways, thereby serving as sorting platforms. These platforms facilitate the efficient and swift transmission of potent signals from the membrane to other cellular locations (Mollinedo and Gajate, 2020). The clustering of lipid rafts into larger platforms enables the recruitment of numerous proteins, allowing them to exert their functions in a secure and conducive environment. Consequently, the functional role of a protein within these rafts is influenced not only by its inherent activity but also by its interactions with the surrounding environment and proteins within the same membrane raft (Mollinedo and Gajate, 2020). Hence, the functionality of raft-localized chaperones, kinases, phosphatases, and other proteins is

likely contingent upon the availability of substrate proteins within the same membrane domain (Mollinedo and Gajate, 2020).

In contrast to this, it has been documented that the destabilisation and reduction of lipid rafts, is a direct consequence of EMT induction. Tisza *et al.* found that by inducing EMT using TGF- $\beta$  or ectopic expression of the transcription factors SNAI1/2 or TWIST1, promoted the destabilisation of lipid raft domains. Normal ordered lipid rafts are characterised by being rich in sphingolipids, saturated lipids, and cholesterol, whereas disordered domains are enriched in unsaturated lipids. They observed that re-stabilisation of lipid rafts reversed motility, mammosphere formation, and importantly inhibited EMT-associated signalling networks (Tisza *et al.*, 2016). This supports the results of this study in which membrane cholesterol levels were lowered by 43% after EMT induction, possibly through lipid raft destabilisation. Similarly, a study by Aulas *et al.* demonstrated that an active EMT program lowers the cholesterol pathway, promoting aggressive subtypes of colon tumour. They hypothesized that EMT necessitates the reduction of cholesterol synthesis to destabilize lipid rafts and enhance cell membrane flexibility for migration (Aulas *et al.*, 2021). Therefore, targeting membrane fluidity may decrease cell motility, stem cell-like properties, and EMT. Although lipid raft destabilisation may seem counter-productive in TGF- $\beta$  signalling, Chen *et al.* discovered that treatment with cholesterol promoted localization of T $\beta$ R-I and T $\beta$ R-II in lipid rafts/caveolae, actually promoting their rapid degradation and suppressed TGF- $\beta$  signalling. Instead, reducing cholesterol levels destabilise lipid rafts increasing the localization of T $\beta$ R-I and T $\beta$ R-II in non-lipid raft microdomains of the plasma membrane potentiating TGF- $\beta$  responsiveness (Chen *et al.*, 2008). This may also be why *TGF- $\beta$ 1* expression increased after EMT induction (Figure 4.14). The role of lipid rafts in cancer cell adhesion and migration remains to be fully elucidated. Notably, there are no studies investigating the role of lipid rafts in the context of EMT in PDAC.

The decrease in membrane cholesterol may also explain the 126% increase in free cholesterol and 70% increase in stored cholesterol as cholesterol is being mobilised from the membrane, where it is then being esterified to prevent free cholesterol-induced cytotoxicity (Tabas, 2002). The accumulation of lipid droplets, have also been implicated in PDAC in which they are able to serve as an energy source, supporting the long-distance spread of cells during invasion (Tabas, 2002; Li *et al.*, 2016; Rozeveld *et al.*, 2020). It has been documented that the promotion of TGF- $\beta$ 2 signalling, promoting EMT, favours the accumulation of lipid droplets. These lipid droplets were implicated in acetylation of SMAD2, increasing its transcription and inducing

invasive capabilities (Corbet *et al.*, 2020). In breast cancer, genes involved in lipid droplet formation were highly expressed and a trait of mesenchymal breast cancer cells (Giudetti *et al.*, 2019). Overall, cholesteryl accumulation and ACAT-1 overexpression has been seen to be prevalent in PDAC specimens and cancer cells lines, promoting metastasis (Li *et al.*, 2016). Additionally, ACAT-1 has been shown to regulate EMT in nasopharyngeal carcinomas (Lu *et al.*, 2021). Interestingly, the inhibition of cholesterol esterification suppressed metastasis via the E2F-1 signalling pathway in prostate cancer, resulting in decrease Ki-67 levels and reduced metastasis in pulmonary metastasis model (Lu *et al.*, 2021). Lipid droplets may hence not only serve as an energy source but as a contributor towards metastasis. However, the importance of lipid droplet accumulation in cell invasion and metastasis is still debatable, particularly why and when lipid mobilization from lipid droplets would be necessary to trigger a more aggressive phenotype in cancer cell (Cruz *et al.*, 2020).

Along with these alterations in cholesterol content, EMT was found to downregulate the expression of *LDLR* (-0.49 log<sub>2</sub> fold change) and *SREBF2* (-1.30 log<sub>2</sub> fold change), while upregulating *ABCA1* expression (1.91 log<sub>2</sub> fold change) (Figure 4.14) indicating a reduction in cholesterol synthesis and uptake along with an increase in cholesterol export. This may be explained by the higher intracellular free cholesterol levels seen after EMT induction. When intracellular cholesterol or cholesterol derived-oxysterols levels are elevated there is a subsequent downregulation of cholesterol synthesis and import and the promotion of cholesterol export, which correspond exactly to the results of this study (Wang *et al.*, 2008). Notably, ABCA1 may be facilitating the export of cholesterol that was once in the membrane and is no longer required for cellular functioning or lipid droplet accumulation. ABCA1 has also been implicated in being necessary for metastasis (Zhao *et al.*, 2016) in which it has been found to be upregulated via MYC-mediated de-repression of its proximal E-box element via EMT induction (Prijic and Chang, 2022). Additionally, ABCA1 has been used to induce EMT in Papillary Thyroid Cancer and has been shown to operate through cooperation with ZEB1 (Park *et al.*, 2023). ABCA1 has also been seen to be regulated by TGF- $\beta$ 1 via the LXR signalling pathway (Hu *et al.*, 2010). ABCA1 overexpression can thus be seen to play a key role in EMT supporting the results of the current study. Although *LDLR* expression was reduced, previous studies have indicated that higher level of *LDLR* expression are associated with advanced stages of colorectal cancer and stemness (C. Wang *et al.*, 2017). Interestingly, low levels of *SREBF2* have been evidenced in the basal subtype of PDAC more than the classical (Gabitova-Cornell *et al.*, 2020). Despite metabolic reprogramming in PDAC leading

to aberrant cholesterol homeostasis, driving disease progression with upregulated cholesterol synthesis and uptake and downregulated efflux (Kuzu *et al.*, 2016; Ricoult *et al.*, 2016; Ruiz *et al.*, 2020; Li *et al.*, 2023), these features align more with epithelial-like tumour cells as described by Aulas *et al.* Gabitova-Cornell *et al.* confirms these speculations by showing that fatty acid and cholesterol metabolism genes were associated with a classical subtype of PDAC, rather than basal. Therefore, mesenchymal cells appear to depend on reduced membrane cholesterol levels, synthesis, and uptake, coupled with increased stored cholesterol and efflux, though this mechanism requires further elucidation. The conflicting interpretations regarding the association between cholesterol and cancer underscore a complex relationship that remains poorly understood. TGF- $\beta$ 1-induced EMT cells therefore seem to rely on reduced membrane cholesterol levels, synthesis, and uptake, coupled with increased stored cholesterol and efflux, which may act to promote invasion, migration and further TGF- $\beta$ 1 signalling.

### **5.2.2 The role of EMT in drug resistance**

EMT plays a central role in the development of chemoresistance by upregulating ABC transporters. This process is further complicated by the intricate relationship between EMT and the cell cycle. Previous studies have shown that EMT induces cell quiescence, which can lead to resistance to conventional chemotherapies such as 5-FU and GEM due to the fact that these therapies primarily target cells in the S and G2/M phases, while the resistant cells reside in the G1/G0 phase (Akhmetkaliyev *et al.*, 2023). The promotion of quiescence as seen in Figure 4.4 and Figure 4.5 may thus be contributing to drug resistance. Although previously believed to be only correlated with drug resistance through ABC transporters, EMT has been shown to directly impact the expression of these transporters. A study by Saxena *et al.* demonstrated that the promoters of ABC transporters contain multiple binding sites for EMT-TFs, and overexpression of TWIST and SNAIL1 increased the promoter activity of 16 ABC transporters (Saxena *et al.*, 2011). Recent studies have also shown that SNAIL1, TWIST1, and ZEB1 overexpress ABCB1, ABCG2, and ABCC5 in various types of cancer cells, including cervical, breast, thyroid papillary, and hepatocellular carcinoma (Chen *et al.*, 2010; Uchibori *et al.*, 2012; Zhu *et al.*, 2012; Tsou *et al.*, 2015; Park *et al.*, 2023).

EMT was shown to promote drug resistance, as evidenced by a 19% decrease in calcein retention (Figure 4.12). Additionally, there was an observed upregulation of *ABCB1* expression with a log<sub>2</sub> fold change of 0.46 (Figure 4.14), further supporting the notion of EMT-induced drug resistance. Moreover, EMT was found to exert a general effect on treatment resistance, as

evidenced by the ability to maintain cell viability even after exposure to various drug combinations. This resistance was particularly evident in the case of plumbagin, as its efficacy in reducing cell viability was significantly diminished (Figure 4.6). It is worth noting that while cell viability can be initial evidence of resistance, further confirmation was sought through a drug resistance assay and RT-qPCR. Surprisingly, EMT was also found to have conflicting effects on the expression of specific drug resistance related-ABC transporters. Specifically, there was a reduction in the expression of *ABCC5* (with a log<sub>2</sub> fold change of -1.08) and *ABCG2* (with a log<sub>2</sub> fold change of -3.95), both of which are known to play a role in drug efflux (Figure 4.14). Interestingly, a side population of PANC-1 cells known to be in an EMT state had an increase in *ABCG2* mRNA levels (Kabashima *et al.*, 2009), whereas in this study a decrease was observed, this may be due to the fact that this study focussed on a sub-population within the PANC-1 cell line that had a high metastatic potential and was in a partial EMT state and not on TGF- $\beta$ 1 EMT-induced PANC-1 cells. Additionally, there was a decrease in the expression of the drug entry gene *hENT1* (with a log<sub>2</sub> fold change of -0.14), which restricts drug import (Figure 4.14). These findings suggest that EMT enhances drug resistance through upregulation of *ABCB1* but may also impact drug import mechanisms. In Saxena *et al.*'s study, different breast cancer cell lines responded differently to EMT, with some promoting multiple ABC transporters while others only promoted one (Saxena *et al.*, 2011). It is possible that TGF- $\beta$  promotes drug resistance through *ABCB1* and other ABC transporters implicated in drug resistance that were not investigated in this study. To date, no studies have examined the specific ABC transporters involved in TGF- $\beta$ -induced EMT resistance in PDAC. Contrastingly to the findings in this study, Subramanian *et al.* showed, using molecular dynamics simulations, that cholesterol accumulation in the membrane increases the activity of the ABC transporter *ABCB1* by preferentially accumulating *ABCB1* substrates in cholesterol-rich regions of the membrane (Subramanian *et al.*, 2016), linking high levels of membrane cholesterol to MDR via ABC transporters. This is; however, a simulation and the exact response may not be elicited *in vitro*. In the case of EMT, cells are reducing their membrane cholesterol and drug resistance via ABC transports may thus be alternatively being promoted through EMT-TFs.

Interestingly, *hENT1* expression was downregulated in this study (Figure 4.14). GEM and 5-FU both use hCNT proteins and ENT proteins to enter the cell. GEM primarily utilises hCNT1, hCNT3, and notably hENT1 (Principe *et al.*, 2021). On the other hand, 5-FU utilises hENT1 and hENT2, with some reports suggesting that organic anionic transporter 2 (hOAT2) is also involved (Kobayashi *et al.*, 2005; Mafi *et al.*, 2023). Interestingly, EMT has been found to

promote drug resistance in PC cells through the functional loss of hENT1, particularly for GEM (Weadick *et al.*, 2021). The promotion of N-cadherin has been found to decrease hENT1 expression and membrane localisation, therefore hENT1 expression is reliant on cadherin switching, and the presence of E-cadherin (Weadick *et al.*, 2021), this is in agreement with the findings of this study that presented a decrease in *hENT1* (Figure 4.14) expression alongside a decrease in E-cadherin expression (Figure 4.11).

In the present study, only gene expression was investigated, but to fully understand the mechanism, protein analysis should also be conducted. EMT cells are thus enhancing drug resistance through increased drug export via *ABCB1*, decreased drug import via *hENT1*, and the induction of cell quiescence. Notably, EMT was found to significantly increase invasive capacity by approximately 51% (Figure 4.13) and hence invasion is facilitated through the induction of EMT, a pivotal characteristic of the process. In general, EMT augments the invasive capacity of cells by orchestrating intricate molecular and cellular modifications that promote their mobility and dissemination within tissues. Remarkably, cell lines characterized by partial EMT typically exhibit invasive properties through the formation of budding clusters and individual cells, whereas cell lines with complete EMT are primarily observed to invade as individual cells (Aiello *et al.*, 2018).

### **5.3 Targeting cholesterol content post-EMT induction promotes altered cholesterol homeostasis, increased drug resistance, invasion, and subsequently EMT.**

Given the significant involvement of cholesterol in various cancer-related processes such as differentiation, proliferation, migration, chemoresistance, and survival, as well as the observed disruption of synthesis, efflux, influx, and metabolism in PDAC, targeting cholesterol depletion has emerged as a potential therapeutic strategy in cancer treatment. Initial studies were conducted in partial-EMT cells to investigate the impact of targeting cholesterol on cell viability in PDAC. Specifically, targeting cholesterol using KS-01 or M $\beta$ CD for 48 hours in a partial-EMT state resulted in reduced viability. Furthermore, the combination of KS-01 with chemotherapies notably enhanced their efficacy (Figure 4.6). This phenomenon has been extensively documented in laboratory settings and has been observed in breast and colorectal cancers. For instance, treatment with HP $\beta$ CD has demonstrated preferential and significant cytotoxic potential in breast cancer cells, inducing apoptosis in both cancer cell lines by depleting cholesterol (Saha *et al.*, 2023). Similarly, in an unpublished dissertation by Pillay *et al.*, the same trend was observed after treating colorectal cancer with KS-01. Both of these

research findings have also been confirmed *in vivo*. However, in the current study, while the efficacy of drug treatments appeared to improve and cell viability decreased upon treatment with KS-01 or M $\beta$ CD, the use of KS-01 resulted in a notable increase in membrane cholesterol levels (74%), with no significant change in CE levels being observed. Conversely, treatment with M $\beta$ CD did not affect membrane cholesterol or CE levels significantly but led to a considerable increase in free cholesterol by 90% (Figure 4.7, Figure 4.8, and Figure 4.9). This difference is most likely due to the use of a different and more aggressive PANC-1 cell line as treatment times and the concentration of KS-01 in this study were kept the same as these breast and colorectal cancer studies.

Without gene expression data or any other experiments performed on the partial-EMT cells, the only mechanism that can be speculated is that targeting cholesterol may lead to cells entering a compensatory state to prevent its reduction. It is important to note that these drug combinations were tested for a duration of only 4 hours, and it is possible that different results may occur over longer periods of time. When cholesterol is depleted through CDs, stored cholesterol is not mobilized; instead, cholesterol synthesis or uptake by LDLR may occur to prevent its loss. This results in the observed increase in free cholesterol in both KS-01 or M $\beta$ CD treatments and the increased membrane cholesterol in KS-01 treated cells. The dysregulation of cholesterol plays a crucial role in PDAC progression, suggesting that this dependence is more significant than previously believed. However, when paired with cell viability assays, these results no longer tell the same story. The mechanisms underlying these results still need to be elucidated and are currently being investigated by Daya *et al.* (unpublished thesis).

Current studies have shed light on the promising role of M $\beta$ CD and HP $\beta$ CD in targeting membrane cholesterol as a potential therapeutic strategy for cancer treatment. Research on breast cancer cells has demonstrated that HP $\beta$ CD treatment effectively depletes cholesterol in lipid rafts, leading to changes in raft construction and affecting the localization of TGF- $\beta$  receptors within these structures (Saha *et al.*, 2023). As a result, TGF- $\beta$ 1-induced migration and invasion signalling pathways are disrupted, highlighting the potential benefits of cholesterol depletion in lipid rafts as a mechanism to inhibit cancer progression (Saha *et al.*, 2023). Studies have also shown that M $\beta$ CD can increase cholesterol levels in the medium in a dose-dependent manner by removing cholesterol from the plasma membrane of human colorectal cancer cells. This decrease in cholesterol levels contributes to the anti-cancer effects of the drug (Ohno *et al.*, 2023b). Another cholesterol-lowering agent, simvastatin, has been

found to reduce raft cholesterol content, inhibit the Akt signalling pathway, and induce apoptosis in certain prostate cancer cells lacking caveolin and PTEN (Zhuang *et al.*, 2005). Additionally, M $\beta$ CD has been shown to suppress proliferation in head and neck carcinoma and non-small cell lung cancer cells by preventing lipid raft aggregation and inhibiting the activation of key signalling molecules such as c-met and c-Src (Zeng *et al.*, 2018)). Collectively, these findings highlight the potential of cholesterol-targeting agents like M $\beta$ CD and HP $\beta$ CD in cancer therapy by disrupting lipid raft organization and impeding cancer cell proliferation and metastasis. This study however, focused on targeting cholesterol in post-EMT PANC-1 cells. The process of EMT entails significant changes in cholesterol levels and gene expression, which reflect alterations in cellular behaviour and phenotype. Our observations revealed that elevated levels of stored cholesterol (CEs stored in lipid droplets), known to play a crucial role in invasion, as well as increased expression of free cholesterol and *ABCA1*, a cholesterol exporter associated with invasiveness in other cancer studies, indicated that targeting cholesterol could serve as a novel therapeutic approach to reduce overall cholesterol levels (Figure 4.8, Figure 4.9, and Figure 4.14). By doing so, we could potentially revert the cells back to a more epithelial-like phenotype and induce cytotoxic effects in PDAC. Preliminary studies have showed the ability of KS-01, statins, and M $\beta$ CD to reverse an EMT state in breast and colorectal cancer (Perumel, *et al* unpublished article based on three research studies conducted in the lab). Thus, we investigated the possibility of targeting cholesterol in order to reverse the EMT state.

Following the induction of EMT, treatment with the compound KS-01 resulted in a significant elevation of membrane cholesterol levels by 128%, coupled with a decrease of 32% in stored cholesterol levels. However, the levels of free cholesterol showed a slight, non-significant decrease, indicating its sustained high expression. In a similar trend, treatment with the agent M $\beta$ CD during the post-EMT phase led to a 57% rise in membrane cholesterol levels and a reduction of 30% in CE levels, with a slight, non-significant drop of 21% in free cholesterol (Figure 4.7, Figure 4.8, and Figure 4.9). Notably, there was a significant upregulation of genes linked to cholesterol metabolism, including *LDLR* (2.71-fold increase) and *SREBF2* (3.31-fold increase), as well as a notable increase in expression of *ABCA1* (1.51-fold increase). Similar to the effects of KS-01 treatment, M $\beta$ CD induced upregulation of *LDLR* (2.63-fold increase), *SREBF2* (1.79-fold increase), and *ABCA1* (0.84-fold increase) (Figure 4.14). Indicating both treatments may be promoting cholesterol synthesis, uptake, and export. Consistent with partial-EMT cells, treatment with cholesterol-depleting agents did not lower the overall levels of

cholesterol, but rather reduced the levels of stored cholesterol. This phenomenon may be a transient response to the removal of cholesterol from the cell. It is postulated that the removal of cholesterol from the membrane via CDs prompts the cell to mobilise its stored cholesterol and stimulate the expression of genes involved in cholesterol synthesis and import as a robust compensatory mechanism. Additionally, the substantial increase in cholesterol levels may further induce the transcription of *ABCA1* in an effort to efflux cholesterol. Notably, this study is the first to document this mechanism and is in contrast to Perumel, *et al.*'s *unpublished* article most likely due to a cancer-specific response to cholesterol depleting agents that is not seen in breast or colorectal cancers, the exact mechanism behind this discrepancy is unknown. The compensatory effects observed appear to be more pronounced with KS-01 compared to M $\beta$ CD. The precise mechanisms underlying this difference remain unknown, and further investigation is warranted to elucidate the specific cholesterol uptake mechanism employed by each CDs. Interestingly, the effect on cholesterol is accompanied by a simultaneous increase in EMT. Following treatment with KS-01, there was a significant upregulation of mesenchymal markers, such as vimentin (115% increase), along with a moderate increase in E-cadherin levels (45% increase), which is somewhat contradictory. Treatment with M $\beta$ CD also led to a significant elevation in vimentin expression (157% increase), while E-cadherin levels remained unaltered (Figure 4.11 and Figure 4.10). KS-01 and M $\beta$ CD caused a 2.44 and 0.93 log<sub>2</sub>-fold change, respectively, in the expression of the EMT transcription factor *SNAIL1*. Additionally, KS-01 increased the expression of *TGF- $\beta$ 1* by 1.11 log<sub>2</sub>-fold change, whereas M $\beta$ CD only slightly increased it by 0.42 log<sub>2</sub>-fold change, which was not statistically significant (Figure 4.14). Interestingly, despite the fact that lipid raft levels were elevated in this study, previous evidence suggests that reduced cholesterol levels and destabilization of lipid rafts are implicated in EMT and TGF- $\beta$  functioning. Hence, alternative mechanisms must be at play to induce EMT. Two important studies in PDAC have demonstrated that targeting cholesterol, either through statins or by knocking out *Nsdhl*, switches the classical subtype of PDAC to a basal subtype. Specifically, Gabitova-Cornell *et al.* showed that decreased cholesterol levels promoted the expression of SREBP1, a key regulator of *de novo* lipogenesis and glycolysis pathways, which in turn increased the expression of TGF- $\beta$ 1 due to the presence of SREBP1 binding motifs. This activation of TGF- $\beta$ 1 leads to the EMT phenotype. Although the study was conducted on epithelial PDAC cells and used cholesterol biosynthesis inhibitors, it is reasonable to speculate that a similar mechanism may occur in EMT-induced cells. Another study by Dorsch *et al.* demonstrated that statins induced a partial EMT phenotype in PDAC, lung cancer, and colon cancer cells. Furthermore, in these PC cells, secondary tumour

formation was reduced, which is attributed to a MET phenotype; however, this effect could be reversed with the development of statin resistance or cessation of statin use, leading to a more metastatic and invasive form of PC (Dorsch *et al.*, 2021). The varying compensatory cholesterol mechanisms may explain the lower overall promotion of *SNAIL1* and *TGF- $\beta$ 1* gene expression observed in M $\beta$ CD-treated cells. Differing levels of TGF- $\beta$ 1 expression could also account for the proportional difference in *ABCA1* expression. As mentioned earlier, TGF- $\beta$ 1 regulates *ABCA1* in THP-1 macrophage-derived foam cells through the LXR signalling pathway (Hu *et al.*, 2010). The upregulation of *SNAIL1* can account for the observed increase in vimentin expression, but it does not fully explain the differences in expression levels, as KS-01, despite having higher *SNAIL1* and TGF- $\beta$ 1 expression, did not exhibit the highest level of vimentin expression. *SNAIL1* is just one of several transcription factors involved in EMT, and the gene expression of all EMT transcription factors would provide further insight into the mechanisms underlying M $\beta$ CD-induced vimentin expression. Interestingly, E-cadherin expression increased alongside vimentin expression after KS-01 treatment, while no change was observed with M $\beta$ CD (Figure 4.11). This observation does not align with the known mechanisms of EMT and warrants further research to elucidate the underlying reasons. It is possible that depleting cholesterol using CDs may induce a hybrid EMT state that maintains an epithelial phenotype. These hybrid EMT states have the highest metastatic potential due to their ability to migrate easily and attach to distant sites, forming metastatic colonies (Pastushenko *et al.*, 2018; Celià-Terrassa and Kang, 2024). It is worth noting that both KS-01 and M $\beta$ CD promoted cell invasion, with M $\beta$ CD inducing the highest level of invasion, which may be attributed to its greater promotion of vimentin expression and consequently enhanced invasive capabilities.

Depleting cholesterol was also implicated in promoting a more aggressive phenotype, by promoting drug resistance, but not through a continued promotion of *ABCB1*. Instead, KS-01 promoted an increase in the expression of *ABCC5* (1.74 log<sub>2</sub> fold change) and a slight, but not significant, increase in *ABCG2* (0.92 log<sub>2</sub> fold change). Treatment with M $\beta$ CD led to slight increases in *ABCC5* expression (0.94-fold increase) and *ABCG2* expression (0.29-fold increase), but these changes were not statistically significant (Figure 4.14). This can be attributed to the increased expression of EMT-TFs, which directly promote the expression of ABC transporters due to their multiple binding sites for EMT-TFs (Saxena *et al.*, 2011). Importantly, *ABCC5* and *ABCG2* are known facilitators of drug resistance to 5-FU and GEM (Hagmann *et al.*, 2009; Li *et al.*, 2011). However, the complete mechanism of drug resistance

through ABC transporters is not documented in this study. One particularly contrasting result observed in this study was the significant decrease in *ABCB1* drug exporter functionality after M $\beta$ CD treatment, despite a 0.91 log<sub>2</sub> fold change increase in gene expression. Investigation of protein expression is needed to understand the mechanism behind this, as gene expression alone does not necessarily indicate functionality or localization to the membrane. This result, however, is supported by a study documenting that M $\beta$ CD abolishes the expression of *ABCB1* and *ABCG2* in ovarian cancer (Kim *et al.*, 2018). The effects of M $\beta$ CD and KS-01 on other ABC transporters contradict studies showing that targeting cholesterol with statins inhibits drug transporter activity, but this disparity may lie in the use of chronic myeloid leukaemia cells and not PC cells in the study as well as the use of statins instead of CDs (Glodkowska-Mrowka *et al.*, 2014). Interestingly, KS-01 significantly promoted the expression of *hENT1* (2.22 log<sub>2</sub> fold change), which is contradictory in terms of drug resistance (Figure 4.14). However, as mentioned earlier, *hENT1* expression is dependent on cadherin switching, and the presence of N-cadherin reduces its expression and localization to the membrane (Weadick *et al.*, 2021). Although EMT was promoted, E-cadherin was upregulated by 45%. Therefore, it can be speculated that the increase in E-cadherin and subsequent downregulation of N-cadherin promoted the expression of *hENT1*. It has also been interestingly found that several PC cell lines were less sensitive to GEM and 5-FU when *hENT1* mRNA levels were high (Tsujiie *et al.*, 2007). This confirms the lack of significant change in *hENT1* expression after M $\beta$ CD treatments, as there was no significant change in E-cadherin levels. Therefore, it can be speculated that instead of combating EMT through cholesterol depletion, CDs enhance EMT, drug resistance, and invasion, thereby promoting the acquisition of an aggressive disease phenotype. This is the first time such results have been documented.

#### **5.4 Combining cholesterol depletion with current chemotherapies 5-FU and GEM**

GEM or 5-FU alone or in combination with other conventional therapeutics is considered the standard of care for the treatment of advanced PDAC. However, this treatment approach has shown limited improvement in overall survival rates and resistance, particularly in mesenchymal PDAC. Consequently, this study aimed to investigate the potential enhancement of the efficacy of GEM and 5-FU in post-EMT PANC-1 cells.

##### **5.4.1 Targeting cholesterol content in combination with 5-FU does not alter the EMT state or drug resistance, but does alter cholesterol homeostasis**

Treatment with either 5-FU alone or the combination of KS-01 with 5-FU showed conflicting results compared to KS-01 treatment alone in PANC-1 cells. Neither treatment exhibited significant changes in expression levels of vimentin or E-cadherin. Interestingly, 5-FU treatment induced a slightly higher increase in *SNAIL1* expression (2.04 log<sub>2</sub> fold change) compared to the combination of 5-FU and KS-01 (1.79 log<sub>2</sub> fold change), although the effect was not as pronounced as in other treatments. Indicating that 5-FU alone may be beginning to promote EMT, as drug treatments were only over 4 hours. Moreover, 5-FU alone did not significantly enhance *TGF-β1* expression (0.64 log<sub>2</sub> fold change alone, 0.56 log<sub>2</sub> fold change combination) beyond the post-EMT levels, although a slight increase was observed (Figure 4.14). However, this increase was not statistically significant and did not reach the level observed in other treatments. Additionally, neither treatment demonstrated an effect on invasion (Figure 4.13). Importantly, the combination of 5-FU with KS-01 exhibited a greater increase in *LDLR* expression (2.69 log<sub>2</sub> fold change) compared to 5-FU alone (0.89 log<sub>2</sub> fold change), while 5-FU alone showed a higher increase in *ABCA1* expression (2.21 log<sub>2</sub> fold change) compared to the combination (1.03 log<sub>2</sub> fold change). Furthermore, the combination of 5-FU with KS-01 (2.41 log<sub>2</sub> fold change) induced a higher increase in *SREBF2* expression compared to 5-FU alone (1.82 log<sub>2</sub> fold change) indicating the same compensatory mechanism was activated in response to KS-01, but the resultant enhancement of EMT was not as present (Figure 4.14).

Studies investigating the impact of 5-FU and cytotoxic compounds on EMT have yielded interesting results. In particular, 5-FU-resistant MCF-7 cells demonstrated EMT features, such as increased invasion and migration, reduced E-cadherin expression, and elevated *SNAIL2* expression (Zhang *et al.*, 2012). The reversal of EMT and invasive behaviour was observed when *SNAIL* was silenced (Zhang *et al.*, 2012). Similarly, 5-FU-resistant DLD1 cells exhibited EMT characteristics, including enhanced invasion and migration, suppressed E-cadherin expression, and increased *SNAIL2* expression (Findlay *et al.*, 2014). Furthermore, cytotoxic compound-induced ER stress has been associated with the promotion of EMT, which seems to be independent of cancer cell type (Shah *et al.*, 2017). Notably, treatment with cisplatin in oral cancer cells has been shown to induce prolonged ER stress, leading to EMT promotion, delayed cell-cycle progression, and S-phase exit (C. Y. Chen *et al.*, 2020). These studies emphasize the multifaceted effects of cytotoxic compounds on EMT regulation and highlight the complex relationship between drug-induced stress responses and cellular phenotypic transitions. Thus, it can be speculated that treatment with 5-FU and subsequent ER stress triggers the

upregulation of EMT-TFs when used alone. However, the unexpected results of gene expression related to cholesterol homeostasis necessitate further investigation, as 5-FU is not known to directly affect cholesterol. Additional observations regarding cholesterol content would provide a better understanding of this mechanism. It is possible that 5-FU disrupts cholesterol homeostasis, resulting in increased synthesis, uptake, and export. Nevertheless, the impact is less significant compared to specifically targeting cholesterol using KS-01, which induces the compensatory mechanism described earlier. The upregulation of all genes observed when 5-FU is combined with KS-01 follows similar trends as KS-01 alone, albeit to a lesser extent, particularly with minimal effects on *TGF-β1* (Figure 4.14). Surprisingly, this did not translate to any changes in vimentin and E-cadherin protein expression. This discrepancy may be attributed to 5-FU's known influence on translation machinery, mainly affecting ribosomal RNA and transfer RNA processing and functions (Bash-Imam *et al.*, 2017). Consequently, this may reduce the propensity of KS-01 to promote an EMT phenotype and thus not increasing invasion. Therefore, the proposed mechanism involving SREBP1 and TGF-β1 may not be the driving force in this combination. Furthermore, it is possible that the observed increase in EMT-TF gene expression is an early event, occurring before significant changes in vimentin or E-cadherin levels become detectable. The downstream effects on protein expression may require more time or additional signalling cascades to manifest. However, further studies are necessary to comprehend these irregular findings fully.

As mentioned earlier, PDAC often demonstrates inherent or acquired resistance to chemotherapy. Surprisingly, treatment with 5-FU alone effectively reduced drug resistance via *ABCB1* in the drug resistance assay (Figure 4.12). Following treatment, *ABCB1* expression was slightly higher (0.37 log<sub>2</sub> fold change), but this increase was not statistically significant. On the other hand, the combination of 5-FU with KS-01 did not affect drug resistance. Additionally, there was minimal change in *ABCB1* expression (0.16 log<sub>2</sub> fold change) in this combination. No significant effects were observed on *ABCG2* or *ABCC5*, although there was a slight increase in *ABCC5* expression post-treatment (0.48 log<sub>2</sub> fold change alone, 0.63 log<sub>2</sub> fold change in combination). Drug influx gene expression increased more with 5-FU alone (1.78 log<sub>2</sub> fold change) compared to the combination of 5-FU and KS-01 (0.91 log<sub>2</sub> fold change) (Figure 4.14). It can be postulated that the absence of significant alterations in the ABC transporters *ABCC5* and *ABCG2* is attributed to the limited increase in EMT-TFs as a result of the treatments. The specific mechanisms underlying these results remain unclear as they have not yet been documented. It is noteworthy that the decreased activity of the ABC transporter

*ABCB1* contradicts previous studies that have highlighted the role of *ABCB1* expression in 5-FU resistance, these studies, however, focussed on colorectal cancer cell lines that were developed to be 5-FU resistant over several passage numbers (T. Wang *et al.*, 2015; Sousa-Squiavinato *et al.*, 2022). These findings also differ from the cell viability results of this study and a previous study that demonstrated a significant increase in cytotoxic effects of 5-FU and patient survival when combined with a statin for cholesterol depletion, but unlike this study it was based on the survival rates of patients with hepatocellular carcinoma (Kawata *et al.*, 2001). Further investigation may be required to fully understand the molecular mechanisms, including drug-drug interactions between KS-01 and 5-FU. It can however be concluded that 5-FU is an ineffective treatment post-EMT and it is not recommended to employ cholesterol depletion as a strategy to increase the efficacy of 5-FU in PDAC.

#### **5.4.2 Targeting cholesterol content in combination with GEM alters cholesterol homeostasis, potentiates EMT induction, chemoresistance, and invasion.**

GEM stands as the cornerstone of first-line therapy for PDAC. GEM became the standard of care due to its modest efficacy and tolerability profile. Despite its widespread use, the overall survival benefit conferred by GEM monotherapy remains limited. The administration of GEM treatment alone did not result in statistically significant changes in the levels of vimentin or E-cadherin expression. However, when used in combination with KS-01, there was an increase in vimentin expression, although to a lesser extent compared to when KS-01 was administered alone (Figure 4.2). Additionally, a small but significant increase in E-cadherin expression was observed, albeit less pronounced than with KS-01 alone. In terms of invasion, GEM alone did not have a significant impact, but when combined with KS-01, it resulted in a 54% increase in invasion (Figure 4.13). However, this increase was not as prominent as when KS-01 or M $\beta$ CD were administered individually. Moreover, GEM alone significantly promoted the expression of *SNAIL1* (with a 1.99 log<sub>2</sub> fold change) and *TGF- $\beta$ 1* (with a 0.44 log<sub>2</sub> fold change) (Figure 4.14). Conversely, when GEM was combined with KS-01, it significantly enhanced *SNAIL1* expression the most, with a 2.57 log<sub>2</sub> fold change, although the increase in *TGF- $\beta$ 1* was less pronounced, with a 0.78 log<sub>2</sub> fold change compared to KS-01 alone (Figure 4.14). GEM, like 5-FU seems to promote the initiation of EMT even without KS-01, and when combined with KS-01 exhibits similar effects to KS-01 alone. Additionally, GEM alone promoted *LDLR* expression with a 0.94 log<sub>2</sub> fold change, *ABCA1* expression more than when in combination with KS-01 (with a 1.94 log<sub>2</sub> fold change), and *SREBF2* expression less than when in

combination (with a 2.27 log<sub>2</sub> fold change), similar to the trend observed with 5-FU treatment, again indicating that the monotherapy induces changes in cholesterol, promoting less import and synthesis and more export than when combined with KS-01. On the other hand, when GEM was combined with KS-01, it significantly promoted *LDLR* expression (with a 2.40 log<sub>2</sub> fold change), *ABCA1* expression (with a 1.17 log<sub>2</sub> fold change), and *SREBF2* expression (with a 3.47 log<sub>2</sub> fold change) in a similar pattern to what was observed with KS-01 alone (Figure 4.14). Hence, combining GEM with KS-01 promotes synthesis and uptake, while promoting cholesterol efflux less than GEM alone.

GEM resistance in PC has been linked to the induction of EMT, a process associated with aggressive tumour behaviour and resistance to therapy. Research has demonstrated that GEM-resistant PC cells undergo additional molecular changes resembling EMT, which are mediated by the ERK-ZEB-1 pathway (El Amrani *et al.*, 2019). Inhibiting the phosphorylation of ERK1/2 or the expression of ZEB-1 has been shown to decrease chemoresistance, indicating the critical role of EMT-related signalling pathways in GEM resistance (El Amrani *et al.*, 2019). Furthermore, induced GEM-resistant cells show an upregulation of Notch-2 and its ligand, Jagged-1, suggesting the involvement of the Notch signalling pathway in EMT acquisition and the emergence of cancer stem-like cell phenotypes (Wang *et al.*, 2009). Moreover, surviving PC cells after GEM treatment exhibit characteristics indicative of stem cell differentiation and EMT, including elevated expression levels of *OCT4*, *CD24*, *EpCAM*, *PDX-1*, *SHH*, *CD44*, *CD133*, and *SNAIL2* (Quint *et al.*, 2012). These findings emphasize the complex relationship between GEM resistance and EMT induction, underscoring the importance of targeting EMT pathways to overcome therapeutic resistance and improve treatment outcomes. This may explain the upregulation of EMT-TFs *SNAIL1* and *TGF-β1* after treatment with GEM alone (Figure 4.14). However, there were no changes observed in vimentin or E-cadherin expression, indicating that the increase in EMT-TF gene expression may be an early event that occurs before significant changes in vimentin or E-cadherin levels can be detected. Additionally, since the drug treatments were only administered for 4 hours, the full effects may not have been observed. In a similar context to 5-FU treatment, ER stress induced by cytotoxic compounds has been associated with the promotion of EMT (Shah *et al.*, 2017) and thus the reason behind the increase in *SNAIL1*. The unexpected gene expression results related to cholesterol homeostasis genes suggest that further investigations are needed to understand this mechanism, considering that GEM is not known to affect cholesterol. Similar trends as observed with KS-01 alone were observed when combining GEM with KS-01;

however, this time there were translational changes in the protein expression of vimentin and E-cadherin, unlike 5-FU treatments (Figure 4.10 and Figure 4.11). This may be due to the different mechanisms of action between 5-FU and GEM, which potentiate the increase in invasion observed in the study. It is speculated that the combination treatment follows a similar mechanism of action as proposed previously with KS-01 alone, with the additional mechanism of GEM explaining some of the minor differences observed. However, GEM does not seem to be functioning as expected, as there is no decrease in cell viability observed after GEM alone or in combination (Figure 4.6). Similarly to KS-01 alone, a hybrid state of EMT that maintains an epithelial phenotype was observed, potentially contributing to a higher metastatic potential (Pastushenko *et al.*, 2018; Celià-Terrassa and Kang, 2024). Nonetheless, the exact mechanism of action underlying the study's results needs further elucidation before drawing specific conclusions.

When administered as a monotherapy, GEM did not have an impact on drug resistance facilitated by *ABCB1*. However, when KS-01 was combined with GEM, drug resistance increased by 25% without any change in *ABCB1* expression (Figure 4.12 and Figure 4.14). It is possible that the upregulation of the transporter's activity was due to increased membrane cholesterol levels (Figure 4.7). This can be speculated because the accumulation of cholesterol in specific regions of the membrane may lead to the preferential accumulation of *ABCB1* substrates (Subramanian *et al.*, 2016). However, this phenomenon was not observed in any other drug treatments, suggesting that the combination of KS-01 and GEM resulted in higher membrane cholesterol levels compared to other treatments. To validate this, further cholesterol analysis is required. GEM alone had no effect on the expression of *ABCC5* and *ABCG2*, but like 5-FU, it promoted the expression of *hENT1*, although to a lesser extent. A similar speculation can be made here as with 5-FU. However, the combination treatment resulted in an increase in *ABCC5* expression (1.35 log<sub>2</sub> fold change), with no change in *ABCB1* expression and a slight increase in *ABCG2* expression, although this change was not statistically significant (Figure 4.14). The promotion of EMT-TF *SNAIL1* may be involved in this phenomenon as these TFs have the ability to bind to the promoters of ABC transporters, thereby promoting their expression and subsequently drug resistance. This is in contrast to a previous study that reported an enhanced anti-neoplastic effect of GEM when combined with a statin to deplete cholesterol levels, although this study was in another PC cell line the use of a statin and for 72 hours instead of a cyclodextrin for 4 hours may explain the differing result (Bocci *et al.*, 2005). The underlying mechanisms behind the increase in *hENT1* expression are not fully

understood. On one hand, it has been found that the promotion of N-cadherin can decrease hENT1 expression and its localization in the membrane, indicating that hENT1 expression depends on the presence of E-cadherin. This may explain the increase in *hENT1* expression observed in the GEM + KS-01 treatment group. On the other hand, *hENT1* expression increased in the GEM monotherapy group without any observed changes in E-cadherin (Figure 4.11 and Figure 4.14). To gain a better understanding of this mechanism across different treatment groups, the activity of the drug importer as well as protein expression should be investigated further. It can be concluded that GEM is an ineffective treatment post-EMT and when combined with cholesterol depletion potentiates EMT, drug resistance, and invasion.

Cholesterol depletion by itself has the potential to activate specific signalling pathways or cause cellular changes that facilitate EMT. When combined with GEM, another promoter of EMT, the two treatments may act in synergy to amplify EMT-related processes. However, when combined with 5-FU, the interaction between cholesterol depletion and the drug leads to a distinct cellular response that may counteract the EMT-promoting effects observed with cholesterol depletion alone. This could be attributed to various factors, such as modifications in intracellular signalling pathways, alterations in patterns of gene expression, or adjustments in cellular metabolism, which ultimately impact the likelihood of EMT induction. Further studies focusing on the mechanisms at the molecular level are necessary to clarify specific molecular processes behind these findings and gain a deeper understanding of the correlation between cholesterol depletion and different chemotherapeutic agents in the regulation of EMT.

## **5.5 Conclusion**

Treating PANC1 cells with 10 ng/mL of TGF- $\beta$ 1 mediated the induction of EMT and promoted a more resistant state. This is evidenced by the promotion of the drug export gene *ABCB1*, the decrease in drug import, and the resistance to chemotherapeutic agents. It is worth noting that this study is the first to document alterations in cellular cholesterol levels following EMT induction in PDAC. Interestingly, TGF- $\beta$ 1-induced EMT seems to rely on reduced membrane cholesterol levels, synthesis, and uptake, coupled with increased stored cholesterol and efflux. Although lipid rafts are key signalling hubs crucial for EMT induction, their destabilisation and decrease facilitated an EMT phenotype, possibly by allowing for a more flexible cell for metastasis. The role of lipid rafts in this context is rather contradictory, as different cancer types demonstrate varying results, and the exact mechanism underlying these discrepancies remains unknown.

Given the significant involvement of cholesterol in various cancer-related processes such as progression, chemoresistance, and invasion along with the successes of previous studies at reversing the EMT phenotype, attempts were made at targeting cellular cholesterol in PDAC to affect both EMT and drug resistance. This, however, led to unexpected results, in which a cholesterol compensatory mechanism was activated, subsequently promoting a hybrid EMT state, drug resistance, and metastatic potential. When combined with GEM, these two treatments are speculated to act collaboratively to enhance EMT-related processes. On the other hand, when paired with 5-FU, the interplay between cholesterol depletion and the drug leads to a unique cellular response that may mitigate the EMT-promoting effects typically associated with cholesterol depletion alone. With regards to this in a clinical setting, patients on cholesterol-lowering agents such as statins should be cautious of the possible repercussions faced if diagnosed with PDAC. Therefore, the findings of this study, along with existing literature, suggest that lowering cholesterol should not be considered a viable therapeutic option for combatting PDAC, particularly when cells are in a mesenchymal state (Figure 5.1).

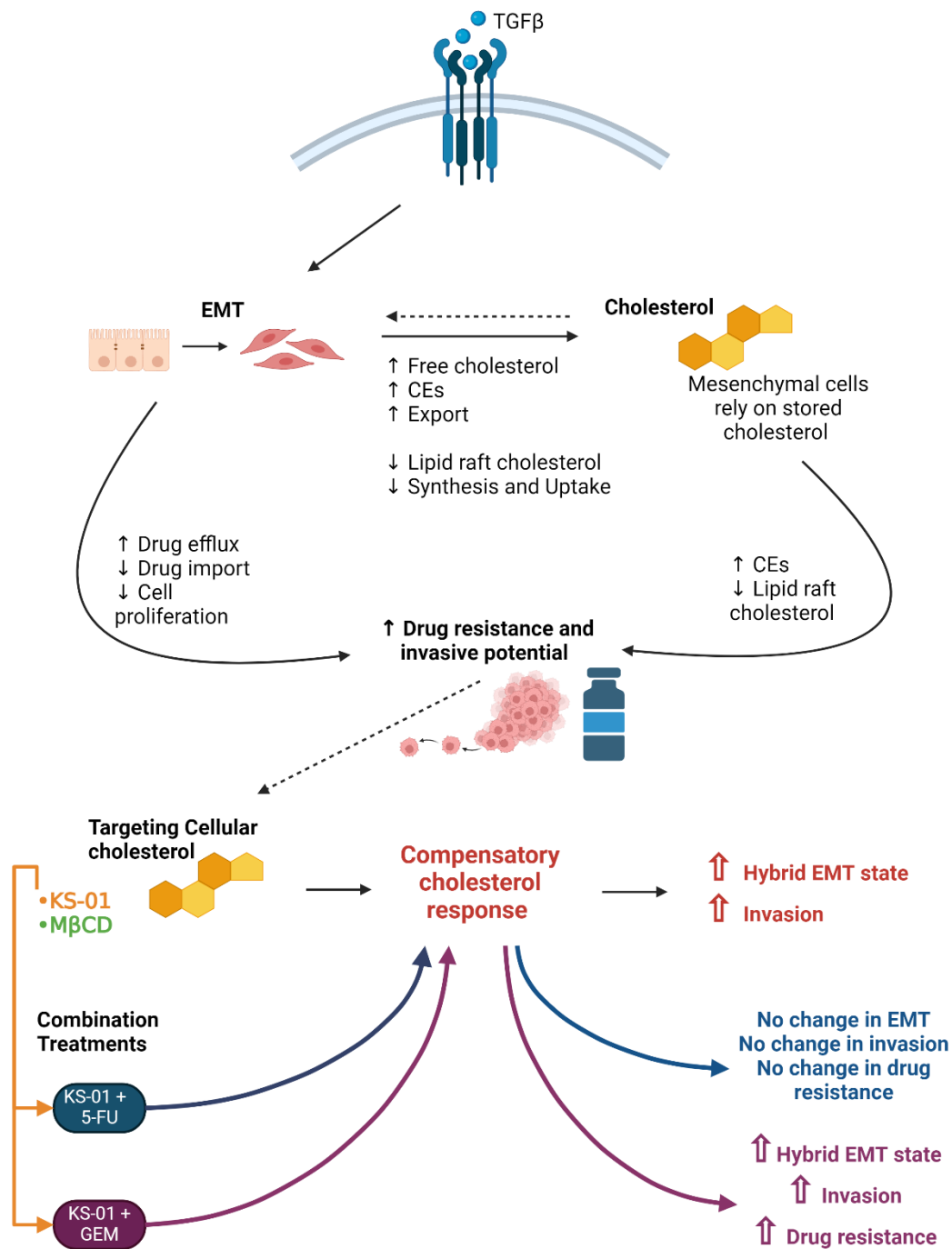


**Figure 5.1: A summary of the main findings of the research**

When EMT is induced using TGF- $\beta$ 1 there is a promotion of drug resistance and invasive potential as a result of increased drug efflux, and decreased drug import and cell proliferation. EMT alters cholesterol homeostasis by increasing levels of free cholesterol and CEs as well as promoting export. Interestingly, lipid raft cholesterol was seen to be decreased and cholesterol synthesis and uptake were promoted. Thus, indicating the reliance of mesenchymal cells on stored cholesterol. These effects on cholesterol, particularly increased CEs and reduced lipid raft cholesterol contribute to the invasive potential of mesenchymal cells. Attempts at targeting cholesterol were then made to see the effects on EMT and drug resistance. Using the CDs KS-01 and M $\beta$ CD resulted in a compensatory cholesterol response, where overall levels of

*cholesterol were not reduced and instead, the PANC-1 cells tried to compensate for this loss by promoting uptake and synthesis of cholesterol, as well as mobilising cholesterol stores. This compensatory effect promoted a hybrid EMT state as indicated by an increase in both vimentin as well as E-cadherin, resulting in the promotion of invasion but yielded conflicting drug resistance responses. When KS-01 was combined with 5-FU, the same cholesterol compensatory response was activated, promoting the expression of EMT-TFs as indicated by changes in gene expression, however, there were no translational changes in the EMT or drug resistance state. Combining KS-01 with GEM, however, promoted a similar mechanism of action to KS-01 alone, but with this treatment drug resistance was also significantly promoted. Therefore, combining cholesterol-depleting agents with chemotherapeutic agents does not promote their efficacy. Hence, based on the outcomes of this investigation and in alignment with prior research, it appears that reducing cholesterol levels may not present a feasible therapeutic avenue for addressing PDAC, especially when cells exhibit a mesenchymal phenotype.*

## **5.6 Limitations and future studies**

Limitations of this study include the reliance on time-point experiments conducted only after 4 hours, which leaves gaps in understanding the temporal dynamics of cellular responses before and after this period, necessitating investigation into long-term effects. Additionally, not utilising the quasi-mesenchymal phenotype resulted in grouping cells together, potentially overlooking variations where one subset of cells may have been more prevalent than another, potentially skewing results. Furthermore, this study focused solely on a single PC cell line, neglecting the exploration of other cell lines representing varying degrees of EMT. The high cost associated with TGF- $\beta$ 1 limited the scope of experiments, resulting in limited sample sizes for invasion and RT-qPCR analyses. Moreover, the exclusive reliance on *in vitro* models overlooks the influence of the TME, intra-tumour heterogeneity, as well as the true metastatic propensity of targeting cholesterol using CDs highlighting the need for complementary *in vivo* studies.

The biological mechanism for the observations made in the current study are still unknown and literature is limited therefore future studies should include cell count assays on post-EMT cells across all drug combinations to elucidate effects on cell growth or viability. Additionally, investigations on partial-EMT cells are essential for accurate comparisons, and hence all experiments should be performed again, but only on partial-EMT cells. Exploring alternative cholesterol-targeting agents such as statins to act as a control for the data observed in this study as well as conducting comprehensive cholesterol studies across all treatment combinations are warranted. Additionally, further experiments should be conducted to assess the dosage and exposure time required for the current cholesterol-depleting agents to effectively reduce

cholesterol levels. These experiments will help determine the specific concentrations and durations that yield the desired outcomes. Subsequently, the findings from these experiments can be used to re-evaluate the results of the current study.

Combining other CDs, such as M $\beta$ CD, and statins with the chemotherapeutic drugs should also be explored. One could even combine statins and CDs and see their collaborative effects on PDAC. Incorporating flow cytometry techniques to understand each subtype of PANC-1 to prevent specific subsets from skewing the reliability of data could also be implemented. Several more genes involved in these pathways should be further investigated possibly through RT<sup>2</sup>-PCR profiler arrays which can further elucidate mechanisms underlying drug resistance, lipoprotein, and cholesterol homeostasis pathways. Western blot analyses on proteins of interest would provide insights into post-transcriptional and post-translational regulatory mechanisms influencing protein expression. Ultimately, transitioning this study to *in vivo* models will be crucial for validating these findings. Nevertheless, the insights gained from this study lay the groundwork for future investigations aimed at elucidating the exact cholesterol-mediated mechanism of EMT in PDAC.

## **6 Troubleshooting**

### **6.1 EMT induction**

In order to optimise EMT induction different times (24 and 48 hours) and concentrations (5 ng/mL and 10ng/mL) of TGF- $\beta$ 1 were tested for EMT induction and can be seen in Figure A2.

### **6.2 MTT assay**

Since the treatment with TGF- $\beta$ 1 extends over 48 hours, which is then followed by drug treatments that extend over 48 hours the resultant time the cells are exposed to TGF- $\beta$ 1 would be 96 hours. RT-qPCR was done to compare EMT induction at 48 and 96 hours, in order to ensure cells were in a comparable EMT state after 96 hours as with 48 hours. It was found that EMT was comparable after 96 hours to 48 hours when TGF- $\beta$ 1 was removed at the 48-hour mark, cells were washed and fresh media was added with the chemotherapies. This was validated through the gene expression of the EMT-TF *SNAIL1* and can be seen in Figure A3

### **6.3 MDR assay**

The Vybrant® MDR Assay Kit is usually read on a plate reader at excitation maximum of 494 nm and an emission maximum of 517 nm utilising black 96-well fluorescent plates (Thermo Fisher Scientific, USA) to prevent background fluorescence due to the scattering and reflection

of light. Owing to the difficult nature of the PANC-1 cell line, the cells did not attach to this type of 96-well plate. The experiment thus needed to be optimised rather to be viewed under a fluorescent microscope, using the GFP channel, in a normal clear 96-well plate which required adaptations to the protocol. Wash steps were extended from two wash steps on a plate shaker for 1 minute to three wash steps on a plate shaker for 5 minutes and lastly cells were left in 45  $\mu$ L of 1 $\times$  PBS for viewing instead of 200  $\mu$ L.

#### **6.4 Invasion Assay**

After following the previously optimised protocol using 40% GelTrex™ and 100 000 cell/mL it was noted that no invasion occurred. To validate if the concentration of GelTrex™ was an issue or if there were other factors such as the Millicell® cell culture inserts pore size (Sigma Aldrich, UK) or lack of invasive capabilities of the cells a range of GelTrex™ concentrations, 0%, 10%, 20%, and 40% as well as cell concentrations (100 000 cells/mL, 200 000 cells/mL, 300 000 cells/mL) were investigated. It was found that maximum invasion occurred at a concentration of 20% GelTrex™ with 300 000 cells/mL. Lastly, cells could not survive in serum free media alone, so varying concentrations of BSA (0.1%, 0.2%, and 0.5%) were tested to support the growth of the PANC-1 cells, cells attached and sustained morphology when treated with at least 0.2% BSA, and this concentration was hence chosen.

#### **6.5 RNA extraction**

RNA from PANC-1 cells was challenging to extract in that yields were extremely low and purity ratios were not usable. The Direct-zol™ RNA MiniPrep kit (Zymo Research, Inqaba Biotec™, SA), Trizol-chloroform method, and RNeasy kit (Qiagen, Netherlands) were all utilised to extract RNA but were unsuccessful. RNA was only successfully extracted after the use of E.Z.N.A.® HP Total RNA Isolation Kit (Omega Bio-Tek, USA).

#### **6.6 RT-qPCR**

The annealing temperatures of the designed primers had to be initially optimised using gradient PCR, using the OneTaq® 2X Master Mix with Standard Buffer (New England Biolabs, USA), prior to RT-qPCR. *SNAIL1*, *ABCBI*, *SREBF2*, *GAPDH*, *LDLR*, *ABCC5*, *ABCG2*, and *ABCA1* were run on a gradient from 57°C to 64°C and *TGF- $\beta$ 1* on a gradient from 57°C to 64°C and can be seen in Figure A4

## 7 References

- Abdulla, N., Vincent, C. T. and Kaur, M. (2021). ‘Mechanistic Insights Delineating the Role of Cholesterol in Epithelial Mesenchymal Transition and Drug Resistance in Cancer’, *Frontiers in Cell and Developmental Biology*. Frontiers Media SA, 9. doi: 10.3389/FCELL.2021.728325.
- Adamska, A. and Falasca, M. (2018). ‘ATP-binding cassette transporters in progression and clinical outcome of pancreatic cancer: What is the way forward?’, *World journal of gastroenterology*. World J Gastroenterol, 24(29), pp. 3222–3236. doi: 10.3748/WJG.V24.I29.3222.
- Adorni, M. P., Ronda, N., Bernini, F. and Zimetti, F. (2021). ‘High Density Lipoprotein Cholesterol Efflux Capacity and Atherosclerosis in Cardiovascular Disease: Pathophysiological Aspects and Pharmacological Perspectives’, *Cells*. Multidisciplinary Digital Publishing Institute, 10(3), p. 574. doi: 10.3390/CELLS10030574.
- Aiello, N. M., Maddipati, R., Norgard, R. J., Balli, D., Li, J., Yuan, S., Yamazoe, T., Black, T., Sahnoud, A., Furth, E. E., Bar-Sagi, D. and Stanger, B. Z. (2018). ‘EMT Subtype Influences Epithelial Plasticity and Mode of Cell Migration’, *Developmental cell*. Dev Cell, 45(6), pp. 681–695.e4. doi: 10.1016/J.DEVCEL.2018.05.027.
- Akhmetkaliyev, A., Alibrahim, N., Shafiee, D. and Tulchinsky, E. (2023). ‘EMT/MET plasticity in cancer and Go-or-Grow decisions in quiescence: the two sides of the same coin?’, *Molecular Cancer*. BMC, 22(1), p. 90. doi: 10.1186/S12943-023-01793-Z.
- Alm, J. J., Qian, H. and Le Blanc, K. (2014). ‘Clinical Grade Production of Mesenchymal Stromal Cells’, *Tissue Engineering: Second Edition*. Academic Press, pp. 427–469. doi: 10.1016/B978-0-12-420145-3.00013-4.
- Almoguera, C., Shibata, D., Forrester, K., Martin, J., Arnheim, N. and Perucho, M. (1988). ‘Most human carcinomas of the exocrine pancreas contain mutant c-K-ras genes’, *Cell*. Cell, 53(4), pp. 549–554. doi: 10.1016/0092-8674(88)90571-5.
- Alvarez, M. A., Freitas, J. P., Mazher Hussain, S. and Glazer, E. S. (2019). ‘TGF- $\beta$  Inhibitors in Metastatic Pancreatic Ductal Adenocarcinoma’, *Journal of gastrointestinal cancer*. J Gastrointest Cancer, 50(2), pp. 207–213. doi: 10.1007/S12029-018-00195-5.
- Ambrosini, G., Dalla Pozza, E., Fanelli, G., Di Carlo, C., Vettori, A., Cannino, G., Cavallini, C., Carmona-Carmona, C. A., Brandi, J., Rinalducci, S., Scupoli, M. T., Rasola, A., Cecconi, D., Palmieri, M. and Dando, I. (2020). ‘Progressively De-Differentiated Pancreatic Cancer Cells Shift from Glycolysis to Oxidative Metabolism and Gain a Quiescent Stem State’, *Cells*. Multidisciplinary Digital Publishing Institute (MDPI), 9(7), p. 1572. doi: 10.3390/CELLS9071572.
- El Amrani, M., Corfiotti, F., Corvaisier, M., Vasseur, R., Fulbert, M., Skrzypczyk, C., Deshorgues, A. C., Gnemmi, V., Tulasne, D., Lahdaoui, F., Vincent, A., Pruvot, F. R., Van Seuning, I., Huet, G. and Truant, S. (2019). ‘Gemcitabine-induced epithelial-mesenchymal transition-like changes sustain chemoresistance of pancreatic cancer cells of mesenchymal-like phenotype’, *Molecular carcinogenesis*. Mol Carcinog, 58(11), pp. 1985–1997. doi: 10.1002/MC.23090.

Arumugam, T., Ramachandran, V., Fournier, K. F., Wang, H., Marquis, L., Abbruzzese, J. L., Gallick, G. E., Logsdon, C. D., McConkey, D. J. and Choi, W. (2009). 'Epithelial to mesenchymal transition contributes to drug resistance in pancreatic cancer', *Cancer Research*. American Association for Cancer Research, 69(14), pp. 5820–5828. doi: 10.1158/0008-5472.CAN-08-2819/654593/P/EPITHELIAL-TO-MESENCHYMAL-TRANSITION-CONTRIBUTES.

Aslantürk, Ö. S. (2018). 'In Vitro Cytotoxicity and Cell Viability Assays: Principles, Advantages, and Disadvantages', in *Genotoxicity - A Predictable Risk to Our Actual World*. InTech. doi: 10.5772/intechopen.71923.

Aulas, A., Liberatoscioli, M. L., Finetti, P., Cabaud, O., Birnbaum, D. J., Birnbaum, D., Bertucci, F. and Mamessier, E. (2021). 'Epithelial-to-mesenchymal transition lowers the cholesterol pathway, which influences colon tumors differentiation', *medRxiv*. Cold Spring Harbor Laboratory Press. doi: 10.1101/2021.10.13.21264887.

Baba, A. B., Rah, B., Bhat, G. R., Mushtaq, I., Parveen, S., Hassan, R., Hameed Zargar, M. and Afroze, D. (2022). 'Transforming Growth Factor-Beta (TGF- $\beta$ ) Signaling in Cancer-A Betrayal Within', *Frontiers in Pharmacology*. Frontiers Media S.A., 13, p. 791272. doi: 10.3389/FPHAR.2022.791272/BIBTEX.

Bailey, P. *et al.* (2016). 'Genomic analyses identify molecular subtypes of pancreatic cancer', *Nature*. Nature, 531(7592), pp. 47–52. doi: 10.1038/NATURE16965.

Barrallo-Gimeno, A. and Nieto, M. A. (2005). 'The Snail genes as inducers of cell movement and survival: implications in development and cancer', *Development*. Development, 132(14), pp. 3151–3161. doi: 10.1242/DEV.01907.

Bascom, C. C., Wolfshohl, J. R., Coffey, R. J., Madisen, L., Webb, N. R., Purchio, A. R., Derynck, R. and Moses, H. L. (1989). 'Complex regulation of transforming growth factor beta 1, beta 2, and beta 3 mRNA expression in mouse fibroblasts and keratinocytes by transforming growth factors beta 1 and beta 2', *Molecular and cellular biology*. Mol Cell Biol, 9(12), pp. 5508–5515. doi: 10.1128/MCB.9.12.5508-5515.1989.

Bash-Imam, Z., Thérizols, G., Vincent, A., Lafôrets, F., Espinoza, M. P., Pion, N., Macari, F., Pannequin, J., David, A., Saurin, J. C., Mertani, H. C., Textoris, J., Auboeuf, D., Catez, F., Venezia, N. D., Dutertre, M., Marcel, V. and Diaz, J. J. (2017). 'Translational reprogramming of colorectal cancer cells induced by 5-fluorouracil through a miRNA-dependent mechanism', *Oncotarget*. Impact Journals, LLC, 8(28), p. 46219. doi: 10.18632/ONCOTARGET.17597.

Battle, E., Sancho, E., Francí, C., Domínguez, D., Monfar, M., Baulida, J. and De Herreros, A. G. (2000). 'The transcription factor snail is a repressor of E-cadherin gene expression in epithelial tumour cells', *Nature cell biology*. Nat Cell Biol, 2(2), pp. 84–89. doi: 10.1038/35000034.

Bayarmagnai, B., Perrin, L., Pourfarhangi, K. E., Graña, X., Tüzel, E. and Gligorijevic, B. (2019). 'Invadopodia-mediated ECM degradation is enhanced in the G1 phase of the cell cycle', *Journal of Cell Science*. Company of Biologists Ltd, 132(20). doi: 10.1242/JCS.227116.

- Biankin, A. V. *et al.* (2012). ‘Pancreatic cancer genomes reveal aberrations in axon guidance pathway genes’, *Nature*. *Nature*, 491(7424), pp. 399–405. doi: 10.1038/NATURE11547.
- Bilimoria, K. Y., Bentrem, D. J., Ko, C. Y., Stewart, A. K., Winchester, D. P. and Talamonti, M. S. (2007). ‘National failure to operate on early stage pancreatic cancer’, *Annals of surgery*. *Ann Surg*, 246(2), pp. 173–180. doi: 10.1097/SLA.0B013E3180691579.
- Bjånes, T. K., Jordheim, L. P., Schjøtt, J., Kamceva, T., Cros-Perrial, E., Langer, A., de Garibay, G. R., Kotopoulis, S., McCormack, E. and Riedel, B. (2020). ‘Intracellular cytidine deaminase regulates gemcitabine metabolism in pancreatic cancer cell lines’, *Drug Metabolism and Disposition*. American Society for Pharmacology and Experimental Therapy, 48(3), pp. 153–158. doi: 10.1124/DMD.119.089334/-/DC1.
- Blum, R. and Kloog, Y. (2014). ‘Metabolism addiction in pancreatic cancer’, *Cell death & disease*. *Cell Death Dis*, 5(2), p. e1065. doi: 10.1038/CDDIS.2014.38.
- Bocci, G., Fioravanti, A., Orlandi, P., Bernardini, N., Collecchi, P., Del Tacca, M. and Danesi, R. (2005). ‘Fluvastatin synergistically enhances the antiproliferative effect of gemcitabine in human pancreatic cancer MIAPaCa-2 cells’, *British journal of cancer*. *Br J Cancer*, 93(3), pp. 319–330. doi: 10.1038/SJ.BJC.6602720.
- Bronsert, P., Kohler, I., Timme, S., Kiefer, S., Werner, M., Schilling, O., Vashist, Y., Makowiec, F., Brabletz, T., Hopt, U. T., Bausch, D., Kulemann, B., Keck, T. and Wellner, U. F. (2014). ‘Prognostic significance of Zinc finger E-box binding homeobox 1 (ZEB1) expression in cancer cells and cancer-associated fibroblasts in pancreatic head cancer’, *Surgery*. *Surgery*, 156(1), pp. 97–108. doi: 10.1016/J.SURG.2014.02.018.
- Brown, A. J. (2007). ‘Cholesterol, statins and cancer’, *Clinical and Experimental Pharmacology and Physiology*, 34(3), pp. 135–141. doi: 10.1111/J.1440-1681.2007.04565.X.
- Brown, M. S. and Goldstein, J. L. (1986). ‘A receptor-mediated pathway for cholesterol homeostasis’, *Science*. *Science*, 232(4746), pp. 34–47. doi: 10.1126/science.3513311.
- Buck, E., Eyzaguirre, A., Barr, S., Thompson, S., Sennello, R., Young, D., Iwata, K. K., Gibson, N. W., Cagnoni, P. and Haley, J. D. (2007). ‘Loss of homotypic cell adhesion by epithelial-mesenchymal transition or mutation limits sensitivity to epidermal growth factor receptor inhibition’, *Molecular cancer therapeutics*. *Mol Cancer Ther*, 6(2), pp. 532–541. doi: 10.1158/1535-7163.MCT-06-0462.
- Bulle, A. and Lim, K. H. (2020). ‘Beyond just a tight fortress: contribution of stroma to epithelial-mesenchymal transition in pancreatic cancer’, *Signal Transduction and Targeted Therapy*. Nature Publishing Group, 5(1), pp. 1–12. doi: 10.1038/s41392-020-00341-1.
- Cano, A., Pérez-Moreno, M. A., Rodrigo, I., Locascio, A., Blanco, M. J., Del Barrio, M. G., Portillo, F. and Nieto, M. A. (2000). ‘The transcription factor snail controls epithelial-mesenchymal transitions by repressing E-cadherin expression’, *Nature cell biology*. *Nat Cell Biol*, 2(2), pp. 76–83. doi: 10.1038/35000025.
- Casas, E., Kim, J., Bendesky, A., Ohno-Machado, L., Wolfe, C. J. and Yang, J. (2011). ‘Snail2 is an essential mediator of Twist1-induced epithelial mesenchymal transition and metastasis’, *Cancer research*. *Cancer Res*, 71(1), pp. 245–254. doi: 10.1158/0008-5472.CAN-10-2330.

Celià-Terrassa, T. and Kang, Y. (2024). 'How important is EMT for cancer metastasis?', *PLOS Biology*. PLOS, 22(2). doi: 10.1371/JOURNAL.PBIO.3002487.

Cerqueira, N. M. F. S. A., Oliveira, E. F., Gesto, D. S., Santos-Martins, D., Moreira, C., Moorthy, H. N., Ramos, M. J. and Fernandes, P. A. (2016). 'Cholesterol Biosynthesis: A Mechanistic Overview', *Biochemistry*. American Chemical Society, 55(39), pp. 5483–5506. doi: 10.1021/ACS.BIOCHEM.6B00342/ASSET/IMAGES/ACS.BIOCHEM.6B00342.SOCIAL.JPEG\_V03.

Chang, T.-Y., Li, B.-L., Chang, C. C. Y. and Urano, Y. (2009). 'Acyl-coenzyme A:cholesterol acyltransferases', *American Journal of Physiology - Endocrinology and Metabolism*. American Physiological Society, 297(1), p. E1. doi: 10.1152/AJPENDO.90926.2008.

Chapiro, J., Sur, S., Savic, L. J., Ganapathy-Kanniappan, S., Reyes, J., Duran, R., Thiruganasambandam, S. C., Moats, C. R., Lin, M. De, Luo, W., Tran, P. T., Herman, J. M., Semenza, G. L., Ewald, A. J., Vogelstein, B. and Geschwind, J. F. (2014). 'Systemic Delivery of Microencapsulated 3-Bromopyruvate for the Therapy of Pancreatic Cancer', *Clinical cancer research : an official journal of the American Association for Cancer Research*. NIH Public Access, 20(24), p. 6406. doi: 10.1158/1078-0432.CCR-14-1271.

Chatterjee, M., Ben-Josef, E., Thomas, D. G., Morgan, M. A., Zalupski, M. M., Khan, G., Andrew Robinson, C., Griffith, K. A., Chen, C. S., Ludwig, T., Bekaii-Saab, T., Chakravarti, A. and Williams, T. M. (2015). 'Caveolin-1 is Associated with Tumor Progression and Confers a Multi-Modality Resistance Phenotype in Pancreatic Cancer', *Scientific reports*. Sci Rep, 5. doi: 10.1038/SREP10867.

Chazotte, B. (2011). 'Labeling Nuclear DNA Using DAPI', *Cold Spring Harbor Protocols*. Cold Spring Harbor Laboratory Press. doi: 10.1101/PDB.PROT5556.

Chen, C. A., Chang, H. H., Kao, C. Y., Tsai, T. H. and Chen, Y. J. (2009). 'Plumbagin, isolated from *plumbago zeylanica*, induces cell death through apoptosis in human pancreatic cancer cells', *Pancreatology*. Elsevier B.V., 9(6), pp. 797–809. doi: 10.1159/000210028.

Chen, C. L., Shuan, S. H. and Jung, S. H. (2008). 'Cholesterol Modulates Cellular TGF- $\beta$  Responsiveness by Altering TGF- $\beta$  Binding to TGF- $\beta$  Receptors', *Journal of cellular physiology*. NIH Public Access, 215(1), p. 223. doi: 10.1002/JCP.21303.

Chen, C. Y., Kawasumi, M., Lan, T. Y., Poon, C. L., Lin, Y. S., Wu, P. J., Chen, Y. C., Chen, B. H., Wu, C. H., Lo, J. F., Weng, R. R., Sun, Y. C. and Hung, K. F. (2020). 'Adaptation to Endoplasmic Reticulum Stress Enhances Resistance of Oral Cancer Cells to Cisplatin by Up-Regulating Polymerase  $\eta$  and Increasing DNA Repair Efficiency', *International Journal of Molecular Sciences 2021, Vol. 22, Page 355*. Multidisciplinary Digital Publishing Institute, 22(1), p. 355. doi: 10.3390/IJMS22010355.

Chen, Limo *et al.* (2014). 'Metastasis is regulated via microRNA-200/ZEB1 axis control of tumour cell PD-L1 expression and intratumoral immunosuppression', *Nature communications*. Nat Commun, 5. doi: 10.1038/NCOMMS6241.

- Chen, M., Xue, X., Wang, F., An, Y., Tang, D., Xu, Y., Wang, H., Yuan, Z., Gao, W., Wei, J., Zhang, J. and Miao, Y. (2012). 'Expression and promoter methylation analysis of ATP-binding cassette genes in pancreatic cancer', *Oncology reports*. *Oncol Rep*, 27(1), pp. 265–269. doi: 10.3892/OR.2011.1475.
- Chen, W. J., Wang, H., Tang, Y., Liu, C. L., Li, H. L. and Li, W. T. (2010). 'Multidrug resistance in breast cancer cells during epithelial-mesenchymal transition is modulated by breast cancer resistant protein', *Chinese journal of cancer*. *Chin J Cancer*, 29(2), pp. 151–157. doi: 10.5732/CJC.009.10447.
- Chen, Y. H., Chen, Y. C., Lin, C. C., Hsieh, Y. P., Hsu, C. S. and Hsieh, M. C. (2020). 'Synergistic anticancer effects of gemcitabine with pitavastatin on pancreatic cancer cell line MIA PaCa-2 in vitro and in vivo', *Cancer Management and Research*. Dove Medical Press Ltd, 12, pp. 4645–4665. doi: 10.2147/CMAR.S247876.
- Cho, J. H., Kim, S. A., Park, S. B., Kim, H. M. and Song, S. Y. (2017). 'Suppression of pancreatic adenocarcinoma upregulated factor (PAUF) increases the sensitivity of pancreatic cancer to gemcitabine and 5FU, and inhibits the formation of pancreatic cancer stem like cells', *Oncotarget*. *Oncotarget*, 8(44), pp. 76398–76407. doi: 10.18632/ONCOTARGET.19458.
- Chowdhury, K., Sharma, A., Sharma, T., Kumar, S. and Mandal, C. C. (2017). 'Simvastatin and MBCD Inhibit Breast Cancer-Induced Osteoclast Activity by Targeting Osteoclastogenic Factors', *Cancer investigation*. *Cancer Invest*, 35(6), pp. 403–413. doi: 10.1080/07357907.2017.1309548.
- Collisson, E. A., Bailey, P., Chang, D. K. and Biankin, A. V. (2019). 'Molecular subtypes of pancreatic cancer', *Nature Reviews Gastroenterology & Hepatology* 2019 16:4. Nature Publishing Group, 16(4), pp. 207–220. doi: 10.1038/s41575-019-0109-y.
- Corbet, C., Bastien, E., Santiago de Jesus, J. P., Dierge, E., Martherus, R., Vander Linden, C., Doix, B., Degavre, C., Guilbaud, C., Petit, L., Michiels, C., Dessy, C., Larondelle, Y. and Feron, O. (2020). 'TGFβ2-induced formation of lipid droplets supports acidosis-driven EMT and the metastatic spreading of cancer cells', *Nature communications*. *Nat Commun*, 11(1). doi: 10.1038/S41467-019-14262-3.
- Corcos, L. and le Jossic-Corcos, C. (2013). 'Statins: Perspectives in cancer therapeutics', *Digestive and Liver Disease*, 45(10), pp. 795–802. doi: 10.1016/J.DLD.2013.02.002.
- Cordes, N., Frick, S., Brunner, T. B., Pilarsky, C., Grützmann, R., Sipos, B., Klöppel, G., McKenna, W. G. and Bernhard, E. J. (2007). 'Human pancreatic tumor cells are sensitized to ionizing radiation by knockdown of caveolin-1', *Oncogene* 2007 26:48. Nature Publishing Group, 26(48), pp. 6851–6862. doi: 10.1038/sj.onc.1210498.
- Cotte, A. K., Aires, V., Fredon, M., Limagne, E., Derangère, V., Thibaudin, M., Humblin, E., Scagliarini, A., De Barros, J. P. P., Hillon, P., Ghiringhelli, F. and Delmas, D. (2018). 'Lysophosphatidylcholine acyltransferase 2-mediated lipid droplet production supports colorectal cancer chemoresistance', *Nature communications*. *Nat Commun*, 9(1). doi: 10.1038/S41467-017-02732-5.

- Cruz, A. L. S., Barreto, E. de A., Fazolini, N. P. B., Viola, J. P. B. and Bozza, P. T. (2020). 'Lipid droplets: platforms with multiple functions in cancer hallmarks', *Cell Death & Disease* 2020 11:2. Nature Publishing Group, 11(2), pp. 1–16. doi: 10.1038/s41419-020-2297-3.
- Daemen, A. *et al.* (2015). 'Metabolite profiling stratifies pancreatic ductal adenocarcinomas into subtypes with distinct sensitivities to metabolic inhibitors', *Proceedings of the National Academy of Sciences of the United States of America*. Proc Natl Acad Sci U S A, 112(32), pp. E4410–E4417. doi: 10.1073/PNAS.1501605112.
- Dandawate, P. R., Vyas, A., Ahmad, A., Banerjee, S., Deshpande, J., Swamy, K. V., Jamadar, A., Dumhe-Klaire, A. C., Padhye, S. and Sarkar, F. H. (2012). 'Inclusion complex of novel curcumin analogue CDF and  $\beta$ -cyclodextrin (1:2) and its enhanced in vivo anticancer activity against pancreatic cancer', *Pharmaceutical Research*, 29(7), pp. 1775–1786. doi: 10.1007/S11095-012-0700-1.
- David, J. M. and Rajasekaran, A. K. (2012). 'Dishonorable Discharge: The Oncogenic Roles of Cleaved E-cadherin Fragments', *Cancer Research*. NIH Public Access, 72(12), p. 2917. doi: 10.1158/0008-5472.CAN-11-3498.
- Davis, M. E. and Brewster, M. E. (2004). 'Cyclodextrin-based pharmaceuticals: Past, present and future', *Nature Reviews Drug Discovery*, 3(12), pp. 1023–1035. doi: 10.1038/NRD1576.
- Di, L. and Kerns, E. H. (2016). 'Formulation', *Drug-Like Properties*. Academic Press, pp. 497–510. doi: 10.1016/B978-0-12-801076-1.00041-1.
- Donatello, S., Babina, I. S., Hazelwood, L. D., Hill, A. D. K., Nabi, I. R. and Hopkins, A. M. (2012). 'Lipid raft association restricts CD44-ezrin interaction and promotion of breast cancer cell migration', *The American journal of pathology*. Am J Pathol, 181(6), pp. 2172–2187. doi: 10.1016/J.AJPATH.2012.08.025.
- Dong, F., Mo, Z., Eid, W., Courtney, K. C. and Zha, X. (2014). 'Akt inhibition promotes ABCA1-mediated cholesterol efflux to apoA-I through suppressing mTORC1', *PLoS ONE*. Public Library of Science, 9(11). doi: 10.1371/journal.pone.0113789.
- Dong, X. D., Zhang, M., Cai, C. Y., Teng, Q. X., Wang, J. Q., Fu, Y. G., Cui, Q., Patel, K., Wang, D. T. and Chen, Z. S. (2022). 'Overexpression of ABCB1 Associated With the Resistance to the KRAS-G12C Specific Inhibitor ARS-1620 in Cancer Cells', *Frontiers in Pharmacology*. Frontiers Media S.A., 13, p. 843829. doi: 10.3389/FPHAR.2022.843829/BIBTEX.
- Dorsch, M. *et al.* (2021). 'Statins affect cancer cell plasticity with distinct consequences for tumor progression and metastasis', *Cell Reports*. Cell Press, 37(8), p. 110056. doi: 10.1016/J.CELREP.2021.110056.
- Drilon, A. *et al.* (2017). 'Safety and Antitumor Activity of the Multitargeted Pan-TRK, ROS1, and ALK Inhibitor Entrectinib: Combined Results from Two Phase I Trials (ALKA-372-001 and STARTRK-1)', *Cancer discovery*. Cancer Discov, 7(4), pp. 400–409. doi: 10.1158/2159-8290.CD-16-1237.

Du, W., Liu, X., Yang, M., Wang, W. and Sun, J. (2021). 'The Regulatory Role of PRRX1 in Cancer Epithelial-Mesenchymal Transition', *OncoTargets and therapy*. Dove Press, 14, p. 4223. doi: 10.2147/OTT.S316102.

Elander, N. O. *et al.* (2018). 'Expression of dihydropyrimidine dehydrogenase (DPD) and hENT1 predicts survival in pancreatic cancer', *British Journal of Cancer* 2018 118:7. Nature Publishing Group, 118(7), pp. 947–954. doi: 10.1038/s41416-018-0004-2.

Ellenrieder, V., Hendler, S. F., Boeck, W., Seufferlein, T., Menke, A., Ruhland, C., Adler, G. and Gress, T. M. (2001). 'Transforming Growth Factor 1 Treatment Leads to an Epithelial-Mesenchymal Transdifferentiation of Pancreatic Cancer Cells Requiring Extracellular Signal-regulated Kinase 2 Activation 1', *CANCER RESEARCH*, 61, pp. 4222–4228. Available at: <http://aacrjournals.org/cancerres/article-pdf/61/10/4222/2484578/ch100104222.pdf> (Accessed: 12 March 2024).

Elsayed, M., Kobayashi, D., Kubota, T., Matsunaga, N., Murata, R., Yoshizawa, Y., Watanabe, N., Matsuura, T., Tsurudome, Y., Ogino, T., Ohdo, S. and Shimazoe, T. (2016). 'Synergistic antiproliferative effects of zoledronic acid and fluvastatin on human pancreatic cancer cell lines: An in Vitro study', *Biological and Pharmaceutical Bulletin*. Pharmaceutical Society of Japan, 39(8), pp. 1238–1246. doi: 10.1248/BPB.B15-00746.

Esue, O., Carson, A. A., Tseng, Y. and Wirtz, D. (2006). 'A direct interaction between actin and vimentin filaments mediated by the tail domain of vimentin', *The Journal of biological chemistry*. J Biol Chem, 281(41), pp. 30393–30399. doi: 10.1074/JBC.M605452200.

Fang, Y. T., Yang, W. W., Niu, Y. R. and Sun, Y. K. (2023). 'Recent advances in targeted therapy for pancreatic adenocarcinoma', *World Journal of Gastrointestinal Oncology*. Baishideng Publishing Group Inc, 15(4), p. 571. doi: 10.4251/WJGO.V15.I4.571.

Farrell, R. E. (2010). 'RNA Isolation Strategies', *RNA Methodologies*. Academic Press, pp. 45–80. doi: 10.1016/B978-0-12-374727-3.00002-4.

Fidai, S. S., Sharma, A. E., Johnson, D. N., Segal, J. P. and Lastra, R. R. (2018). 'Dihydropyrimidine dehydrogenase deficiency as a cause of fatal 5-Fluorouracil toxicity', *Autopsy & Case Reports*. Universidade de São Paulo, Hospital Universitário, 8(4). doi: 10.4322/ACR.2018.049.

Findlay, V. J., Wang, C., Nogueira, L. M., Hurst, K., Quirk, D., Ethier, S. P., Staveley O'Carroll, K. F., Watson, D. K. and Camp, E. R. (2014). 'SNAI2 modulates colorectal cancer 5-fluorouracil sensitivity through miR145 repression', *Molecular cancer therapeutics*. Mol Cancer Ther, 13(11), pp. 2713–2726. doi: 10.1158/1535-7163.MCT-14-0207.

Fouad, Y. A. and Aanei, C. (2017). 'Revisiting the hallmarks of cancer', *American Journal of Cancer Research*. E-Century Publishing Corporation, pp. 1016–1036. Available at: [www.ajcr.us/ISSN:2156-6976/ajcr0053932](http://www.ajcr.us/ISSN:2156-6976/ajcr0053932) (Accessed: 7 September 2020).

Fox, C. H., Johnson, F. B., Whiting, J. and Roller, P. P. (1985). 'Formaldehyde fixation.', *The journal of histochemistry and cytochemistry : official journal of the Histochemistry Society*. SAGE PublicationsSage CA: Los Angeles, CA, 33(8), pp. 845–853. doi: 10.1177/33.8.3894502/ASSET/33.8.3894502.FP.PNG\_V03.

- Fu, J., Qin, L., He, T., Qin, J., Hong, J., Wong, J., Liao, L. and Xu, J. (2011). 'The TWIST/Mi2/NuRD protein complex and its essential role in cancer metastasis', *Cell Research*. Nature Publishing Group, 21(2), p. 275. doi: 10.1038/CR.2010.118.
- Furusawa, T., Moribe, H., Kondoh, H. and Higashi, Y. (1999). 'Identification of CtBP1 and CtBP2 as corepressors of zinc finger-homeodomain factor deltaEF1', *Molecular and cellular biology*. Mol Cell Biol, 19(12), pp. 8581–8590. doi: 10.1128/MCB.19.12.8581.
- Gabitova-Cornell, L. *et al.* (2020). 'Cholesterol Pathway Inhibition Induces TGF- $\beta$  Signaling to Promote Basal Differentiation in Pancreatic Cancer', *Cancer Cell*. Cell Press, 38(4), pp. 567-583.e11. doi: 10.1016/J.CCELL.2020.08.015.
- Gadade, D. D. and Pekamwar, S. S. (2020). 'Cyclodextrin Based Nanoparticles for Drug Delivery and Theranostics', *Advanced Pharmaceutical Bulletin*. Tabriz University of Medical Sciences, 10(2), p. 166. doi: 10.34172/APB.2020.022.
- Gagliano, N., Celesti, G., Tacchini, L., Pluchino, S., Sforza, C., Rasile, M., Valerio, V., Laghi, L., Conte, V. and Procacci, P. (2016). 'Epithelial-to-mesenchymal transition in pancreatic ductal adenocarcinoma: Characterization in a 3D-cell culture model', *World Journal of Gastroenterology*. Baishideng Publishing Group Inc, 22(18), p. 4466. doi: 10.3748/WJG.V22.I18.4466.
- Galván, J. A., Zlobec, I., Wartenberg, M., Lugli, A., Gloor, B., Perren, A. and Karamitopoulou, E. (2015). 'Expression of E-cadherin repressors SNAIL, ZEB1 and ZEB2 by tumour and stromal cells influences tumour-budding phenotype and suggests heterogeneity of stromal cells in pancreatic cancer', *British Journal of Cancer*. Nature Publishing Group, 112(12), p. 1944. doi: 10.1038/BJC.2015.177.
- Giudetti, A. M., De Domenico, S., Ragusa, A., Lunetti, P., Gaballo, A., Franck, J., Simeone, P., Nicolardi, G., De Nuccio, F., Santino, A., Capobianco, L., Lanuti, P., Fournier, I., Salzet, M., Maffia, M. and Vergara, D. (2019). 'A specific lipid metabolic profile is associated with the epithelial mesenchymal transition program', *Biochimica et biophysica acta. Molecular and cell biology of lipids*. Biochim Biophys Acta Mol Cell Biol Lipids, 1864(3), pp. 344–357. doi: 10.1016/J.BBALIP.2018.12.011.
- Globocan (2020a). *Breast*.
- Globocan (2020b). *Pancreas*. Available at: <https://gco.iarc.fr/today> (Accessed: 25 May 2021).
- Globocan (2020c). *South Africa*. Available at: <https://gco.iarc.fr/today/data/factsheets/populations/710-south-africa-fact-sheets.pdf> (Accessed: 8 April 2022).
- Globocan (2020d). *World*.
- Glodkowska-Mrowka, E., Mrowka, P., Basak, G. W., Niesiobedzka-Krezel, J., Seferynska, I., Wlodarski, P. K., Jakobisiak, M. and Stoklosa, T. (2014). 'Statins inhibit ABCB1 and ABCG2 drug transporter activity in chronic myeloid leukemia cells and potentiate antileukemic effects of imatinib', *Experimental hematology*. Exp Hematol, 42(6), pp. 439–447. doi: 10.1016/J.EXPHEM.2014.02.006.

- Gong, J., Sachdev, E., Robbins, L. A., Lin, E., Hendifar, A. E. and Mita, M. M. (2017). 'Statins and pancreatic cancer', *Oncology Letters*. Spandidos Publications, 13(3), pp. 1035–1040. doi: 10.3892/OL.2017.5572.
- Gonyeau, M. J. and Yuen, D. W. (2010). 'A clinical review of statins and cancer: Helpful or harmful?', *Pharmacotherapy*, 30(2), pp. 177–194. doi: 10.1592/PHCO.30.2.177.
- Gould, S. and Scott, R. C. (2005). '2-Hydroxypropyl- $\beta$ -cyclodextrin (HP- $\beta$ -CD): A toxicology review', *Food and Chemical Toxicology*. Pergamon, 43(10), pp. 1451–1459. doi: 10.1016/J.FCT.2005.03.007.
- Gracia-Rubio, I., Martín, C., Civeira, F. and Cenarro, A. (2021). 'SR-B1, a Key Receptor Involved in the Progression of Cardiovascular Disease: A Perspective from Mice and Human Genetic Studies', *Biomedicines 2021, Vol. 9, Page 612*. Multidisciplinary Digital Publishing Institute, 9(6), p. 612. doi: 10.3390/BIOMEDICINES9060612.
- Grände, M., Franzen, Å., Karlsson, J. O., Ericson, L. E., Heldin, N. E. and Nilsson, M. (2002). 'Transforming growth factor- $\beta$  and epidermal growth factor synergistically stimulate epithelial to mesenchymal transition (EMT) through a MEK-dependent mechanism in primary cultured pig thyrocytes', *Journal of Cell Science*, 115(22), pp. 4227–4236. doi: 10.1242/jcs.00091.
- Griesmann, H., Ripka, S., Pralle, M., Ellenrieder, V., Baumgart, S., Buchholz, M., Pilarsky, C., Aust, D., Gress, T. M. and Michl, P. (2013). 'WNT5A-NFAT Signaling Mediates Resistance to Apoptosis in Pancreatic Cancer', *Neoplasia (New York, N.Y.)*. Neoplasia Press, 15(1), p. 11. doi: 10.1593/NEO.121312.
- Gu, L., Saha, S. T., Thomas, J. and Kaur, M. (2019). 'Targeting cellular cholesterol for anticancer therapy', *The FEBS Journal*. John Wiley & Sons, Ltd, 286(21), pp. 4192–4208. doi: 10.1111/FEBS.15018.
- Guillaumond, F. *et al.* (2015). 'Cholesterol uptake disruption, in association with chemotherapy, is a promising combined metabolic therapy for pancreatic adenocarcinoma', *Proceedings of the National Academy of Sciences of the United States of America*. National Academy of Sciences, 112(8), pp. 2473–2478. doi: 10.1073/PNAS.1421601112/SUPPL\_FILE/PNAS.1421601112.SD03.XLSX.
- Gzil, A., Zarębska, I., Bursiewicz, W., Antosik, P., Grzanka, D. and Szyłberg, Ł. (2019). 'Markers of pancreatic cancer stem cells and their clinical and therapeutic implications', *Molecular Biology Reports 2019 46:6*. Springer, 46(6), pp. 6629–6645. doi: 10.1007/S11033-019-05058-1.
- Hagmann, W., Jesnowski, R., Faissner, R., Guo, C. and Löhr, J. M. (2009). 'ATP-binding cassette C transporters in human pancreatic carcinoma cell lines. Upregulation in 5-fluorouracil-resistant cells', *Pancreatology: official journal of the International Association of Pancreatology (IAP) ... [et al.]*. Pancreatology, 9(1–2), pp. 136–144. doi: 10.1159/000178884.
- He, X., Wang, J., Wei, W., Shi, M., Xin, B., Zhang, T. and Shen, X. (2016). 'Hypoxia regulates ABCG2 activity through the activation of ERK1/2/HIF-1 $\alpha$  and contributes to

chemoresistance in pancreatic cancer cells', *Cancer biology & therapy*. *Cancer Biol Ther*, 17(2), pp. 188–198. doi: 10.1080/15384047.2016.1139228.

Van Heek, N. T., Meeker, A. K., Kern, S. E., Yeo, C. J., Lillemoe, K. D., Cameron, J. L., Offerhaus, G. J. A., Hicks, J. L., Wilentz, R. E., Goggins, M. G., De Marzo, A. M., Hruban, R. H. and Maitra, A. (2002). 'Telomere shortening is nearly universal in pancreatic intraepithelial neoplasia', *The American journal of pathology*. *Am J Pathol*, 161(5), pp. 1541–1547. doi: 10.1016/S0002-9440(10)64432-X.

Hosein, A. N., Dougan, S. K., Aguirre, A. J. and Maitra, A. (2022). 'Translational advances in pancreatic ductal adenocarcinoma therapy', *Nature Cancer 2022 3:3*. Nature Publishing Group, 3(3), pp. 272–286. doi: 10.1038/s43018-022-00349-2.

Hotz, B., Arndt, M., Dullat, S., Bhargava, S., Buhr, H. J. and Hotz, H. G. (2007). 'Epithelial to mesenchymal transition: expression of the regulators snail, slug, and twist in pancreatic cancer', *Clinical cancer research : an official journal of the American Association for Cancer Research*. *Clin Cancer Res*, 13(16), pp. 4769–4776. doi: 10.1158/1078-0432.CCR-06-2926.

Hou, Z., Peng, H., Ayyanathan, K., Yan, K.-P., Langer, E. M., Longmore, G. D. and Frank J. Rauscher, I. (2008). 'The LIM Protein AJUBA Recruits Protein Arginine Methyltransferase 5 To Mediate SNAIL-Dependent Transcriptional Repression', *Molecular and Cellular Biology*. Taylor & Francis, 28(10), p. 3198. doi: 10.1128/MCB.01435-07.

Hruban, R. H., Adsay, N. V., Albores-Saavedra, J., Compton, C., Garrett, E. S., Goodman, S. N., Kern, S. E., Klimstra, D. S., Klöppel, G., Longnecker, D. S., Lüttges, J. and Offerhaus, G. J. A. (2001). 'Pancreatic intraepithelial neoplasia: a new nomenclature and classification system for pancreatic duct lesions', *The American journal of surgical pathology*. *Am J Surg Pathol*, 25(5), pp. 579–586. doi: 10.1097/00000478-200105000-00003.

Hu, H. feng, Ye, Z., Qin, Y., Xu, X. wu, Yu, X. jun, Zhuo, Q. feng and Ji, S. rong (2021). 'Mutations in key driver genes of pancreatic cancer: molecularly targeted therapies and other clinical implications', *Acta pharmacologica Sinica*. *Acta Pharmacol Sin*, 42(11), pp. 1725–1741. doi: 10.1038/S41401-020-00584-2.

Hu, Y. W., Wang, Q., Ma, X., Li, X. X., Liu, X. H., Xiao, J., Liao, D. F., Xiang, J. and Tang, C. K. (2010). 'TGF-beta1 up-regulates expression of ABCA1, ABCG1 and SR-BI through liver X receptor alpha signaling pathway in THP-1 macrophage-derived foam cells', *Journal of atherosclerosis and thrombosis*. *J Atheroscler Thromb*, 17(5), pp. 493–502. doi: 10.5551/JAT.3152.

Huang, H., Xie, H., Pan, Y., Zheng, K., Xia, Y. and Chen, W. (2018). 'Plumbagin Triggers ER Stress-Mediated Apoptosis in Prostate Cancer Cells via Induction of ROS', *Cellular Physiology and Biochemistry*. S. Karger AG, 45(1), pp. 267–280. doi: 10.1159/000486773.

Iacobazzi, R. M., Cutrignelli, A., Stefanachi, A., Porcelli, L., Lopodota, A. A., Di Fonte, R., Lopalco, A., Serrati, S., Laquintana, V., Silvestris, N., Franco, M., Cellamare, S., Leonetti, F., Azzariti, A. and Denora, N. (2020). 'Hydroxy-Propyl-β-Cyclodextrin Inclusion Complexes of two Biphenylnicotinamide Derivatives: Formulation and Anti-Proliferative Activity Evaluation in Pancreatic Cancer Cell Models', *International Journal of Molecular Sciences*

2020, Vol. 21, Page 6545. Multidisciplinary Digital Publishing Institute, 21(18), p. 6545. doi: 10.3390/IJMS21186545.

Ikenouchi, J., Matsuda, M., Furuse, M. and Tsukita, S. (2003). 'Regulation of tight junctions during the epithelium-mesenchyme transition: direct repression of the gene expression of claudins/occludin by Snail', *Journal of cell science*. J Cell Sci, 116(Pt 10), pp. 1959–1967. doi: 10.1242/JCS.00389.

Ikonen, E. (2008). 'Cellular cholesterol trafficking and compartmentalization', *Nature Reviews Molecular Cell Biology*, 9(2), pp. 125–138. doi: 10.1038/NRM2336.

Ikushima, H. and Miyazono, K. (2010). 'TGFbeta signalling: a complex web in cancer progression', *Nature reviews. Cancer*. Nat Rev Cancer, 10(6), pp. 415–424. doi: 10.1038/NRC2853.

Jain, A. G., Wazir, M., Zafar, H., Zhou, J., Khanal, K., Khan, A. K. and Ahmad, S. (2019). 'Epidermal growth factor receptor role in pancreatic cancer', *Theranostic Approach for Pancreatic Cancer*. Academic Press, pp. 295–324. doi: 10.1016/B978-0-12-819457-7.00015-3.

Jakic, B., Buszko, M., Cappellano, G. and Wick, G. (2017). 'Elevated sodium leads to the increased expression of HSP60 and induces apoptosis in HUVECs', *PLoS ONE*. PLOS, 12(6). doi: 10.1371/JOURNAL.PONE.0179383.

Jeannot, P., Nowosad, A., Perchey, R., Callot, C., Bennana, E., Katsube, T., Mayeux, P., Guillonneau, F., Manenti, S. and Besson, A. (2017). 'P27kip1 promotes invadopodia turnover and invasion through the regulation of the PAK1/cortactin pathway', *eLife*. eLife Sciences Publications Ltd, 6. doi: 10.7554/ELIFE.22207.

Ji, T., Li, S., Zhang, Y., Lang, J., Ding, Y., Zhao, X., Zhao, R., Li, Y., Shi, J., Hao, J., Zhao, Y. and Nie, G. (2016). 'An MMP-2 Responsive Liposome Integrating Antifibrosis and Chemotherapeutic Drugs for Enhanced Drug Perfusion and Efficacy in Pancreatic Cancer', *ACS applied materials & interfaces*. ACS Appl Mater Interfaces, 8(5), pp. 3438–3445. doi: 10.1021/ACSAMI.5B11619.

Jiang, W., Hu, J. W., He, X. R., Jin, W. L. and He, X. Y. (2021). 'Statins: a repurposed drug to fight cancer', *Journal of Experimental & Clinical Cancer Research : CR*. BioMed Central, 40(1), p. 241. doi: 10.1186/S13046-021-02041-2.

Jiang, Y. and Sohal, D. P. S. (2023). 'Pancreatic Adenocarcinoma Management', *JCO Oncology Practice*. American Society of Clinical Oncology (ASCO), 19(1), pp. 19–32. doi: 10.1200/op.22.00328.

Jones, S. *et al.* (2008). 'Core Signaling Pathways in Human Pancreatic Cancers Revealed by Global Genomic Analyses', *Science (New York, N.Y.)*. NIH Public Access, 321(5897), p. 1801. doi: 10.1126/SCIENCE.1164368.

Kabashima, A., Higuchi, H., Takaishi, H., Matsuzaki, Y., Suzuki, S., Izumiya, M., Iizuka, H., Sakai, G., Hozawa, S., Azuma, T. and Hibi, T. (2009). 'Side population of pancreatic cancer cells predominates in TGF-beta-mediated epithelial to mesenchymal transition and invasion', *International journal of cancer*. Int J Cancer, 124(12), pp. 2771–2779. doi: 10.1002/IJC.24349.

Kar, R., Jha, N. K., Jha, S. K., Sharma, A., Dholpuria, S., Asthana, N., Chaurasiya, K., Singh, V. K., Burgee, S. and Nand, P. (2019). 'A "NOTCH" Deeper into the Epithelial-To-Mesenchymal Transition (EMT) Program in Breast Cancer', *Genes*. Multidisciplinary Digital Publishing Institute (MDPI), 10(12). doi: 10.3390/GENES10120961.

Karthic, A., Roy, A., Lakkakula, J., Alghamdi, S., Shakoori, A., Babalghith, A. O., Emran, T. Bin, Sharma, R., Lima, C. M. G., Kim, B., Park, M. N., Safi, S. Z., de Almeida, R. S. and Coutinho, H. D. M. (2022). 'Cyclodextrin nanoparticles for diagnosis and potential cancer therapy: A systematic review', *Frontiers in Cell and Developmental Biology*. Frontiers Media SA, 10. doi: 10.3389/FCELL.2022.984311.

Kawata, S., Yamasaki, E., Nagase, T., Inui, Y., Ito, N., Matsuda, Y., Inada, M., Tamura, S., Noda, S., Imai, Y. and Matsuzawa, Y. (2001). 'Effect of pravastatin on survival in patients with advanced hepatocellular carcinoma. A randomized controlled trial', *British journal of cancer*. Br J Cancer, 84(7), pp. 886–891. doi: 10.1054/BJOC.2000.1716.

Kim, S., Lee, M., Dhanasekaran, D. N. and Song, Y. S. (2018). 'Activation of LXRA/β by cholesterol in malignant ascites promotes chemoresistance in ovarian cancer', *BMC Cancer*. BMC, 18(1). doi: 10.1186/S12885-018-5152-5.

Kobayashi, Y., Ohshiro, N., Sakai, R., Ohbayashi, M., Kohyama, N. and Yamamoto, T. (2005). 'Transport mechanism and substrate specificity of human organic anion transporter 2 (hOat2 [SLC22A7])', *The Journal of pharmacy and pharmacology*. J Pharm Pharmacol, 57(5), pp. 573–578. doi: 10.1211/0022357055966.

Komori, S., Osada, S. and Yoshida, K. (2011). 'Novel Strategy with Gemcitabine for Advanced Pancreatic Cancer', *ISRN Oncology*. Hindawi Limited, 2011, pp. 1–5. doi: 10.5402/2011/936893.

Kondo, A., Yamamoto, S., Nakaki, R., Shimamura, T., Hamakubo, T., Sakai, J., Kodama, T., Yoshida, T., Aburatani, H. and Osawa, T. (2017). 'Extracellular Acidic pH Activates the Sterol Regulatory Element-Binding Protein 2 to Promote Tumor Progression', *Cell Reports*. Elsevier B.V., 18(9), pp. 2228–2242. doi: 10.1016/j.celrep.2017.02.006.

Kopan, R. and Ilagan, M. X. G. (2009). 'The canonical Notch signaling pathway: unfolding the activation mechanism', *Cell*. Cell, 137(2), pp. 216–233. doi: 10.1016/J.CELL.2009.03.045.

Kosenko, T., Golder, M., Leblond, G., Weng, W. and Lagace, T. A. (2013). 'Low Density Lipoprotein Binds to Proprotein Convertase Subtilisin/Kexin Type-9 (PCSK9) in Human Plasma and Inhibits PCSK9-mediated Low Density Lipoprotein Receptor Degradation', *The Journal of Biological Chemistry*. American Society for Biochemistry and Molecular Biology, 288(12), p. 8279. doi: 10.1074/JBC.M112.421370.

Kuo, A., Lee, M. Y., Yang, K., Gross, R. W. and Sessa, W. C. (2018). 'Caveolin-1 regulates lipid droplet metabolism in endothelial cells via autocrine prostacyclin-stimulated, cAMP-mediated lipolysis', *The Journal of Biological Chemistry*. American Society for Biochemistry and Molecular Biology, 293(3), p. 973. doi: 10.1074/JBC.RA117.000980.

Kuo, Y. C., Kou, H. W., Hsu, C. P., Lo, C. H. and Hwang, T. L. (2023). 'Identification and Clinical Significance of Pancreatic Cancer Stem Cells and Their Chemotherapeutic Drug

Resistance', *International Journal of Molecular Sciences*. Multidisciplinary Digital Publishing Institute (MDPI), 24(8). doi: 10.3390/IJMS24087331.

Kurata, N., Fujita, H., Ohuchida, K., Mizumoto, K., Mahawithitwong, P., Sakai, H., Onimaru, M., Manabe, T., Ohtsuka, T. and Tanaka, M. (2011). 'Predicting the chemosensitivity of pancreatic cancer cells by quantifying the expression levels of genes associated with the metabolism of gemcitabine and 5-fluorouracil', *International journal of oncology*. *Int J Oncol*, 39(2), pp. 473–482. doi: 10.3892/IJO.2011.1058.

Kuzu, O. F., Noory, M. A. and Robertson, G. P. (2016). 'The role of cholesterol in cancer', *Cancer Research*. American Association for Cancer Research Inc., 76(8), pp. 2063–2070. doi: 10.1158/0008-5472.CAN-15-2613.

Lamouille, S., Xu, J. and Derynck, R. (2014). 'Molecular mechanisms of epithelial–mesenchymal transition', *Nature reviews. Molecular cell biology*. NIH Public Access, 15(3), p. 178. doi: 10.1038/NRM3758.

Lei, J., Ma, J., Ma, Q., Li, X., Liu, H., Xu, Q., Duan, W., Sun, Q., Xu, J., Wu, Z. and Wu, E. (2013). 'Hedgehog signaling regulates hypoxia induced epithelial to mesenchymal transition and invasion in pancreatic cancer cells via a ligand-independent manner', *Molecular Cancer*. BioMed Central, 12(1), pp. 1–11. doi: 10.1186/1476-4598-12-66/FIGURES/7.

Li, C., Heidt, D. G., Dalerba, P., Burant, C. F., Zhang, L., Adsay, V., Wicha, M., Clarke, M. F. and Simeone, D. M. (2007). 'Identification of pancreatic cancer stem cells', *Cancer Research*. *Cancer Res*, 67(3), pp. 1030–1037. doi: 10.1158/0008-5472.CAN-06-2030.

Li, J., Gu, D., Lee, S. S. Y., Song, B., Bandyopadhyay, S., Chen, S., Konieczny, S. F., Ratliff, T. L., Liu, X., Xie, J. and Cheng, J. X. (2016). 'Abrogating cholesterol esterification suppresses growth and metastasis of pancreatic cancer', *Oncogene*. *Oncogene*, 35(50), pp. 6378–6388. doi: 10.1038/ONC.2016.168.

Li, J., Qu, X., Tian, J., Zhang, J. T. and Cheng, J. X. (2018). 'Cholesterol esterification inhibition and gemcitabine synergistically suppress pancreatic ductal adenocarcinoma proliferation', *PLoS ONE*. *PLOS*, 13(2). doi: 10.1371/JOURNAL.PONE.0193318.

Li, Y. C., Park, M. J., Ye, S. K., Kim, C. W. and Kim, Y. N. (2006). 'Elevated Levels of Cholesterol-Rich Lipid Rafts in Cancer Cells Are Correlated with Apoptosis Sensitivity Induced by Cholesterol-Depleting Agents', *The American Journal of Pathology*. Elsevier, 168(4), pp. 1107–1118. doi: 10.2353/AJPATH.2006.050959.

Li, Y., Revalde, J. L., Reid, G. and Paxton, J. W. (2011). 'Modulatory effects of curcumin on multi-drug resistance-associated protein 5 in pancreatic cancer cells', *Cancer chemotherapy and pharmacology*. *Cancer Chemother Pharmacol*, 68(3), pp. 603–610. doi: 10.1007/S00280-010-1515-6.

Li, Y., Wu, S., Zhao, X., Hao, S., Li, F., Wang, Yuxiong, Liu, B., Zhang, D., Wang, Yishu and Zhou, H. (2023). 'Key events in cancer: Dysregulation of SREBPs', *Frontiers in Pharmacology*. Frontiers Media SA, 14, p. 1130747. doi: 10.3389/FPHAR.2023.1130747/BIBTEX.

- Li, Z., Liu, H. and Luo, X. (2020). 'Lipid droplet and its implication in cancer progression', *American Journal of Cancer Research*. e-Century Publishing Corporation, 10(12), p. 4112. Available at: [/pmc/articles/PMC7783747/](https://pubmed.ncbi.nlm.nih.gov/41392021/) (Accessed: 26 February 2024).
- Liao, J., Chung, Y. T., Yang, A. L., Zhang, M., Li, H., Zhang, W., Yan, L. and Yang, G. Y. (2013). 'Atorvastatin inhibits pancreatic carcinogenesis and increases survival in LSL-KrasG12D-LSL-Trp53R172H-Pdx1-Cre mice', *Molecular Carcinogenesis*, 52(9), pp. 739–750. doi: 10.1002/MC.21916.
- Liu, J., Xiao, Q., Xiao, J., Niu, C., Li, Y., Zhang, X., Zhou, Z., Shu, G. and Yin, G. (2022). 'Wnt/ $\beta$ -catenin signalling: function, biological mechanisms, and therapeutic opportunities', *Signal Transduction and Targeted Therapy* 2021 7:1. Nature Publishing Group, 7(1), pp. 1–23. doi: 10.1038/s41392-021-00762-6.
- Livak, K. J. and Schmittgen, T. D. (2001). 'Analysis of relative gene expression data using real-time quantitative PCR and the 2<sup>-Delta Delta C(T)</sup> Method', *Methods (San Diego, Calif.)*. Methods, 25(4), pp. 402–408. doi: 10.1006/METH.2001.1262.
- Loftsson, T., Jarho, P., Masson, M. and Jarvinen, T. (2005). 'Cyclodextrins in drug delivery', *Expert opinion on drug delivery*. Expert Opin Drug Deliv, 2(2), pp. 335–351. doi: 10.1517/17425247.2.1.335.
- Loh, C. Y., Chai, J. Y., Tang, T. F., Wong, W. F., Sethi, G., Shanmugam, M. K., Chong, P. P. and Looi, C. Y. (2019). 'The E-Cadherin and N-Cadherin Switch in Epithelial-to-Mesenchymal Transition: Signaling, Therapeutic Implications, and Challenges', *Cells*. Multidisciplinary Digital Publishing Institute (MDPI), 8(10). doi: 10.3390/CELLS8101118.
- Longley, D. B., Harkin, D. P. and Johnston, P. G. (2003). '5-Fluorouracil: Mechanisms of action and clinical strategies', *Nature Reviews Cancer*, 3(5), pp. 330–338. doi: 10.1038/nrc1074.
- Lowery, J., Kuczmarski, E. R., Herrmann, H. and Goldma, R. D. (2015). 'Intermediate Filaments Play a Pivotal Role in Regulating Cell Architecture and Function', *The Journal of biological chemistry*. J Biol Chem, 290(28), pp. 17145–17153. doi: 10.1074/JBC.R115.640359.
- Lu, Y., Zhou, Xiaohui, Zhao, W., Liao, Z., Li, B., Han, P., Yang, Y., Zhong, X., Mo, Y., Li, P., Huang, G., Xiao, X., Zhang, Z. and Zhou, Xiaoying (2021). 'Epigenetic Inactivation of Acetyl-CoA Acetyltransferase 1 Promotes the Proliferation and Metastasis in Nasopharyngeal Carcinoma by Blocking Ketogenesis', *Frontiers in Oncology*. Frontiers Media S.A., 11, p. 667673. doi: 10.3389/FONC.2021.667673/BIBTEX.
- Luo, J., Yang, H. and Song, B. L. (2020). 'Mechanisms and regulation of cholesterol homeostasis', *Nature Reviews Molecular Cell Biology*. Nature Research, 21(4), pp. 225–245. doi: 10.1038/S41580-019-0190-7.
- Mafi, A., Rezaee, M., Hedayati, N., Hogan, S. D., Reiter, R. J., Aarabi, M. H. and Asemi, Z. (2023). 'Melatonin and 5-fluorouracil combination chemotherapy: opportunities and efficacy in cancer therapy', *Cell Communication and Signaling : CCS*. BMC, 21(1). doi: 10.1186/S12964-023-01047-X.

- Maier, H. J., Schmidt-Straßburger, U., Huber, M. A., Wiedemann, E. M., Beug, H. and Wirth, T. (2010). 'NF-kappaB promotes epithelial-mesenchymal transition, migration and invasion of pancreatic carcinoma cells', *Cancer letters*. *Cancer Lett*, 295(2), pp. 214–228. doi: 10.1016/J.CANLET.2010.03.003.
- Maitra, A., Fukushima, N., Takaori, K. and Hruban, R. H. (2005). 'Precursors to invasive pancreatic cancer', *Advances in anatomic pathology*. *Adv Anat Pathol*, 12(2), pp. 81–91. doi: 10.1097/01.PAP.0000155055.14238.25.
- Maitra, A. and Hruban, R. H. (2008). 'Pancreatic cancer', *Annual review of pathology*. *Annu Rev Pathol*, 3, pp. 157–188. doi: 10.1146/ANNUREV.PATHMECHDIS.3.121806.154305.
- Makena, M. R., Gatla, H., Verlekar, D., Sukhavasi, S., Pandey, M. K. and Pramanik, K. C. (2019). 'Wnt/ $\beta$ -Catenin Signaling: The Culprit in Pancreatic Carcinogenesis and Therapeutic Resistance', *International Journal of Molecular Sciences*. Multidisciplinary Digital Publishing Institute (MDPI), 20(17). doi: 10.3390/IJMS20174242.
- Mann, K. M., Ying, H., Juan, J., Jenkins, N. A. and Copeland, N. G. (2016). 'KRAS-related proteins in pancreatic cancer', *Pharmacology & therapeutics*. *Pharmacol Ther*, 168, pp. 29–42. doi: 10.1016/J.PHARMTHERA.2016.09.003.
- Mantovani, F., Collavin, L. and Del Sal, G. (2019). 'Mutant p53 as a guardian of the cancer cell', *Cell death and differentiation*. *Cell Death Differ*, 26(2), pp. 199–212. doi: 10.1038/S41418-018-0246-9.
- Marabelle, A. *et al.* (2020). 'Efficacy of Pembrolizumab in Patients With Noncolorectal High Microsatellite Instability/Mismatch Repair-Deficient Cancer: Results From the Phase II KEYNOTE-158 Study', *Journal of clinical oncology : official journal of the American Society of Clinical Oncology*. *J Clin Oncol*, 38(1), pp. 1–10. doi: 10.1200/JCO.19.02105.
- Marques, L. R., Diniz, T. A., Antunes, B. M., Rossi, F. E., Caperuto, E. C., Lira, F. S. and Gonçalves, D. C. (2018). 'Reverse Cholesterol Transport: Molecular Mechanisms and the Non-medical Approach to Enhance HDL Cholesterol', *Frontiers in Physiology*. *Frontiers Media SA*, 9(MAY). doi: 10.3389/FPHYS.2018.00526.
- Masoodi, K. Z., Lone, S. M. and Rasool, R. S. (2021). 'Total RNA isolation', *Advanced Methods in Molecular Biology and Biotechnology*. Academic Press, pp. 73–78. doi: 10.1016/B978-0-12-824449-4.00013-X.
- Massagué, J., Blain, S. W. and Lo, R. S. (2000). 'TGF $\beta$  Signaling in Growth Control, Cancer, and Heritable Disorders', *Cell*. Elsevier, 103(2), pp. 295–309. doi: 10.1016/S0092-8674(00)00121-5.
- Másson, M., Loftsson, T., Másson, G. and Stefánsson, E. (1999). 'Cyclodextrins as permeation enhancers: Some theoretical evaluations and in vitro testing', *Journal of Controlled Release*, 59(1), pp. 107–118. doi: 10.1016/S0168-3659(98)00182-5.
- Mathews, L. A., Cabarcas, S. M., Hurt, E. M., Zhang, X., Jaffee, E. M. and Farrar, W. L. (2011). 'Increased expression of DNA repair genes in invasive human pancreatic cancer cells', *Pancreas*. NIH Public Access, 40(5), p. 730. doi: 10.1097/MPA.0B013E31821AE25B.

Matsuda, Y., Ishiwata, T., Izumiyama-Shimomura, N., Hamayasu, H., Fujiwara, M., Tomita, K. I., Hiraishi, N., Nakamura, K., Ishikawa, N., Aida, J., Takubo, K. and Arai, T. (2015). 'Gradual Telomere Shortening and Increasing Chromosomal Instability among PanIN Grades and Normal Ductal Epithelia with and without Cancer in the Pancreas', *PLOS ONE*. Public Library of Science, 10(2), p. e0117575. doi: 10.1371/JOURNAL.PONE.0117575.

Maxfield, F. R. and Wüstner, D. (2012). 'Analysis of cholesterol trafficking with fluorescent probes', *Methods in cell biology*. NIH Public Access, 108, p. 367. doi: 10.1016/B978-0-12-386487-1.00017-1.

Mazur, P. K., Einwächter, H., Lee, M., Sipos, B., Nakhai, H., Rad, R., Zimmer-Strobl, U., Strobl, L. J., Radtke, F., Klöppel, G., Schmid, R. M. and Siveke, J. T. (2010). 'Notch2 is required for progression of pancreatic intraepithelial neoplasia and development of pancreatic ductal adenocarcinoma', *Proceedings of the National Academy of Sciences of the United States of America*. National Academy of Sciences, 107(30), pp. 13438–13443. doi: 10.1073/PNAS.1002423107/SUPPL\_FILE/PNAS.201002423SI.PDF.

Medicines Agency, E. (2014). 'Background review for cyclodextrins used as excipients'.

Mehra, S., Deshpande, N. and Nagathihalli, N. (2021). 'Targeting PI3K Pathway in Pancreatic Ductal Adenocarcinoma: Rationale and Progress', *Cancers*. Multidisciplinary Digital Publishing Institute (MDPI), 13(17). doi: 10.3390/CANCERS13174434.

Mendez, M. G., Kojima, S.-I. and Goldman, R. D. (2010). 'Vimentin induces changes in cell shape, motility, and adhesion during the epithelial to mesenchymal transition', *The FASEB Journal*. The Federation of American Societies for Experimental Biology, 24(6), p. 1838. doi: 10.1096/FJ.09-151639.

Meng, J., Chen, S., Han, J. X., Qian, B., Wang, X. R., Zhong, W. L., Qin, Y., Zhang, H., Gao, W. F., Lei, Y. Y., Yang, W., Yang, L., Zhang, C., Liu, H. J., Liu, Y. R., Zhou, H. G., Sun, T. and Yang, C. (2018). 'Twist1 Regulates Vimentin through Cul2 Circular RNA to Promote EMT in Hepatocellular Carcinoma', *Cancer research*. Cancer Res, 78(15), pp. 4150–4162. doi: 10.1158/0008-5472.CAN-17-3009.

Mikesh, L. M., Kumar, M., Erdag, G., Hogan, K. T., Molhoek, K. R., Mayo, M. W. and Slingluff, C. L. (2010). 'Evaluation of molecular markers of mesenchymal phenotype in melanoma', *Melanoma Research*. NIH Public Access, 20(6), pp. 485–495. doi: 10.1097/CMR.0b013e32833fafb4.

Miller, I., Min, M., Yang, C., Tian, C., Gookin, S., Carter, D. and Spencer, S. L. (2018). 'Ki67 is a Graded Rather than a Binary Marker of Proliferation versus Quiescence', *Cell reports*. NIH Public Access, 24(5), p. 1105. doi: 10.1016/J.CELREP.2018.06.110.

Mistafa, O. and Stenius, U. (2009). 'Statins inhibit Akt/PKB signaling via P2X7 receptor in pancreatic cancer cells', *Biochemical Pharmacology*, 78(9), pp. 1115–1126. doi: 10.1016/J.BCP.2009.06.016.

Mizrahi, J. D., Surana, R., Valle, J. W. and Shroff, R. T. (2020). 'Pancreatic cancer', *The Lancet*. Lancet Publishing Group, 395(10242), pp. 2008–2020. doi: 10.1016/S0140-6736(20)30974-0.

Moffitt, R. A., Marayati, R., Flate, E. L., Volmar, K. E., Loeza, S. G. H., Hoadley, K. A., Rashid, N. U., Williams, L. A., Eaton, S. C., Chung, A. H., Smyla, J. K., Anderson, J. M., Kim, H. J., Bentrem, D. J., Talamonti, M. S., Iacobuzio-Donahue, C. A., Hollingsworth, M. A. and Yeh, J. J. (2015). 'Virtual microdissection identifies distinct tumor- and stroma-specific subtypes of pancreatic ductal adenocarcinoma', *Nature Genetics* 2015 47:10. Nature Publishing Group, 47(10), pp. 1168–1178. doi: 10.1038/ng.3398.

Mohammad, N., Malvi, P., Meena, A. S., Singh, S. V., Chaube, B., Vannuruswamy, G., Kulkarni, M. J. and Bhat, M. K. (2014). 'Cholesterol depletion by methyl- $\beta$ -cyclodextrin augments tamoxifen induced cell death by enhancing its uptake in melanoma', *Molecular Cancer*. BioMed Central Ltd., 13(1), pp. 1–13. doi: 10.1186/1476-4598-13-204/FIGURES/6.

Mollinedo, F. and Gajate, C. (2019). 'Novel therapeutic approaches for pancreatic cancer by combined targeting of RAF→MEK→ERK signaling and autophagy survival response', *Annals of Translational Medicine*. AME Publications, 7(Suppl 3), pp. S153–S153. doi: 10.21037/ATM.2019.06.40.

Mollinedo, F. and Gajate, C. (2020). 'Lipid rafts as signaling hubs in cancer cell survival/death and invasion: implications in tumor progression and therapy: Thematic Review Series: Biology of Lipid Rafts', *Journal of lipid research*. J Lipid Res, 61(5), pp. 611–635. doi: 10.1194/JLR.TR119000439.

Morandi, A., Taddei, M. L., Chiarugi, P. and Giannoni, E. (2017). 'Targeting the Metabolic Reprogramming That Controls Epithelial-to-Mesenchymal Transition in Aggressive Tumors', *Frontiers in Oncology*. Frontiers Media SA, 7(MAR), p. 1. doi: 10.3389/FONC.2017.00040.

Moustakas, A. and Heldin, C. H. (2007). 'Signaling networks guiding epithelial-mesenchymal transitions during embryogenesis and cancer progression', *Cancer science*. Cancer Sci, 98(10), pp. 1512–1520. doi: 10.1111/J.1349-7006.2007.00550.X.

Moustakas, A. and Heldin, C. H. (2016). 'Mechanisms of TGF $\beta$ -Induced Epithelial–Mesenchymal Transition', *Journal of Clinical Medicine*. Multidisciplinary Digital Publishing Institute (MDPI), 5(7). doi: 10.3390/JCM5070063.

Mukhopadhyay, U. K. *et al.* (2019). 'TP53 Status as a Determinant of Pro- vs Anti-Tumorigenic Effects of Estrogen Receptor-Beta in Breast Cancer', *JNCI: Journal of the National Cancer Institute*. Oxford Academic, 111(11), pp. 1202–1215. doi: 10.1093/JNCI/DJZ051.

Murai, T., Maruyama, Y., Mio, K., Nishiyama, H., Suga, M. and Sato, C. (2011). 'Low cholesterol triggers membrane microdomain-dependent CD44 shedding and suppresses tumor cell migration', *Journal of Biological Chemistry*, 286(3), pp. 1999–2007. doi: 10.1074/JBC.M110.184010.

Nagafuchi, A. (2001). 'Molecular architecture of adherens junctions', *Current opinion in cell biology*. Curr Opin Cell Biol, 13(5), pp. 600–603. doi: 10.1016/S0955-0674(00)00257-X.

Nagathihalli, N. S., Castellanos, J. A., Van Saun, M. N., Dai, X., Ambrose, M., Guo, Q., Xiong, Y. and Merchant, N. B. (2016). 'Pancreatic stellate cell secreted IL-6 stimulates STAT3 dependent invasiveness of pancreatic intraepithelial neoplasia and cancer cells', *Oncotarget*. Impact Journals, LLC, 7(40), p. 65982. doi: 10.18632/ONCOTARGET.11786.

Nestler, L., Evege, E., Mclaughlin, J., Munroe, D., Tan, T.-S., Wagner, K. and Stiles, B. (2004). 'TrypLE™ Express: A Temperature Stable Replacement for Animal Trypsin in Cell Dissociation Applications'.

Nieto, M. A. (2013). 'Epithelial plasticity: a common theme in embryonic and cancer cells', *Science (New York, N.Y.)*. Science, 342(6159). doi: 10.1126/SCIENCE.1234850.

Oberstein, P. E. and Olive, K. P. (2013). 'Pancreatic cancer: why is it so hard to treat?', *Therapeutic Advances in Gastroenterology*. SAGE Publications, 6(4), p. 321. doi: 10.1177/1756283X13478680.

Ohno, Y., Toshino, M., Mohammed, A. F. A., Fujiwara, Y., Komohara, Y., Onodera, R., Higashi, T. and Motoyama, K. (2023a). 'Mannose-methyl- $\beta$ -cyclodextrin suppresses tumor growth by targeting both colon cancer cells and tumor-associated macrophages', *Carbohydrate Polymers*. Elsevier, 305, p. 120551. doi: 10.1016/J.CARBPOL.2023.120551.

Ohno, Y., Toshino, M., Mohammed, A. F. A., Fujiwara, Y., Komohara, Y., Onodera, R., Higashi, T. and Motoyama, K. (2023b). 'Mannose-methyl- $\beta$ -cyclodextrin suppresses tumor growth by targeting both colon cancer cells and tumor-associated macrophages', *Carbohydrate Polymers*. Elsevier, 305, p. 120551. doi: 10.1016/J.CARBPOL.2023.120551.

Oken, M. M., Creech, R. H., Tormey, D. C., Horton, J., Davis, T. E., McFadden, E. T. and Carbone, P. P. (1982). 'Toxicity and response criteria of the Eastern Cooperative Oncology Group - PubMed', *American journal of clinical oncology*, 5(6), pp. 49–55. Available at: <https://pubmed.ncbi.nlm.nih.gov/7165009/> (Accessed: 9 April 2022).

Ong, H. S. (2018). 'Comparative genomics analysis', *Encyclopedia of Bioinformatics and Computational Biology: ABC of Bioinformatics*. Elsevier, 1–3, pp. 425–431. doi: 10.1016/B978-0-12-809633-8.20126-X.

Oni, T. E. *et al.* (2020). 'SOAT1 promotes mevalonate pathway dependency in pancreatic cancer', *The Journal of experimental medicine*. J Exp Med, 217(9). doi: 10.1084/JEM.20192389.

O'Reilly, E. M. *et al.* (2020). 'Randomized, Multicenter, Phase II Trial of Gemcitabine and Cisplatin With or Without Veliparib in Patients With Pancreas Adenocarcinoma and a Germline BRCA/PALB2 Mutation', *Journal of clinical oncology : official journal of the American Society of Clinical Oncology*. J Clin Oncol, 38(13), pp. 1378–1388. doi: 10.1200/JCO.19.02931.

Ottinger, E. A. *et al.* (2014). 'Collaborative Development of 2-Hydroxypropyl- $\beta$ -Cyclodextrin for the Treatment of Niemann-Pick Type C1 Disease', *Current topics in medicinal chemistry*. NIH Public Access, 14(3), p. 330. doi: 10.2174/1568026613666131127160118.

Paavilainen, L., Edvinsson, Å., Asplund, A., Hober, S., Kampf, C., Pontén, F. and Wester, K. (2010). 'The Impact of Tissue Fixatives on Morphology and Antibody-based Protein Profiling in Tissues and Cells', *Journal of Histochemistry and Cytochemistry*. Histochemical Society, 58(3), p. 237. doi: 10.1369/JHC.2009.954321.

Palamaris, K., Felekouras, E. and Sakellariou, S. (2021). 'Epithelial to Mesenchymal Transition: Key Regulator of Pancreatic Ductal Adenocarcinoma Progression and

Chemoresistance', *Cancers*. Multidisciplinary Digital Publishing Institute (MDPI), 13(21). doi: 10.3390/CANCERS13215532.

Panda, P. K., Mukhopadhyay, S., Das, D. N., Sinha, N., Naik, P. P. and Bhutia, S. K. (2015). 'Mechanism of autophagic regulation in carcinogenesis and cancer therapeutics', *Seminars in cell & developmental biology*. Semin Cell Dev Biol, 39, pp. 43–55. doi: 10.1016/J.SEMCDB.2015.02.013.

Park, J. H., Myung, J. K., Lee, S. J., Kim, H., Kim, S., Lee, S. B., Jang, H., Jang, W. Il, Park, S., Yang, H., Shim, S. and Kim, M. J. (2023). 'ABCA1-Mediated EMT Promotes Papillary Thyroid Cancer Malignancy through the ERK/Fra-1/ZEB1 Pathway', *Cells*. Cells, 12(2). doi: 10.3390/CELLS12020274.

Pastushenko, I. *et al.* (2018). 'Identification of the tumour transition states occurring during EMT', *Nature*. Nature, 556(7702). doi: 10.1038/S41586-018-0040-3.

Patteson, A. E., Vahabikashi, A., Pogoda, K., Adam, S. A., Mandal, K., Kittisopikul, M., Sivagurunathan, S., Goldman, A., Goldman, R. D. and Janmey, P. A. (2019). 'Vimentin protects cells against nuclear rupture and DNA damage during migration', *The Journal of Cell Biology*. The Rockefeller University Press, 218(12), p. 4079. doi: 10.1083/JCB.201902046.

Peinado, H., Ballestar, E., Esteller, M. and Cano, A. (2004). 'Snail Mediates E-Cadherin Repression by the Recruitment of the Sin3A/Histone Deacetylase 1 (HDAC1)/HDAC2 Complex', *Molecular and Cellular Biology*. Taylor & Francis, 24(1), p. 306. doi: 10.1128/MCB.24.1.306-319.2004.

Peinado, H., Olmeda, D. and Cano, A. (2007). 'Snail, Zeb and bHLH factors in tumour progression: an alliance against the epithelial phenotype?', *Nature reviews. Cancer*. Nat Rev Cancer, 7(6), pp. 415–428. doi: 10.1038/NRC2131.

Pinho, A. V., Rooman, I. and Real, F. X. (2011). 'p53-dependent regulation of growth, epithelial-mesenchymal transition and stemness in normal pancreatic epithelial cells', *Cell cycle (Georgetown, Tex.)*. Cell Cycle, 10(8), pp. 1312–1321. doi: 10.4161/CC.10.8.15363.

Van Der Poel-Van De Luytgaarde, S. C. P. A. M., Geertsma-Kleinekoort, W. M. C., Goudswaard, C. S., Hogenbirk-Hupkes, P. E., Van Hoven-Beijen, M. A., Van De Werf, M., Chu, I. W. T., Van Kapel, J. and Valk, P. J. M. (2013). 'Addition of  $\beta$ -Mercaptoethanol Is a Prerequisite for High-Quality RNA Isolation Using QIA-symphony Technology as Demonstrated by Detection of Molecular Aberrations in Hematologic Malignancies', <https://home.liebertpub.com/gtmb>. Mary Ann Liebert, Inc. 140 Huguenot Street, 3rd Floor New Rochelle, NY 10801 USA , 17(6), pp. 475–480. doi: 10.1089/GTMB.2012.0448.

Porter, R. L. *et al.* (2019). 'Epithelial to mesenchymal plasticity and differential response to therapies in pancreatic ductal adenocarcinoma', *Proceedings of the National Academy of Sciences of the United States of America*. Proc Natl Acad Sci U S A, 116(52), pp. 26835–26845. doi: 10.1073/PNAS.1914915116.

Preta, G. (2020). 'New Insights Into Targeting Membrane Lipids for Cancer Therapy', *Frontiers in Cell and Developmental Biology*. Frontiers Media S.A., 8, p. 876. doi: 10.3389/fcell.2020.571237.

- Prijic, S. and Chang, J. T. (2022). 'ABCA1 Expression Is Upregulated in an EMT in Breast Cancer Cell Lines via MYC-Mediated De-Repression of Its Proximal Ebox Element', *Biomedicines*. MDPI, 10(3). doi: 10.3390/BIOMEDICINES10030581/S1.
- Principe, D. R., Underwood, P. W., Korc, M., Trevino, J. G., Munshi, H. G. and Rana, A. (2021). 'The Current Treatment Paradigm for Pancreatic Ductal Adenocarcinoma and Barriers to Therapeutic Efficacy', *Frontiers in Oncology*. Frontiers Media S.A., 11, p. 688377. doi: 10.3389/FONC.2021.688377/BIBTEX.
- Puleo, F. *et al.* (2018). 'Stratification of Pancreatic Ductal Adenocarcinomas Based on Tumor and Microenvironment Features', *Gastroenterology*. *Gastroenterology*, 155(6), pp. 1999-2013.e3. doi: 10.1053/J.GASTRO.2018.08.033.
- Qiu, N., Li, X. and Liu, J. (2017). 'Application of cyclodextrins in cancer treatment', *Journal of Inclusion Phenomena and Macrocyclic Chemistry*. Springer Netherlands, 89(3–4), pp. 229–246. doi: 10.1007/S10847-017-0752-2.
- Quint, K., Tonigold, M., Di Fazio, P., Montalbano, R., Lingelbach, S., Rückert, F., Alinger, B., Ocker, M. and Neureiter, D. (2012). 'Pancreatic cancer cells surviving gemcitabine treatment express markers of stem cell differentiation and epithelial-mesenchymal transition', *International journal of oncology*. *Int J Oncol*, 41(6), pp. 2093–2102. doi: 10.3892/IJO.2012.1648.
- Ramkumar, S., Raghunath, A. and Raghunath, S. (2016). 'Statin Therapy: Review of Safety and Potential Side Effects', *Acta Cardiologica Sinica*. Taiwan Society of Cardiology, 32(6), p. 631. doi: 10.6515/ACS20160611A.
- Resnik, N., Repnik, U., Kreft, M. E., Sepčić, K., Maček, P., Turk, B. and Veranič, P. (2015). 'Highly Selective Anti-Cancer Activity of Cholesterol-Interacting Agents Methyl- $\beta$ -Cyclodextrin and Ostreolysin A/Pleurotolysin B Protein Complex on Urothelial Cancer Cells', *PLOS ONE*. Public Library of Science, 10(9), p. e0137878. doi: 10.1371/JOURNAL.PONE.0137878.
- Rhim, A. D., Mirek, E. T., Aiello, N. M., Maitra, A., Bailey, J. M., McAllister, F., Reichert, M., Beatty, G. L., Rustgi, A. K., Vonderheide, R. H., Leach, S. D. and Stanger, B. Z. (2012). 'EMT and dissemination precede pancreatic tumor formation', *Cell*. *Cell*, 148(1–2), pp. 349–361. doi: 10.1016/J.CELL.2011.11.025.
- Ribatti, D., Tamma, R. and Annese, T. (2020). 'Epithelial-Mesenchymal Transition in Cancer: A Historical Overview', *Translational Oncology*. Neoplasia Press, 13(6), p. 100773. doi: 10.1016/J.TRANON.2020.100773.
- Ricoult, S. J. H., Yecies, J. L., Ben-Sahra, I. and Manning, B. D. (2016). 'Oncogenic PI3K and K-Ras stimulate de novo lipid synthesis through mTORC1 and SREBP', *Oncogene*. NIH Public Access, 35(10), p. 1250. doi: 10.1038/ONC.2015.179.
- Rio, D. C., Ares, M., Hannon, G. J. and Nilsen, T. W. (2010). 'Ethanol precipitation of RNA and the use of carriers', *Cold Spring Harbor protocols*. Cold Spring Harb Protoc, 2010(6). doi: 10.1101/PDB.PROT5440.

Riss, T. L., Moravec, R. A., Niles, A. L., Duellman, S., Benink, H. A., Worzella, T. J. and Minor, L. (2004). *Cell Viability Assays, Assay Guidance Manual*. Eli Lilly & Company and the National Center for Advancing Translational Sciences.

Rozeveld, C. N., Johnson, K. M., Zhang, L. and Razidlo, G. L. (2020). 'KRAS controls pancreatic cancer cell lipid metabolism and invasive potential through the lipase HSL', *Cancer research*. NIH Public Access, 80(22), p. 4932. doi: 10.1158/0008-5472.CAN-20-1255.

Ruiz, C. F., Montal, E. D., Haley, J. A., Bott, A. J. and Haley, J. D. (2020). 'SREBP1 regulates mitochondrial metabolism in oncogenic KRAS expressing NSCLC', *FASEB journal : official publication of the Federation of American Societies for Experimental Biology*. NIH Public Access, 34(8), p. 10574. doi: 10.1096/FJ.202000052R.

Rustgi, A. K. (2006). 'The molecular pathogenesis of pancreatic cancer: Clarifying a complex circuitry', *Genes and Development*. Cold Spring Harbor Laboratory Press, 20(22), pp. 3049–3053. doi: 10.1101/gad.1501106.

Saha, S. T., Abdulla, N., Zininga, T., Shonhai, A., Wadee, R. and Kaur, M. (2023). '2-Hydroxypropyl- $\beta$ -cyclodextrin (HP $\beta$ CD) as a Potential Therapeutic Agent for Breast Cancer', *Cancers*. MDPI, 15(10), p. 2828. doi: 10.3390/CANCERS15102828/S1.

Saiki, Y. *et al.* (2012). 'DCK is frequently inactivated in acquired gemcitabine-resistant human cancer cells', *Biochemical and biophysical research communications*. Biochem Biophys Res Commun, 421(1), pp. 98–104. doi: 10.1016/J.BBRC.2012.03.122.

Sallam, T., Jones, M. C., Gilliland, T., Zhang, L., Wu, X., Eskin, A., Sandhu, J., Casero, D., Vallim, T. Q. D. A., Hong, C., Katz, M., Lee, R., Whitelegge, J. and Tontonoz, P. (2016). 'Feedback modulation of cholesterol metabolism by the lipid-responsive non-coding RNA LeXis', *Nature*. Nature, 534(7605), pp. 124–128. doi: 10.1038/NATURE17674.

Sánchez-Tilló, E., Lázaro, A., Torrent, R., Cuatrecasas, M., Vaquero, E. C., Castells, A., Engel, P. and Postigo, A. (2010). 'ZEB1 represses E-cadherin and induces an EMT by recruiting the SWI/SNF chromatin-remodeling protein BRG1', *Oncogene 2010 29:24*. Nature Publishing Group, 29(24), pp. 3490–3500. doi: 10.1038/onc.2010.102.

Satoh, K., Hamada, S. and Shimosegawa, T. (2015). 'Involvement of epithelial to mesenchymal transition in the development of pancreatic ductal adenocarcinoma', *Journal of Gastroenterology*. Springer Japan, 50(2), pp. 140–146. doi: 10.1007/S00535-014-0997-0/FIGURES/1.

Saxena, M., Stephens, M. A., Pathak, H. and Rangarajan, A. (2011a). 'Transcription factors that mediate epithelial-mesenchymal transition lead to multidrug resistance by upregulating ABC transporters', *Cell death & disease*. Cell Death Dis, 2(7). doi: 10.1038/CDDIS.2011.61.

Saxena, M., Stephens, M. A., Pathak, H. and Rangarajan, A. (2011b). 'Transcription factors that mediate epithelial–mesenchymal transition lead to multidrug resistance by upregulating ABC transporters', *Cell Death & Disease 2011 2:7*. Nature Publishing Group, 2(7), pp. e179–e179. doi: 10.1038/cddis.2011.61.

Shah, P. P., Dupre, T. V., Siskind, L. J. and Beverly, L. J. (2017). 'Common cytotoxic chemotherapeutics induce epithelial-mesenchymal transition (EMT) downstream of ER

stress', *Oncotarget*. Impact Journals, LLC, 8(14), p. 22625. doi: 10.18632/ONCOTARGET.15150.

Sharma, A., Bandyopadhyaya, S., Chowdhury, K., Sharma, T., Maheshwari, R., Das, A., Chakrabarti, G., Kumar, V. and Mandal, C. C. (2019). 'Metformin exhibited anticancer activity by lowering cellular cholesterol content in breast cancer cells', *PLoS ONE*. PLOS, 14(1). doi: 10.1371/JOURNAL.PONE.0209435.

Shichi, Y., Sasaki, N., Michishita, M., Hasegawa, F., Matsuda, Y., Arai, T., Gomi, F., Aida, J., Takubo, K., Toyoda, M., Yoshimura, H., Takahashi, K. and Ishiwata, T. (2019). 'Enhanced morphological and functional differences of pancreatic cancer with epithelial or mesenchymal characteristics in 3D culture', *Scientific Reports 2019 9:1*. Nature Publishing Group, 9(1), pp. 1–10. doi: 10.1038/s41598-019-47416-w.

Shields, M. A., Dangi-Garimella, S., Krantz, S. B., Bentrem, D. J. and Munshi, H. G. (2011). 'Pancreatic Cancer Cells Respond to Type I Collagen by Inducing Snail Expression to Promote Membrane Type 1 Matrix Metalloproteinase-dependent Collagen Invasion', *Journal of Biological Chemistry*. Elsevier, 286(12), pp. 10495–10504. doi: 10.1074/JBC.M110.195628.

Silva Afonso, M., Marcondes Machado, R., Ferrari Lavrador, M. S., Rocha Quintao, E. C., Moore, K. J. and Lottenberg, A. M. (2018). 'Molecular Pathways Underlying Cholesterol Homeostasis', *Nutrients 2018, Vol. 10, Page 760*. Multidisciplinary Digital Publishing Institute, 10(6), p. 760. doi: 10.3390/NU10060760.

Simón, L., Campos, A., Leyton, L. and Quest, A. F. G. (2020). 'Caveolin-1 function at the plasma membrane and in intracellular compartments in cancer', *Cancer Metastasis Reviews*. Springer, 39(2), p. 435. doi: 10.1007/S10555-020-09890-X.

Smeenk, H. G., Tran, T. C. K., Erdmann, J., van Eijck, C. H. J. and Jeekel, J. (2005). 'Survival after surgical management of pancreatic adenocarcinoma: Does curative and radical surgery truly exist?', *Langenbeck's Archives of Surgery*. Langenbecks Arch Surg, 390(2), pp. 94–103. doi: 10.1007/s00423-004-0476-9.

Sohal, D. P. S., Mangu, P. B., Khorana, A. A., Shah, M. A., Philip, P. A., O'Reilly, E. M., Uronis, H. E., Ramanathan, R. K., Crane, C. H., Engebretson, A., Ruggiero, J. T., Copur, M. S., Lau, M., Urba, S. and Laheru, D. (2016). 'Metastatic Pancreatic Cancer: American Society of Clinical Oncology Clinical Practice Guideline', *Journal of clinical oncology : official journal of the American Society of Clinical Oncology*. J Clin Oncol, 34(23), pp. 2784–2796. doi: 10.1200/JCO.2016.67.1412.

Sommariva, M. and Gagliano, N. (2020). 'E-Cadherin in Pancreatic Ductal Adenocarcinoma: A Multifaceted Actor during EMT', *Cells*. Multidisciplinary Digital Publishing Institute (MDPI), 9(4). doi: 10.3390/CELLS9041040.

Sorrentino, A., Thakur, N., Grimsby, S., Marcusson, A., Von Bulow, V., Schuster, N., Zhang, S., Heldin, C. H. and Landström, M. (2008). 'The type I TGF-beta receptor engages TRAF6 to activate TAK1 in a receptor kinase-independent manner', *Nature cell biology*. Nat Cell Biol, 10(10), pp. 1199–1207. doi: 10.1038/NCB1780.

- Sousa-Squiavinato, A. C. M., Arregui Ramos, D. A., Wagner, M. S., Tessmann, J. W., de-Freitas-Junior, J. C. M. and Morgado-Díaz, J. A. (2022). 'Long-term resistance to 5-fluorouracil promotes epithelial-mesenchymal transition, apoptosis evasion, autophagy, and reduced proliferation rate in colon cancer cells', *European journal of pharmacology*. Eur J Pharmacol, 933. doi: 10.1016/J.EJPHAR.2022.175253.
- Stockwell, B. R. *et al.* (2017). 'Ferroptosis: A Regulated Cell Death Nexus Linking Metabolism, Redox Biology, and Disease', *Cell*. Cell Press, 171(2), pp. 273–285. doi: 10.1016/J.CELL.2017.09.021.
- Subramanian, N., Schumann-Gillett, A., Mark, A. E. and O'Mara, M. L. (2016). 'Understanding the accumulation of P-glycoprotein substrates within cells: The effect of cholesterol on membrane partitioning', *Biochimica et Biophysica Acta (BBA) - Biomembranes*. Elsevier, 1858(4), pp. 776–782. doi: 10.1016/J.BBAMEM.2015.12.025.
- Sung, H., Ferlay, J., Siegel, R. L., Laversanne, M., Soerjomataram, I., Jemal, A. and Bray, F. (2021). 'Global Cancer Statistics 2020: GLOBOCAN Estimates of Incidence and Mortality Worldwide for 36 Cancers in 185 Countries', *CA: a cancer journal for clinicians*. CA Cancer J Clin, 71(3), pp. 209–249. doi: 10.3322/CAAC.21660.
- Szejtli, J. (1998). 'Introduction and general overview of cyclodextrin chemistry', *Chemical Reviews*. American Chemical Society, 98(5), pp. 1743–1753. doi: 10.1021/CR970022C.
- Tabas, I. (2002). 'Consequences of cellular cholesterol accumulation: basic concepts and physiological implications', *The Journal of Clinical Investigation*. American Society for Clinical Investigation, 110(7), p. 905. doi: 10.1172/JCI16452.
- Takano, S., Reichert, M., Bakir, B., Das, K. K., Nishida, T., Miyazaki, M., Heeg, S., Collins, M. A., Marchand, B., Hicks, P. D., Maitra, A. and Rustgi, A. K. (2016). 'Prrx1 isoform switching regulates pancreatic cancer invasion and metastatic colonization', *Genes & Development*. Cold Spring Harbor Laboratory Press, 30(2), p. 233. doi: 10.1101/GAD.263327.115.
- Thiery, J. P., Acloque, H., Huang, R. Y. J. and Nieto, M. A. (2009). 'Epithelial-Mesenchymal Transitions in Development and Disease', *Cell*. Elsevier, 139(5), pp. 871–890. doi: 10.1016/J.CELL.2009.11.007/ATTACHMENT/7E0CAE36-4693-4EE3-AF81-C2E478E595A2/MMC1.PDF.
- Timmerman, L. A., Grego-Bessa, J., Raya, A., Bertrán, E., Pérez-Pomares, J. M., Díez, J., Aranda, S., Palomo, S., McCormick, F., Izpisua-Belmonte, J. C. and De La Pompa, J. L. (2004). 'Notch promotes epithelial-mesenchymal transition during cardiac development and oncogenic transformation', *Genes & Development*. Cold Spring Harbor Laboratory Press, 18(1), p. 99. doi: 10.1101/GAD.276304.
- Tisza, M. J., Zhao, W., Fuentes, J. S. R., Prijic, S., Chen, X., Levental, I. and Chang, J. T. (2016). 'Motility and stem cell properties induced by the epithelial-mesenchymal transition require destabilization of lipid rafts', *Oncotarget*. Impact Journals, LLC, 7(32), p. 51553. doi: 10.18632/ONCOTARGET.9928.
- Topacio, B. R., Zatulovskiy, E., Cristea, S., Xie, S., Tambo, C. S., Rubin, S. M., Sage, J., Kõivomägi, M. and Skotheim, J. M. (2019). 'Cyclin D-Cdk4,6 Drives Cell-Cycle Progression

via the Retinoblastoma Protein's C-Terminal Helix', *Molecular cell*. NIH Public Access, 74(4), p. 758. doi: 10.1016/J.MOLCEL.2019.03.020.

Tsou, S. H., Chen, T. M., Hsiao, H. T. and Chen, Y. H. (2015). 'A critical dose of doxorubicin is required to alter the gene expression profiles in MCF-7 cells acquiring multidrug resistance', *PloS one*. PLoS One, 10(1). doi: 10.1371/JOURNAL.PONE.0116747.

Tsuji, K., Ojima, M., Otabe, K., Horie, M., Koga, H., Sekiya, I. and Muneta, T. (2017). 'Effects of Different Cell-Detaching Methods on the Viability and Cell Surface Antigen Expression of Synovial Mesenchymal Stem Cells', *Cell Transplantation*. SAGE Publications, 26(6), p. 1089. doi: 10.3727/096368917X694831.

Tsujie, M., Nakamori, S., Nakahira, S., Takahashi, Y., Hayashi, N., Okami, J., Nagano, H., Dono, K., Umeshita, K., Sakon, M. and Monden, M. (2007). 'Human Equilibrative Nucleoside Transporter 1, as a Predictor of 5-Fluorouracil Resistance in Human Pancreatic Cancer', *Anticancer Research*. International Institute of Anticancer Research, 27(4B), pp. 2241–2249. Available at: <https://ar.iijournals.org/content/27/4B/2241> (Accessed: 7 November 2023).

Turabelidze, A., Guo, S. and Dipietro, L. A. (2010). 'Importance of Housekeeping gene selection for accurate RT-qPCR in a wound healing model', *Wound repair and regeneration : official publication of the Wound Healing Society [and] the European Tissue Repair Society*. NIH Public Access, 18(5), p. 460. doi: 10.1111/J.1524-475X.2010.00611.X.

Uchibori, K., Kasamatsu, A., Sunaga, M., Yokota, S., Sakurada, T., Kobayashi, E., Yoshikawa, M., Uzawa, K., Ueda, S., Tanzawa, H. and Sato, N. (2012). 'Establishment and characterization of two 5-fluorouracil-resistant hepatocellular carcinoma cell lines', *International Journal of Oncology*. Spandidos Publications, 40(4), p. 1005. doi: 10.3892/IJO.2011.1300.

Ungefroren, H., Groth, S., Sebens, S., Lehnert, H., Gieseler, F. and Fändrich, F. (2011). 'Differential roles of Smad2 and Smad3 in the regulation of TGF- $\beta$ 1-mediated growth inhibition and cell migration in pancreatic ductal adenocarcinoma cells: control by Rac1', *Molecular cancer*. Mol Cancer, 10. doi: 10.1186/1476-4598-10-67.

Ungefroren, H., Thürling, I., Färber, B., Kowalke, T., Fischer, T., De Assis, L. V. M., Braun, R., Castven, D., Oster, H., Konukiewicz, B., Wellner, U. F., Lehnert, H. and Marquardt, J. U. (2022). 'The Quasimesenchymal Pancreatic Ductal Epithelial Cell Line PANC-1—A Useful Model to Study Clonal Heterogeneity and EMT Subtype Shifting', *Cancers*. MDPI, 14(9), p. 2057. doi: 10.3390/CANCERS14092057/S1.

Usman, S., Waseem, N. H., Nguyen, T. K. N., Mohsin, S., Jamal, A., Teh, M. T. and Waseem, A. (2021). 'Vimentin Is at the Heart of Epithelial Mesenchymal Transition (EMT) Mediated Metastasis', *Cancers*. Multidisciplinary Digital Publishing Institute (MDPI), 13(19), p. 4985. doi: 10.3390/CANCERS13194985.

Vega, S., Morales, A. V., Ocaña, O. H., Valdés, F., Fabregat, I. and Nieto, M. A. (2004). 'Snail blocks the cell cycle and confers resistance to cell death', *Genes & development*. Genes Dev, 18(10), pp. 1131–1143. doi: 10.1101/GAD.294104.

- Vesuna, F., van Diest, P., Chen, J. H. and Raman, V. (2008). 'Twist is a transcriptional repressor of E-cadherin gene expression in breast cancer', *Biochemical and biophysical research communications*. NIH Public Access, 367(2), p. 235. doi: 10.1016/J.BBRC.2007.11.151.
- Vincent, T., Neve, E. P. A., Johnson, J. R., Kukalev, A., Rojo, F., Albanell, J., Pietras, K., Virtanen, I., Philipson, L., Leopold, P. L., Crystal, R. G., de Herreros, A. G., Moustakas, A., Pettersson, R. F. and Fuxe, J. (2009). 'A SNAIL1-SMAD3/4 transcriptional repressor complex promotes TGF-beta mediated epithelial-mesenchymal transition', *Nature cell biology*. Nat Cell Biol, 11(8), pp. 943–950. doi: 10.1038/NCB1905.
- Vona, R., Iessi, E. and Matarrese, P. (2021). 'Role of Cholesterol and Lipid Rafts in Cancer Signaling: A Promising Therapeutic Opportunity?', *Frontiers in Cell and Developmental Biology*. Frontiers Media S.A., 9, p. 622908. doi: 10.3389/FCELL.2021.622908/BIBTEX.
- Waddell, N. *et al.* (2015). 'Whole genomes redefine the mutational landscape of pancreatic cancer', *Nature*. Nature, 518(7540), pp. 495–501. doi: 10.1038/NATURE14169.
- Wainberg, Z. A., Feeney, K., Lee, M. A., Muñoz, A., Gracián, A. C., Lonardi, S., Ryoo, B. Y., Hung, A., Lin, Y., Bendell, J. and Hecht, J. R. (2020). 'Meta-analysis examining overall survival in patients with pancreatic cancer treated with second-line 5-fluorouracil and oxaliplatin-based therapy after failing first-line gemcitabine-containing therapy: effect of performance status and comparison with other regimens', *BMC Cancer*. BioMed Central, 20(1), pp. 1–9. doi: 10.1186/S12885-020-07110-X/TABLES/4.
- Wakana, Y., Hayashi, K., Nemoto, T., Watanabe, C., Taoka, M., Angulo-Capel, J., Garcia-Parajo, M. F., Kumata, H., Umemura, T., Inoue, H., Arasaki, K., Campelo, F. and Tagaya, M. (2021). 'The ER cholesterol sensor SCAP promotes CARTS biogenesis at ER–Golgi membrane contact sites', *The Journal of Cell Biology*. The Rockefeller University Press, 220(1). doi: 10.1083/JCB.202002150.
- Wang, B. and Tontonoz, P. (2018). 'Liver X receptors in lipid signalling and membrane homeostasis', *Nature reviews. Endocrinology*. NIH Public Access, 14(8), p. 452. doi: 10.1038/S41574-018-0037-X.
- Wang, C., Li, P., Xuan, J., Zhu, C., Liu, J., Shan, L., Du, Q., Ren, Y. and Ye, J. (2017). 'Cholesterol Enhances Colorectal Cancer Progression via ROS Elevation and MAPK Signaling Pathway Activation', *Cellular physiology and biochemistry: international journal of experimental cellular physiology, biochemistry, and pharmacology*. Cell Physiol Biochem, 42(2), pp. 729–742. doi: 10.1159/000477890.
- Wang, C., Zhang, W., Juan Fu, M., Yang, A., Huang, H. and Xie, J. (2015). 'Establishment of human pancreatic cancer gemcitabine-resistant cell line with ribonucleotide reductase overexpression', *Oncology reports*. Oncol Rep, 33(1), pp. 383–390. doi: 10.3892/OR.2014.3599.
- Wang, F., Ma, L., Zhang, Z., Liu, X., Gao, H., Zhuang, Y., Yang, P., Kornmann, M., Tian, X. and Yang, Y. (2016). 'Hedgehog Signaling Regulates Epithelial-Mesenchymal Transition in Pancreatic Cancer Stem-Like Cells', *Journal of Cancer*. Ivyspring International Publisher, 7(4), p. 408. doi: 10.7150/JCA.13305.

Wang, H., Wu, J., Zhang, Y., Xue, X., Tang, D., Yuan, Z., Chen, M., Wei, J., Zhang, J. and Miao, Y. (2012). 'Transforming growth factor  $\beta$ -induced epithelial-mesenchymal transition increases cancer stem-like cells in the PANC-1 cell line', *Oncology Letters*. Spandidos Publications, 3(1), p. 229. doi: 10.3892/OL.2011.448.

Wang, S., Huang, S. and Sun, Y. L. (2017). 'Epithelial-Mesenchymal Transition in Pancreatic Cancer: A Review', *BioMed Research International*. Hindawi Limited, 2017. doi: 10.1155/2017/2646148.

Wang, T., Chen, Z., Zhu, Y., Pan, Q., Liu, Y., Qi, X., Jin, L., Jin, J., Ma, X. and Hua, D. (2015). 'Inhibition of Transient Receptor Potential Channel 5 Reverses 5-Fluorouracil Resistance in Human Colorectal Cancer Cells', *The Journal of Biological Chemistry*. American Society for Biochemistry and Molecular Biology, 290(1), p. 448. doi: 10.1074/JBC.M114.590364.

Wang, Y., Rogers, P. M., Su, C., Varga, G., Stayrook, K. R. and Burris, T. P. (2008). 'Regulation of cholesterologenesis by the oxysterol receptor, LXR $\alpha$ ', *Journal of Biological Chemistry*. American Society for Biochemistry and Molecular Biology, 283(39), pp. 26332–26339. doi: 10.1074/jbc.M804808200.

Wang, Z., Li, Y., Kong, D., Banerjee, S., Ahmad, A., Azmi, A. S., Ali, S., Abbruzzese, J. L., Gallick, G. E. and Sarkar, F. H. (2009). 'Acquisition of epithelial-mesenchymal transition phenotype of gemcitabine-resistant pancreatic cancer cells is linked with activation of the notch signaling pathway', *Cancer research*. *Cancer Res*, 69(6), pp. 2400–2407. doi: 10.1158/0008-5472.CAN-08-4312.

Ward, N. C., Watts, G. F. and Eckel, R. H. (2019). 'Statin Toxicity: Mechanistic Insights and Clinical Implications', *Circulation Research*. Lippincott Williams and Wilkins, 124(2), pp. 328–350. doi: 10.1161/CIRCRESAHA.118.312782.

Weadick, B., Nayak, D., Persaud, A. K., Hung, S. W., Raj, R., Campbell, M. J., Chen, W., Li, J., Williams, T. M. and Govindarajan, R. (2021). 'EMT-Induced Gemcitabine Resistance in Pancreatic Cancer Involves the Functional Loss of Equilibrative Nucleoside Transporter 1', *Molecular cancer therapeutics*. *Mol Cancer Ther*, 20(2), pp. 410–422. doi: 10.1158/1535-7163.MCT-20-0316.

De Wever, O., Derycke, L., Hendrix, A., De Meerleer, G., Godeau, F., Depypere, H. and Bracke, M. (2007). 'Soluble cadherins as cancer biomarkers', *Clinical and Experimental Metastasis*. Springer, 24(8), pp. 685–697. doi: 10.1007/S10585-007-9104-8/FIGURES/3.

Williams, E. D., Gao, D., Redfern, A. and Thompson, E. W. (2019). 'Controversies around epithelial–mesenchymal plasticity in cancer metastasis', *Nature reviews. Cancer*. NIH Public Access, 19(12), p. 716. doi: 10.1038/S41568-019-0213-X.

Wong, J., Quinn, C. M. and Brown, A. J. (2006). 'SREBP-2 positively regulates transcription of the cholesterol efflux gene, ABCA1, by generating oxysterol ligands for LXR', *Biochemical Journal*. Portland Press Ltd, 400(Pt 3), p. 485. doi: 10.1042/BJ20060914.

Wong, T. S., Gao, W. and Chan, J. Y. W. (2014). 'Transcription Regulation of E-Cadherin by Zinc Finger E-Box Binding Homeobox Proteins in Solid Tumors', *BioMed Research International*. Hindawi Limited, 2014. doi: 10.1155/2014/921564.

- Wu, Y., Diab, I., Zhang, X., Izmailova, E. S. and Zehner, Z. E. (2004). 'Stat3 enhances vimentin gene expression by binding to the antisilencer element and interacting with the repressor protein, ZBP-89', *Oncogene*. *Oncogene*, 23(1), pp. 168–178. doi: 10.1038/SJ.ONC.1207003.
- Wu, Y., Zhang, X., Salmon, M., Lin, X. and Zehner, Z. E. (2007). 'TGFbeta1 regulation of vimentin gene expression during differentiation of the C2C12 skeletal myogenic cell line requires Smads, AP-1 and Sp1 family members', *Biochimica et biophysica acta*. *Biochim Biophys Acta*, 1773(3), pp. 427–439. doi: 10.1016/J.BBAMCR.2006.11.017.
- Xian, G., Zhao, J., Qin, C., Zhang, Z., Lin, Y. and Su, Z. (2017). 'Simvastatin attenuates macrophage-mediated gemcitabine resistance of pancreatic ductal adenocarcinoma by regulating the TGF- $\beta$ 1/Gfi-1 axis', *Cancer Letters*. Elsevier Ireland Ltd, 385, pp. 65–74. doi: 10.1016/J.CANLET.2016.11.006.
- Xiao, B., Jiang, Z. Q., Hu, J. X., Zhang, X. M. and Xu, H. B. (2019). 'Differentiating pancreatic neuroendocrine tumors from pancreatic ductal adenocarcinomas by the "Duct-Road Sign": A preliminary magnetic resonance imaging study', *Medicine*. Wolters Kluwer Health, 98(35). doi: 10.1097/MD.00000000000016960.
- Xu, J., Lamouille, S. and Derynck, R. (2009). 'TGF- $\beta$ -induced epithelial to mesenchymal transition', *Cell research*. NIH Public Access, 19(2), p. 156. doi: 10.1038/CR.2009.5.
- Xu, T. P., Shen, H., Liu, L. X. and Shu, Y. Q. (2013). 'Plumbagin from plumbago zeylanica 1 induces apoptosis in human non-small cell lung cancer cell lines through NF Kb inactivation', *Asian Pacific Journal of Cancer Prevention*. Asian Pacific Organization for Cancer Prevention, 14(4), pp. 2325–2331. doi: 10.7314/APJCP.2013.14.4.2325.
- Yamaguchi, R., Perkins, G. and Hirota, K. (2015). 'Targeting cholesterol with  $\beta$ -cyclodextrin sensitizes cancer cells for apoptosis', *FEBS Letters*. John Wiley & Sons, Ltd, 589(24PartB), pp. 4097–4105. doi: 10.1016/J.FEBSLET.2015.11.009.
- Yamashita, M., Fatyol, K., Jin, C., Wang, X., Liu, Z. and Zhang, Y. E. (2008). 'TRAF6 mediates Smad-independent activation of JNK and p38 by TGF-beta', *Molecular cell*. *Mol Cell*, 31(6), pp. 918–924. doi: 10.1016/J.MOLCEL.2008.09.002.
- Yang, C. Y., Chang, P. W., Hsu, W. H., Chang, H. C., Chen, C. L., Lai, C. C., Chiu, W. T. and Chen, H. C. (2019). 'Src and SHP2 coordinately regulate the dynamics and organization of vimentin filaments during cell migration', *Oncogene*. *Oncogene*, 38(21), pp. 4075–4094. doi: 10.1038/S41388-019-0705-X.
- Yang, Q., Miyagawa, M., Liu, X., Zhu, B., Munemasa, S., Nakamura, T., Murata, Y. and Nakamura, Y. (2018). 'Methyl- $\beta$ -cyclodextrin potentiates the BITC-induced anti-cancer effect through modulation of the Akt phosphorylation in human colorectal cancer cells', *Bioscience, biotechnology, and biochemistry*. *Biosci Biotechnol Biochem*, 82(12), pp. 2158–2167. doi: 10.1080/09168451.2018.1514249.
- Ye, D., Lammers, B., Zhao, Y., Meurs, I., J.C. Van Berkel, T. and Van Eck, M. (2011). 'ATP-binding cassette transporters A1 and G1, HDL metabolism, cholesterol efflux, and inflammation: important targets for the treatment of atherosclerosis', *Current drug targets*. *Curr Drug Targets*, 12(5), pp. 647–660. doi: 10.2174/138945011795378522.

- Ye, X. and Weinberg, R. A. (2015). 'Epithelial-Mesenchymal Plasticity: A central regulator of cancer progression', *Trends in cell biology*. NIH Public Access, 25(11), p. 675. doi: 10.1016/J.TCB.2015.07.012.
- Yonezawa, S., Higashi, M., Yamada, N. and Goto, M. (2008). 'Precursor Lesions of Pancreatic Cancer', *Gut and Liver*. The Editorial Office of Gut and Liver, 2(3), pp. 137–154. doi: 10.5009/gnl.2008.2.3.137.
- Zadran, S., Arumugam, R., Herschman, H., Phelps, M. E. and Levine, R. D. (2014). 'Surprisal analysis characterizes the free energy time course of cancer cells undergoing epithelial-to-mesenchymal transition', *Proceedings of the National Academy of Sciences of the United States of America*. Proc Natl Acad Sci U S A, 111(36), pp. 13235–13240. doi: 10.1073/PNAS.1414714111.
- Van Der Zee, J. A., Van Eijck, C. H. J., Hop, W. C. J., Van Dekken, H., Dicheva, B. M., Seynhaeve, A. L. B., Koning, G. A., Eggermont, A. M. M. and Ten Hagen, T. L. M. (2012). 'Expression and prognostic significance of thymidylate synthase (TS) in pancreatic head and periampullary cancer.', *European Journal of Surgical Oncology : the Journal of the European Society of Surgical Oncology and the British Association of Surgical Oncology*, 38(11), pp. 1058–1064. doi: 10.1016/J.EJSO.2012.04.013.
- Zeisberg, M. and Neilson, E. G. (2009). 'Biomarkers for epithelial-mesenchymal transitions', *The Journal of Clinical Investigation*. American Society for Clinical Investigation, 119(6), p. 1429. doi: 10.1172/JCI36183.
- Zeng, J., Zhang, H., Tan, Y., Sun, C., Liang, Y., Yu, J. and Zou, H. (2018). 'Aggregation of lipid rafts activates c-met and c-Src in non-small cell lung cancer cells', *BMC Cancer*. BioMed Central Ltd., 18(1), pp. 1–11. doi: 10.1186/S12885-018-4501-8/FIGURES/7.
- Zhang, J. H., Chung, T. D. Y. and Oldenburg, K. R. (1999). 'A Simple Statistical Parameter for Use in Evaluation and Validation of High Throughput Screening Assays', *Journal of biomolecular screening*. J Biomol Screen, 4(2), pp. 67–73. doi: 10.1177/108705719900400206.
- Zhang, Q., Zhao, Y. P., Liao, Q., Hu, Y., Xu, Q., Zhou, L. and Shu, H. (2011). 'Associations between gene polymorphisms of thymidylate synthase with its protein expression and chemosensitivity to 5-fluorouracil in pancreatic carcinoma cells', *Chinese Medical Journal*, 124(2), pp. 262–267. doi: 10.3760/CMA.J.ISSN.0366-6999.2011.02.021.
- Zhang, S., Zhu, N., Li, H. F., Gu, J., Zhang, C. J., Liao, D. F. and Qin, L. (2022). 'The lipid rafts in cancer stem cell: a target to eradicate cancer', *Stem Cell Research & Therapy*. BMC, 13(1). doi: 10.1186/S13287-022-03111-8.
- Zhang, W., Feng, M., Zheng, G., Chen, Y., Wang, X., Pen, B., Yin, J., Yu, Y. and He, Z. (2012). 'Chemoresistance to 5-fluorouracil induces epithelial-mesenchymal transition via up-regulation of Snail in MCF7 human breast cancer cells', *Biochemical and biophysical research communications*. Biochem Biophys Res Commun, 417(2), pp. 679–685. doi: 10.1016/J.BBRC.2011.11.142.

- Zhang, X. M., Guo, K., Li, L. H., Zhang, S. and Li, B. J. (2015). 'Multi-stimuli-responsive magnetic assemblies as tunable releasing carriers', *Journal of Materials Chemistry B*. Royal Society of Chemistry, 3(29), pp. 6026–6031. doi: 10.1039/C5TB00845J.
- Zhang, Y., Li, C., Xia, C., Wah To, K. K., Guo, Z., Ren, C., Wen, L., Wang, F., Fu, L. and Liao, N. (2022). 'Adagrasib, a KRAS G12C inhibitor, reverses the multidrug resistance mediated by ABCB1 in vitro and in vivo', *Cell Communication and Signaling : CCS*. BMC, 20(1). doi: 10.1186/S12964-022-00955-8.
- Zhang, Z., Duan, Q., Zhao, H., Liu, T., Wu, H., Shen, Q., Wang, C. and Yin, T. (2016). 'Gemcitabine treatment promotes pancreatic cancer stemness through the Nox/ROS/NF- $\kappa$ B/STAT3 signaling cascade', *Cancer letters*. Cancer Lett, 382(1), pp. 53–63. doi: 10.1016/J.CANLET.2016.08.023.
- Zhao, B., Qin, C., Li, Z., Wang, Y., Li, Tianhao, Cao, H., Yang, X., Li, Tianyu and Wang, W. (2022). 'Multidrug resistance genes screening of pancreatic ductal adenocarcinoma based on sensitivity profile to chemotherapeutic drugs', *Cancer Cell International*. BioMed Central Ltd, 22(1), pp. 1–12. doi: 10.1186/S12935-022-02785-7/FIGURES/7.
- Zhao, H., Wu, S., Li, H., Duan, Q., Zhang, Z., Shen, Q., Wang, C. and Yin, T. (2019). 'ROS/KRAS/AMPK Signaling Contributes to Gemcitabine-Induced Stem-like Cell Properties in Pancreatic Cancer', *Molecular Therapy - Oncolytics*. Cell Press, 14, pp. 299–312. doi: 10.1016/j.omto.2019.07.005.
- Zhao, W., Prijic, S., Urban, B. C., Tisza, M. J., Zuo, Y., Li, L., Tan, Z., Chen, X., Mani, S. A. and Chang, J. T. (2016). 'Candidate Antimetastasis Drugs Suppress the Metastatic Capacity of Breast Cancer Cells by Reducing Membrane Fluidity', *Cancer research*. Cancer Res, 76(7), pp. 2037–2049. doi: 10.1158/0008-5472.CAN-15-1970.
- Zhao, X., Li, Z. and Gu, Z. (2022). 'A new era: tumor microenvironment in chemoresistance of pancreatic cancer', *Journal of cancer science and clinical therapeutics*. NIH Public Access, 6(1), p. 61. doi: 10.26502/JCSCT.5079146.
- Zhao, Y., He, L., Wang, T., Zhu, L. and Yan, N. (2021). '2-hydroxypropyl- $\beta$ -cyclodextrin regulates the epithelial to mesenchymal transition in breast cancer cells by modulating cholesterol homeostasis and endoplasmic reticulum stress', *Metabolites*. MDPI, 11(8). doi: 10.3390/METABO11080562/S1.
- Zheng, C., Jiao, X., Jiang, Y. and Sun, S. (2013). 'ERK1/2 activity contributes to gemcitabine resistance in pancreatic cancer cells', *The Journal of international medical research*. J Int Med Res, 41(2), pp. 300–360. doi: 10.1177/0300060512474128.
- Zheng, X., Carstens, J. L., Kim, J., Scheible, M., Kaye, J., Sugimoto, H., Wu, C. C., Lebleu, V. S. and Kalluri, R. (2015). 'Epithelial-to-mesenchymal transition is dispensable for metastasis but induces chemoresistance in pancreatic cancer', *Nature*. Nature, 527(7579), pp. 525–530. doi: 10.1038/NATURE16064.
- Zhu, K., Chen, L., Han, X., Wang, Jia and Wang, Jue (2012). 'Short hairpin RNA targeting Twist1 suppresses cell proliferation and improves chemosensitivity to cisplatin in HeLa human cervical cancer cells', *Oncology reports*. Oncol Rep, 27(4), pp. 1027–1034. doi: 10.3892/OR.2012.1633.

Zhu, Q. Q., Ma, C., Wang, Q., Song, Y. and Lv, T. (2016). 'The role of TWIST1 in epithelial-mesenchymal transition and cancers', *Tumor Biology*. Springer Science and Business Media B.V., 37(1), pp. 185–197. doi: 10.1007/S13277-015-4450-7/FIGURES/2.

Zhuang, L., Kim, J., Adam, R. M., Solomon, K. R. and Freeman, M. R. (2005). 'Cholesterol targeting alters lipid raft composition and cell survival in prostate cancer cells and xenografts', *The Journal of clinical investigation*. J Clin Invest, 115(4), pp. 959–968. doi: 10.1172/JCI19935.

## 8 Appendix

### Optimising GEM and 5-FU concentrations in the PANC-1 cell line

In order to optimise the concentrations of drugs 5-FU and GEM for downstream experiments, MTT assays were performed using a range of drug concentrations alone or in combination with the cholesterol depleting agent, 10 mM KS-01. The drugs 5-FU and GEM demonstrated resistance to cell death at all concentrations and thus chosen concentrations were chosen based off their effect in combination with KS-01. A concentration of 1  $\mu\text{M}$  was chosen for GEM and a concentration of 10  $\mu\text{M}$  for 5-FU for downstream experiments.

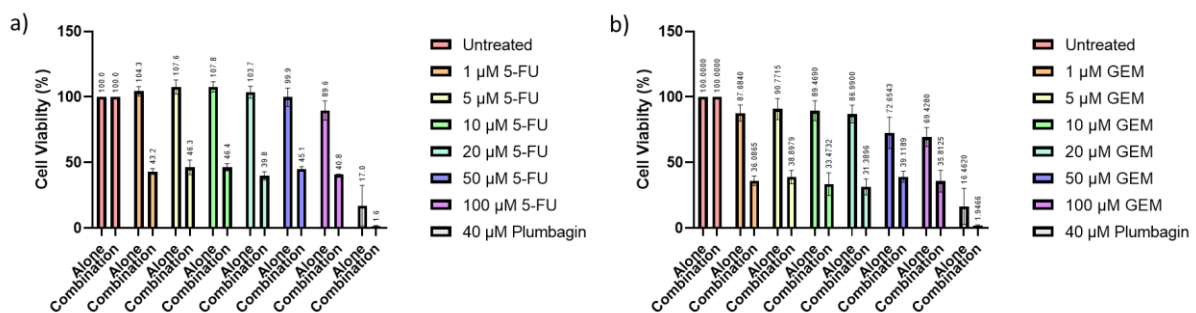


**Figure A1: Changes in cell viability in PANC-1 cells after a range of concentrations of 5-FU or GEM alone or in combination with a cholesterol depleting agent KS-01.**

The graphs depict (a) The percentage cell viability of PANC-1 cells after treatment with various concentrations of 5-FU alone or in combination with 10mM KS-01 after 48 hours, normalised to untreated. (b) The percentage cell viability of PANC-1 cells after treatment with various concentrations of GEM alone or in combination with 10mM KS-01 after 48 hours, normalised to untreated. Cells were plated, treated for 48 hours and MTT was then added for 4 hours, formazan crystals solubilised overnight, and viewed using a VICTOR™ Nivo plate reader at 570 nm. Cells were treated with 1  $\mu\text{M}$ , 5  $\mu\text{M}$ , 10  $\mu\text{M}$ , 20  $\mu\text{M}$ , 50  $\mu\text{M}$ , and 100  $\mu\text{M}$  5-FU or GEM as well as these same concentrations combined with 10 mM ks-01. A positive control (Plumbagin at 40  $\mu\text{M}$ ) was used for all conditions, as it is known to have pro-apoptotic properties. Quantification indicated that in cells treated with 5-FU (a) there was a reduction in viability when treated with a combination of 5-FU and KS-01, there was no reduction in viability when treated with 5-FU alone and a concentration of 10  $\mu\text{M}$  5-FU was chosen for all downstream experiments. In GEM treated cells (b) the same was seen, there was a reduction in viability when treated with a combination of GEM and KS-01, there was no reduction in viability when treated with GEM alone and a concentration of 1  $\mu\text{M}$  GEM was chosen for all downstream experiments. Treatment groups were compared to the (a) untreated control and (b) untreated control. Cell viability was assessed using an MTT assay relative to the untreated control (100% viability). Data are mean  $\pm$  SD; (n = 3) from raw data. The z-factor was >0.6 for each 96-well plate.

### Optimising EMT induction in the PANC-1 cell line

In order to optimise the concentration of TGF- $\beta$ 1 to successfully induce EMT, 24- and 48-hours incubations were investigated using 5 ng/mL and 10 ng/mL of TGF- $\beta$ 1. The only

significant change in vimentin expression, a mesenchymal marker, was after 48 hours with a concentration of 10 ng/mL and was hence chosen to be investigated further using the epithelial marker E-cadherin and the proliferation marker Ki-67 which then resulted in the use of 10 ng/mL TGF- $\beta$ 1 for downstream experiments.

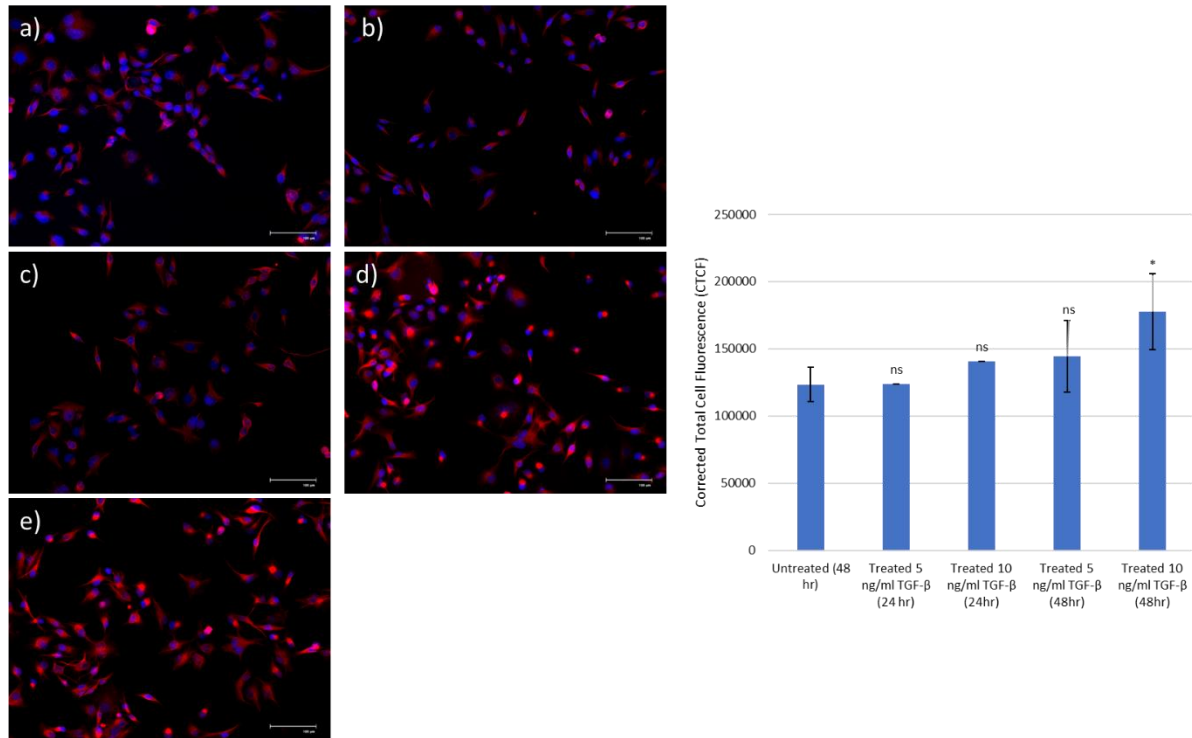


**Figure A2: Changes in vimentin fluorescence in PANC-1 cells after TGF- $\beta$ 1 treatment**

The representative immunofluorescent images illustrate the impact of various TGF- $\beta$ 1 treatments on vimentin expression levels. (i) The images correspond to the following conditions: (a) Untreated, (b) 5 ng/mL TGF- $\beta$ 1 for 24 hours, (c) 5 ng/mL TGF- $\beta$ 1 for 24 hours, (d) 5 ng/mL TGF- $\beta$ 1 for 48 hours, (e) 10 ng/mL TGF- $\beta$ 1 for 48 hours. Cells were labelled with Rabbit Anti-Human Vimentin primary antibody and Goat Anti-Rabbit Texas Red secondary antibody. Nuclei are stained with DAPI and shown in blue, and vimentin in red. (ii) Quantification revealed a significant increase vimentin, a mesenchymal marker, only after treatment with 10 ng/mL of TGF- $\beta$ 1 for 48 hours. Images were captured using EVOS Flويد™ Cell Imaging Station at 20 $\times$  magnification and subsequently quantified using Image J. A corresponding bar graph depicting mean values of the corrected total cell fluorescence (CTCF) from three independent repeats, is included. Treatment groups were compared to the untreated control. Scale bar represents 100  $\mu$ M. Data are mean  $\pm$  SD; (n = 3) from raw data. Treatment groups were compared to the untreated control. Statistical analysis was calculated using a two-tailed students t-test, where \* $p$  < .05, \*\* $p$  < .01, \*\*\* $p$  < .001, \*\*\*\* $p$  < .0001, and ns = non-significant indicates a significant or non-significant difference to the untreated control.

### Optimising MTT assay conditions

In the MTT assay, treatment with TGF- $\beta$ 1 extends over 48 hours, which is then followed by drug treatments that extend over 48 hours the resultant time the cells are exposed to TGF- $\beta$ 1 would be 96 hours. It was then confirmed if there are comparable levels of expression of *SNAIL1*, and EMT-TF gene, after these treatment times. A 48-hour treatment with 10 ng/mL TGF- $\beta$ 1 was found to be comparable to a treatment for 96 hours of 10 ng/ml TGF- $\beta$ 1 with a media change after 48 hours and these conditions were kept for all MTT assays involving EMT induction.

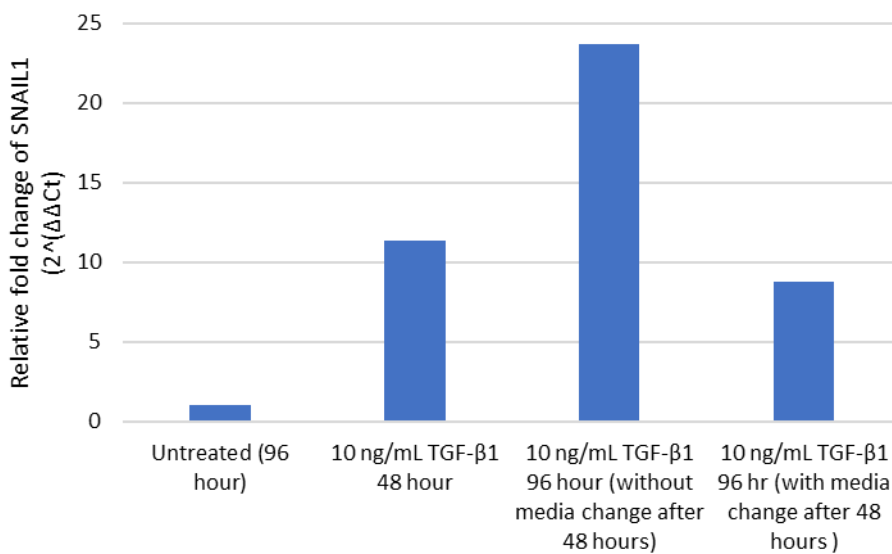


**Figure A3: Changes in *SNAIL1* expression after TGF- $\beta$ 1-induced EMT and combination treatments.**

The graph depicts the  $2^{-\Delta\Delta Ct}$  fold change of a gene involved in EMT (*SNAIL1*) in PANC-1 cells normalized to the untreated. Cells were treated with 10 ng/ml TGF- $\beta$ 1 for 48 hours, 10 ng/ml TGF- $\beta$ 1 for 96 hours without any media change after 48 hours, and 10 ng/ml TGF- $\beta$ 1 for 96 hours with a media change after 48 hours. TGF- $\beta$ 1-induced EMT promotes the gene expression of *SNAIL1* at comparable levels after either 48 hours of 10 ng/mL TGF- $\beta$ 1 or 96 hours of 10 ng/ml TGF- $\beta$ 1 with a media change after 48 hours.  $n=1$ .

### **Determining the optimal annealing temperatures of genes for RT-qPCR**

As to determine the optimal annealing temperature for RT-qPCR, gradient PCR was run on all of the utilised genes and their PCR products run on an agarose gel.

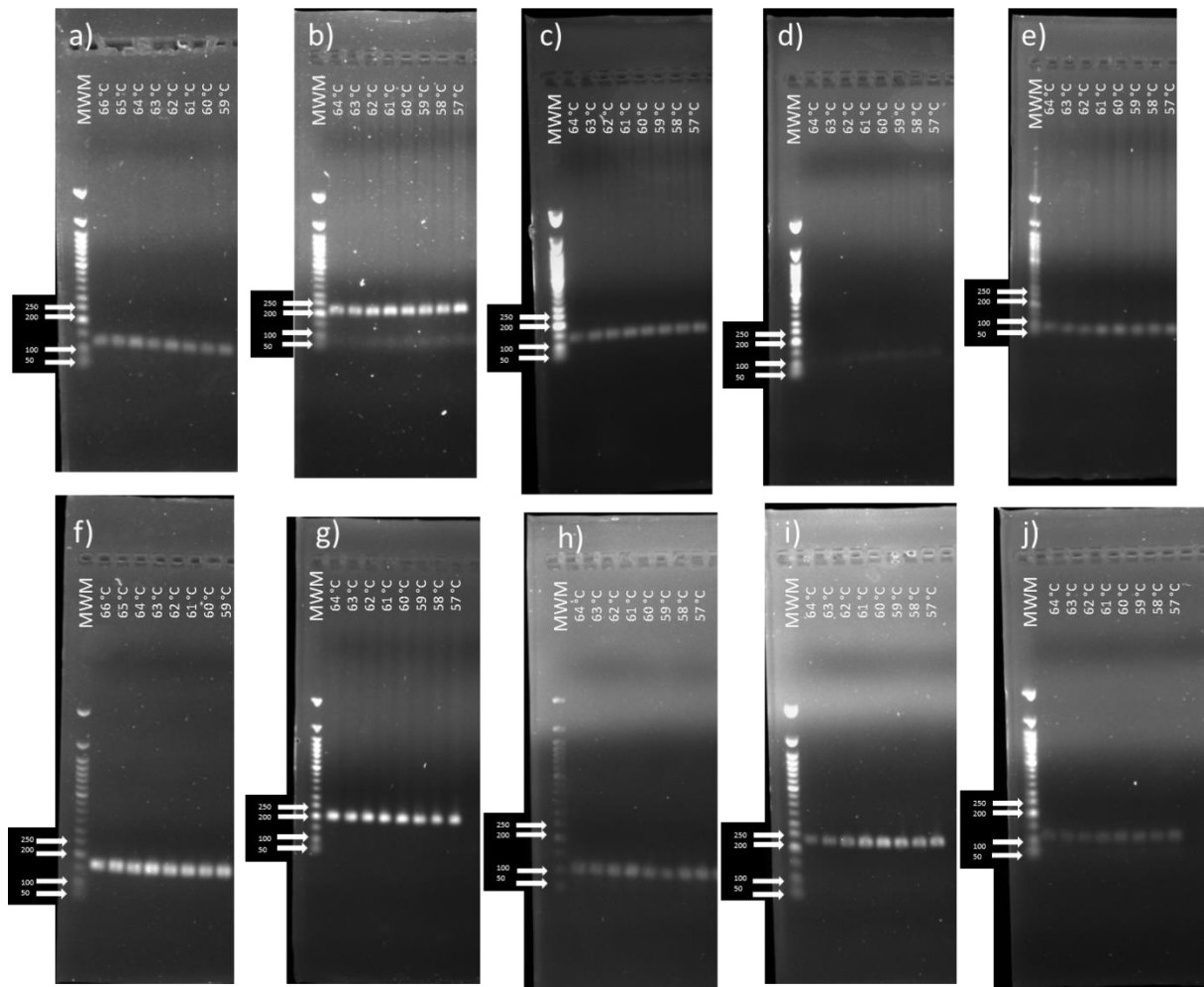


**Figure A4: Agarose gel electrophoresis of gradient PCR products for various genes.**

Each panel represents the specific PCR product band corresponding to the gene indicated, with the expected sizes determined by comparison to the 50 bp DNA ladder. The images correspond to the following genes. (a) *TGF- $\beta$ 1*, (b) *SREBF2*, (c) *SNAIL1*, (d) *ABCB1*, (e) *LDLR*, (f) *hENT1*, (g) *GAPDH*, (h) *ABCG2*, (i) *ABCC5*, (j) *ABCA1*. The genes in panels (a) and (f) were run on a gradient of 59 to 66°C and the rest of the genes run on a gradient of 57 to 64 °C. Gradient PCR optimization was employed to achieve specific amplification of each target gene, facilitating precise assessment of the correct annealing temperature for use in RT-qPCR.